# Hydrological Implications of Woody Encroachment in the Semi-Arid Savannas of South Africa

**by**

**TIFFANY ANTHEA ALDWORTH**

**Submitted in fulfilment of the academic requirements of Doctor of Philosophy**

in Hydrology

School of Agriculture, Earth and Environmental Sciences

College of Agriculture, Engineering and Science

University of KwaZulu-Natal

Pietermaritzburg

South Africa

March 2025

# PREFACE

The research contained in this thesis was completed by the candidate while based in the Discipline of Hydrology, School of Agricultural, Earth and Environmental Sciences of the College of Agriculture, Engineering and Science, University of KwaZulu-Natal, Pietermaritzburg Campus, South Africa. The research was financially supported by the National Research Foundation.

The contents of this work have not been submitted in any form to another university and, except where the work of others is acknowledged in the text, the results reported are due to investigations by the candidate.

Signed: Dr M.L. Toucher

Date: March 2025

Signed: Professor A.D. Clulow

Date: March 2025

## DECLARATION 1: PLAGIARISM

I, *Tiffany Aldworth*, declare that:

(i) the research reported in this thesis, except where otherwise indicated or acknowledged, is my original work;

(ii) this thesis has not been submitted in full or in part for any degree or examination to any other university;

(iii) this thesis does not contain other persons' data, pictures, graphs or other information, unless specifically acknowledged as being sourced from other persons;

(iv) this thesis does not contain other persons' writing, unless specifically acknowledged as being sourced from other researchers. Where other written sources have been quoted, then:

a) their words have been re-written but the general information attributed to them has been referenced;

b) where their exact words have been used, their writing has been placed inside quotation marks, and referenced;

(v) where I have used material for which publications followed, I have indicated in detail my role in the work;

(vi) this thesis is primarily a collection of material, prepared by myself, published as journal articles or presented as a poster and oral presentations at conferences. In some cases, additional material has been included;

(vii) this thesis does not contain text, graphics or tables copied and pasted from the Internet, unless specifically acknowledged, and the source being detailed in the thesis and in the References sections.

Signed: T.A. Aldworth

Date: March 2025

## DECLARATION 2: PUBLICATIONS

**DETAILS OF CONTRIBUTION TO PUBLICATIONS** that form part of and/or include research presented in this thesis (including publications submitted and published, giving details of the contributions of each author to the research and writing of each publication):

### Chapter 2

Aldworth, T.A., Toucher, M.L., Clulow, A.D., 2023. The Potential Impact of Woody Encroachment on Evapotranspiration Losses in South Africa's Savannas: A Combined Systematic Review and Meta-Analysis Approach. Ecohydrology & Hydrobiology 24, 25-35. https://doi.org/10.1016/j.ecohyd.2023.08.016.

The review of relevant literature, methodological design and data analysis was conducted by TA Aldworth. Advice on paper structure and content were provided by ML Toucher and AD Clulow. The publication was written in its entirety by TA Aldworth and all results, figures, tables and graphs were produced by the same, unless otherwise stated within the text of the paper. Final editing and comment were provided by the co-authors and anonymous reviewers of the publication.

### Chapter 3

Aldworth, T.A., Toucher, M.L., Clulow, A.D., Swemmer, A.M., 2023. The Effect of Woody Encroachment on Evapotranspiration in a Semi-Arid Savanna. Hydrology 10, 9. https://doi.org/10.3390/hydrology10010009.

Pre-site setup and programming of equipment was conducted by TA Aldworth, ML Toucher, AD Clulow, BA Gray and MJ Savage. The setup and installation of the equipment was conducted by TA Aldworth, ML Toucher, AD Swemmer, BA Gray, R Lerm and P Nkuna. AD Swemmer, R Lerm and P Nkuna were responsible for maintenance of the equipment and data collection. Data processing, analysis and interpretation was conducted by TA Aldworth with assistance from ML Toucher, AD Clulow, AD Swemmer and BA Gray. The manuscript was written in its entirety along with all figures and tables were created by TA Aldworth unless otherwise referenced. Final editing and comment were provided by the co-authors and anonymous reviewers of the publication.

**Chapter 4**

Aldworth, T.A., Toucher, M.L., Clulow, A.D., Swemmer, A.M. The Influence of Woody Plant Thinning on Soil Hydrological Processes: A Paired Plot Experiment in a Woody-Encroached, Semi-Arid Savanna. Submitted to Hydrological Processes.

Pre-site setup and programming of equipment was conducted by TA Aldworth, ML Toucher, AD Clulow, BA Gray and MJ Savage. The setup and installation of the equipment was conducted by TA Aldworth, ML Toucher, AD Swemmer, BA Gray, R Lerm and P Nkuna. AD Swemmer, R Lerm and P Nkuna were responsible for maintenance of the equipment and data collection. Preparation and processing of the soil samples for analysis was undertaken by TA Aldworth with assistance from V Naiken and K Reddy. Data processing, analysis and interpretation was conducted by TA Aldworth with assistance from ML Toucher, AD Clulow, AD Swemmer and BA Gray. The manuscript was written in its entirety along with all figures and tables were created by TA Aldworth unless otherwise referenced. Final editing and comment were provided by the co-authors and examiners.

**Chapter 5**

Aldworth, T.A., Toucher, M.L., Gokool, S., Clulow, A.D. Assessing the Relationship Between Woody Cover and Evapotranspiration Across Various Spatio-Temporal Scales in a Semi-Arid Savanna Catchment. Intention to submit to Agricultural and Forest Meteorology.

Advice on methodological approaches, and paper structure and content were provided by S Gokool and ML Toucher. Data processing, analysis and interpretation was conducted by TA Aldworth with assistance from ML Toucher, S Gokool and AD Clulow. The manuscript was written in its entirety along with all figures and tables were created by TA Aldworth unless otherwise referenced. Final editing and comment were provided by the co-authors and examiners.

Signed: T.A. Aldworth

Date: March 2025

## ABSTRACT

Many grasslands and savannas across the globe are undergoing large-scale degradation in the form of woody encroachment, a phenomenon where native woody plants are gradually increasing in abundance at the expense of grasses and other herbaceous vegetation. Given the notion that increases in woody cover lead to increases in evapotranspiration (ET), and that some of the most severe cases of woody encroachment have been reported in drylands, concern has been expressed that woody encroachment may be placing further strain on already limited water supplies.

Given this concern, a considerable number of hydrological studies pertaining to woody encroachment have been undertaken across the globe, mostly in the southern Great Plains and southwest regions of the United States. These studies have demonstrated that the hydrological response to woody encroachment is highly variable and is largely dependent on the local climate. The studies carried out in more mesic climates have mostly corroborated the belief that woody encroachment increases ET, resulting in reductions in streamflow and/or groundwater recharge. Fewer studies have been carried out in more arid climates, and their findings have varied from little influence to a decrease or increase in streamflow and groundwater recharge, with soil properties and geology also having a significant influence on the hydrological impact.

The Greater Kruger National Park is South Africa's largest conservation area and is heavily encroached by indigenous woody species. There has been significant concern about the impact on water resources in the park's northern part, which experiences the driest conditions, and future climate projections indicate that these conditions will only worsen. The northern Greater Kruger National Park region also has a high cover of *Colophospermum mopane* (Mopane). Mopane is a protected species of high socio-economic importance, but it has become a dominant encroacher species growing in monospecific stands, and climatic models project that it will extend its current distribution range as a result of climate change. Mopane is thought to be an aggressive competitor for water, tapping into soil water stores that are critical for groundwater recharge.

The hydrological implications of woody encroachment in South Africa's savannas have received little research attention to date. The ground-based research equipment required to fully explore the impact of woody encroachment on ET is capital and human resource demanding.

However, developing countries such as South Africa have limited financial resources and technical expertise to pursue such research. A further challenge has been that the high spatio-temporal variability in ET necessitates data collection and analysis at large spatial scales as well as over several years to be able to draw meaningful conclusions for land and water management planning purposes. However, advances in ground-based observation methods, as well as access to remote sensing technologies, have allowed for many of the limitations to be overcome. Therefore, the aim of this study was to advance our understanding of the impact of woody encroachment on ET and other components of the water balance in a semi-arid savanna in South Africa by employing cheaper, simpler, yet robust in situ measurements, and to further evaluate these findings across various spatio-temporal scales using freely available remote sensing resources.

A combined systematic review and meta-analysis approach was undertaken first to explore trends in previous research on the water use of different vegetation types located in various climates across South Africa, to ultimately evaluate the likelihood of woody encroachment increasing ET losses in South Africa's semi-arid savannas. The results revealed mixed support for this idea. On the one hand, the fact that woody encroacher species replace grasses and form dense thickets with extensive rooting systems indicated that there is a high potential for woody encroachment to increase ET. On the other hand, rainfall appeared to be a primary factor limiting ET in semi-arid climates, indicating little potential for woody encroachment to have any effect on ET, unless there is an above-average rainfall year, or the vegetation has access to an additional water source. It was noted that there was relatively little ground-based research available on woody encroachment, especially in the South African context, and that further research was warranted in dryland and susceptible areas.

In situ ET measurements were therefore carried out in a semi-arid South African savanna to determine the effect of woody encroachment. Over three hydrological years, ET was measured at an experimental woody plant clearing trial using surface renewal, a simpler, more affordable alternative to the well-established eddy covariance method. Two surface renewal approaches, surface renewal 1 (SR1) and surface renewal dissipation theory (SRDT), were tested against eddy covariance in order to assess their potential for sensible heat flux (H) measurement. The SR1 approach best agreed with eddy covariance, and therefore, ET measurements derived from SR1 were compared at two adjacent plots differing in woody plant density; one encroached plot and

one plot thinned of Mopane trees. For the two drier years of the study, thinning had little effect on ET. However, for the wettest year of the study, thinning decreased ET by 12%, supporting the theory that woody encroachment can increase ET, at least during years of above-average rainfall.

It was also important to evaluate the influence of woody plant thinning on soil hydrological processes because any changes to the movement and distribution of water in the soil can have a direct impact on the production of surface runoff and groundwater recharge. Therefore, at the same site, a field-scale paired-plot experiment was conducted, with soil water content, soil temperature and ET measured in three paired plots over a two-and-a-half-year period. Surface infiltration tests were also carried out. Thinning had minor effects on soil water in the soil profile and soil temperature, and no pronounced effect on daily ET. Only one set of infiltration tests indicated a significant increase in infiltration following thinning.

Finally, freely available and relatively user-friendly resources provided by Google Earth Engine were leveraged to assess the relationship between woody cover and ET across various spatio-temporal scales in a woody-encroached, semi-arid savanna catchment. Woody cover in the study catchment was mapped using Sentinel-2 imagery and Gradient Tree Boost algorithms within the Google Earth Engine platform, while remotely sensed ET estimates were obtained from Earth Engine Evapotranspiration Flux (EEFlux) validated by in situ surface renewal measurements. It was found that while woody encroachment can increase ET in semi-arid savannas, this increase occurs gradually over time and typically only during wet seasons and wet years. Moreover, this increase only becomes evident at larger scales.

The key conclusions from the research were as follows:

- Woody encroachment in semi-arid savannas can increase ET losses, however, this is a gradual process that is only distinguishable during wet seasons or extended wet periods;

- The increase in ET in semi-arid savannas caused by woody encroachment is more evident at larger scales;

- The SR1 approach with eddy covariance calibration produced reliable ET estimates with reasonable accuracy over semi-arid savanna-type vegetation;
- ET in semi-arid savannas is highly seasonal, rising during the wet season in response to increased soil water availability and higher net radiation (Rn), and dropping significantly during the dry season due to low soil water availability and the deciduous nature of the vegetation;

- Woody plant thinning had little effect on infiltration and soil water in the soil profile;

- Sentinel-2 imagery and supervised pixel-based classification algorithms within Google Earth Engine accurately mapped woody cover in densely wooded areas, but in sparsely wooded areas, woody cover was either over- or under-classified; and

- EEFlux was able to estimate daily ET in semi-arid savanna vegetation with a reasonable level of accuracy, despite an underestimation of ET.

While there is still a need to continue ET monitoring, further improve remote sensing-based ET models for use in natural environments, and better understand how woody encroachment affects deep drainage and groundwater recharge, this research added to our understanding of the hydrological implications of the woody encroachment phenomenon in drylands. It further provided invaluable insight for developing land and water management strategies to increase resilience under a changing climate and increasing socio-ecological pressures.

## ACKNOWLEDGEMENTS

Michele Toucher, thank for guiding me on this tough yet incredible journey. You've been with me since before my post-grad days, and I would never have gotten this far if it weren't for you!

Alistair Clulow, you have been an amazing mentor to me over the years. Thank you for always encouraging me and being someone I can always on count on when I have left my work to the last minute.

Tony Swemmer, thank you sharing your incredible knowledge of the bush and the Mthimkhulu reserve. I have been so fortunate to be a part of one of your projects.

Shaeden Gokool, for showing me that remote sensing isn't as intimidating as I had previously thought. The knowledge you have shared while preparing our paper has taught me so much.

To the National Research Foundation (NRF), thank you for funding this research and for making it possible for students, such as myself, to study further.

Sue van Rensburg and the staff and students of the SAEON: Grasslands-Forest-Wetlands Node thank you for the support and for hosting me, even though my project did not fall within your node.

I'd also like to acknowledge the SAEON: Ndlovu Node for hosting me in the Kruger Park when I visited to carry out field work. Rion Lerm and Peace Nkuna thank you for your assistance with the field work.

The Mthimkhulu Tribal Authority for permitting the research at your site

To the University of KwaZulu-Natal (UKZN) and the Centre for Water Resources Research (CWRR), thank you for the use of facilities and equipment required for our in situ monitoring. A huge thank you to Vivek Naiken and Kyle Reddy for your patience in the lab.

Byron Gray, thank you for your assistance with the set-up of instrumentation, and for helping me better understand eddy covariance and surface renewal. You made these instruments less daunting.

My examiners, thank you for taking the time and effort to provide feedback and suggestions. Your input has been invaluable to this final draft of my thesis.

Kent, thank you for sticking with me over these last few years, despite having to spend most weekends on your own. It's finally time for us to go on those trips we have been talking about.

And finally, to my family – thank you for your unwavering support from afar and for always cheering me on. Mom and dad, this one is for you. Kim and I are beyond grateful for all the sacrifices you made so that we could receive a quality education.

# TABLE OF CONTENTS

**Page**

# LIST OF TABLES

**Table** **Page**

# LIST OF FIGURES

**Figure** **Page**

# 1 INTRODUCTION

## 1.1 Background

Grasslands and savannas are among the world's most extensive vegetation types, occupying approximately 23% of the Earth's terrestrial surface, yet they are also among the most severely threatened (Ford 2010, Stevens *et al*. 2017, Tsalyuk *et al*. 2017). Natural land cover loss and fragmentation of these vegetation types is occurring due to land use and land cover change (LULCC) caused by urban expansion, agricultural intensification, commercial tree planting and other anthropogenic activities (Stevens *et al*. 2017, Tsalyuk *et al*. 2017). A form of LULCC affecting many grasslands and savannas across the globe is woody encroachment, a phenomenon also commonly termed bush or shrub encroachment, woody thickening, thicketization or xerification (Archer *et al*. 2017, Olariu *et al*. 2022). Woody encroachment involves the gradual thickening of indigenous trees and/or shrubs within their natural geographic range or expansion beyond this range, displacing grasses and other herbaceous vegetation (Archer *et al*. 2017). Grasslands and savannas, which have been open grassy landscapes since the late Miocene-Pliocene, have evolved into landscapes that more resemble dense shrublands and forests (Strömberg 2011, Hoetzel *et al*. 2013, Olariu *et al*. 2022). Woody encroachment has been documented on every continent except Antarctica, with rates of increase in woody cover ranging between 0.1 and 2.3% per annum (Archer *et al*. 2017, Liu *et al*. 2021).

The origin and drivers of woody encroachment have fueled considerable debate and discussion over the years, but there is consensus that a variety of factors act either alone, or in combination, to facilitate the growth of encroacher species under different land uses, land management and environmental conditions. These factors may be of local (e.g., changes in grazing regimes, fire suppression), regional (e.g., shifts in temperature and precipitation patterns), or global (e.g., rising atmospheric $CO_2$ concentrations) origin (Stevens *et al*. 2016, Archer *et al.* 2017). Most of the discussion has centered around heavy grazing and the consequent reductions in fire frequency and intensity, which are thought to promote woody encroachment by restricting grass competition for resources (i.e., water and nutrients) (Stevens *et al*. 2017). In more recent research, rising atmospheric $CO_2$ concentrations have emerged as a major driver, as $CO_2$ favours the growth of $C_3$ woody plants over $C_4$ grasses. Under elevated $CO_2$, $C_3$ woody plants have higher photosynthesis

rates relative to $C_4$ grasses, allowing for faster growth rates and better water use efficiency, hence improving competitive ability (Saha *et al*. 2015, Stevens *et al*. 2016, Stevens *et al*. 2017).

Woody encroachment is of significance for a number of reasons. It has been recognized as a form of land degradation since the early 20$^{th}$ century, due to its ability to reduce the carrying capacity of land for domestic and wild grazers (Venter *et al.* 2018). The negative consequences for biodiversity, soil erosion and soil organic carbon storage have also been long-standing concerns (Huxman *et al*. 2005). However, in the last two decades or so, as global concerns surrounding water security have intensified, the hydrological implications of woody encroachment have drawn increasing attention (Otieno and Ochieng 2004, Zou *et al*. 2018). Some of the most severe cases of woody encroachment have been observed in drylands, prompting fears that woody encroachment is placing further strain on already limited streamflow and groundwater resources (Puttock *et al*. 2013, Acharya *et al*. 2018, Wang *et al*. 2018). The majority of scientific research on the processes via which woody encroachment might affect streamflow and/or groundwater has focused on evapotranspiration (ET) as the primary mechanism (Wang *et al*. 2018). Evapotranspiration is the transport of water vapour to the atmosphere by plant transpiration, soil and plant evaporation, and essentially translates into a loss of water from the terrestrial system (Allen *et al*. 1998). Woody plants have been reported to have greater ET than grasses because of their deeper and greater root biomass, taller stature, longer growing seasons, larger leaf areas, higher interception ratios and higher air turbulence in the canopy boundary layer (Huxman *et al*. 2005, Acharya *et al*. 2017, Dye *et al*. 217, Acharya *et al*. 2018). The result is that, as landscapes become woodier, ET losses are expected to rise, resulting in less water available to replenish streamflow and groundwater stores (Acharya *et al*. 2017, Acharya *et al*. 2018). Prior hydrological research pertaining to woody encroachment has also investigated how woody encroachment may alter soil hydrological processes, such as soil water storage, soil infiltrability and deep drainage. Any change in these processes is significant because they may directly affect the amount of surface runoff and groundwater recharge (Wilcox and Huang 2010, Acharya *et al*. 2018).

A considerable number of hydrological studies pertaining to woody encroachment have been undertaken across the globe at various spatial scales, utilizing both field-based and modelling approaches. These studies have demonstrated that the hydrological response to woody encroachment is highly variable, and it is not always the case that woody encroachment increases

ET while decreasing streamflow and groundwater (Acharya *et al.* 2018). Rather, the hydrological changes that occur concomitant with woody encroachment can vary depending on the climate, soils and geology of a given area (Zou *et al*. 2015).

Most studies have been carried out in the southern Great Plains and southwest regions of the United States, a vast area with a number of ecoregions and climates (Zou *et al*. 2015). The studies carried out in more mesic climates (i.e., subhumid or relatively wet semi-arid climates) have mostly corroborated the belief that woody encroachment increases ET, resulting in reductions in streamflow and/or groundwater recharge (Wilcox *et al*. 2022, Sadayappan *et al*. 2023, Keen *et al*. 2024). Fewer studies have been carried out in more arid climates (i.e., arid and drier semi-arid climates) in the United States, and their findings have varied, with soil properties and geology having a significant influence on the hydrological impact (Wilcox *et al*. 2022). In shrublands in south Texas, woody encroachment was found to slightly increase ET and deep drainage, with little influence on total groundwater recharge (Wilcox *et al*. 2022). In the Rolling Plains of Texas, woody encroachment caused higher soil infiltrability, which reduced overland flow. This led to large reductions in streamflow since, in this area, streamflow was mainly generated as infiltration-excess overland flow (Wilcox *et al.* 2022). Another study conducted in a semi-arid rangeland in the state of Oregon agreed that woody encroachment reduced streamflow, and they ascribed this to the high rainfall interception of woody canopies, which significantly reduced the soil water beneath the canopies and in the canopy interspace (Ochoa *et al.* 2018). As a result, high ET losses occurred and less rainfall was available to generate streamflow. In the Chihuahuan Desert, a very arid site in New Mexico, woody encroachment led to increased overland flow and groundwater recharge. This is because woody encroachment increased the amount of bare ground in a process called ‘xerification’, resulting in lower surface roughness and soil infiltrability, which greatly facilitated surface runoff into stream channels (Schreiner-McGraw *et al.* 2020, Wilcox *et al.* 2022). This ultimately led to higher groundwater recharge through deep percolation in stream channels (Wilcox *et al.* 2022). In the Edwards Plateau in central Texas, geology played a more important role than climate in determining the hydrological impact of woody encroachment (Wilcox and Huang 2010, Acharya *et al*. 2018). The climate of the Edwards plateau ranges between semi-arid to subhumid, and the plateau has a karst geology, which is permeable and deep drainage occurs mainly via conduit flow. Some studies conducted on the Edwards Plateau reported that woody encroachment, along with the high permeability of the karst substrate, enhanced soil infiltrability,

resulting in significant increases in streamflow and groundwater recharge. On the other hand, several studies reported that, even while woody encroachment increased ET, woody encroachment or its removal had minimal impact on streamflow or groundwater recharge (Leite *et al*. 2020, Wilcox *et al*. 2022). Streamflow and groundwater recharge were reported to be primarily dependent on rainfall, unaffected by changes in vegetation cover (Wilcox *et al*. 2005, Bazan *et al*. 2012, Cardella Dammeyer *et al.* 2016).

There have also been a fair number of hydrological studies relating to woody encroachment in Brazil, where woody plant cover has increased in the native Cerrado savanna vegetation. These studies have agreed with the United States studies in more mesic climates that woody encroachment reduces streamflow and groundwater recharge (Honda and Durigan 2016, Oliviera *et al*. 2016). They attributed this to the high transpiration and rainfall interception of woody canopies at densely encroached sites.

### 1.2 Rationale for the research

South Africa's savannas have undergone widespread woody encroachment during the last century (O'Connor and Crow 1999, Hudak and Wessman 2001, Britz and Ward 2007, Wigley *et al.* 2009, Wigley *et al*. 2010, Munyati *et al*. 2011, Buitenwerf *et al*. 2012, Puttick *et al*. 2014, Symeonakis and Higginbottom 2014, Ward *et al*. 2014, Munyati and Sinthumule 2016, Symeonakis *et al*. 2016, Marston *et al*. 2017, Skowno *et al*. 2017, Hoffman *et al*. 2018, Zhou *et al*. 2021, Maphanga *et al*. 2024). Although the exact extent of woody encroachment is yet to be determined, it is estimated that between 10 and 20 million hectares of land have been affected (Stafford *et al*. 2017). Given that South Africa's savannas host a large and rapidly growing proportion of the country's human population, and because they typically have semi-arid climates with limited water resources, the hydrological implications of woody encroachment have been of considerable concern (Wessels *et al*. 2010, Whitecross *et al*. 2016, Andreu *et al*. 2019). Semi-arid climates experience low rainfall with a mean annual precipitation (MAP) of less than 700 mm. Rainfall can also be highly variable between seasons with a distinct dry season experiencing little or no rainfall and high temperatures (Kambatuku *et al*. 2012). Furthermore, droughts naturally occur resulting in severe and extensive dry periods (Andreu *et al*. 2019). South Africa's semi-arid savannas are also believed to be highly vulnerable to the adverse effects of global warming and climate change, potentially aggravating water shortages (Andreu *et al*. 2019). In the Kruger National Park, South Africa's largest

conservation area (Ferreria and Harmse 2014), projected data indicates an increase in temperatures of more than 1°C and a slight decrease in precipitation (1%) by 2080, with minimal change in the seasonal dynamics of rainfall (Bunting *et al*. 2016). Additionally, the Kruger National Park has noted a rise in the frequency of extremely high maximum temperatures, as well as upward trends in the mean minimum and maximum temperatures (Kruger and Sekele 2013, Malherbe *et al*. 2020). Kruger and Shongwe (2004) have predicted a rise in the annual maximum temperature of 1.2°C per century in the Kruger National Park. Global circulation models also predict that climate change will lead to more frequent and severe drought in savanna regions in South Africa, a trend that has already been observed in recent decades (Gizaw and Gan 2017, Malherbe *et al*. 2020). The most recent severe drought occurred in 2015-2016, due to El Niño, and was associated with extremely high temperatures, heat waves and lower than normal rainfall. As a result of these effects, water levels in dams, reservoirs and groundwater stores declined, causing water shortages in many parts of the country (Baudoin *et al*. 2017).

To our knowledge, no research on the hydrological implications of woody encroachment in South Africa's semi-arid savannas has provided any conclusive findings. There have, however, been extensive hydrological studies on the uncontrolled spread of invasive alien plants in the country. These studies have demonstrated that ET increases with woody plant cover, leading to a decline in streamflow and groundwater recharge (Le Maitre *et al*. 2020). This led to the development of a national-scale invasive alien plant clearing programme called 'Working for Water' in 1995 (van Wilgen *et al*. 1998). It has been well established that invasive alien trees consume greater amounts of water than indigenous trees (Calder and Dye 2001), and most of the invasive alien plant studies have been conducted in higher rainfall regions of the country, or in riparian zones, where vegetation likely has access to more water (Aldworth *et al*. 2023). Therefore, we cannot infer that these findings hold true for the woody encroachment phenomenon in South Africa's semi-arid savannas. Furthermore, it is difficult to infer the impact of woody encroachment in South Africa from international research, since the research has demonstrated that the hydrological impact of woody encroachment can vary significantly depending on location, due to varying climatic, geologic and soil conditions (Wilcox *et al*. 2022). The few woody encroachment-related hydrological studies conducted in drier climates in the United States have also yielded mixed findings (Acharya *et al*. 2018, Wilcox *et al*. 2022). The annual rainfall totals in South Africa's semi-arid savannas are typically lower and more variable than in the semi-arid locations

of the international studies. Another important difference between the semi-arid locations of the international studies and semi-arid savannas in South Africa is the intercanopy vegetation. Because of their wetter climates, woody encroachment usually causes thicketization in the semi-arid locations of the international studies, where intercanopy spaces remain vegetated with herbaceous plants year-round (Schreiner-McGraw *et al*. 2020). Whereas in South Africa's semi-arid savannas, climates are drier and cattle farming causes heavy grazing, resulting in xerification. Landscapes affected by xerification have little, if any, grass cover, and bare soil exists in the intercanopy spaces, especially during the dry season (Schreiner-McGraw *et al*. 2020). The soils are highly susceptible to surface crusting and compaction because of exposure to raindrop impact and trampling by large mammals (Smit and Rethman 2000). Soil crusting and compaction slows and/or prevents infiltration, promoting high surface runoff losses and reduced soil water recharge, which affects streamflow and/or groundwater recharge (Acharya *et al*. 2018).

Hydrological research relating to woody encroachment in South Africa's savannas has been hindered by the expense and complexity of the instrumentation necessary to carry out ET field measurements (Khosa *et al.* 2019, Awada *et al*. 2021, Gray *et al*. 2021). The preferred method for ET field measurements is eddy covariance, which provides direct and reliable results (Pozníková *et al*. 2018). Eddy covariance measures the covariance of vertical wind velocity and water vapor exchange between the atmosphere and plant canopy, to measure latent heat flux (LE), from which ET is calculated (Rosa *et al*. 2013). However, only three eddy covariance systems are currently monitoring ET at savanna sites in South Africa; the Skukuza, Malopeni and Agincourt flux towers operated by the Council for Scientific and Industrial Research (CSIR). The main reasons preventing the widespread use of eddy covariance in South Africa are the high cost of the eddy covariance sensors and the high degree of expertise required to operate the sensors and interpret their data (Zapata and Martínez-Cob 2002, Rosa *et al*. 2013). As a developing country, South Africa has limited funds, resources and technical skills for such research (Khosa *et al.* 2019, Gray *et al*. 2021). South Africa also faces a significant risk of theft and damage to valuable equipment due to the country's high poverty rate, and the occurrence of wildfires which are common in many vegetation types including savannas (Clulow *et al.* 2012, Gray *et al*. 2021). Other disadvantages of eddy covariance include sensitive sensors that must be maintained and monitored on a regular basis for accurate readings, the necessity for extensive fetch and site homogeneity, and the inability to consistently achieve energy balance closure (Suvočarev *et al.* 2014, Haymann *et al*. 2019).

For the reasons mentioned above, simple and more affordable alternatives to eddy covariance have been sought. One such method that has gained popularity in recent years is surface renewal (Rosa *et al*. 2013). Surface renewal uses high-frequency air temperature measurements taken near or above the vegetation canopy to calculate sensible heat flux (H). The H measurements along with simple measurements of net radiation (Rn) and soil heat flux (G), and the shortened surface energy balance equation, are then used to indirectly calculate LE (Rosa and Tanny 2015). Surface renewal overcomes many of the limitations of eddy covariance; 1) it makes use of simple, cheaper sensors increasing the possibility of replicating measurements; 2) the sensors are less sensitive to wind speed and don't require as careful positioning as eddy covariance sensors 3) the sensors are more suitable for use in remote, easily accessible areas since they require little maintenance and have lower power requirements (Castellví 2004, Mengistu and Savage 2010, Poblete-Echeverría *et al*. 2014, Hu *et al*. 2018), and 4) surface renewal can operate satisfactorily under smaller fetch conditions than eddy covariance (Castellví and Snyder 2009a, Haymann *et al*. 2019). The surface renewal method does have a significant drawback, though, in that accurate H values cannot be obtained unless calibration against a standard method, such as eddy covariance, is performed (Suvočarev *et al.* 2014). Nonetheless, efforts have been made to develop alternative surface renewal approaches that avoid the use of a calibration factor, although they still require significant testing and refining over different surfaces (Castellví 2002; 2004, Castellví and Snyder 2009b). Promising results have been found when the original surface renewal method has been tested against eddy covariance and other micrometeorological methods for measuring ET. However, these experiments have mostly been made in agricultural croplands in wetter climates (Hu *et al*. 2018). Few investigations on the accuracy of surface renewal over natural vegetation have been undertaken, especially in dry environments.

Researching the hydrological impact of woody encroachment is further complicated by the fact that the hydrological response of a catchment can be highly scale dependent, meaning that impacts may only become evident or even change as the scale of observation increases (Wilcox *et al*. 2022). If we are to develop land-based mitigation and adaptation strategies under global environmental change, it is essential that we understand the impact of woody encroachment on ET and other water balance components across various scales (Qiao *et al*. 2015). Eddy covariance, surface renewal and other micrometeorological methods only provide ET measurements at the field- or point-scale and are unable to account for the spatial variability of ET across a catchment (Alemayehu *et al*.

2017, Nisa *et al*. 2021). There are also many constraints that prevent these measurements from being replicated or carried out over extended periods (i.e., high costs, a lack of technical skills, site remoteness, vandalism, etc.), therefore the in situ ET data records that exist are limited and only cover short time periods (Aldworth *et al*. 2023).

Recent advances in remote sensing-based surface energy balance models may be able to provide promising ET data to fill these observational gaps (Alemayehu *et al*. 2017, Weerasinghe *et al.* 2020, Laipelt *et al*. 2021). Prior validation research has demonstrated that surface energy balance models are capable of mapping ET at various spatial and temporal scales with reasonable accuracy (Alemayehu *et al*. 2017, Weerasinghe *et al*. 2020). Significant advancements have also been made in cloud computing platforms, including Google Earth Engine, Earth on Amazon Web Services and Microsoft Azure (Amani *et al*. 2020, Xu *et al*. 2022). These platforms have the ability to handle computationally-intensive processing tasks and simplify remote sensing applications for non-expert users (Xu *et al*. 2022). The Mapping Evapotranspiration at High Resolution using Internalized Calibration (METRIC) Model, a surface energy balance model, was recently implemented into the Google Earth Engine platform via a graphical user interface called Earth Engine Evapotranspiration Flux (EEFlux) (Kadam *et al.* 2021, Poudel *et al.* 2021). Earth Engine Evapotranspiration Flux allows users to almost instantaneously obtain daily ET images with a spatial resolution of 30 m and a temporal resolution of eight days for any terrestrial land area across the globe from 1984 to the present (de Oliveira Costa *et al*. 2020, Carrasco-Benavides *et al.* 2022, Blin and Suárez 2023). As with surface renewal, EEFlux has mostly been tested over agricultural crops and in wetter climates (Bchir *et al*. 2021, Kadam *et al*. 2021, Nisa *et al*. 2021, Poudel *et al.* 2021, Rojas-Villalobos *et al*. 2022), and the potential for use in natural, drier landscapes still requires testing.

### 1.3 Woody encroachment in the study region

The study catchment of the research described within this thesis is the quaternary catchment B82J (796 $km^2$), located in the north-east region of South Africa (Figure 1.1). The catchment is one of 23 quaternary sub-catchments, South Africa's principal water management units, that comprise the Letaba River catchment. The Letaba River catchment encompasses a large portion of the Kruger National Park, as well as several private game reserves, large towns (e.g., Tzaneen and Giyani) and rural villages, and thus provides an important supply of water to many people, animals

and the environment (Pollard and du Toit 2011, Kanjere *et al*. 2014). Quaternary B82J drains into the Klein Letaba River, a major tributary of the Letaba River. The quaternary B82J was chosen for this research because it consists primarily of intact savanna landscapes that have undergone woody encroachment. An experimental woody plant clearing trial is also located within the quaternary B82J. This experimental trial was established in 2014 by the South African Environmental Observation Network (SAEON) and is located in Mthimkhulu, a private game reserve owned by a local traditional authority.

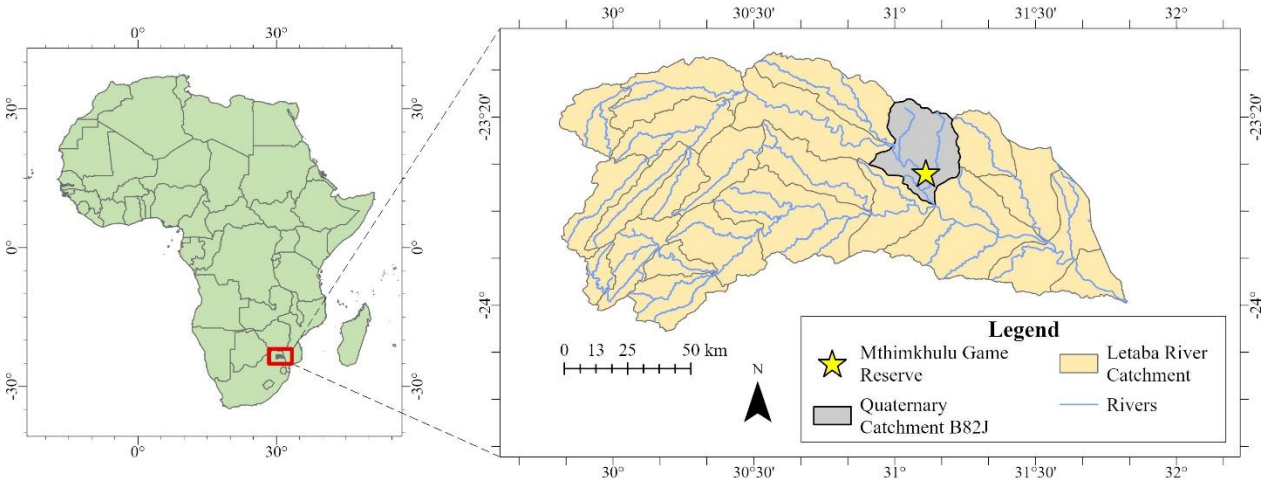


**Figure 1.1 The location of the Mthimkhulu Game Reserve and the quaternary B82J within the Letaba River catchment in southern Africa.**

The vegetation of the quaternary catchment B82J can be classified as Lowveld Mopaneveld (Mucina and Rutherford 2006), a semi-arid savanna characterized by dense, monospecific *Colophospermum mopane* (Mopane) stands interspersed with *Combretum imberbe* (Leadwood), *Vachellia tortilis* (Umbrella thorn) and *Combretum apiculatum* (Red bushwillow) trees, and *Grewia bicolor* (Twotone raisin) shrubs. The grass layer is sparse, mostly dominated by annual *Aristida* species, scattered with tufts of *Urochloa mosambicensis* (Gonyagrass) and *Panicum maximum* (Guinea grass). Although Mopane naturally grows in dense monospecific stands in mopaneveld savanna, its density has increased in this vegetation type in recent decades (Jordaan *et al*. 2004, O'Connor 2015). In the communal areas of the quaternary B82J, this is most likely in response to poor land management practices, such as overgrazing by cattle and fire suppression. However, because most of the quaternary B82J is covered by the Kruger National Park, which is

a protected area, regional- and global-scale changes in temperature, precipitation and atmospheric $CO_2$ concentrations are likely, or at least believed to have played a role in causing woody encroachment.

*Colophospermum mopane* (Kirk ex Benth) Kirk éx J. Léonard is one of the most dominant woody plant species in the dry savanna regions of southern Africa, covering an area of around 550 500 $km^2$ (Makhado *et al.* 2018). Its range spans from southern Angola, northern Namibia and northern Botswana across Zambia and Zimbabwe into central and southern Malawi and Mozambique, to northern South Africa, with its southern-most distribution just south of the Olifants River in Kruger National Park (Figure 1.2, Makhado *et al.* 2018). This distribution appears to be heavily influenced by altitude, temperature and rainfall, with the species occurring in low-lying (400-700 m above sea level), hot, dry (200-800 mm rainfall per annum) areas (Mapaure 1994, Whitecross *et al*. 2012). Mopane usually grows in monospecific stands, or in dense clusters either as a multi-stemmed shrub, or a small- to medium-sized single-stemmed tree less than 5 m in height (Stevens *et al*. 2013). In the past 100-200 years, the density of Mopane in southern Africa's savannas has significantly increased within its existing range, and climatic models project that it will extend southward and westward of its current distribution range due to climate change (Stevens *et al*. 2013). It is thought that Mopane is an aggressive encroacher species that uses its roots to successfully compete with other woody and herbaceous plants for available soil water. Mopane roots have been observed to be shallow with a large biomass, extending horizontally in the upper soil layers well beyond the canopy extent (Smit and Rethman 1998, Macgregor and O'Connor 2002, Smit 2004). Unpublished root excavation data from a study conducted within the Greater Kruger National Park found that the highest mean root concentration was within the first 0.5 m of soil, and that most coarse roots extended horizontally to a distance of approximately 2 m from the tree stem. The species has also been reported to have a deep taproot of up to 3 m long (Sebego 1999). As a result, Mopane likely have access to available soil water across an extended area in both the upper and lower soil layers. It has also been demonstrated that Mopane germinates and establishes root growth at soil matric potentials lower than those at which other species can tolerate (Macgregor and O'Connor 2002, Smit 2004). However, there has been hesitancy to clear encroaching Mopane because it is a protected species of high socio-economic importance (Mashabane 2001). Mopane is used for firewood, building materials, traditional medicine, and the leaves and pods provide an important food source for many animals (Mashabane 2001, Ferreria

2003, Poilecot and Gaidet 2010). Mopane is also the host plant for the 'Mopane worm' (*Gonimbra siabelina*), a popular delicacy and protein source in the diet of indigenous African people (Ferreria 2003). In southern Africa, Mopane worms are also traded both commercially and informally for profit (Baiyegunhi and Oppong 2016).

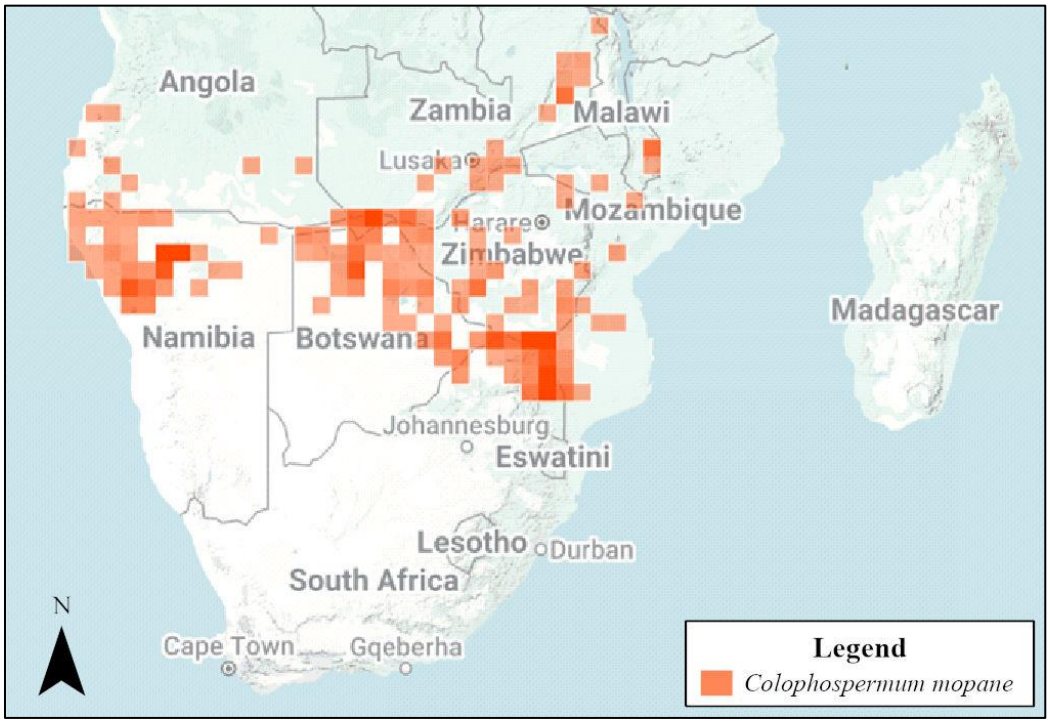


**Figure 1.2 Distribution map of *Colophospermum mopane* in southern Africa (iNaturalist 2024).**

To visualise woody cover in the quaternary catchment B82J, historical aerial photographs taken in 1937/1938 and 1971 sourced from the South African CDNGI Geospatial Portal (http://www.cdngiportal.co.za/CDNGIPortal/) were compared to Google Earth Pro imagery taken in 2023 for selected areas (Figure 1.3). This comparison demonstrated that there was a significant amount of woody cover in the catchment in the 1930s and 1970s, but there has been an increase in the density of woody plants in some areas in recent decades. Increases were also evident in areas within the boundaries of the protected Kruger National Park.

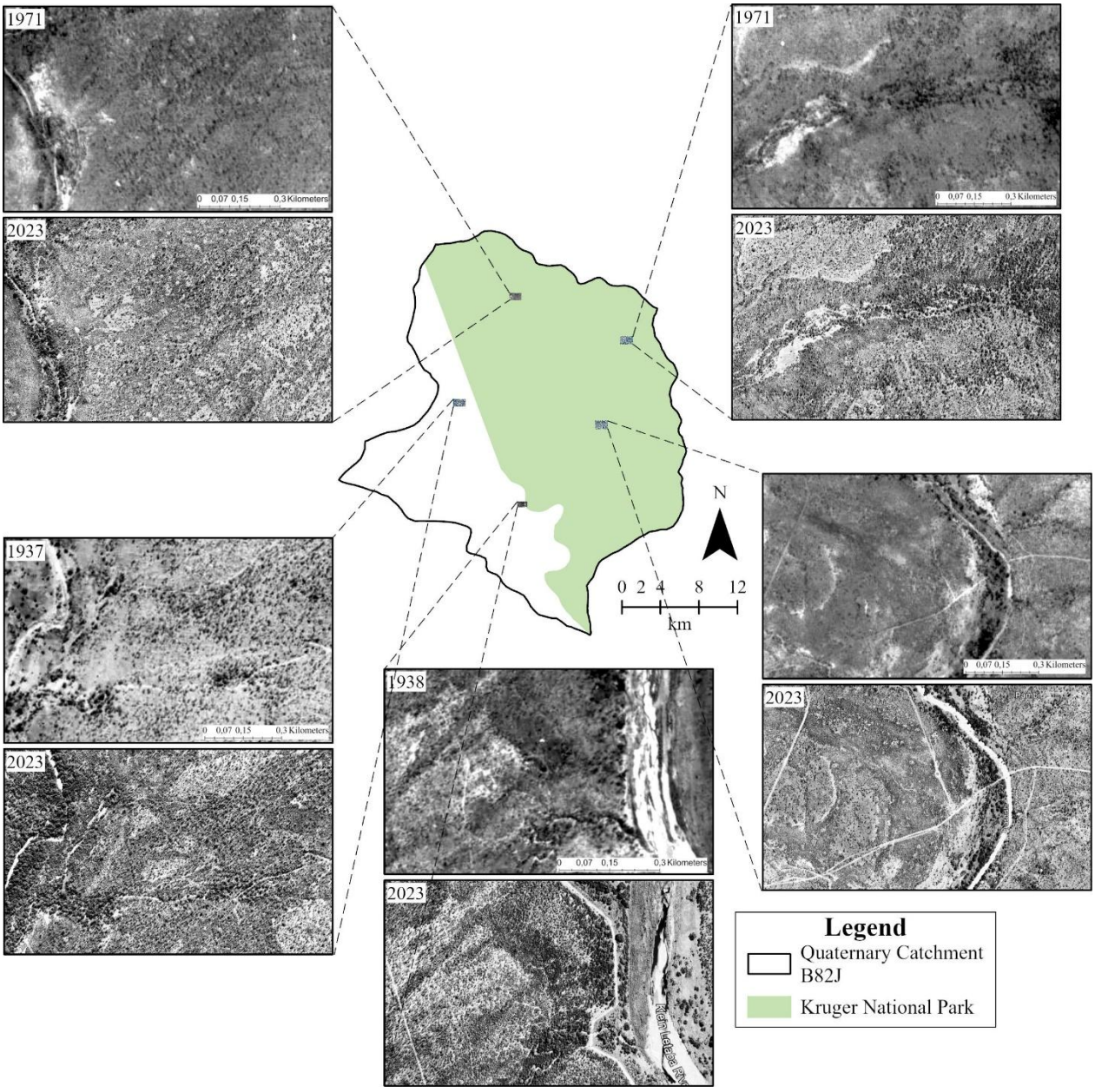


**Figure 1.3 Imagery depicting woody cover in 1937/1938, 1971 and 2023 in selected areas of quaternary catchment B82J.**

### 1.4 Research aim and objectives

The overall aim of this thesis was to advance our understanding of the impact of woody encroachment on ET and other components of the water balance in a semi-arid savanna in South Africa by employing cheaper, simpler, yet robust in situ measurements, and to further evaluate

these findings across various spatio-temporal scales using freely available remote sensing resources.

To achieve the overall aim, the following objectives were defined:

- Explore trends in the water use of different vegetation types located in various climates across South Africa to evaluate the potential of woody encroachment to increase ET losses in South Africa's savannas (Chapter 2).

- Determine the effect of woody encroachment on ET in a semi-arid savanna at the field scale using a simple and cost-effective in situ measurement method (Chapter 3).

- Investigate the influence of woody plant thinning on soil hydrological processes in a woody-encroached, semi-arid savanna (Chapter 4).

- Assess the relationship between woody cover and ET across various spatio-temporal scales in a woody-encroached, semi-arid savanna catchment by leveraging freely available and relatively user-friendly resources provided by Google Earth Engine (Chapter 5).

### 1.5 Outline of the thesis structure

This thesis consists of six chapters. The first chapter provides an overall introduction to the thesis, while chapters two to five are a series of individual research papers presenting the findings of the research. The last chapter provides a synthesis of the thesis. Each research paper contains a literature review, materials and methods, results, discussion, and conclusion. They have been published, are in press, submitted, or are intended for submission, following the approach that has been accepted by the University of KwaZulu-Natal. As recommended by the University of KwaZulu-Natal's thesis guidelines, the references for each of the research papers conform to the referencing style of the journal in which the paper was published, to which it has been submitted or will be submitted.

Figure 1.4 depicts a "road map" of the structure of the thesis, outlining the overall aim of the thesis, as well as the objectives and approach employed in each chapter to achieve that aim.

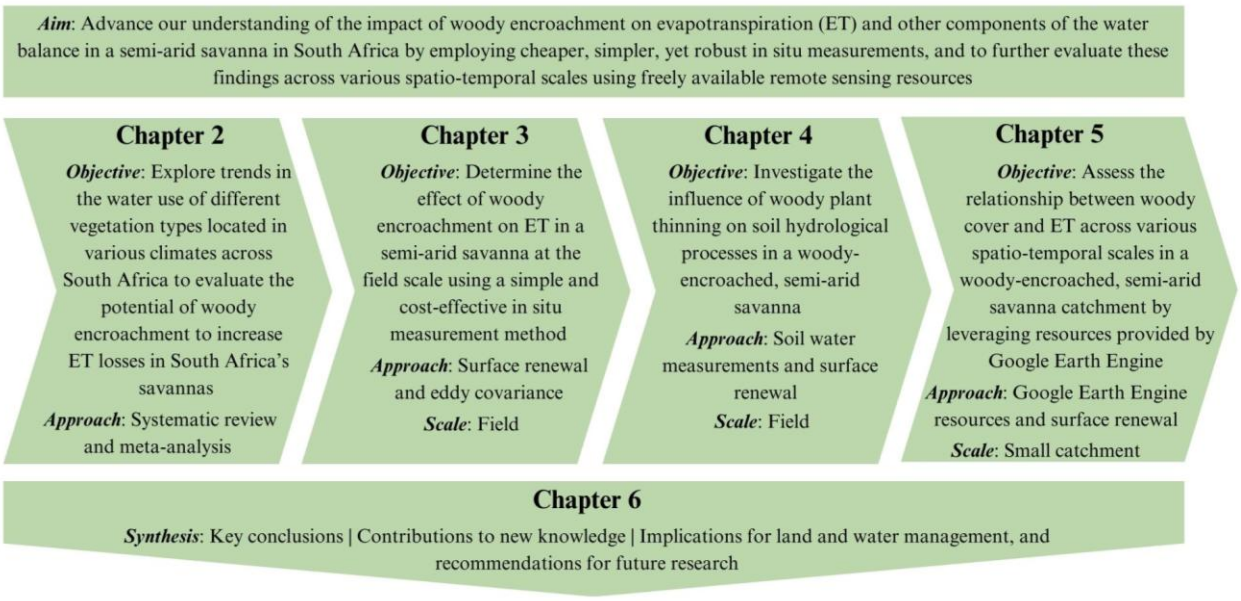


**Figure 1.4 A "road map" showing the structure of the thesis.**

Chapter 2 undertook systematic review methods to provide an overview of the vegetation water use measurements conducted in South Africa to date. A meta-analysis was then conducted to identify the common trends in vegetation water use and highlight how they vary with climate and vegetation type. Using this knowledge of vegetation water use trends, the potential of woody encroachment to increase ET losses in South Africa's savannas was discussed.

Chapter 3 assessed the validity of two surface renewal approaches, surface renewal 1 (SR1) and surface renewal dissipation theory (SRDT), for estimating ET in semi-arid savanna vegetation against eddy covariance, and thereafter the surface renewal approach which best agreed with eddy covariance was used in a paired-plot experiment to determine the effect of woody encroachment on ET in a semi-arid savanna.

Chapter 4 evaluated the influence of woody plant thinning on soil hydrological processes in a woody-encroached, semi-arid savanna ecosystem using a paired-plot experiment and field measurements of soil water content, soil temperature, ET and infiltration.

Chapter 5 leveraged resources provided by Google Earth Engine to assess the relationship between woody cover and ET across various spatio-temporal scales in a woody-encroached, semi-arid savanna catchment.

Chapter 6, the final synthesis chapter, revisited the aims and objectives, and discussed key conclusions from the study, new knowledge contributions, research limitations and challenges and recommendations for future research.

Each chapter begins with a repetition of Figure 1.4, with the relevant parts of the figure in the chapter that follows highlighted, placing each chapter in the context of the overall thesis.

## 1.6 References


Acharya, B.S., Hao, Y., Ochsner, T.E. and Zou, C.B., 2017. Woody plant encroachment alters soil hydrological properties and reduces downward flux of water in tallgrass prairie. *Plant and Soil*, *414*, 379-391.

Acharya, B.S., Kharel, G., Zou, C.B., Wilcox, B.P. and Halihan, T., 2018. Woody plant encroachment impacts on groundwater recharge: A review. *Water*, *10*(10), 1466.

Aldworth, T.A., Toucher, M.L. and Clulow, A.D., 2023. The Potential Impact of Woody Encroachment on Evapotranspiration Losses in South Africa's Savannas: A combined Systematic Review and meta-Analysis Approach. *Ecohydrology & Hydrobiology*, 24, 25-35.

Alemayehu, T., Van Griensven, A., Senay, G.B. and Bauwens, W., 2017. Evapotranspiration mapping in a heterogeneous landscape using remote sensing and global weather datasets: Application to the Mara Basin, East Africa. *Remote Sensing*, *9*(4), 390.

Allen, R.G., Pereira, L.S., Raes, D. and Smith, M., 1998. Crop evapotranspiration-Guidelines for computing crop water requirements-FAO Irrigation and drainage paper 56. *Fao, Rome*, *300*(9), D05109.

Amani, M., Ghorbanian, A., Ahmadi, S.A., Kakooei, M., Moghimi, A., Mirmazloumi, S.M., Moghaddam, S.H.A., Mahdavi, S., Ghahremanloo, M., Parsian, S. and Wu, Q., 2020. Google earth engine cloud computing platform for remote sensing big data applications: A comprehensive review. *IEEE Journal of Selected Topics in Applied Earth Observations and Remote Sensing*, *13*, 5326-5350.

Andreu, A., Dube, T., Nieto, H., Mudau, A.E., González-Dugo, M.P., Guzinski, R. and Hülsmann, S., 2019. Remote sensing of water use and water stress in the African savanna ecosystem at local scale–Development and validation of a monitoring tool. *Physics and Chemistry of the Earth, Parts A/B/C*, *112*, 154-164.

Archer, S.R., Andersen, E.M., Predick, K.I., Schwinning, S., Steidl, R.J. and Woods, S.R., 2017. Woody plant encroachment: causes and consequences. *Rangeland systems: Processes, management and challenges*, 25-84.

Awada, H., Di Prima, S., Sirca, C., Giadrossich, F., Marras, S., Spano, D. and Pirastru, M., 2021. Daily actual evapotranspiration estimation in a mediterranean ecosystem from landsat observations using SEBAL approach. *Forests*, *12*(2), 189.

Baiyegunhi, L.J.S. and Oppong, B.B., 2016. Commercialisation of Mopane worm (Imbrasia belina) in rural households in Limpopo Province, South Africa. *Forest Policy and Economics*, *62*, 141-148.

Baudoin, M.A., Vogel, C., Nortje, K. and Naik, M., 2017. Living with drought in South Africa: lessons learnt from the recent El Niño drought period. *International Journal of Disaster Risk Reduction*, *23*, 128-137.

Bazan, R.A., Wilcox, B.P., Munster, C. and Gary, M., 2012. Removing woody vegetation has little effect on conduit flow recharge. *Ecohydrology*, *6*(3), 435-443.

Bchir, A., M'nassri, S., Dhib, S., Amri, A.E. and Mulla, D., 2021. Estimating and mapping evapotranspiration in olive groves of semi-arid Tunisia using empirical formulas and satellite remote sensing. *Arabian Journal of Geosciences*, *14*(24), 2717.

Blin, N. and Suárez, F., 2023. Evaluating the contribution of satellite-derived evapotranspiration in the calibration of numerical groundwater models in remote zones using the EEFlux tool. *Science of the Total Environment*, *858*, 159764.

Bunting, E.L., Fullman, T., Kiker, G. and Southworth, J., 2016. Utilization of the SAVANNA model to analyze future patterns of vegetation cover in Kruger National Park under changing climate. *Ecological Modelling*, *342*, 147-160.

Calder, I.R. and Dye, P., 2001. Hydrological impacts of invasive alien plants. *Land use and water resources research*, *1*(1732-2016-140259).

Cardella Dammeyer, H., Schwinning, S., Schwartz, B.F. and Moore, G.W., 2016. Effects of juniper removal and rainfall variation on tree transpiration in a semi-arid karst: evidence of complex water storage dynamics. *Hydrological Processes*, *30*(24), 4568-4581.

Carrasco-Benavides, M., Ortega-Farías, S., Gil, P.M., Knopp, D., Morales-Salinas, L., Lagos, L.O., de la Fuente, D., López-Olivari, R. and Fuentes, S., 2022. Assessment of the vineyard water footprint by using ancillary data and EEFlux satellite images. Examples in the Chilean central zone. *Science of The Total Environment*, *811*, 152452.

Castellvi, F., Perez, P.J. and Ibanez, M., 2002. A method based on high-frequency temperature measurements to estimate the sensible heat flux avoiding the height dependence. *Water Resources Research*, *38*(6), 20-1.

Castellví, F., 2004. Combining surface renewal analysis and similarity theory: A new approach for estimating sensible heat flux. *Water Resources Research*, *40*(5).

Castellví, F. and Snyder, R.L., 2009a. On the performance of surface renewal analysis to estimate sensible heat flux over two growing rice fields under the influence of regional advection. *Journal of Hydrology*, *375*(3-4), 546-553.

Castellvi, F. and Snyder, R.L., 2009b. Combining the dissipation method and surface renewal analysis to estimate scalar fluxes from the time traces over rangeland grass near Ione (California). *Hydrological Processes: An International Journal*, *23*(6), 842-857.

Clulow, A.D., Everson, C.S., Mengistu, M.G., Jarmain, C., Jewitt, G.P.W., Price, J.S. and Grundling, P.L., 2012. Measurement and modelling of evaporation from a coastal wetland in Maputaland, South Africa. *Hydrology and Earth System Sciences*, *16*(9), 3233-3247.

de Oliveira Costa, J., José, J.V., Wolff, W., de Oliveira, N.P.R., Oliveira, R.C., Ribeiro, N.L., Coelho, R.D., da Silva, T.J.A., Bonfim-Silva, E.M. and Schlichting, A.F., 2020. Spatial variability quantification of maize water consumption based on Google EEflux tool. *Agricultural Water Management*, *232*, 106037.

Dye, P., Naiken, V., Clulow, A., Prinsloo, E., Crichton, M., & Weiersbye, I., 2017. Sap flow in *Searsia pendulina* and *Searsia lancea* trees established on gold mining sites in central South Africa. *South African Journal of Botany*, *109*, 81-89.

Ferreira, D., Marais, J.P. and Slade, D., 2003. Phytochemistry of the Mopane, *Colophospermum mopane*. *Phytochemistry*, *64*(1), 31-51.

Ferreira, S. and Harmse, A., 2014. Kruger National Park: Tourism development and issues around the management of large numbers of tourists. *Journal of Ecotourism*, *13*(1), 16-34.

Ford, P.L., 2010. *Grasslands and Savannas*. Singapore: EOLSS Publisher.

Gizaw, M.S. and Gan, T.Y., 2017. Impact of climate change and El Niño episodes on droughts in sub-Saharan Africa. *Climate Dynamics*, *49*, 665-682.

Gray, B.A., Toucher, M.L., Savage, M.J. and Clulow, A.D., 2021. The potential of surface renewal for determining sensible heat flux for indigenous vegetation for a first-order montane catchment. *Hydrological Sciences Journal*, *66*(6), 1015-1027.

Haymann, N., Lukyanov, V. and Tanny, J., 2019. Effects of variable fetch and footprint on surface renewal measurements of sensible and latent heat fluxes in cotton. *Agricultural and Forest Meteorology*, *268*, 63-73.

Hoetzel, S., Dupont, L., Schefuß, E., Rommerskirchen, F. and Wefer, G., 2013. The role of fire in Miocene to Pliocene C4 grassland and ecosystem evolution. *Nature Geoscience*, *6*(12), 1027-1030.

Hoffman, M.T., Rohde, R.F. and Gillson, L., 2019. Rethinking catastrophe? Historical trajectories and modelled future vegetation change in southern Africa. *Anthropocene*, *25*, 100189.

Honda, E.A. and Durigan, G., 2016. Woody encroachment and its consequences on hydrological processes in the savannah. *Philosophical Transactions of the Royal Society B: Biological Sciences*, *371*(1703), 20150313.

Hu, Y., Buttar, N.A., Tanny, J., Snyder, R.L., Savage, M.J. and Lakhiar, I.A., 2018. Surface renewal application for estimating evapotranspiration: A review. *Advances in Meteorology*, 2018(1), 1690714.

Huxman, T.E., Wilcox, B.P., Breshears, D.D., Scott, R.L., Snyder, K.A., Small, E.E., Hultine, K., Pockman, W.T. and Jackson, R.B., 2005. Ecohydrological implications of woody plant encroachment. *Ecology*, *86*(2), 308-319.

iNaturalist. Available from https://www.inaturalist.org. Accessed 08 December 2024.

Jordaan, J.J., Wessels, D.C.J., Dannhauser, C.S. and Rootman, G.T., 2004. Secondary succession in the Mopani veld of the Limpopo Valley, South Africa. *African Journal of Range and Forage Science*, *21*(3), 205-210.

Kadam, S.A., Stöckle, C.O., Liu, M., Gao, Z. and Russell, E.S., 2021. Suitability of Earth Engine Evaporation Flux (EEFlux) estimation of evapotranspiration in rainfed crops. *Remote Sensing*, *13*(19), 3884.

Kambatuku, J.R., Cramer, M.D. and Ward, D., 2013. Overlap in soil water sources of savanna woody seedlings and grasses. *Ecohydrology*, *6*(3), 464-473. https://doi.org/10.1002/eco.1273.

Kanjere, M., Thaba, K. and Lekoana, M., 2014. Water Shortage Management at Letaba Water Catchment Area in Limpopo Province, of South Africa. *Mediterr. J. Soc. Sci*, *5*, 1356.

Keen, R.M., Sadayappan, K., Jarecke, K.M., Li, L., Kirk, M.F., Sullivan, P.L. and Nippert, J.B., 2024. Unexpected hydrologic response to ecosystem state change in tallgrass prairie. *Journal of Hydrology*, *643*, 131937.

Khosa, F.V., Feig, G.T., Van der Merwe, M.R., Mateyisi, M.J., Mudau, A.E. and Savage, M.J., 2019. Evaluation of modeled actual evapotranspiration estimates from a land surface, empirical and satellite-based models using in situ observations from a South African semi-arid savanna ecosystem. *Agricultural and Forest Meteorology*, *279*, 107706.

Kruger, A.C. and Shongwe, S., 2004. Temperature trends in South Africa: 1960-2003. *International journal of Climatology*, *24*(15), 1929-1945.

Kruger, A.C. and Sekele, S.S., 2013. Trends in extreme temperature indices in South Africa: 1962-2009. *International Journal of Climatology*, *33*(3).

Laipelt, L., Kayser, R.H.B., Fleischmann, A.S., Ruhoff, A., Bastiaanssen, W., Erickson, T.A. and Melton, F., 2021. Long-term monitoring of evapotranspiration using the SEBAL algorithm and Google Earth Engine cloud computing. *ISPRS Journal of Photogrammetry and Remote Sensing*, *178*, 81-96.

Leite, P.A., Wilcox, B.P. and McInnes, K.J., 2020. Woody plant encroachment enhances soil infiltrability of a semiarid karst savanna. *Environmental Research Communications*, *2*(11), 115005.

Le Maitre, D.C., Blignaut, J.N., Clulow, A., Dzikiti, S., Everson, C.S., Görgens, A.H. and Gush, M.B., 2020. Impacts of plant invasions on terrestrial water flows in South Africa. In *Biological Invasions in South Africa* (pp. 431-457). Cham: Springer International Publishing.

Liu, X., Feng, S., Liu, H. and Ji, J., 2021. Patterns and determinants of woody encroachment in the eastern Eurasian steppe. *Land Degradation & Development*, *32*(13), 3536-3549.

Macgregor, S.D. and O'Connor, T.G., 2002. Patch dieback of *Colophospermum mopane* in a dysfunctional semi-arid African savanna. *Austral Ecology*, *27*(4), 385-395.

Makhado, R.A., Potgieter, M.J. and Luus-Powell, W.J., 2018. *Colophospermum mopane* Leaf Production and Phenology in Southern Africa's Savanna Ecosystem-A Review. *Insights of Forest Research*, *2*(1), 84-90.

Malherbe, J., Smit, I.P., Wessels, K.J. and Beukes, P.J., 2020. Recent droughts in the Kruger National Park as reflected in the extreme climate index. *African Journal of Range & Forage Science*, *37*(1), 1-17.

Mapaure, I., 1994. The distribution of *Colophospermum mopane* (Leguminosae-caesalpinioideae) in Africa. *Kirkia*, 1-5.

Mashabane, L.G., Wessels, D.C.J. and Potgieter, M.J., 2001. The utilisation of *Colophospermum mopane* by the Vatsonga in the Gazankulu region (eastern Northern Province, South Africa). *South African Journal of Botany*, *67*(2), 199-205.

Mengistu, M.G. and Savage, M.J., 2010. Surface renewal method for estimating sensible heat flux. *Water SA*, *36*(1).

Mucina, L. and Rutherford, M.C., 2006. The vegetation of South Africa, Lesotho and Swaziland. Strelitzia 19.,(South African National Biodiversity Institute: Pretoria, South Africa). *Memoirs of the Botanical Survey of South Africa*.

Nisa, Z., Khan, M.S., Govind, A., Marchetti, M., Lasserre, B., Magliulo, E. and Manco, A., 2021. Evaluation of SEBS, METRIC-EEFlux, and QWaterModel actual evapotranspiration for a Mediterranean cropping system in southern Italy. *Agronomy*, *11*(2), 345.

Ochoa, C.G., Caruso, P., Ray, G., Deboodt, T., Jarvis, W.T. and Guldan, S.J., 2018. Ecohydrologic connections in semiarid watershed systems of central Oregon USA. *Water*, *10*(2), 181.

O'Connor, T.G., 2015. Long-term response of an herbaceous sward to reduced grazing pressure and rainfall variability in a semi-arid South African savanna. *African Journal of Range & Forage Science*, *32*(4), 261-270.

Olariu, H.G., Malambo, L., Popescu, S.C., Virgil, C. and Wilcox, B.P., 2022. Woody plant encroachment: Evaluating methodologies for semiarid woody species classification from drone images. *Remote Sensing*, *14*(7), 1665.

Oliveira, P.T.S., Leite, M.B., Mattos, T., Nearing, M.A., Scott, R.L., de Oliveira Xavier, R., da Silva Matos, D.M. and Wendland, E., 2016. Groundwater recharge decrease with increased vegetation density in the Brazilian cerrado. *Ecohydrology*, *10*(1), 1759.

Otieno, F.A. and Ochieng, G.M., 2004. Water management tools as a means of averting a possible water scarcity in South Africa by the year 2025. *Water SA*, *30*(5), 120-124.

Poblete-Echeverría, C., Sepúlveda-Reyes, D. and Ortega-Farías, S., 2014. Effect of height and time lag on the estimation of sensible heat flux over a drip-irrigated vineyard using the surface renewal (SR) method across distinct phenological stages. *Agricultural Water Management*, *141*, 74-83.

Poilecot, P. and Gaidet, N., 2011. A quantitative study of the grass and woody layers of a Mopane (*Colophospermum mopane*) savannah in the mid-Zambezi Valley, Zimbabwe. *African Journal of Ecology*, *49*(2), 150-164.

Pollard, S. and Du Toit, D., 2011. Towards adaptive integrated water resources management in southern Africa: The role of self-organisation and multi-scale feedbacks for learning and responsiveness in the Letaba and Crocodile catchments. *Water Resources Management*, *25*(15), 4019-4035.

Poudel, U., Stephen, H. and Ahmad, S., 2021. Evaluating irrigation performance and water productivity using EEFlux ET and NDVI. *Sustainability*, *13*(14), 7967.

Pozníková, G., Fischer, M., van Kesteren, B., Orság, M., Hlavinka, P., Žalud, Z. and Trnka, M., 2018. Quantifying turbulent energy fluxes and evapotranspiration in agricultural field conditions: A comparison of micrometeorological methods. *Agricultural Water Management*, *209*, 249-263.

Puttock, A., Macleod, C.J., Bol, R., Sessford, P., Dungait, J. and Brazier, R.E., 2013. Changes in ecosystem structure, function and hydrological connectivity control water, soil and carbon losses in semi-arid grass to woody vegetation transitions. *Earth Surface Processes and Landforms*, *38*(13), 1602-1611.

Qiao, L., Zou, C.B., Will, R.E. and Stebler, E., 2015. Calibration of SWAT model for woody plant encroachment using paired experimental watershed data. *Journal of Hydrology*, *523*, 231-239.

Rojas Villalobos, H.L., 2022. Comparison of evaporation estimates from the REEM and EEFlux models in a shallow water body. Case: Bustillos Lake, Chihuahua, Mexico. *Instituto de Arquitectura Diseño y Arte*.

Rosa, R., Dicken, U. and Tanny, J., 2013. Estimating evapotranspiration from processing tomato using the surface renewal technique. *Biosystems Engineering*, *114*(4), 406-413.

Rosa, R. and Tanny, J., 2015. Surface renewal and eddy covariance measurements of sensible and latent heat fluxes of cotton during two growing seasons. *Biosystems Engineering*, *136*, 149-161.

Sadayappan, K., Keen, R., Jarecke, K.M., Moreno, V., Nippert, J.B., Kirk, M.F., Sullivan, P.L. and Li, L., 2023. Drier streams despite a wetter climate in woody-encroached grasslands. *Journal of Hydrology*, *627*, 130388.

Schreiner-McGraw, A.P., Vivoni, E.R., Ajami, H., Sala, O.E., Throop, H.L. and Peters, D.P., 2020. Woody Plant encroachment has a larger impact than climate change on Dryland water budgets. *Scientific Reports*, *10*(1), 8112.

Sebego, R.J., 1999. The ecology and distribution limits of *Colophospermum mopane* in southern Africa. *Botswana Notes & Records*, *31*(1), 53-72.

Smit, G.N. and Rethman, N.F.G., 1998. Root biomass, depth distribution and relations with leaf biomass of *Colophospermum mopane*. *South African Journal of Botany*, *64*(1), 38-43.

Smit, G.N. and Rethman, N.F.G., 2000. The influence of tree thinning on the soil water in a semi-arid savanna of southern Africa. *Journal of Arid Environments*, *44*(1), 41-59.

Smit, G.N., 2004. An approach to tree thinning to structure southern African savannas for long-term restoration from bush encroachment. *Journal of Environmental Management*, *71*(2), 179-191.

Stafford, W., Birch, C., Etter, H., Blanchard, R., Mudavanhu, S., Angelstam, P., Blignaut, J., Ferreira, L. and Marais, C., 2017. The economics of landscape restoration: Benefits of controlling bush encroachment and invasive plant species in South Africa and Namibia. *Ecosystem Services*, *27*, 193-202.

Stevens, N., Swemmer, A.M., Ezzy, L. and Erasmus, B.F., 2013. Investigating potential determinants of the distribution limits of a savanna woody plant: *Colophospermum mopane*. *Journal of Vegetation Science*, *25*(2), 363-373.

Stevens, N., Erasmus, B.F.N., Archibald, S. and Bond, W.J., 2016. Woody encroachment over 70 years in South African savannahs: overgrazing, global change or extinction aftershock? *Philosophical Transactions of the Royal Society B: Biological Sciences*, *371*(1703), 20150437.

Stevens, N., Lehmann, C.E., Murphy, B.P. and Durigan, G., 2017. Savanna woody encroachment is widespread across three continents. *Global Change Biology*, *23*(1), 235-244. https://doi.org/10.1111/gcb.13409.

Strömberg, C.A., 2011. Evolution of grasses and grassland ecosystems. *Annual review of Earth and Planetary Sciences*, *39*, 517-544.

Suvočarev, K., Shapland, T.M., Snyder, R.L. and Martínez-Cob, A., 2014. Surface renewal performance to independently estimate sensible and latent heat fluxes in heterogeneous crop surfaces. *Journal of Hydrology*, *509*, 83-93.

Tsalyuk, M., Kelly, M. and Getz, W.M., 2017. Improving the prediction of African savanna vegetation variables using time series of MODIS products. *ISPRS Journal of Photogrammetry and Remote Sensing*, *131*, 77-91.

Van Wilgen, B.W., Le Maitre, D.C. and Cowling, R.M., 1998. Ecosystem services, efficiency, sustainability and equity: South Africa's Working for Water programme. *Trends in Ecology & Evolution*, *13*(9), 378.

Venter, Z.S., Cramer, M.D. and Hawkins, H.J., 2018. Drivers of woody plant encroachment over Africa. *Nature Communications*, *9*(1), 2272. https://doi.org/10.1038/s41467-018-04616-8.

Wang, J., Xiao, X., Zhang, Y., Qin, Y., Doughty, R.B., Wu, X., Bajgain, R. and Du, L., 2018. Enhanced gross primary production and evapotranspiration in juniper-encroached grasslands. *Global Change Biology*, *24*(12), 5655-5667.

Weerasinghe, I., Bastiaanssen, W., Mul, M., Jia, L. and Van Griensven, A., 2020. Can we trust remote sensing evapotranspiration products over Africa? *Hydrology and Earth System Sciences*, *24*(3), 1565-1586.

Wessels, K.J., Mathieu, R., Erasmus, B.F.N., Asner, G.P., Smit, I.P.J., Van Aardt, J.A.N., Main, R., Fisher, J., Marais, W., Kennedy-Bowdoin, T. and Knapp, D.E., 2011. Impact of communal land use and conservation on woody vegetation structure in the Lowveld savannas of South Africa. *Forest Ecology and Management*, *261*(1), 19-29.

Whitecross, M.A., Archibald, S. and Witkowski, E.T.F., 2012. Do freeze events create a demographic bottleneck for *Colophospermum mopane*? *South African Journal of Botany*, *83*, 9-18.

Whitecross, M.A., Witkowski, E.T.F. and Archibald, S., 2016. No two are the same: Assessing variability in broad-leaved savanna tree phenology, with watering, from 2012 to 2014 at Nylsvley, South Africa. *South African Journal of Botany*, *105*, 123-132.

Wilcox, B.P., Owens, M.K., Knight, R.W. and Lyons, R.K., 2005. Do woody plants affect streamflow on semiarid karst rangelands? *Ecological Applications*, *15*(1), 127-136.

Wilcox, B.P. and Huang, Y., 2010. Woody plant encroachment paradox: Rivers rebound as degraded grasslands convert to woodlands. *Geophysical Research Letters*, *37*(7).

Wilcox, B.P., Basant, S., Olariu, H. and Leite, P.A., 2022. Ecohydrological connectivity: A unifying framework for understanding how woody plant encroachment alters the water cycle in drylands. *Frontiers in Environmental Science*, *10*, 934535.

Xu, C., Du, X., Fan, X., Giuliani, G., Hu, Z., Wang, W., Liu, J., Wang, T., Yan, Z., Zhu, J. and Jiang, T., 2022. Cloud-based storage and computing for remote sensing big data: a technical review. *International Journal of Digital Earth*, *15*(1), 1417-1445.

Zapata, N. and Martınez-Cob, A., 2002. Evaluation of the surface renewal method to estimate wheat evapotranspiration. *Agricultural Water Management*, *55*(2), 141-157.

Zou, C.B., Qiao, L. and Wilcox, B.P., 2015. Woodland expansion in central Oklahoma will significantly reduce streamflows–a modelling analysis. *Ecohydrology*, *9*(5), 807-816.

Zou, C.B., Twidwell, D., Bielski, C.H., Fogarty, D.T., Mittelstet, A.R., Starks, P.J., Will, R.E., Zhong, Y. and Acharya, B.S., 2018. Impact of eastern redcedar proliferation on water resources in the Great Plains USA—current state of knowledge. *Water*, *10*(12), 1768.

**Lead into Chapter 2**

It was first necessary to understand the current state of knowledge. Therefore, the objective of Chapter 2 was to explore trends in the water use of different vegetation types located in various climates across South Africa to evaluate the potential of woody encroachment to increase evapotranspiration (ET) losses in South Africa's savannas. First, an overview of the vegetation water use measurements conducted in South Africa to date was provided using systematic review methods. These measurements were then used in a meta-analysis to identify the common trends in vegetation water use and highlight how they vary with climate and vegetation type. This knowledge of vegetation water use trends was used to discuss the potential of woody encroachment to increase ET losses in South Africa's savannas.

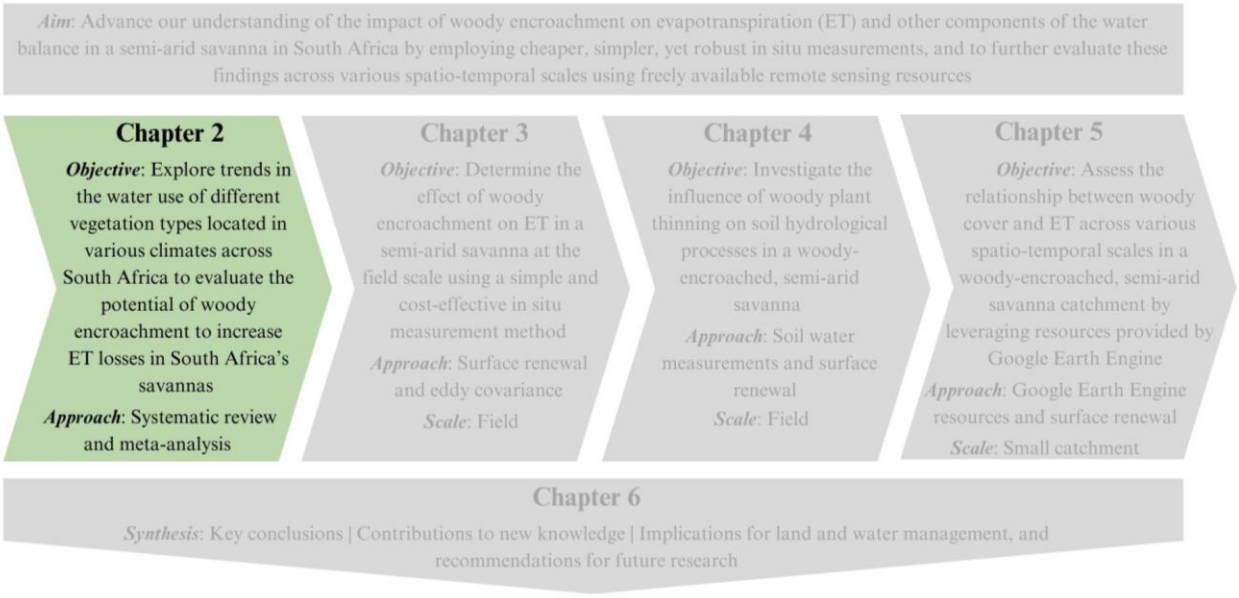

# 2 THE POTENTIAL IMPACT OF WOODY ENCROACHMENT ON EVAPOTRANSPIRATION LOSSES IN SOUTH AFRICA'S SAVANNAS: A COMBINED SYSTEMATIC REVIEW AND META-ANALYSIS APPROACH[1]

## 2.1 Abstract

Woody vegetation cover in South Africa has increased over the past 100-150 years owing to the establishment of commercial forestry plantations, the spread of invasive alien plants and indigenous woody encroachment. Extensive research conducted over the past 50 years has shown that invasive alien plants can lead to dramatic declines in catchment water yields as a result of their high evapotranspiration (ET) rates. This has raised concern that woody encroachment may also be responsible for increasing ET losses and adversely impacting the country's limited water resources. In this paper, we used a combined systematic review and meta-analysis approach to explore trends in the water use of different vegetation types located in various climates across South Africa, to ultimately evaluate the likelihood of woody encroachment increasing ET losses in South Africa's savannas. This study revealed mixed support for whether woody encroachment in South Africa's savannas is increasing ET losses. On one hand, the fact that woody encroachment species replace grasses and form dense thickets indicates that there is high potential for woody encroachment to increase ET losses. On the other hand, rainfall, appears to be a primary factor limiting ET in semi-arid climates, indicating little potential for woody encroachment to have any effect on ET, unless there is an above-average rainfall year, or the vegetation has access to an additional water source. This study justifies the need for additional ET monitoring in South Africa's savannas in order to determine whether large-scale woody encroachment control should be implemented to conserve water resources in one of the country's driest regions.

***Keywords****: Indigenous vegetation, invasive alien plants, commercial afforestation, vegetation water use, woody encroachment control*

## 2.2 Introduction

The loss of trees through deforestation has been well-documented across the globe, but in South Africa there has been a shift toward greater woody vegetation cover over the past 100-150 years (Nel *et al.* 2004, van Wilgen and Richardson 2012, Dye 2013). This is largely attributed to the establishment of commercial forestry plantations and the uncontrolled spread of invasive alien



[1]Aldworth, T.A., Toucher, M.L. and Clulow, A.D., 2024. The Potential Impact of Woody Encroachment on Evapotranspiration Losses in South Africa's Savannas: A combined Systematic Review and meta-Analysis Approach. *Ecohydrology & Hydrobiology*, *24*(1), 25-35. https://doi.org/10.1016/j.ecohyd.2023.08.016.

plants, which have been introduced into the country either deliberately or accidentally via human activities (Le Maitre *et al*. 2020). The most recent national survey estimated that approximately 10 million hectares of South Africa and Lesotho have been invaded by invasive alien plants to some degree (Le Maitre *et al*. 2000), but this area is expected to be much larger today. Given that invasive alien plants are known to be excessive water users (Calder and Dye 2001), and that South Africa is a water-scarce country with a mean annual precipitation (MAP) of only about 500 mm (Le Maitre *et al*. 2020), a substantial proportion of the country's hydrological research conducted over the past 50 or so years has focused on the impact of invasive alien plants on water resources. This research has shown that invasive alien plants, especially the introduction of tall trees, can lead to dramatic declines in streamflow and groundwater recharge in catchment areas as a result of their higher evapotranspiration (ET) rates relative to the native vegetation they replace (Dzikiti *et al*. 2016, Mkunyane *et al*. 2018).

The research on invasive alien plants has raised concern that another widespread phenomenon in South Africa, commonly termed woody encroachment, may also be responsible for increasing ET losses and adversely impacting water resources (Dzikiti *et al*. 2017). Woody encroachment is the gradual proliferation of indigenous trees or shrubs, which either increase in density within their natural geographic range or expand outside of this range (Hoffman 2014). Reports of woody encroachment have been made for grass-dominated vegetation types in many regions of the world, including southern Africa (O'Connor *et al*. 2014), southwestern United States (Weber-Grullon *et al*. 2021), central Brazil (Rosan *et al*. 2019), northern China (Peng *et al*. 2013) and eastern Australia (Eldridge and Soliveres 2014). Long-established drivers have centered around anthropogenic changes to herbivory numbers and fire regimes, but more recent research suggests that global climate change effects on temperature, rainfall and atmospheric $CO_2$ may be the primary drivers, or further promote woody encroachment (O'Connor *et al*. 2014, Stevens *et al*. 2016, Archer *et al*. 2017). In South Africa, woody encroachment has been most prevalent in the grassland and savanna biomes, but it has been of most hydrological concern in the country's savannas as they mostly have semi-arid climates (Whitecross *et al.* 2016). Semi-arid climates have low annual rainfall totals (< 700 mm), and annual potential ET is many times greater than precipitation, therefore, water resources in South Africa's savannas are generally limited (Kambatuku *et al.* 2012). Furthermore, climate change projections indicate that the savanna

regions of South Africa are going to get hotter and drier by 2080, which will put these water resources under further strain (Bunting *et al*. 2016).

To our knowledge, no studies investigating the effect of woody encroachment on ET in southern African savannas have provided any conclusive findings. However, there have been a significant number of studies conducted in the western United States, the majority of which have reported that ET increased with increasing indigenous woody vegetation cover (Acharya *et al*. 2018). For example, in Arizona, Scott *et al*. (2014) measured ET over a riparian grassland, shrubland and woodland (representing a woody encroachment gradient of *Prosopis velutina*) over a five-year period. A higher mean annual ET of 692 mm was measured for the woodland, compared to the shrubland and grassland sites, which measured 564 mm and 548 mm, respectively. In a remote sensing study of all grasslands in the state of Oklahoma, Wang *et al*. (2018) found that the mean annual ET was 45% higher when grasslands completely transitioned to *Juniperus* spp. woodland. In another study in Oklahoma, Qiao *et al.* (2015) found that the annual ET for a *Juniperus virginiana* woodland was on average 100 mm greater than for a grassland. Near the Idaho-Oregon border, Kormos *et al.* (2016) estimated ET over a *Juniperus occidentalis* woodland and a shrubland for six years and found that the woodland had a higher mean annual ET of 531 mm, compared with 348 mm for the shrubland. In Texas, Dugas *et al*. (1998) and Afinowicz *et al*. (2005) estimated ET in a catchment before and after the removal of *Juniperus ashei* and found that the *Juniperus ashei* catchments had a higher mean annual ET than the treated catchments. At the study site of Afinowicz *et al*. (2005), the *Juniperus ashei* catchment only had a 31.9 mm higher mean annual ET, whereas the *Juniperus ashei* catchment of the Dugas *et al*. (1998) study had a 110 mm higher mean annual ET than the treated catchments. However, this significant increase for the Dugas *et al*. (1998) study was only observed for the first two years following removal of *Juniperus ashei*, after which it decreased.

The question of whether woody encroachment in South Africa's savannas also increases ET is debatable, largely due to their semi-arid climates. In mesic climates, increases in woody vegetation cover are believed to increase ET because high rainfall allows the potential for high transpiration and interception rates, and in arid climates, increases in woody vegetation cover are believed to have minimal effect on ET because most, if not all, precipitation is used for ET irrespective of the type of vegetation. However, there is still much uncertainty surrounding whether increases in

woody vegetation cover effect ET in semi-arid climates (Huxman *et al.* 2005, Schreier-McGraw *et al.* 2020). A recent study by Wilcox *et al.* (2022) studied six case studies carried out across a subhumid to arid climatic gradient in the Great Plains and Chihuahuan Desert regions of the United States. Their findings supported those of Huxman *et al.* (2005) and Schreier-McGraw *et al.* (2020), as they discovered that woody encroachment resulted in a significant increase in ET in the subhumid or mesic case studies, but had minimal influence on ET in the arid case studies. However, in one of their semi-arid case studies in a south Texas shrubland (MAP of 660 mm), woody encroachment resulted in a small increase in ET. Most of the invasive alien plant studies in South Africa and woody encroachment studies in the United States, which found an increase in ET with increasing woody vegetation cover, have been conducted at sites with more mesic climates (MAP > 700 mm). Several studies did have sites with semi-arid climates, however, they were located in riparian zones where the vegetation likely had access to additional water sources besides rainfall, including river water or shallow groundwater (Scott *et al*. 2014, Dzikiti *et al*. 2016, Kormos *et al.* 2016).

Vegetation characteristics of the common woody encroacher species have also caused some debate as to whether woody encroachment has an effect on ET. Woody encroacher species tend to grow in mono-specific stands forming dense thickets, which should permit high transpiration rates and evaporation from canopy interception given these high densities (Kennedy and Potgieter 2003). A recent interception study carried out in a heavily encroached South African savanna reported that *Dichrostachys cinereal* canopies intercepted approximately 44% of rainfall (Skhosana *et al*. 2023). Woody encroacher species also tend to have shallow root systems that occupy the same soil niche as grass roots enabling them to actively compete for available soil water with grasses (Smit and Rethman 1998). In addition, the roots of many woody encroacher species have been observed to extend horizontally enabling them to take up water from a larger surface area (Smit 2004). For example, the roots of the *Colophospermum mopane* (Mopane) tree, have been observed to extend horizontally to a distance of approximately 7.6 times their height and 12.5 times the extent of their canopies (Smit 2004). Woody species also have lower albedo and greater air turbulence in the canopy boundary layer compared to grasses, thus potential ET should be higher in woody-encroached sites than in grasslands (Archer *et al*. 2017). However, woody encroacher species are argued to be conservative water users owing to the fact that they are indigenous (Dye *et al.* 2008). Indigenous species are generally slow-growing indicating low water

use (Dye *et al.* 2008, Scott-Shaw and Everson 2019), and they are mostly deciduous or semi-deciduous, therefore, they lose their leaves during the dry season, inhibiting year-round transpiration (Tomlinson *et al*. 2013). Furthermore, in dry environments, indigenous species have been found to have physiological adaptations which allow them to survive with little, if not any water (de Blécourt *et al.* 2021). One of the most significant physiological adaptations observed for *Senegalia mellifera* and Mopane is stomatal conductance, where species close the stomata of their leaves in order to limit transpiration when soil water availability is low (Makhado *et al.* 2014, de Blécourt *et al.* 2021).

In this paper, we explore trends in the water use of different vegetation types located in various climates across South Africa to evaluate the likelihood that woody encroachment is increasing ET losses in South Africa's savannas and therefore potentially threatening water resources. We had two specific objectives. First, we used systematic review methods to provide an overview of the vegetation water use measurements that have been conducted in South Africa to date. Second, we performed a meta-analysis using these measurements to identify the common trends in vegetation water use and highlight how they vary with climate and vegetation type. Using this knowledge of vegetation water use trends, we discussed the potential of woody encroachment to increase ET losses in South Africa's savannas. These findings would benchmark the value of additional ET measurements, which can be used by studies to determine the impact of woody encroachment on water resources in South Africa's savannas. This knowledge will contribute towards a more sustainable management of water resources in one of South Africa's driest regions.

## 2.3 Methods

### *2.3.1 Literature search*

To retrieve studies relating to the measurement of vegetation water use in South Africa, a systematic search of the Google Scholar, ScienceDirect and Wiley databases was undertaken. The keywords 'vegetation water use', 'evapotranspiration', 'total evaporation' and 'transpiration' were searched in combination with 'South Africa'. After screening the titles and abstracts of studies resulting from the database searches, relevant studies were selected. The selected studies were limited to peer-reviewed journal papers and grey literature (e.g. reports, conference proceedings),

excluding unpublished academic theses and crop water use studies. The search yielded a total of 50 studies published between 1993 and 2022.

### *2.3.2 Database compilation and data extraction*

The full texts of the 50 selected studies were searched for measurements of vegetation water use. Measurements included ET and/or transpiration measurements conducted using in situ, modelling or remote sensing methods, or a combination of methods. Measurements were first filtered for duplicate measurements where studies used the same datasets. Many studies provided water use measurements for more than one vegetation type or measurement site, in which case each vegetation type or measurement site was counted as a separate measurement. If more than one measurement was made at the same site by different studies or using different methods, this was counted as one measurement. If a study measured both ET and transpiration at the same study site, this was also counted as one measurement. In total, 59 measurements of vegetation water use were identified.

The measurements were grouped according to their respective vegetation types (i.e., invasive alien plant, grassland, savanna, etc.) and key information associated with each measurement was collected from the studies to compile a database. This information included the source, location where the measurement took place, dominant vegetation or species at the site, methods used for estimating ET or transpiration and the measurement period covered by the data. Characteristics of the measurement sites were also noted, including the MAP, climate zone and whether the site was located in a riparian or non-riparian zone. The measurements were categorized into different climate zones according to their MAP; sites receiving less than 250 mm were classified as being arid, sites receiving between 250 mm and 700 mm as semi-arid and sites receiving more than 700 mm as mesic.

For the meta-analysis, measurements of annual ET or transpiration were graphed, to allow the general trends in vegetation water use to be identified. These measurements were extracted directly from given numeric values in the text. Transpiration measurements were only included if they were upscaled to the stand scale (i.e., no individual tree transpiration measurements were included) and given in units of mm, which allowed for comparison. In addition, the measurement period had to be at least one year in order to account for seasonal variation in water use. If measurements were

available for more than one year, an average annual value was captured. The meta-analysis also included the annual reference evapotranspiration ($ET_o$) and the annual rainfall for the year of measurement provided they were given in the study, to gain a better understanding of the influence of climate factors on vegetation water use.

### 2.4 Overview of vegetation water use measurements in South Africa

The distribution of the 59 measurements of vegetation water use across South Africa is shown in Figure 2.1 and key information related to each measurement is listed in a database in Table 2.1 of *Appendix A*. Measurements are unevenly distributed among the climate zones, with the largest proportion conducted in mesic climates (33), followed by semi-arid (21) and arid (5) climates (Figure 2.1). Indigenous vegetation types make up almost three-quarters of the total measurements (43), whereas considerably fewer measurements have been conducted for alien vegetation types (16). Regarding the more specific vegetation type, the majority of measurements are for invasive alien plants and grasslands (12 each). The invasive alien plant measurements are mostly in mesic catchments located in the Western Cape Province and invaded by one or more tree species of the Acacia, Pinus, Eucalyptus or Prosopis genera. The grassland measurements are mostly for mesic, natural grasslands located in the KwaZulu-Natal and the Eastern Cape provinces. A total of seven water use measurements have been conducted for commercial forestry plantations; four of which have been made for alien plantations, and three for indigenous plantations. Fynbos and indigenous forest are also well represented with six measurements each. The indigenous forest measurements have been made for a variety of different forest types, including a peat swamp, dune, evergreen, afrotemperate and mistbelt forest. Only four measurements have been made for savannas, all of which are in semi-arid climates in the Mpumalanga and Limpopo provinces. However, many different studies have used these same datasets, particularly the dataset for the Skukuza eddy covariance flux tower, where several studies used different periods of the dataset. Very few measurements have been made for woodland (3), shrubland (3) and thicket (2) vegetation types, and only one for each of wetlands, fern, renosterveld and bushveld. The majority of ET measurements were obtained in situ using micro-meteorological methods, such as eddy covariance, scintillometers, Bowen Ratio Energy Balance and surface renewal. Most transpiration measurements were obtained using the heat pulse velocity (HPV) technique, which measures xylem sap flow of individual trees (Burgess *et al*. 2001), however, the transpiration measurements included in these studies were upscaled to stand level transpiration. There were also several studies

that used remotely sensed ET data products and remote sensing models to estimate ET. Very few long-term in situ measurements have been conducted, the longest being the Skukuza and Malopeni eddy covariance flux towers located in the Mpumalanga and Limpopo provinces, which have been monitoring ET since 2000 and 2009, respectively, and are still operating today (Ramoelo *et al.* 2014). More than half of the in situ measurements were conducted over only one year or less, many of these being short measurement campaigns of up to a few days or weeks. Therefore, in many cases, hydrological models were used to extend in situ data records. The longest simulation was conducted by Dye *et al*. (2008), who used scintillometer data and a Penman-Monteith model to simulate ET for 21 years in an evergreen indigenous mixed forest in the Western Cape Province.

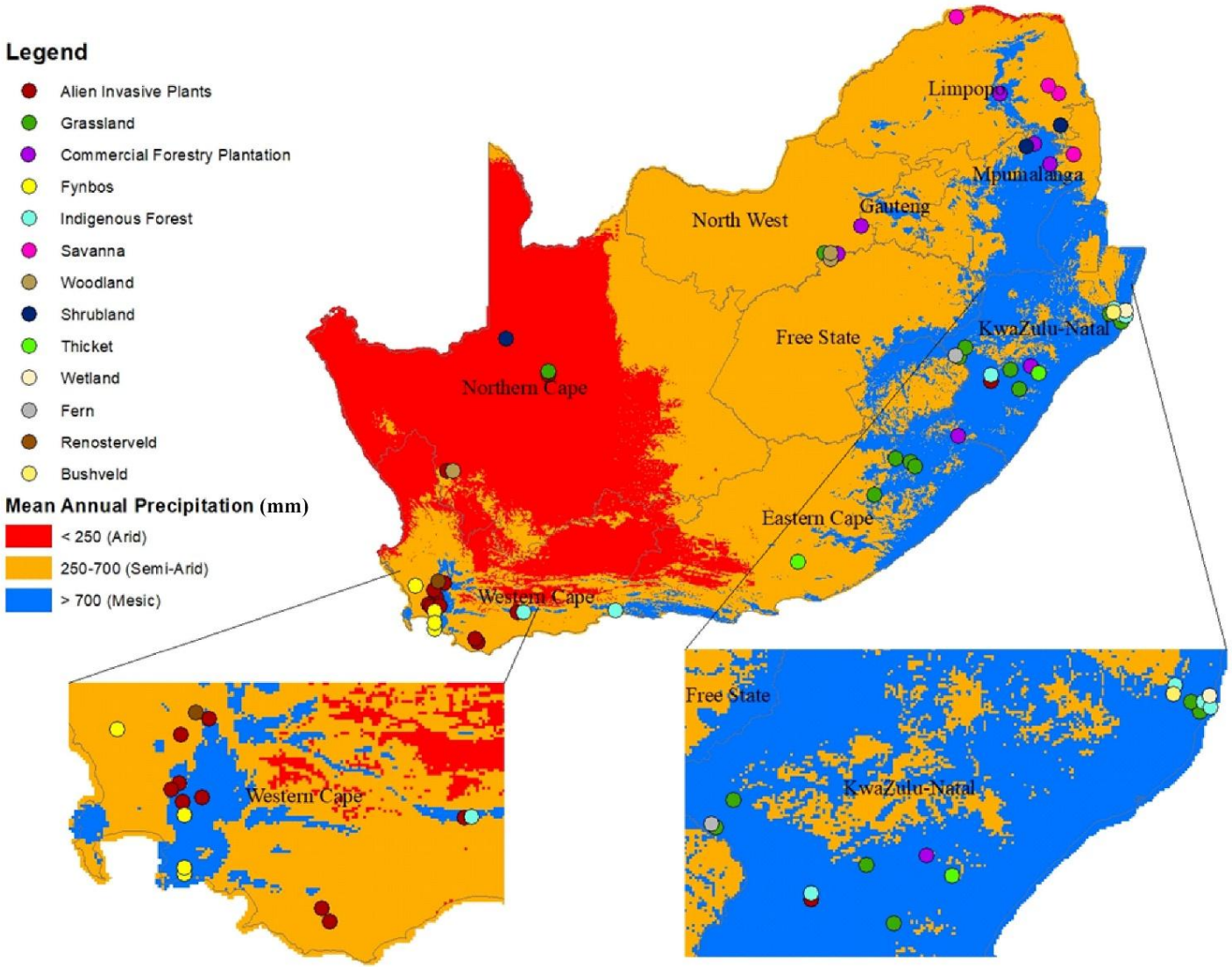


**Figure 2.1 Distribution of the vegetation water use measurements across South Africa according to their respective vegetation type and climatic zone.**

## 2.5 General trends in vegetation water use

Following a review of the literature and an analysis of the annual ET and transpiration measurements for the different vegetation types (Figures 2.2a-b and 2.3a-b), commonalities and patterns relating to the water use of vegetation in South Africa were identified. Some of these general trends are discussed in the following section.

### *2.5.1 Vegetation water use increases with decreasing aridity*

The comparison of annual ET and transpiration measurements for the different vegetation types reveals that vegetation types located in arid climates were the lowest water users. The ET measurement made by Palmer and Yunusa (2011) in a Nama-Karoo shrubland was the only ET measurement for an arid climate and was the lowest annual ET measured, totaling ~120 mm. Five annual transpiration measurements were available for arid climates, three of which were very low totaling ~140 mm or less, whereas, two annual transpiration measurements, made by Ntshidi *et al*. (2015) and Dzikiti *et al*. (2017), were much higher roughly totaling ~350 mm and ~540 mm, respectively. In fact, they were higher than some vegetation types located in mesic climates. These measurements were from the same study site investigating *Prosopis* invasion, but the studies were conducted over different years. They attributed the high water use of the *Prosopis* to the site being located in a riparian zone, where the trees likely had access to additional water sources besides rainfall, including river water or shallow groundwater. Isotopic analysis at the site confirmed that the *Prosopis* used significant groundwater sources.

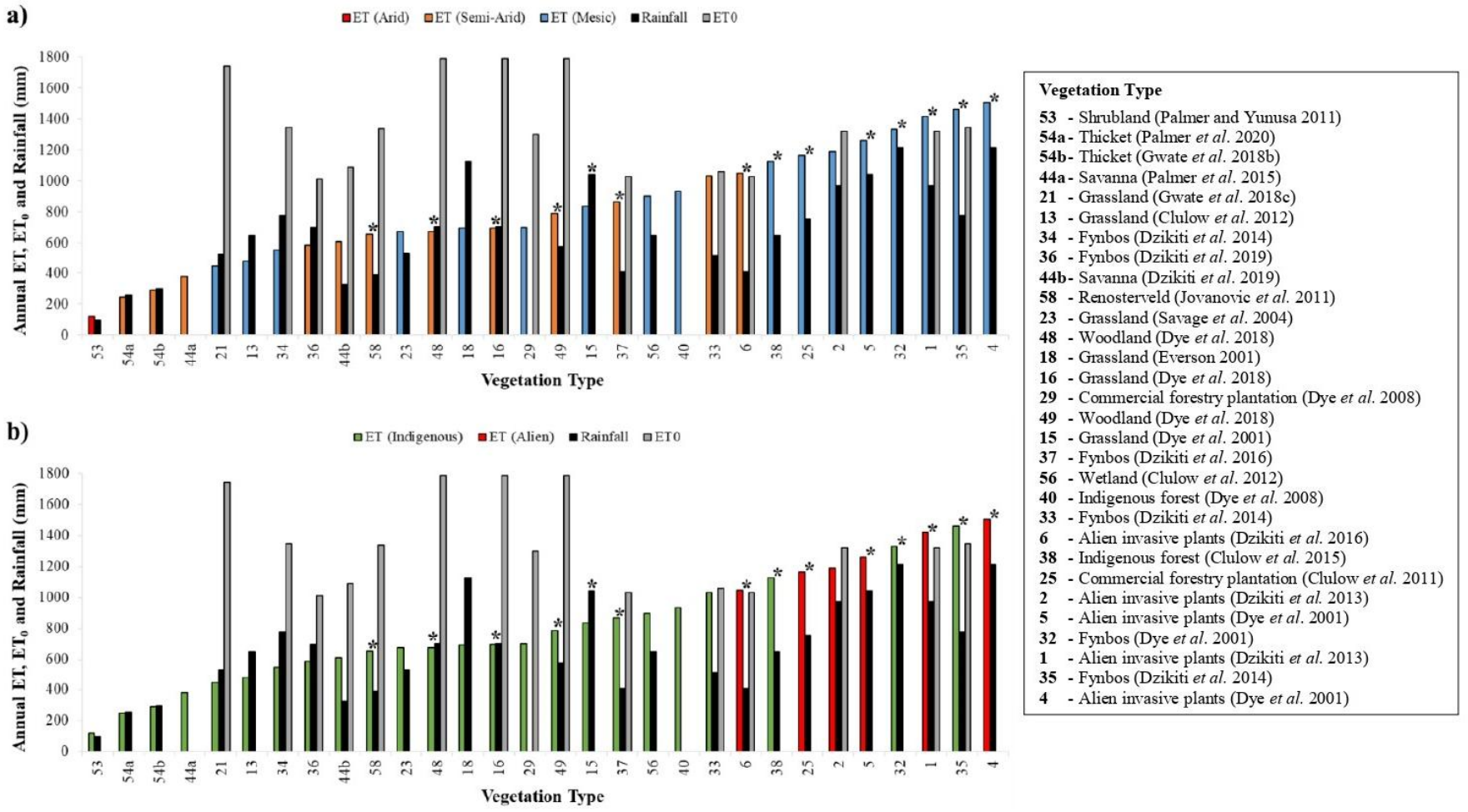


**Figure 2.2 The annual evapotranspiration (ET) estimates for various vegetation types and the annual reference evapotranspiration ($ET_0$) and rainfall measurements for these sites in South Africa. The top graph a) shows the ET colour-coded according to climate zone and the bottom graph b) shows the ET colour-coded according to whether the vegetation type is indigenous or alien. The stars (*) represent the sites located in riparian zones.**

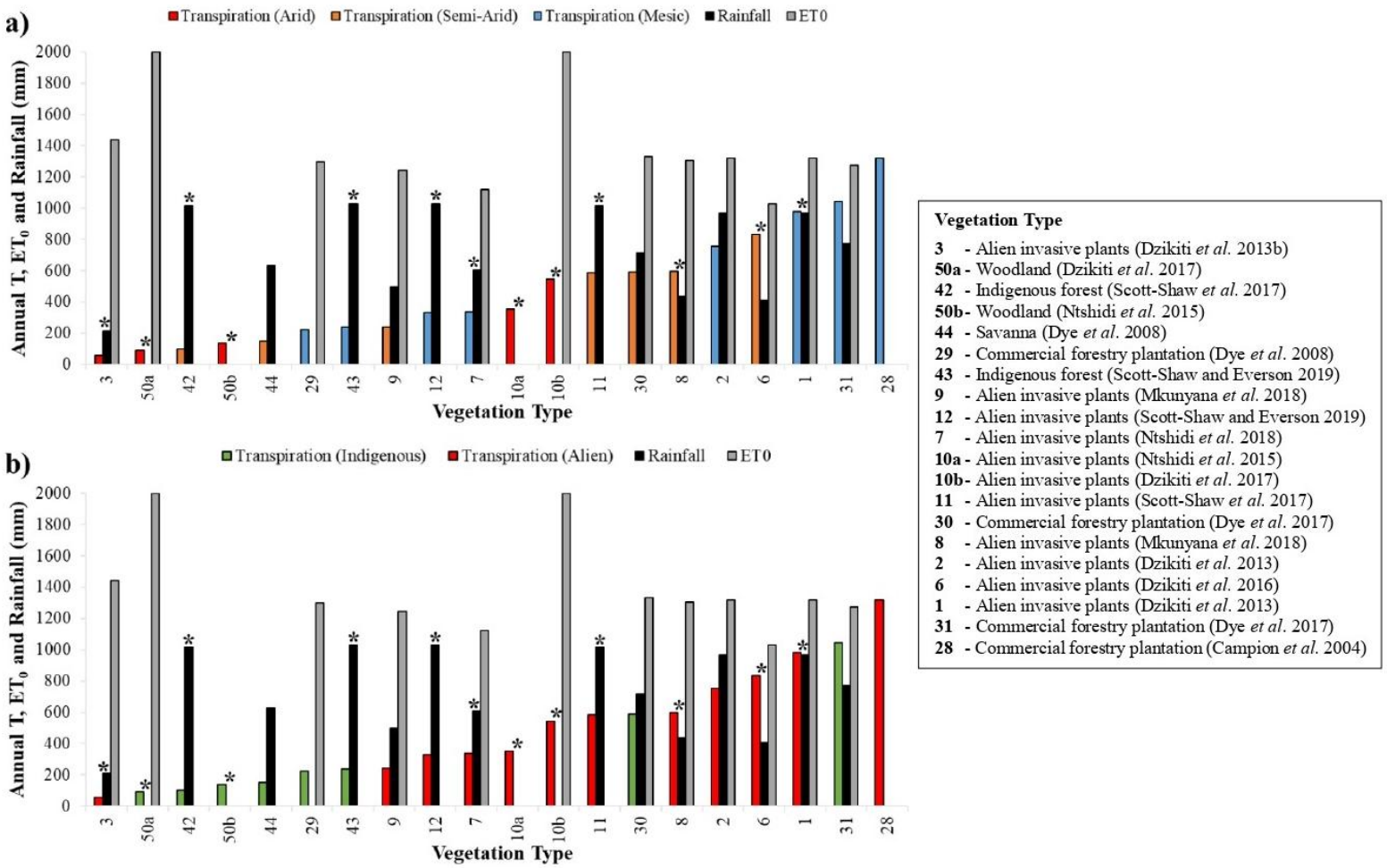


**Figure 2.3 The annual transpiration (T) estimates for various vegetation types and the annual reference evapotranspiration ($ET_o$) and rainfall measurements for these sites in South Africa. The top graph a) shows the transpiration colour-coded according to climate zone and the bottom graph b) shows the transpiration colour-coded according to whether the vegetation type is indigenous or alien. The stars (*) represent the sites located in riparian zones.**

Vegetation types located in semi-arid climates were generally the next highest water users with annual ET estimates ranging between ~250 mm and ~1050 mm, and annual transpiration estimates ranging between ~100 mm and ~830 mm. There were, however, several vegetation types with semi-arid climates that exceeded the water use of vegetation types with mesic climates. These vegetation types were located in riparian zones and many of their ET and transpiration measurements exceeded the annual rainfall, confirming that the vegetation had access to additional water sources. The fynbos (Dzikiti *et al*. 2017) and commercial forestry plantation (Dye *et al*. 2017) vegetation types had semi-arid climates and measured a higher water use than many mesic vegetation types, however, they were not located in riparian zones. The fynbos's higher water use was explained by the fact that the measurement site had a shallow water table which the fynbos roots could access, while the measurement for the commercial forestry plantation was made during an above-average rainfall year when soil water availability was high.

Vegetation types located in mesic climates were usually the highest water users with annual ET estimates ranging between ~450 mm and ~1500 mm, and annual transpiration estimates ranging between ~220 mm and ~1320 mm. Most of the mesic vegetation types with the highest water use measurements were also located in riparian zones, or they had access to an additional source of water. For example, the commercial forestry plantation of Dye *et al*. (2017) was located at a mining site with a shallow water table and strong lateral flow of mine water occurred during the summer growing season. Measurements for mesic vegetation types that were not comparably high compared to other mesic vegetation types were usually made during low-rainfall years when the annual rainfall was much lower than the MAP of the site. For example, the grassland site of Clulow *et al*. (2012) had a mesic climate with a MAP of 1200 mm, but an annual ET of only ~480 mm was measured. Clulow *et al*. (2012) reported that there was a drought during the measurement year and only 650 mm of rainfall occurred. The measurement sites of Gwate *et al*. (2018c) and Savage *et al*. (2004) also experienced significantly low annual rainfall totals compared to their typical MAP and their ET totals were lower than those measured for other mesic sites.

### *2.5.2 Vegetation water use is primarily limited by climatic factors*

Climatic factors, including rainfall and atmospheric demand, played a primary role in limiting vegetation ET. Atmospheric demand determines the energy available to drive ET and is governed

by factors such as solar radiation, temperature, relative humidity, wind speed and vapour pressure deficit (Calder and Dye 2001).

Vegetation types located in arid and semi-arid climates measured an annual ET that was either comparable to, lower than, or higher than annual rainfall, but generally lower than the annual $ET_o$ provided this data was available. In this case, atmospheric demand is high, but ET is rainfall- or water-limited. This included the fynbos (Dzikiti *et al*. 2016, Dzikiti *et al*. 2019), savanna (Dzikiti *et al*. 2019), renosterveld (Jovanovic *et al.* 2011), woodland (Dye *et al*. 2018) and grassland (Dye *et al*. 2018) vegetation types. There were, however, two exceptions; the fynbos (Dzikiti *et al*. 2014) and invasive alien plant (Dzikiti *et al*. 2016) vegetation types that were located in semi-arid climates measured an annual ET that was comparable to, or slightly higher, than the annual $ET_o$. The fynbos site had a shallow groundwater table, while the invasive alien plant site was located in a riparian zone, therefore, the ET of these vegetation types was likely not limited by rainfall.

Given that about half of the vegetation types located in mesic climates were also in riparian zones and likely had access to additional water sources, it was not possible to determine if their water use was limited by rainfall. However, several mesic vegetation types that were not in riparian zones measured an annual ET that was lower than the annual $ET_o$, suggesting that their ET was limited by rainfall. This included the grassland (Gwate *et al*. 2018c), fynbos (Dzikiti *et al.* 2014) and invasive alien plant (Dzikiti *et al.* 2013) vegetation types. Dzikiti *et al.* (2014) also measured the ET of an adjacent fynbos site that was located within a riparian zone. The annual ET of the fynbos in the riparian zone was almost three times higher than that of the dryland fynbos, confirming that the dryland fynbos ET was rainfall- or water-limited. In mesic climates, it was also found that atmospheric demand could limit vegetation ET. For example, the grassland vegetation type of Everson (2001) measured an annual ET that was significantly lower than the annual rainfall over a four-year period. Everson (2001) reported low ET variation between the years, even in the lower rainfall years, indicating that ET was limited by atmospheric demand. Clulow *et al*. (2012) also reported that atmospheric demand limited the ET of their wetland vegetation type. Wetlands typically have year-round access to water, however, the site observed a much lower annual ET than typically measured for wetlands. Clulow *et al*. (2012) attributed this to the prevailing cloudy conditions, which often persisted until nearly midday, particularly during the rainy summer season. Cloud cover reduces solar radiation and net irradiance, and therefore atmospheric demand,

resulting in lower ET. The reduced atmospheric evaporative demand and lower ET was also attributed to the low vapour pressure deficit caused by the humid coastal conditions of the area.

### *2.5.3 Indigenous vegetation types use less water than alien vegetation types*

Indigenous vegetation types were generally the lowest water users, with lower annual ET and transpiration measurements compared to alien vegetation types. There was an exception where the lowest annual transpiration was measured for an alien plant invasion of *Prosopis* trees (Dzikiti *et al.* 2013b), however, this site was extremely arid with a MAP of 75-200 mm, and there was likely very little soil water available for plant uptake or evaporation. The invasive alien plants and alien commercial forestry plantations were generally the highest water users, with the highest annual ET of ~1500 mm measured for an *Acacia mearnsii* invasion and the highest annual transpiration of ~1300 mm measured for a *Eucalyptus grandis* plantation. It is important to note that the measurements for alien vegetation types have mostly been conducted in riparian zones and/or mesic climates, where vegetation often has unlimited access to water. Furthermore, the measurements for alien vegetation types are mostly for tree-dominated vegetation types, which generally use more water than grass- and shrub-dominated vegetation types. Some indigenous vegetation types did, however, measure high annual ET and transpiration totals that were comparable to alien vegetation types. This included two riparian fynbos sites (Dye *et al*. 2001, Dzikiti *et al.* 2014), which measured annual ET rates of over ~1320 mm, and two commercial forestry plantations (Dye *et al*. 2017), which measured annual transpiration rates of ~590 mm and ~1040 mm.

### *2.5.4 Grass- and shrub-dominated vegetation types use less water than tree-dominated vegetation types*

The annual ET measurements indicate that grass- and shrub-dominated vegetation types (i.e., shrubland, thicket, savanna and grassland) were typically lower water users. For grass and shrub vegetation types, an annual ET ranging between ~120 mm and ~840 mm was measured, with grasslands typically measuring the highest rates. Fynbos is also considered a shrub vegetation type, however, fynbos tended to have a higher water use than grasslands and other shrub vegetation types, with annual ET estimates ranging between ~550 mm and ~1460 mm. In fact, some of the highest annual ET estimates were measured at fynbos sites, some of which were higher than the invasive alien plants and commercial forestry plantations. These fynbos sites were either located

in riparian zones, or where there were very shallow groundwater tables (i.e., Dzikiti *et al*. 2014). The higher water use of fynbos shrubs can also be explained by their deep root systems and by the fact that they are evergreen, which means they can use water all year round (Dye *et al*. 2001, Tomlinson *et al.* 2013, Dzikiti *et al*. 2014).

Tree-dominated vegetation types (i.e., woodlands, indigenous forests, invasive alien plants and commercial forestry plantations) generally measured higher annual ET rates, ranging between ~670 mm and ~1500 mm. The highest annual ET estimate of ~1500 mm was measured for an *Acacia mearnsii* invasion (Dye *et al.* 2001). There are many reasons why tree-dominated vegetation types are high water users. To begin with, trees are large in size due to their great heights, large canopies and thick stem diameters, which results in a high demand for water (Calder and Dye 2001, Le Maitre *et al.* 2015). Their tall canopies also have a high aerodynamic roughness and they increase air turbulence in the canopy boundary layer, which allows them to utilize advective energy more effectively and increase ET rates, particularly in wet climates (Calder and Dye 2001). Furthermore, tree-dominated vegetation types tend to have a higher leaf area index, and therefore the potential for greater transpiration (Le Maitre *et al.* 2015). A higher leaf area index also allows for a greater precipitation interception capacity, and given that most intercepted water evaporates back to the atmosphere, this evaporation contributes to ET (Le Maitre *et al.* 2015). Very few interception studies have been carried out in South Africa, but they indicate significant interception losses for tree-dominated vegetation types. For example, Bulcock and Jewitt (2012) found that the canopies of *Eucalyptus grandis, Acacia mearnsii*, and *Pinus patula* commercial forestry stands intercepted approximately 14.9%, 27.7% and 21.4% of the gross precipitation, respectively. In a savanna, Skhosana *et al*. (2023) reported that between 20.5% and 43.6% of rainfall was intercepted across a woody encroachment gradient of *Dichrostachys cinereal* and *Terminalia sericea* trees. Trees also have larger rooting systems, which are able to access and transpire water from both shallow and deeper soil layers, thus a larger soil water store is available. Therefore, during dry periods when water in upper soil layers dries up, the deep roots of trees enable sustained transpiration from more stable soil water supplies found in deeper soil layers, or from groundwater if their roots intercept with the capillary rise of groundwater, or the water table itself (Calder and Dye 2001, Le Maitre *et al.* 2015). The high transpiration of the *Acacia mearnsii* trees in the Clulow *et al*. (2011) and Scott-Shaw *et al.* (2017) studies was attributed to their deep root systems, which allowed access to groundwater reserves. The *Acacia mearnsii* roots at the

study site of Clulow *et al*. (2011) grew deeper than 8 m (Everson *et al*. 2014), and at the study site of Scott-Shaw *et al.* (2017), they grew to depths of 5 m.

### *2.5.5 Tree water use increases with height, stem diameter and stem density*

The water use of individual trees with access to adequate soil water availability was found to be closely correlated to their height and stem diameter. Generally, the taller the tree and the larger its stem diameter, the higher its transpiration rate (Dye *et al*. 2001, Dzikiti *et al.* 2013, Scott-Shaw *et al.* 2017, Mkunyana *et al*. 2018). When upscaling transpiration from the individual tree scale to the stand scale, the stem density, or the number of trees per unit area, became important in determining the transpiration of the stand. Many studies attributed the high water use of their tree-dominated vegetation types to the high stem densities at the sites (Nshidi *et al*. 2015, Dzikiti *et al*. 2016, Dzikiti *et al*. 2017, Scott-Shaw *et al*. 2017, Mkunyana *et al*. 2018, Scott-Shaw and Everson 2019). Dzikiti *et al*. (2017) found that co-occurring individual *Prosopis* and *Vachellia karroo* trees of the same size transpired a similar amount of water. However, at the stand scale, *Prosopis* transpired greater than five times more water than *Vachellia karroo* since there were six times more *Prosopis* trees than *Vachellia karroo* per unit area.

### *2.5.6 Vegetation water use is determined by the length of the growing season*

Many studies attributed the lower water use of grass-dominated vegetation types to the fact that grass species generally become dormant during the dry season. (Dye *et al*. 2001, Everson 2001, Savage *et al.* 2010, Dye *et al*. 2018). During the dry season, grasses senesce in response to drying soils and lower temperatures, ultimately reducing their transpiration (Calder and Dye 2001). On the other hand, trees are either evergreen, deciduous, or semi-deciduous. Evergreen trees retain their leaves year-round, allowing them to transpire water throughout the year, hence they are generally higher water users. Deciduous and semi-deciduous trees shed their leaves during the dry season when water resources are limited, hence they have a shorter growing season and are generally lower water users (Tomlinson *et al*. 2013). The meta-analysis studies revealed that generally alien species were evergreen, whereas indigenous species were generally deciduous. Studies comparing the water use of alien and indigenous tree-dominated vegetation types attributed indigenous vegetation types' lower water use to their deciduous nature (Dye *et al*. 2017, Scott-Shaw *et al*. 2017, Dye *et al*. 2018, Scott-Shaw and Everson 2019). For example, Dye *et al*. (2017) measured the annual transpiration of two adjacent indigenous commercial forestry

plantations, one planted with deciduous *Searsia pendulina*, and the other, with evergreen *Searsia lancea*. Dye *et al*. (2017) found that the annual transpiration of the *Searsia lancea* (~1044 mm) was nearly double that of the *Searsia penduline* (~591 mm). The ability of the *Searsia lancea* to maintain its green leaves and transpire throughout the year was believed to be one of the main reasons for this difference in water use.

## 2.6 The likelihood that woody encroachment is increasing ET losses in South Africa's savannas

Considerable debate and discussion surrounds the issue of whether woody encroachment in South Africa's savannas is adversely impacting water resources. Previous research has clearly demonstrated that increasing woody vegetation cover causes an increase in ET in mesic climates (Huxman *et al*. 2005, Gwate *et al*. 2018c), but it is unclear whether woody encroachment has the same effect in South Africa's savannas, owing to the fact that these ecosystems mostly have semi-arid climates and woody encroachment species are indigenous. Using a meta-analysis of annual ET and transpiration measurements from 50 studies across South Africa, six general trends in vegetation water use relating to climate and vegetation characteristics were identified. First, vegetation water use increases with decreasing aridity. Second, vegetation water use is primarily limited by climatic factors. Third, indigenous vegetation types use less water than alien vegetation types. Fourth, grass- and shrub-dominated vegetation types use less water than tree-dominated vegetation types. Fifth, tree water use increases with tree height, stem diameter and stem density. Finally, vegetation water use is determined by the length of the growing season. Knowledge of these trends limiting vegetation water use allowed us to evaluate the likelihood that woody encroachment is increasing ET losses in South Africa's savannas.

The first two vegetation water use trends revealed that climate factors play a primary role in limiting ET. In summary, vegetation types located in arid climates were generally the lowest water users, followed by those in semi-arid climates, while vegetation types located in mesic climates were generally the highest water users. This trend is largely due to the second trend, i.e., vegetation water use is typically limited by rainfall, however, some studies did show that vegetation water use can be limited by atmospheric demand in mesic climates. Savannas in South Africa typically have semi-arid climates and low annual rainfall totals (Kambatuku *et al.* 2012, Whitecross *et al.* 2016), therefore, it is expected that their annual ET will be comparable to their annual rainfall, and

any change in woody vegetation cover is unlikely to have an effect on ET during years with average rainfall. However, rainfall in semi-arid climates can be extremely variable from year-to-year (Kambatuku *et al*. 2012), and invasive alien plant studies have demonstrated that increasing woody vegetation cover at higher rainfall sites can increase ET. Hence, woody encroachment may have the potential to increase ET losses in semi-arid savannas during above-average rainfall years. This meta-analysis also revealed that vegetation ET can exceed the rainfall total if the vegetation is located in a riparian zone, or where there are very shallow groundwater tables that the vegetation roots can access. When there is higher water availability, ET may become limited by atmospheric demand, or vegetation characteristics (size, leaf area index, rooting structures, etc.) may have more of an effect on ET. Therefore, in above-average rainfall years, or in areas with an additional water source, an increase in woody vegetation cover should allow for an increase in ET.

One of the main arguments in support of woody encroachment having a minimal effect on ET is that woody encroachment species are indigenous and indigenous species are believed to be conservative water users. Previous South African studies demonstrating that ET increases with increasing woody vegetation cover have involved the replacement of indigenous species with alien species, which are known to use significantly more water (Calder and Dye 2001). The results of this meta-analysis agree that alien vegetation types use more water than indigenous vegetation types, however, the indigenous vegetation types in these studies were mostly grass- or shrub-dominated, whereas the alien vegetation types were tree-dominated and trees naturally use more water. Furthermore, the alien trees were reported to be taller, have larger stem diameters, grow in greater densities than the indigenous trees and use water year-round, which likely contributed to their higher water use. A global meta-analysis that used over 40 published studies from around the world to examine the water use of invasive alien plants and indigenous plants of the same growth form (Cavaleri and Sack 2010), agreed with the findings of this meta-analysis that alien vegetation types had greater transpiration rates than indigenous vegetation types at the stand scale. However, this meta-analysis also reported that when they compared the little ET data that was available at the ecosystem-scale, invasive alien plant- and indigenous-dominated ecosystems of the same growth form were equally likely to have greater ET. This meta-analysis did not compare the transpiration of individual alien trees to that of individual indigenous trees, however, studies in South Africa have reported mixed findings on this. For example, Dzikiti *et al*. (2017) found that alien and indigenous trees had similar transpiration rates, whereas Scott-Shaw *et al*. (2017) and

Scott-Shaw and Everson (2019) found that alien trees had higher transpiration rates. The meta-analysis by Cavaleri and Sack (2010) agreed with Dzikiti *et al*. (2017) that invasive alien plants and indigenous plants were equally likely to have higher transpiration rates at the plant scale.

The remaining vegetation water use trends relating to vegetation characteristics provided positive support for the idea that woody encroachment increases ET losses in South Africa's savannas. The first of these trends revealed that tree-dominated vegetation types use more water than grass-dominated vegetation types, which supports the idea that woody encroachment increases ET losses owing to the fact that woody encroachment involves the replacement of grasses by trees. Furthermore, woody encroachment species tend to form dense, mono-specific stands, and many of the meta-analysis studies demonstrated that high stem densities can be a significant factor contributing to high transpiration losses. High stem densities were also reported to result in high canopy interception following rainfall events, resulting in high evaporation losses. The final trend revealed that savanna grasses and woody species likely have a similar growing season length, given that savanna grasses go dormant during the dry season and most woody encroachment species in South Africa's savannas are deciduous (Tomlinson *et al*. 2013). Therefore, if there are any water use differences between the different vegetation states (i.e., encroached vs not encroached), this would be a result of other vegetation or climate factors.

## 2.7 Conclusions

This study revealed mixed support for whether woody encroachment in South Africa's savannas is increasing ET losses. On one hand, the fact that woody encroachment species replace grasses and form dense thickets of trees and shrubs indicates that there is high potential for woody encroachment to increase ET losses through larger canopies and extensive rooting systems. However, on the other hand, rainfall, appears to be a primary factor limiting ET in semi-arid climates, indicating little potential for woody encroachment to have any effect on ET, unless there is an above-average rainfall year, or the vegetation has access to an additional water source. This study justifies the need for additional ET monitoring in South Africa's savannas in order to predict the net change in ET following woody encroachment. If woody encroachment does result in increased ET losses, there would be justification for large-scale woody encroachment clearing. There are currently no policies in place in South Africa to clear woody encroachment and clearing of indigenous woody species is prohibited. Only with in situ ET measurements can we determine

whether woody encroachment control should be implemented in South Africa in an effort to conserve water resources.

## 2.8 References


Acharya, B. S., Kharel, G., Zou, C. B., Wilcox, B. P., & Halihan, T. (2018). Woody plant encroachment impacts on groundwater recharge: A review. *Water*, *10*(10), 1466. https://doi.org/10.3390/w10101466.

Afinowicz, J. D., Munster, C. L., & Wilcox, B. P. (2005). Modelling effects of brush management on the rangeland water budget: Edwards Plateau, Texas. *JAWRA Journal of the American Water Resources Association*, *41*(1), 181-193. https://doi.org/10.1111/j.1752-1688.2005.tb03727.x.

Andreu, A., Dube, T., Nieto, H., Mudau, A. E., González-Dugo, M. P., Guzinski, R., & Hülsmann, S. (2019). Remote sensing of water use and water stress in the African savanna ecosystem at local scale–Development and validation of a monitoring tool. *Physics and Chemistry of the Earth, Parts A/B/C*, *112*, 154-164. https://doi.org/10.1016/j.pce.2019.02.004.

Archer, S. R., Andersen, E. M., Predick, K. I., Schwinning, S., Steidl, R. J., & Woods, S. R. (2017). Woody plant encroachment: causes and consequences. *Rangeland Systems: Processes, Management and Challenges*, 25-84. https://doi.org/10.1007/978-3-319-46709-2.

Bulcock, H. H., & Jewitt, G. P. W. (2012). Field data collection and analysis of canopy and litter interception in commercial forest plantations in the KwaZulu-Natal Midlands, South Africa. *Hydrology and Earth System Sciences*, *16*(10), 3717-3728. https://doi.org/10.5194/hess-16-3717-2012.

Bunting, E. L., Fullman, T., Kiker, G., & Southworth, J. (2016). Utilization of the SAVANNA model to analyze future patterns of vegetation cover in Kruger National Park under changing climate. *Ecological Modelling*, *342*, 147-160. http://doi.org/10.1016/j.ecolmodel.2016.09.012.

Burgess, S. S., Adams, M. A., Turner, N. C., Beverly, C. R., Ong, C. K., Khan, A. A., & Bleby, T. M. (2001). An improved heat pulse method to measure low and reverse rates of sap flow in woody plants. *Tree Physiology*, *21*(9), 589-598. https://doi.org/10.1093/treephys/21.9.589.

Calder, I., & Dye, P. (2001). Hydrological impacts of invasive alien plants. *Land Use Water Resour. Res*, *1*(7), 1-8. https://doi.org/10.22004/ag.econ.47855.

Campion, J. M., Dye, P. J., & Scholes, M. C. (2004). Modelling maximum canopy conductance and transpiration in Eucalyptus grandis stands not subjected to soil water deficits. *The Southern African Forestry Journal*, *202*(1), 4-11. https://doi.org/10.1080/20702620.2004.10431784.

Cavaleri, M. A., & Sack, L. (2010). Comparative water use of native and invasive plants at multiple scales: a global meta-analysis. *Ecology*, *91*(9), 2705-2715. https://doi.org/10.1890/09-0582.1.

Clulow, A. D., Everson, C. S., & Gush, M. B. (2011). The long-term impact of Acacia mearnsii trees on evaporation, streamflow and ground water resources. *Water Research Commission Report No. TT505/11, WRC, Pretoria, South Africa*.

Clulow, A. D., Everson, C. S., Mengistu, M. G., Jarmain, C., Jewitt, G. P. W., Price, J. S., & Grundling, P. L. (2012). Measurement and modelling of evaporation from a coastal wetland in Maputaland, South Africa. *Hydrology and Earth System Sciences*, *16*(9), 3233-3247.

Clulow, A. D., Everson, C. S., Jarmain, C., & Mengistu, M. (2012b). *Water-use of the dominant natural vegetation types of the Eastern Shores area, Maputaland* (No. 1926/1, p. 12). WRC report. https://doi.org/10.5194/hess-16-3233-2012.

Clulow, A. D., Everson, C. S., Price, J. S., Jewitt, G. P. W., & Scott-Shaw, B. C. (2013). Water-use dynamics of a peat swamp forest and a dune forest in Maputaland, South Africa. *Hydrology and Earth System Sciences*, *17*(5), 2053-2067. https://doi.org/10.5194/hess-17-2053-2013.

Clulow, A. D., Everson, C. S., Mengistu, M. G., Price, J. S., Nickless, A., & Jewitt, G. P. W. (2015). Extending periodic eddy covariance latent heat fluxes through tree sap-flow measurements to estimate long-term total evaporation in a peat swamp forest. *Hydrology and Earth System Sciences*, *19*(5), 2513-2534. https://doi.org/10.5194/hess-19-2513-2015.

de Blécourt, M., Gröngröft, A., Thomsen, S., & Eschenbach, A. (2021). Temporal variation and controlling factors of tree water consumption in the thornbush savanna. *Journal of Arid Environments*, *189*, 104500. https://doi.org/10.1016/j.jaridenv.2021.104500.

Dugas, W. A., Hicks, R. A., & Wright, P. (1998). Effect of removal of Juniperus ashei on evapotranspiration and runoff in the Seco Creek watershed. *Water Resources Research*, *34*(6), 1499-1506. https://doi.org/10.1029/98WR00556.

Dye, P. J., & Olbrich, B. W. (1993). Estimating transpiration from 6-year-old Eucalyptus grandis trees: development of a canopy conductance model and comparison with independent sap flux measurements. *Plant, Cell & Environment*, *16*(1), 45-53. https://doi.org/10.1111/j.1365-3040.1993.tb00843.x.

Dye, P. J., Poulter, A. G., Soko, S., & Maphanga, D. (1997). The determination of the relationship between transpiration rate and declining available water for Eucalyptus grandis. *Water Research Commission Report*, (441/1), 97.

Dye, P., Moses, G., Vilakazi, P., Ndlela, R., & Royappen, M. (2001). Comparative water use of wattle thickets and indigenous plant communities at riparian sites in the Western Cape and KwaZulu-Natal. *Water SA*, *27*(4), 529-538. http://dx.doi.org/10.4314/wsa.v27i4.4967.

Dye, P. J., Gush, M. B., Everson, C. S., Jarmain, C., Clulow, A., Mengistu, M., ... & Savage, M. J. (2008). Water-use in relation to biomass of indigenous tree species in woodland, forest and/or plantation conditions. *Water Research Commission Report*, (361/08).

Dye, P. (2013). A review of changing perspectives on Eucalyptus water-use in South Africa. *Forest Ecology and Management*, *301*, 51-57. https://doi.org/10.1016/j.foreco.2012.08.027.

Dye, P., Naiken, V., Clulow, A., Prinsloo, E., Crichton, M., & Weiersbye, I. (2017). Sap flow in Searsia pendulina and Searsia lancea trees established on gold mining sites in central South Africa. *South African Journal of Botany*, *109*, 81-89. https://doi.org/10.1016/j.sajb.2016.12.016.

Dye, P. J., Jarmain, C., Clulow, A. D., Everson, C. S., Mengistu, M. G., & Weiersbye, I. M. (2018). Evapotranspiration from mine-affected riparian sites along the Vaal River in central South Africa. *South African Geographical Journal*, *100*(1), 62-81. http://dx.doi.org/10.1080/03736245.2017.1299640.

Dzikiti, S., Schachtschneider, K., Naiken, V., Gush, M., & Le Maitre, D. (2013). Comparison of water-use by alien invasive pine trees growing in riparian and non-riparian zones in the Western Cape Province, South Africa. *Forest Ecology and Management*, *293*, 92-102. http://dx.doi.org/10.1016/j.foreco.2013.01.003.

Dzikiti, S., Schachtschneider, K., Naiken, V., Gush, M., Moses, G., & Le Maitre, D. C. (2013b). Water relations and the effects of clearing invasive *Prosopis* trees on groundwater in an arid environment in the Northern Cape, South Africa. *Journal of Arid Environments*, *90*, 103-113. http://dx.doi.org/10.1016/j.jaridenv.2012.10.015.

Dzikiti, S., Jovanovic, N. Z., Bugan, R., Israel, S., & Le Maitre, D. C. (2014). Measurement and modelling of evapotranspiration in three fynbos vegetation types. *Water SA*, *40*(2), 189-198. http://dx.doi.org/10.4314/wsa.v40i2.1.

Dzikiti, S., Gush, M. B., Le Maitre, D. C., Maherry, A., Jovanovic, N. Z., Ramoelo, A., & Cho, M. A. (2016). Quantifying potential water savings from clearing invasive alien Eucalyptus camaldulensis using in situ and high-resolution remote sensing data in the Berg River Catchment, Western Cape, South Africa. *Forest Ecology and Management*, *361*, 69-80. http://dx.doi.org/10.1016/j.foreco.2015.11.009.

Dzikiti, S., Ntshidi, Z., Le Maitre, D. C., Bugan, R. D., Mazvimavi, D., Schachtschneider, K., ... & Pienaar, H. H. (2017). Assessing water use by *Prosopis* invasions and Vachellia karroo trees: Implications for groundwater recovery following alien plant removal in an arid catchment in South Africa. *Forest Ecology and Management*, *398*, 153-163. http://dx.doi.org/10.1016/j.foreco.2017.05.009.

Dzikiti, S., Jovanovic, N. Z., Bugan, R. D., Ramoelo, A., Majozi, N. P., Nickless, A., ... & Pienaar, H. H. (2019). Comparison of two remote sensing models for estimating evapotranspiration: algorithm evaluation and application in seasonally arid ecosystems in South Africa. *Journal of Arid Land*, *11*, 495-512. https://doi.org/10.1007/s40333-019-0098-2.

Dzikiti, S., Ntuli, N. R., Nkosi, N. N., Ntshidi, Z., Ncapai, L., Gush, M. B., ... & Pienaar, H. H. (2022). Contrasting water use patterns of two drought adapted native fruit tree species growing

on nutrient poor sandy soils in northern KwaZulu-Natal. *South African Journal of Botany*, *147*, 197-207. https://doi.org/10.1016/j.sajb.2022.01.003.

Eldridge, D. J., & Soliveres, S. (2014). Are shrubs really a sign of declining ecosystem function? Disentangling the myths and truths of woody encroachment in Australia. *Australian Journal of Botany*, *62*(7), 594-608. http://dx.doi.org/10.1071/BT14137.

Everson, C. S. (2001). The water balance of a first order catchment in the montane grasslands of South Africa. *Journal of Hydrology*, *241*(1-2), 110-123. https://doi.org/10.1016/S0022-1694(00)00376-0.

Everson, C., Clulow, A., & Mengitsu, M. (2009). *Feasibility study on the determination of riparian evaporation in non-perennial systems*. Pretoria: Water Research Commission.

Gokool, S., Jarmain, C., Riddell, E., Swemmer, A., Lerm Jr, R., & Chetty, K. T. (2017). Quantifying riparian total evaporation along the Groot Letaba River: A comparison between infilled and spatially downscaled satellite derived total evaporation estimates. *Journal of Arid Environments*, *147*, 114-124. http://dx.doi.org/10.1016/j.jaridenv.2017.07.014.

Gokool, S., Riddell, E. S., Swemmer, A., Nippert, J. B., Raubenheimer, R., & Chetty, K. T. (2018). Estimating groundwater contribution to transpiration using satellite-derived evapotranspiration estimates coupled with stable isotope analysis. *Journal of Arid Environments*, *152*, 45-54. https://doi.org/10.1016/j.jaridenv.2018.02.002.

Gray, B. A., Toucher, M. L., Savage, M. J., & Clulow, A. D. (2022). Seasonal evapotranspiration over an invader vegetation (Pteridium aquilinum) in a degraded montane grassland using surface renewal. *Journal of Hydrology: Regional Studies*, *40*, 101012. https://doi.org/10.1016/j.ejrh.2022.101012.

Gwate, O., Mantel, S. K., Palmer, A. R., & Gibson, L. A. (2016). Measuring evapotranspiration using an eddy covariance system over the Albany Thicket of the Eastern Cape, South Africa. In *Remote Sensing for Agriculture, Ecosystems, and Hydrology XVIII* (Vol. 9998, pp. 247-266). https://doi.org/10.1117/12.2245426.

Gwate, O., Mantel, S. K., Palmer, A. R., & Gibson, L. A. (2016b). Modelling evapotranspiration using the modified Penman-Monteith equation and MODIS data over the Albany Thicket in South Africa. In *Remote Sensing for Agriculture, Ecosystems, and Hydrology XVIII* (Vol. 9998, pp. 218-236). https://doi.org/10.1117/12.2245439.

Gwate, O., Mantel, S. K., Finca, A., Gibson, L. A., Munch, Z., & Palmer, A. R. (2018). Estimating evapotranspiration in semi-arid rangelands: connecting reference to actual evapotranspiration and the role of soil evaporation. *African Journal of Range & Forage Science*, *36*(1), 17-25. https://doi.org/10.2989/10220119.2018.1505779.

Gwate, O., Mantel, S. K., Palmer, A. R., & Gibson, L. A. (2018b). Biophysical controls of water vapour and energy fluxes: Towards the development of biome scale predictive models of evapotranspiration in the Albany Thicket, South Africa. *Ecohydrology*, *11*(8), e2031. https://doi.org/10.1002/eco.2031.

Gwate, O., Mantel, S. K., Gibson, L. A., Munch, Z., & Palmer, A. R. (2018c). Exploring dynamics of evapotranspiration in selected land cover classes in a sub-humid grassland: A case study in quaternary catchment S50E, South Africa. *Journal of Arid Environments*, *157*, 66-76. https://doi.org/10.1016/j.jaridenv.2018.05.011.

Hoffman, M. T. (2014). Changing patterns of rural land use and land cover in South Africa and their implications for land reform. *Journal of Southern African Studies*, *40*(4), 707-725. http://dx.doi.org/10.1080/03057070.2014.943525.

Huxman, T. E., Wilcox, B. P., Breshears, D. D., Scott, R. L., Snyder, K. A., Small, E. E., ... & Jackson, R. B. (2005). Ecohydrological implications of woody plant encroachment. *Ecology*, *86*(2), 308-319. https://doi.org/10.1890/03-0583.

Jarmain, C., Govender, M., & Everson, C. S. (2004). Improving the basis for predicting total evaporation from natural veld types in South Africa. *Water Research Commission Report*, *1219*(1), 04.

Jovanovic, N. Z., Jarmain, C., De Clercq, W. P., Vermeulen, T., & Fey, M. V. (2011). Total evaporation estimates from a Renosterveld and dryland wheat/fallow surface at the Voëlvlei Nature Reserve (South Africa). *Water SA*, *37*(4), 471-482. http://dx.doi.org/10.4314/wsa.v40i2.3.

Kambatuku, J. R., Cramer, M. D., & Ward, D. (2012). Overlap in soil water sources of savanna woody seedlings and grasses. *Ecohydrology*, *6*(3), 464-473. https://doi.org/10.1002/eco.1273.

Kennedy, A. D., & Potgieter, A. L. F. (2003). Fire season affects size and architecture of *Colophospermum mopane* in southern African savannas. *Plant Ecology*, *167*, 179-192. http://dx.doi.org/10.1023/A:1023964815201.

Khosa, F. V., Feig, G. T., Van der Merwe, M. R., Mateyisi, M. J., Mudau, A. E., & Savage, M. J. (2019). Evaluation of modeled actual evapotranspiration estimates from a land surface, empirical and satellite-based models using in situ observations from a South African semi-arid savanna ecosystem. *Agricultural and Forest Meteorology*, *279*, 107706. https://doi.org/10.1016/j.agrformet.2019.107706.

Kongo, M. V., Jewitt, G. W. P., & Lorentz, S. A. (2011). Evaporative water use of different land uses in the upper-Thukela river basin assessed from satellite imagery. *Agricultural Water Management*, *98*(11), 1727-1739. https://doi.org/10.1016/j.agwat.2010.06.005.

Kormos, P. R., Marks, D., Pierson, F. B., Williams, C. J., Hardegree, S. P., Havens, S., ... & Svejcar, T. J. (2016). Ecosystem water availability in juniper versus sagebrush snow-dominated rangelands. *Rangeland Ecology & Management*, *70*(1), 116-128. http://dx.doi.org/10.1016/j.rama.2016.05.003.

Le Maitre, D. C., Versfeld, D. B., & Chapman, R. A. (2000). Impact of invading alien plants on surface water resources in South Africa: A preliminary assessment.

Le Maitre, D. C., Blignaut, J. N., Clulow, A., Dzikiti, S., Everson, C. S., Görgens, A. H., & Gush, M. B. (2020). Impacts of plant invasions on terrestrial water flows in South Africa. In *Biological Invasions in South Africa* (pp. 431-457). Cham: Springer International Publishing. http://dx.doi.org/10.1007/978-3-030-32394-3_15.

Makhado, R. A., Mapaure, I., Potgieter, M. J., Luus-Powell, W. J., & Saidi, A. T. (2014). Factors influencing the adaptation and distribution of *Colophospermum mopane* in southern Africa's Mopane savannas-A review. *Bothalia-African Biodiversity & Conservation*, *44*(1), 1-9. https://doi.org/10.4102/abc.v44i1.152.

Mkunyana, Y. P., Mazvimavi, D., Dzikiti, S., & Ntshidi, Z. (2018). A comparative assessment of water use by Acacia longifolia invasions occurring on hillslopes and riparian zones in the Cape Agulhas region of South Africa. *Physics and Chemistry of the Earth, Parts A/B/C*, *112*, 255-264. https://doi.org/10.1016/j.pce.2018.10.002.

Nel, J. L., Richardson, D. M., Rouget, M., Mgidi, T. N., Mdzeke, N., Le Maitre, D. C., ... & Neser, S. (2004). A proposed classification of invasive alien plant species in South Africa: towards prioritizing species and areas for management action: working for water. *South African Journal of Science*, *100*(1), 53-64.

Ntshidi, Z., Dzikiti, S., Mazvimavi, D., BUGAN, R., Le Maitre, D. C., Gush, M. B., & Jovanovic, N. Z. (2015). Comparative use of groundwater by invasive alien *Prosopis* spp. and co-occurring indigenous V. karroo in a semi-arid catchment. In *14th Biennial Ground Water Division Conference and Exhibition* (pp. 21-23).

Ntshidi, Z., Gush, M. B., Dzikiti, S., & Le Maitre, D. C. (2018). Characterising the water use and hydraulic properties of riparian tree invasions: A case study of *Populus canescens* in South Africa. *Water SA*, *44*(2), 328-337. http://dx.doi.org/10.4314/wsa.v44i2.18.

O'Connor, T. G., Puttick, J. R., & Hoffman, M. T. (2014). Bush encroachment in southern Africa: changes and causes. *African Journal of Range & Forage Science*, *31*(2), 67-88. http://dx.doi.org/10.2989/10220119.2014.939996.

Palmer, A. R., & Yunusa, I. A. M. (2011). Biomass production, evapotranspiration and water use efficiency of arid rangelands in the Northern Cape, South Africa. *Journal of Arid Environments*, *75*(11), 1223-1227. http://dx.doi.org/10.1016/j.jaridenv.2011.05.009.

Palmer, A. R., Weideman, C., Finca, A., Everson, C. S., Hanan, N., & Ellery, W. (2015). Modelling annual evapotranspiration in a semi-arid, African savanna: functional convergence theory, MODIS LAI and the Penman–Monteith equation. *African Journal of Range & Forage Science*, *32*(1), 33-39. https://doi.org/10.2989/10220119.2014.931305.

Palmer, A. R., Ezenne, G. I., Choruma, D. J., Gwate, O., Mantel, S. K., & Tanner, J. L. (2020). A comparison of three models used to determine water fluxes over the Albany Thicket, Eastern Cape, South Africa. *Agricultural and Forest Meteorology*, *288*, 107984. https://doi.org/10.1016/j.agrformet.2020.107984.

Peng, H. Y., Li, X. Y., Li, G. Y., Zhang, Z. H., Zhang, S. Y., Li, L., ... & Ma, Y. J. (2013). Shrub encroachment with increasing anthropogenic disturbance in the semiarid Inner Mongolian grasslands of China. *Catena*, *109*, 39-48. http://dx.doi.org/10.1016/j.catena.2013.05.008.

Qiao, L., Zou, C. B., Will, R. E., & Stebler, E. (2015). Calibration of SWAT model for woody plant encroachment using paired experimental watershed data. *Journal of Hydrology*, *523*, 231-239. http://dx.doi.org/10.1016/j.jhydrol.2015.01.056.

Ramoelo, A., Majozi, N., Mathieu, R., Jovanovic, N., Nickless, A., & Dzikiti, S. (2014). Validation of global evapotranspiration product (MOD16) using flux tower data in the African savanna, South Africa. *Remote Sensing*, *6*(8), 7406-7423. http://doi:10.3390/rs6087406.

Riddell, E. S., Gokool, S., Raubenheimer, R., Strydom, T., Nel, J. M., Jarmain, C., & Swemmer, A. (2016). *Quantification of transmission loss processes along the Letaba River* (No. K5/2338, p. 1). WRC Report.

Rosan, T. M., Aragao, L. E., Oliveras, I., Phillips, O. L., Malhi, Y., Gloor, E., & Wagner, F. H. (2019). Extensive 21st-century woody encroachment in South America's savanna. *Geophysical Research Letters*, *46*(12), 6594-6603. http://dx.doi.org/10.1029/2019GL082327.

Saha, M.V., Scanlon, T.M. and D'odorico, P., 2015. Examining the linkage between shrub encroachment and recent greening in water-limited southern Africa. *Ecosphere*, *6*(9), 1-16. https://doi.org/10.1890/ES15-00098.1.

Savage, M. J., Everson, C. S., Odhiambo, G. O., Mengistu, M. G., & Jarmain, C. (2004). Theory and practice of evaporation measurement, with special focus on surface layer scintillometry as an operational tool for the estimation of spatially averaged evaporation. *Water Research Commission Report*, *1335*(1).

Savage, M. J. (2009). Estimation of evaporation using a dual-beam surface layer scintillometer and component energy balance measurements. *Agricultural and Forest Meteorology*, *149*(3-4), 501-517. http://doi:10.1016/j.agrformet.2008.09.012.

Savage, M. J., Odhiambo, G. O., Mengistu, M. G., Everso, C. S., & Jarmain, C. (2010). Measurement of grassland evaporation using a surface-layer scintillometer. *Water SA*, *36*(1). http://dx.doi.org/10.4314/wsa.v36i1.50901.

Schreiner-McGraw, A. P., Vivoni, E. R., Ajami, H., Sala, O. E., Throop, H. L., & Peters, D. P. (2020). Woody Plant encroachment has a larger impact than climate change on Dryland water budgets. *Scientific Reports*, *10*(1), 8112. https://doi.org/10.1038/s41598-020-65094-x.

Scott, R. L., Huxman, T. E., Barron-Gafford, G. A., Darrel Jenerette, G., Young, J. M., & Hamerlynck, E. P. (2014). When vegetation change alters ecosystem water availability. *Global Change Biology*, *20*(7), 2198-2210. https://doi.org/10.1111/gcb.12511.

Scott-Shaw, B. C., Everson, C. S., & Clulow, A. D. (2017). Water-use dynamics of an alien-invaded riparian forest within the Mediterranean climate zone of the Western Cape, South

Africa. *Hydrology and Earth System Sciences, 21*(9), 4551-4562. https://doi.org/10.5194/hess-21-4551-2017.

Scott-Shaw, B. C., & Everson, C. S. (2019). Water-use dynamics of an alien-invaded riparian forest within the summer rainfall zone of South Africa. *Hydrology and Earth System Sciences*, *23*(3), 1553-1565. https://doi.org/10.5194/hess-23-1553-2019.

Skhosana, F. V., Thenga, H. F., Mateyisi, M. J., von Maltitz, G., Midgley, G. F., & Stevens, N. (2023). Steal the rain: Interception loses and rainfall partitioning by a broad-leaf and a fine-leaf woody encroaching species in a southern African semi-arid savanna. *Ecology and Evolution*, *13*(3), e9868. https://doi.org/10.1002/ece3.9868.

Smit, G. N., & Rethman, N. F. G. (1998). Root biomass, depth distribution and relations with leaf biomass of *Colophospermum mopane*. *South African Journal of Botany*, *64*(1), 38-43. https://doi.org/10.1016/S0254-6299(15)30825-5.

Smit, G. N., & Rethman, N. F. G. (2000). The influence of tree thinning on the soil water in a semi-arid savanna of southern Africa. *Journal of Arid Environments*, *44*(1), 41-59. https://doi.org/10.1006/jare.1999.0576.

Smit, G. N. (2004). An approach to tree thinning to structure southern African savannas for long-term restoration from bush encroachment. *Journal of Environmental Management*, *71*(2), 179-191. https://doi.org/10.1016/j.jenvman.2004.02.005.

Stevens, N., Lehmann, C. E., Murphy, B. P., & Durigan, G. (2016). Savanna woody encroachment is widespread across three continents. *Global Change Biology*, *23*(1), 235-244. https://doi.org/10.1111/gcb.13409.

Tomlinson, K. W., Poorter, L., Sterck, F. J., Borghetti, F., Ward, D., de Bie, S., & van Langevelde, F. (2013). Leaf adaptations of evergreen and deciduous trees of semi-arid and humid savannas on three continents. *Journal of Ecology*, *101*(2), 430-440. https://doi.org/10.1111/1365-2745.12056.

van Huyssteen, C. V., Zere, T. B., & Hensley, M. (2009). Soil water variability in the Weatherley grassland catchment, South Africa: I. Evapotranspiration. *South African Journal of Plant and Soil*, *26*(3), 170-178. https://doi.org/10.1080/02571862.2009.10639952.

van Wilgen, B. W., & Richardson, D. M. (2012). Three centuries of managing introduced conifers in South Africa: benefits, impacts, changing perceptions and conflict resolution. *Journal of Environmental Management, 106,* 56-68. http://dx.doi.org/10.1016/j.jenvman.2012.03.052.

Wang, J., Xiao, X., Zhang, Y., Qin, Y., Doughty, R. B., Wu, X., Bajgaun, R., & Du, L. (2018). Enhanced gross primary production and evapotranspiration in juniper-encroached grasslands. *Global Change Biology, 24*(12), 5655-5667. https://doi.org/10.1111/gcb.14441.

Weber-Grullon, L., Gherardi, L., Rutherford, W. A., Archer, S. R., & Sala, O. E. (2022). Woody-plant encroachment: Precipitation, herbivory, and grass-competition interact to affect shrub recruitment. *Ecological Applications*, *32*(3), e2536. https://doi.org/10.1002/eap.2536.

Whitecross, M. A., Witkowski, E. T. F., & Archibald, S. (2016). No two are the same: Assessing variability in broad-leaved savanna tree phenology, with watering, from 2012 to 2014 at Nylsvley, South Africa. *South African Journal of Botany*, *105*, 123-132. https://doi.org/10.1016/j.sajb.2016.03.016.

Wilcox, B. P., Basant, S., Olariu, H., & Leite, P. A. (2022). Ecohydrological connectivity: A unifying framework for understanding how woody plant encroachment alters the water cycle in drylands. *Frontiers in Environmental Science*, *10*, 934535. https://doi.org/10.3389/fenvs.2022.934535.

## APPENDIX A

**Table 2.1 Overview of the vegetation water use measurements conducted in South Africa using in situ, modelling or remote sensing methods. Studies are grouped according to their respective vegetation type. The abbreviations are defined below the table.**

| | Measurement No. | Source | Dominant Vegetation or Species | Location | Method and Measurement Period | MAP (mm) | Climate | Riparian |
|---|---|---|---|---|---|---|---|---|
| **Invasive Alien Plants** | **1** | Dzikiti *et al*. 2013 | *Pinus pinaster* and *Pinus halepensis* (A) | Simonsberg Mountain, WC | HPV (Jul 2011 - Apr 2012)<br>Scintillometer (Mar 2011, Jun 2011, Oct–Nov 2011, Feb 2012)<br>PM model (May 2011-Apr 2012) | 812 | Mesic | Yes |
| | **2** | Dzikiti *et al*. 2013 | *Pinus pinaster* and *Pinus halepensis* (A) | Simonsberg Mountain, WC | HPV (Jul 2011 - Apr 2012)<br>Scintillometer (Mar 2011, Jun-Jul 2011, Nov 2011, Feb–Mar 2012)<br>PM model (May 2011-Apr 2012) | 812 | Mesic | - |
| | **3** | Dzikiti *et al.* 2013b | *Prosopis* (A) | Rugseer river, NC | HPV + PM model (Nov 2010 - Dec 2011)<br>EC (Nov 2010, Feb 2011, Jul 2011) | 75-200 | Arid | Yes |
| | **4** | Dye *et al.* 2001 | *Acacia mearnsii* (A) | Wellington, WC | HPV (Aug 1997- Feb 1998) | 1050 | Mesic | Yes |
| | **5** | Dye *et al.* 2001 | *Acacia mearnsii* (A) | Gilboa. KZN/Groot Drakenstein Mountains, WC | HPV (Aug 1998 - Feb 1999) | 906 | Mesic | Yes |
| | **6** | Dzikiti *et al*. 2016 | *Eucalyptus camaldulensis* (A) | Berg River Catchment, WC | HPV (Nov 2013-Dec 2014)<br>SEBAL + PM model (Nov 2013-Dec 2014) | 450-500 | Semi-arid | Yes |
| | **7** | Ntshidi *et al.* 2018 | *Populus canescens* (A) | Berg River Catchment, WC | HPV (Feb 2015- Feb 2016) | 863 | Mesic | Yes |
| | **8** | Mkunyana *et al.* 2018 | *Acacia longifolia* (A) | Nuwejaars Catchment, WC | HPV (Jun 2016- Jun 2017) | 400-600 | Semi-arid | Yes |
| | **9** | Mkunyana *et al*. 2018 | *Acacia longifolia* (A) | Nuwejaars Catchment, WC | HPV (Jun 2016- Jun 2017) | 400-600 | Semi-arid | - |
| | **10** | Ntshidi *et al.* 2015, Dzikiti *et al.* 2017 | *Prosopis* (A) | Brandkop farm, NC | HPV + model (Aug 2013-Jan 2016) | 150 | Arid | Yes |
| | **11** | Scott-Shaw *et al.* 2017 | *Acacia mearnsii* (A) | Buffeljags River, WC | HPV (Jan 2012-Mar 2015) | 636 | Semi-arid | Yes |
| | **12** | Scott-Shaw and Everson 2019 | *Acacia mearnsii*, *Eucalyptus nitens* and *Solanum mauritianum* (A) | New Forest, KZN | HPV + SSS techniques (Jan 2013- Dec 2014) | 941-1000 | Mesic | Yes |

| | | | | | | | | |
|---|---|---|---|---|---|---|---|---|
| **Grassland** | **13** | Clulow *et al*. 2012, Clulow *et al*. 2012b | *Trachypogon spicatus, Imperata cylindrica, Helichrysum kraussii, Cyperus obtusiflorus, Crassula alba* and *Parinari capensis* (I) | iSimangaliso Wetland Park, KZN | SR (Oct 2009-Sep 2010)<br>EC (Aug 2009, Nov 2009, Mar 2010) | 844-1200 | Mesic | - |
| | **14** | Clulow *et al*. 2012b | *Graminoids Sporobolus subtilis and Ischaemum fasciculatum* and *Restio zuluensis* (I) | iSimangaliso Wetland Park, KZN | EC (Aug, Nov 2009, Mar 2010) | 844-1200 | Mesic | Yes |
| | **15** | Dye *et al*. 2001 | *Andropogon appendiculatus, Helictotrichon turgidulum, Tristachya leucothrix, Harpechloa falx, Helichrysum aureonitens* and *Aristida congesta* (I) | Gilboa, KZN | BR (Sep 1998-Sep 1999) | 867 | Mesic | Yes |
| | **16** | Dye *et al.* 2018 | *Cynodon sp*. and *Schoenoplectis sp*. (I) | R.G. Williams Nature Reserve, NW | EC (Nov 2006- Apr 2007)<br>Model (Nov 2006-May 2007) | 657 | Semi-Arid | Yes |
| | **17** | Dzikiti *et al.* 2013b | - (I) | Rugseer River, NC | EC (Nov 2010, Feb 2011, Jul 2011) | 75-200 | Arid | Yes |
| | **18** | Everson *et al.* 2001, Jarmain *et al.* 2004 | *Themeda triandra* (I) | Cathedral Peak Catchments, KZN | BR (Sep 1990 - Jun 1995)<br>ACRU/SWAT model (Jan - Dec 1992) | 1299 | Mesic | - |
| | **19** | Gwate *et al.* 2018 | - (I) | Southern Drakensberg, EC | Scintillometer (Sep - Nov 2015) | 786 | Mesic | - |
| | **20** | Gwate *et al.* 2018 | - (I) | East Griqualand, EC | Scintillometer (Nov 2015-Apr 2016) | 756 | Mesic | - |
| | **21** | Gwate *et al*. 2018c | - (I) | Quaternary catchment S50E, EC | Mod 16 ET data product (Jan 2000-Dec 2014) | 772 | Mesic | - |
| | **22** | Kongo *et al*. 2011 | - (I) | Potshini Catchment, KZN | Scintillometer (May-Aug 2006)<br>SEBAL/MODIS (Jun 2005-Sep 2006) | 700 | Mesic | - |
| | **23** | Savage *et al.* 2004, Savage 2009, Savage 2010 | - (I) | Pietermaritzburg, KZN | Scintillometer and EC (Jan 2003- Jun 2005)<br>BR (Dec 2003 -Jun 2005) | 928 | Mesic | - |
| | **24** | van Huyssteen *et al.* 2009 | *Themeda triandra, Heteropogon contortus, Tristachya leucothrix, Eragrostis curvula, Elionurus muticus, Digitaria setifera* and *Andropogon appendiculatus* (I) | Weatherly catchment, EC | Soil water balance equation (Jun 1999-Jun 2003) | 1013 | Mesic | - |
| **Commercial Forestry Plantation** | **25** | Clulow *et al.* 2011 | *Acacia mearnsii* (A) | Two Streams catchment, KZN | Scintillometer (Aug 2006 - Dec 2008) | 920 | Mesic | Yes |
| | **26** | Dye *et al.* 1997, Dye and Olbrich 1993, Campion *et al*. 2004 | *Eucalyptus grandis* (A) | Frankfort State Forest, MP | HPV (Mar and Aug 1989, Jun 1992 - Jun 1993), PM model | 1459/1240 | Mesic | - |
| | **27** | Dye *et al.* 1997 | *Eucalyptus grandis* (A) | White River, MP | HPV (Feb 1994 - Dec 1995) | 950 | Mesic | - |

| | | | | | | | | |
|---|---|---|---|---|---|---|---|---|
| | **28** | Campion *et al*. 2004 | *Eucalyptus grandis* (A) | Came, KZN | HPV (Aug 2001 – Nov 2001), PM Model (Aug 2001 – Nov 2001) | 919 | Mesic | - |
| | **29** | Dye *et al.* 2008 | *Podocarpus falcatus* (I) | De Hoek Forest Plantation, LP | EC, SR (Sep 2005, Feb 2006, Aug 2006)<br>HPV (Sep 2004-Aug 2006)<br>PM model (Oct 2005-Sep2006) | 1001 | Mesic | - |
| | **30** | Dye *et al.* 2017 | *Searsia pendulina* (I) | Vaal River, FS | HPV (Oct 2008-Oct 2009) | 646 | Semi-arid | - |
| | **31** | Dye *et al.* 2017 | *Searsia lancea* (I) | West Wits, GP | HPV (Mar 2009-Mar 2010) | 704 | Mesic | - |
| **Fynbos** | **32** | Dye *et al.* 2001 | *Pteridium aquilinum, Elegia capensis, Cannomois virgate* and *Ischyrolepis gaudichaudiana* (I) | Jonkershoek, WC | BR (Aug 1998-Jul 1999) | 1324 | Mesic | Yes |
| | **33** | Dzikitit *et al*. 2014, Jovanovic *et al*. 2014 | - (I) | Riverlands Nature Reserve, WC | Scintillometer (Oct 2010)<br>LANDSAF (Oct 2010) | 450 | Semi-arid | - |
| | **34** | Dzikitit *et al*. 2014 | - (I) | Kogelberg Nature Reserve, WC | Scintillometer (Apr-Jun 2011) | - | Mesic | - |
| | **35** | Dzikitit *et al*. 2014 | - (I) | Kogelberg Nature Reserve, WC | Scintillometer (Sep-Oct 2011) | - | Mesic | Yes |
| | **36** | Dzikitit *et al*. 2014, Dzikitit *et al*. 2019 | - (I) | Elandsberg Nature Reserve, WC | Scintillometer (Oct 2011 - Oct 2013) | 470/600 | Semi-arid | - |
| | **37** | Dzikiti *et al*. 2016 | *Kiggelaria Africana, Olea europea subsp. Africana, Salix mucronate* and *Podocarpus elongatus* (I) | Berg River Catchment, WC | Scintillometer (Nov 2013-Dec 2014)<br>SEBAL + PM model + MOD16 (Nov 2013-Dec 2014) | 450-500 | Semi-arid | Yes |
| **Indigenous Forest** | **38** | Clulow *et al*. 2012b, Clulow *et al*. 2013, Clulow *et al*. 2015 | Peat Swamp Forest - *Syzygium cordatum, Shirakiopsis elliptica, Macaranga capensis, Bridelia macrantha, Tarenna pavettoides* and *Stenochlaena tenuifolia* (I) | iSimangaliso Wetland Park, KZN | EC (Aug and Nov 2009, and Mar 2010)<br>HPV (Sep 2009 - May 2011)<br>PM model + Priestley-Taylor model (Oct 2009-Sep 2010) | 844-1200 | Mesic | - |
| | **39** | Clulow *et al*. 2012b, Clulow *et al*. 2013 | Dune Forest - *Drypetes natalensis, Eugenia natalitia and Mimusops caffra, Strychnos gerrardii, Garcinia livingstonei* and *Casearia gladiiformis* (I) | iSimangaliso Wetland Park, KZN | HPV (Sep 2009 - May 2011)<br>Scintillometer (Aug and Nov 2009, Mar 2010) | 844-1200 | Mesic | - |
| | **40** | Dye *et al*. 2008 | Evergreen Forest - *Podocarpus latifolius, Curtisia dentata* and *Burchellia bubaline* (I) | Groenkop forest, WC | EC, Scintillometer, BR (Feb 2004, Jun 2004, Sep-Oct 2004)<br>PM model (1970-1990)<br>WAVES (Jan-Dec 2004) | 860 | Mesic | - |

| | | | | | | | | |
|---|---|---|---|---|---|---|---|---|
| | **41** | Dzikitit *et al*. 2022 | *Sclerocaryea birrea* and *Strychnos spinosa* (I) | Bonamanzi Game Reserve, KZN | HPV + PM Model (Jan 2018 - Dec 2019) | 650 | Semi-arid | - |
| | **42** | Scott-Shaw *et al*. 2017 | Afrotemperate Forest - *Celtis africana, V. lanceolata, Prunus africana, Rapanea melanophloeos* and *Afrocarpus (Podocarpus falcatus)* (I) | Buffeljags River, WC | HPV (Jan 2012-Mar 2015) | 636 | Semi-arid | Yes |
| | **43** | Scott-Shaw and Everson 2019 | Mistbelt forest - *Leucosidea sericea, Halleria lucida, Celtis Africana* and *Afrocarpus falcatus* (I) | New Forest, KZN | HPV + stem steady state (SSS) techniques (Jan 2013- Dec 2014) | 941-1000 | Mesic | Yes |
| **Savanna** | **44** | Andreu *et al.* 2019, Dye *et al.* 2008, Dzikitit *et al.* 2019, Khosa *et al*. 2019, Palmer *et al*. 2015, Ramoelo *et al*. 2014 | *Combretum apiculatum* and *Senegalia nigrescens* (I) | Skukuza, MP | EC (2000-present)<br>Scintillometer (Aug-Sep 2004, Jan-Feb 2005, May 2005)<br>HPV (Aug 2004-May2005), TSEB (2010-2012), KC-FAO56 model (2010-2012), CENTURY Model (Jul 2005 - Jun 2006), MOD-16 (2000-2010) | 547 | Semi-arid | - |
| | **45** | Andreu *et al*. 2019, Dzikitit *et al*. 2019, Ramoelo *et al*. 2014 | *Colophospermum mopane* (I) | Malopeni, LP | EC (2009-present), TSEB (2010-2012), KC-FAO56 model (2010-2012), MOD16 global ET product (2009) | 472 | Semi-arid | - |
| | **46** | Gokool *et al*. 2017, Gokool *et al*. 2018, Riddel *et al*. 2017 | *Phragmites Mauritianus, Ficus sycomorus (Fig), Philonoptera violecia (Apple leaf)* and *Diospyros mespiliformis* (I) | Groot Letaba River, LP | EC (Jun 2015 - Oct 2015, May 2016-Oct 2016)<br>SEBS Model | 418/612 | Semi-arid | Yes |
| | **47** | Smit and Rethman 2000 | *Colophospermum mopane, Boscia foetida subsp. Rehmanniana, Salvadora angustifolia, Enneapogon cenchroides, Aristida adscensionis, Brachiaria deflexa, Cenchrus ciliaris* and *Digitaria eriantha* (I) | LP | Soil water balance equation (1990-1992) | 376 | Semi-arid | - |
| **Woodland** | **48** | Dye *et al*. 2018 | *Vachellia karroo* and *Ziziphus mucronate* (I) | R.G. Williams Nature Reserve, NW | EC (Nov-2010)<br>HPV (Nov 2010-Jan 2011)<br>Model of T and ET (Sep 2006-May 2007) | 657 | Semi-arid | Yes |
| | **49** | Dye *et al.* 2018 | *Vachellia karroo* and *Asparagus suaveolens* (I) | R.G. Williams Nature Reserve, NW | Soil water balance equation (Oct 2007-Mar 2009) | 657 | Semi-arid | Yes |
| | **50** | Dzikiti *et al*. 2017, Ntshidi *et al.* 2015 | *Vachellia karroo* (I) | Brandkop farm, NC | HPV + model (Aug 2013-Jan 2016) | 150 | Arid | Yes |
| **Shrubland** | **51** | Everson *et al.* 2009 | *Juncus spp (tall sedge)* and *Phragmites reeds* (I) | Seekoei River, LP | Scintillometer (October 2007, February 2008) | 300-420 | Semi-arid | Yes |

| | | | | | | | | |
|---|---|---|---|---|---|---|---|---|
| | **52** | Everson *et al.* 2009 | *Willow trees, Rhus lancea, Acacia karoo and Phragmites* and *Juncus spp.* (I) | Seekoei River, LP | Scintillometer (October 2007, February 2008) | 300-420 | Semi-arid | Yes |
| | **53** | Palmer and Yunusa 2011 | Nama-Karoo shrubland (I) | Riemvasmaak Rural Area, NC | $ET_o$ and the MODIS fPAR product (Jan-Dec 2009) | 130 | Arid | - |
| **Thicket** | **54** | Gwate *et al.* 2016, Gwate *et al.* 2016b, Gwate *et al.* 2018, Gwate *et al.* 2018b, Palmer *et al.* 2020 | Albany thicket - *Portulacaria afra, Pappea capensis* and *Euclea undulata* (I) | eZulu Game Reserve, EC | EC (Oct 2015 -May 2018)<br>BGC-MAN model<br>PM-Leuning (PML) MOD16 model (Oct 2015 -May 2018) | 400 | Semi-arid | - |
| | **55** | Jarmain *et al.* 2004 | Valley thicket - *Acacia sieberiana* (I) | Noodsberg, KZN | BR (May 2002 to September 2003)<br>ACRU/SWAT/SWAP (May 2002-Feb 2003) | 843 | Mesic | - |
| **Wetland** | **56** | Clulow *et al.* 2012, Clulow *et al.* 2012b | *Rhynchospora holoschoenoides, Fimbristylis bivalvis, Panicum glandulopaniculatum* and *Ischaemum fasciculatum* (I) | iSimangaliso Wetland Park, KZN | SR (Oct 2009-Sep 2010) EC (Aug and Nov 2009, Mar 2010) | 844-1200 | Mesic | - |
| **Fern** | **57** | Gray *et al.* 2022 | *Pteridium aquilinum* (I) | Cathedral Peak, KZN | SR (Nov 2018-Oct 2020)<br>EC (Dec 2019, Jul-Aug 2020) | 1564 | Mesic | - |
| **Renosterveld** | **58** | Jovanovic *et al.* 2011 | - (I) | Voëlvlei Nature Reserve, WC | Scintillometer (Aug-Sep 2005, Jan-Feb 2007, Jun 2007)<br>SEBAL model + MODIS (Jul 2000-Jun 2003, Jul 2006-Jun 2007) | 450 | Semi-arid | Yes |
| **Bushveld** | **59** | Jarmain *et al.* 2004 | - (I) | Bonamanzi Nature Reserve, KZN | BR (Apr 2002-Aug 2003)<br>ACRU/SWAT/SWAP (June 2002-Mar 2003) | 758 | Mesic | - |

Acronym key: Alien (A), Indigenous (I) Western Cape (WC), Northern Cape (NC), KwaZulu-Natal (KZN), North-West (NW), Eastern Cape (EC), Mpumalanga (MP), Limpopo (LP), Gauteng (GP), Free State (FS), Heat Pulse Velocity technique (HPV), Penman-Monteith (PM), Eddy Covariance (EC), Surface Energy Balance Algorithm for Land (SEBAL), stem steady state (SSS), Surface Renewal (SR), Bowen Ratio (BR), Agricultural Catchments Research Unit (ACRU), Soil and Water Assessment Tool (SWAT), Moderate Imaging Spectroradiometer (MODIS), Land Surface Analyses Satellite Applications Facility (LANDSAF), Surface Energy Balance System (SEBS), Soil Water Atmosphere Plant (SWAP).

**Lead into Chapter 3**

After establishing that more research on the thesis topic was necessary, in situ evapotranspiration (ET) measurements were carried out in a semi-arid savanna in South Africa to determine the effect of woody encroachment on ET in these environments. Over three hydrological years, ET was measured at an experimental woody plant clearing trial using surface renewal, a simpler, more cost-effective alternative to the well-established eddy covariance method. Two surface renewal approaches, surface renewal 1 (SR1) and surface renewal dissipation theory (SRDT), were tested against eddy covariance in order to assess their potential for sensible heat flux (H) measurement. The surface renewal approach which best agreed with eddy covariance was then used to estimate ET at two adjacent plots differing in woody plant density, and hence, determine the effect of woody encroachment on ET.

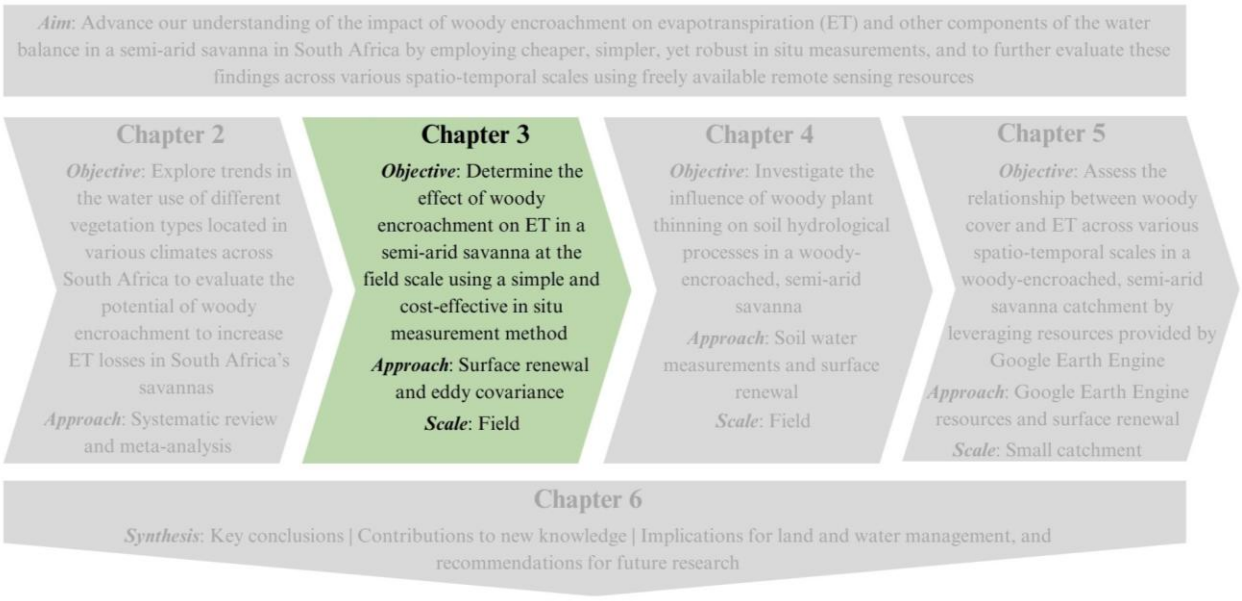

# 3 THE EFFECT OF WOODY ENCROACHMENT ON EVAPOTRANSPIRATION IN A SEMI-ARID SAVANNA[2]


## 3.1 Abstract

Over the past century, increases in indigenous woody plant species, also known as woody encroachment, has occurred in grasslands and savannas across the globe. While the impact on grassland and savanna composition and productivity has been well studied, little is known of the impacts on the hydrological cycle. Woody encroachment may increase evapotranspiration (ET) losses, leading to reduced infiltration and ultimately reduced freshwater availability, which is of particular concern in arid and semi-arid areas. The aim of this study was to determine the effect of *Colophospermum mopane* (Mopane) encroachment on ET in a semi-arid savanna located in South Africa. Mopane is widely distributed across southern Africa, and is one of the main encroaching species of the region. Following an assessment of the validity of two surface renewal approaches, surface renewal 1 (SR1) and surface renewal dissipation theory (SRDT), against short eddy covariance campaigns for sensible heat flux estimation, the SR1 approach was used to estimate ET at an experimental woody plant clearing trial from November 2019 to July 2022. For the two drier years of the study, the removal of Mopane trees had little effect on ET. However, for the wettest year of the study, the removal of Mopane trees decreased ET by 12%, supporting the hypothesis that the conversion from grass dominance to woody dominance can increase ET. Annual ET exceeded annual rainfall in all three years, indicating that the vegetation supplements its water use with soil water that has accumulated during previous wet seasons, or that tree roots facilitate hydraulic lift of deep soil water, or groundwater, to depths within the rooting depth of both trees and grasses. Further research is needed to confirm the exact mechanism involved, and the consequences of this for groundwater and streamflow at landscape scales.



***Keywords****: South Africa; indigenous vegetation; water-limited ecosystems; Colophospermum mopane; eddy covariance; surface renewal*


## 3.2 Introduction

Increases in the density and cover of indigenous woody plants at the expense of the grass layer, a phenomenon termed woody encroachment, has occurred in grasslands and savannas across the globe over the past century, and is still occurring in many areas (Sala and Maestra 2014, Deng *et al*. 2021). For decades, debate has surrounded the causes of woody encroachment, with varying degrees of evidence for overgrazing, a loss of browser herbivores, fire suppression,

[2]Aldworth, T.A., Toucher, M.L., Clulow, A.D. and Swemmer, A.M., 2022. The Effect of Woody Encroachment on Evapotranspiration in a Semi-Arid Savanna. *Hydrology*, *10*(1), 9. https://doi.org/10.3390/hydrology10010009.

warmer temperatures, altered rainfall patterns and increasing atmospheric $CO_2$ concentrations being responsible (Archer *et al*. 2017). In southern Africa, woody encroachment has been particularly widespread in arid and semi-arid savannas, with as much as 20 million hectares affected in South Africa alone (Stafford *et al*. 2017). These savannas typically have low total precipitation coupled with high seasonal variability (Kambatuku *et al*. 2012), and water is a key limitation on ecosystem productivity and economic development. There is growing concern that woody encroachment may escalate the risk of water shortages by increasing evapotranspiration (ET) losses, as woody plants are typically taller, have larger leaf areas, longer growing periods and deeper roots compared to the grasses they replace. Therefore, with increased woody densities, less water will be available in the system to supply stormflow and baseflow for streams and/or groundwater stores (Huxman *et al*. 2005, Acharya *et al*. 2017). One of the dominant encroacher tree species in the semi-arid savannas of South Africa is *Colophospermum mopane* (Kirk ex Benth) Kirk éx J. Léonard (Mopane) (Stevens 2021). Mopane is considered to be an aggressive competitor for available soil water with shallow-rooted grasses and other woody plants because it tends to grow in dense, monotypic stands with little to no grass cover (Macgregor and O'Connor 2002, Whitecross *et al*. 2012). Mopane's competitive advantage for water is largely attributed to the structural, physical and physiological adaptations of its roots and leaves, which at the same time allow it to survive in extremely dry conditions (Macgregor and O'Connor 2002, Makhado *et al*. 2014). Although the roots of Mopane are not as deep as other trees, the species has a large root biomass which extends horizontally well beyond the extent of its canopy (Macgregor and O'Connor 2002, Smit 2004), allowing access to soil water over a large area. Mopane roots can also extract water when soils are very dry as they have the ability to utilize soil water at lower matric water potentials than those tolerated by grasses and other woody plants (Smit and Rethman 2000). The leaves of Mopane are compound and compose of two ovate leaflets, which have the ability to fold together during hot periods to limit transpiration (Makhado *et al*. 2014). Mopane is deciduous and limits its transpiration during the dry winter season by shedding its leaves, but typically retains its leaves longer into the dry season than co-occurring woody species and grasses (Whitecross *et al*. 2012, Makhado *et al*. 2014).

The effect of woody encroachment by Mopane on ET is yet to be established. In fact, few studies have measured changes in ET in response to any encroaching species anywhere in Africa. Theory and ecohydrological models predict that woody encroachment can increase ET

losses in mesic environments because high rainfall allows the potential for high transpiration and interception rates (Huxman *et al*. 2005, Schreier-McGraw *et al*. 2020). In arid environments, Huxman *et al*. (2005) reported that woody encroachment has less of an effect on ET because most precipitation is evaporated irrespective of the type of vegetation, whereas Schreier-McGraw *et al*. (2020) predicted that woody encroachment decreases ET, due to a reduction of infiltration caused by increases in bare soil cover. While several international studies have found evidence that woody encroachment increased ET losses in semi-arid savanna vegetation types (Afinowicz *et al*. 2005, Scott *et al*. 2006, Kormos *et al*. 2017), similar studies are needed from southern African systems to confirm that these results can be generalized to the region.

A variety of micrometeorological methods are available for field-scale ET estimation, including eddy covariance, large weighing lysimeters, optical scintillation and the Bowen Ratio Energy Balance method (Hu *et al*. 2018). However, the expense of the sophisticated instrumentation required by most of these methods, as well as a shortage of experienced technicians equipped with the necessary skills to setup and operate the equipment, has hindered their use in the developing southern African region (Poblete-Echeverría *et al*. 2014, Castellví and Gavilán 2021, Gray *et al*. 2021). The method considered to be most universally accurate is eddy covariance (Pozníková *et al*. 2018). Eddy covariance directly calculates latent heat flux (LE) (and ET) as the covariance between turbulent fluctuations of vertical wind speed and water vapor exchange between the atmosphere and plant canopy (Rosa *et al*. 2013). In addition to the high-cost, continuous maintenance and complex operation of eddy covariance, a number of issues have prevented its widespread use (Zapata and Martínez-Cob 2002, Rosa *et al*. 2013). Eddy covariance sensors require installation in the inertial sublayer above the roughness sublayer, which is generally estimated as twice the canopy height. The higher the sensor is installed, the larger the area of fetch (i.e., upwind distance from the sensor with uniform features) required to achieve representative measurements for the vegetation of interest. Therefore, the use of eddy covariance is limited in small experimental plots, and a lack of fetch is a common reason why energy balance closure from eddy covariance measurements is not accomplished (Suvočarev *et al*. 2014, Haymann *et al*. 2019). Furthermore, eddy covariance sensors are sensitive and their accuracy can be affected by terrain properties, sensor positioning and alignment, low wind speeds and unfavorable wind directions (Zapata and Martínez-Cob 2002, Haymann *et al*. 2019).

In recent years, simpler alternative methods for estimating ET that overcome the shortcomings of eddy covariance have been sought. One of these methods that has drawn attention in the literature is surface renewal (Rosa *et al*. 2013). While surface renewal is not a new method, an increasing number of studies are reporting on its successful application for estimating ET over a wide range of surfaces, including water, bare soil, wetlands, grasses and a variety of agricultural crops (Hu *et al*. 2018). Surface renewal has not yet been widely used in southern Africa, but to date, it has been successfully tested against eddy covariance, scintillometer and Bowen Ratio Energy Balance measurements over a mesic grassland (Savage 2017), an open water reservoir (Mengistu and Savage 2010a), a wetland (Clulow *et al*. 2012), a *Podocarpus falcatus* plantation (Dye *et al*. 2008), a grassland encroached by *Leucosidea sericea* (Gray *et al*. 2021) and a grassland invaded by *Pteridium aquilinium* (Gray *et al*. 2022).

Surface renewal analysis, first introduced by Paw U *et al*. (1995), is based on the turbulent exchange of sensible heat between the plant canopy and the atmosphere caused by the continuous exchange of air parcels (Rosa *et al*. 2013). High frequency air temperature readings collected above the vegetation canopy and the analysis of their ramp structures are used to estimate sensible heat flux (H). Thereafter, LE is calculated indirectly as the residual of the shortened surface energy balance equation, along with net radiation (Rn) and soil heat flux (G) measurements (i.e., $LE = Rn - G - H$) (Rosa and Tanny 2015). Surface renewal systems comprise of a simple design, requiring a minimum of one inexpensive fine-wire thermocouple, in addition to sensors for the measurements of Rn and G, which are also relatively inexpensive. The low-cost of the thermocouples not only makes it affordable to duplicate ET measurements in field experiments, but also allows for back-up sensors to be used, limiting data record gaps in the case of thermocouple damage (Castellví 2004, Mengistu and Savage 2010b, Poblete-Echeverría *et al*. 2014, Hu *et al*. 2018). The thermocouples and Rn and G sensors also have a low power consumption permitting fewer site visits (Clulow *et al*. 2012). All of these factors make surface renewal a particularly useful method for long-term, unattended use in remote sites. Another significant attraction of surface renewal is that a relatively small fetch is sufficient for reliable H measurements. Thermocouples capture very small eddies so a more localized process of H exchange can be examined, allowing for them to be deployed in the roughness sublayer, within or close to the canopy. This also makes surface renewal a useful method at remote sites, because the measurement height does not have to be adjusted as the vegetation grows or dies back (Castellví and Snyder 2009a, Haymann *et al*. 2019).

Several variations of the surface renewal method exist (Haymann *et al*. 2019). Surface renewal 1 (SR1, Snyder *et al*. 1996) is the original, most documented and well tested surface renewal approach. It is based on classical structure function analysis and only requires high frequency air temperature measurements for H estimation (Mengistu and Savage 2010b, Poblete-Echeverría *et al*. 2014). Surface renewal 1 H estimates require site-specific calibration against a standard flux measurement method, such as eddy covariance. Calibration involves correcting H estimated with surface renewal by means of a calibration factor (α), to account for uneven heating of air parcels below the thermocouple (Mengistu and Savage 2010b, Suvočarev *et al*. 2014). To avoid the dependency of surface renewal on other methods, surface renewal approaches exempt from calibration have been developed, including surface renewal 2 (SR2, Castellví 2002; 2004) and surface renewal dissipation Theory (SRDT, Castellví and Snyder 2009b). Surface renewal 2 incorporates the principles of the Monin-Obukhov Similarity Theory (MOST) with structure function analysis (Castellví 2004). In addition to high frequency air temperature measurements, SR2 requires horizontal wind speed measurements and specific flux parameters, such as zero-plane displacement height, roughness sub-layer depth and canopy parameters (i.e., leaf area index, canopy height and vertical extent of the foliage) to estimate H (Poblete-Echeverría *et al*. 2014). Surface Renewal Dissipation Theory combines the Hsieh and Katul (2007) dissipation method with structure function analysis and only requires air temperature measurements to estimate H (Castellví and Snyder 2009b). Although the SRDT approach is the least tested approach, it has produced good H estimates over rangeland grass in California (Castellví and Snyder 2009b) and *Leucosidea sericea* and *Pteridium aquilinium* canopies in South Africa (Gray *et al*. 2021, Gray *et al*. 2022).

In this study, we used surface renewal to determine the effect of Mopane encroachment on ET in a semi-arid savanna ecosystem located in north-eastern South Africa. Evapotranspiration was measured continuously for three years from November 2019 to July 2022 at an experimental woody plant clearing trial. The validity of surface renewal at the site was first tested by comparing two surface renewal approaches, SR1 and SRDT, against the eddy covariance method. Thereafter, the surface renewal approach which best agreed with eddy covariance, was used to estimate ET at two adjacent plots differing in woody plant density. To our knowledge, this is the first validation test of surface renewal over semi-arid savanna-type vegetation worldwide.

## 3.3 Materials and methods

### *3.3.1 Study site*

The study was carried out at the Mthimkhulu Game Reserve (23°31′46″ S; 31°06′12″ E, elevation 335 m above sea level) in the Limpopo Province, South Africa (Figure 3.1). The Mthimkhulu Game Reserve is owned by a local tribal authority but is part of the greater Kruger National Park, South Africa's largest conservation area, and shares open borders with the north-eastern side of the park (Ferreria and Harmse 2014). The vegetation of Mthimkhulu Game Reserve is classified as Lowveld Mopaneveld (Acocks 1988, Mucina and Rutherford 2006), a semi-arid savanna characterized by a dense cover of Mopane shrubs, sparsely scattered trees and a limited grass understory. According to a nearby rainfall station at Mahlangeni in the Kruger National Park, the area receives a mean annual precipitation (MAP) of 467 mm. Rainfall is highly seasonal, falling in the form of thunderstorms during the spring-summer months of October to March (Kennedy and Potgieter 2003, Mucina and Rutherford 2006). Temperatures are high in summer and mild in winter with a mean annual temperature of 21.6°C (Mucina and Rutherford 2006, Stevens *et al*. 2013). The landscape is mostly flat and homogeneous with Goudplaats and Makhutswi Gneiss underlying shallow and well drained red-yellow apedal soils (Mucina and Rutherford 2006). The seasonal Klein Letaba river, which is a tributary of the Letaba River, is situated adjacent to the site.

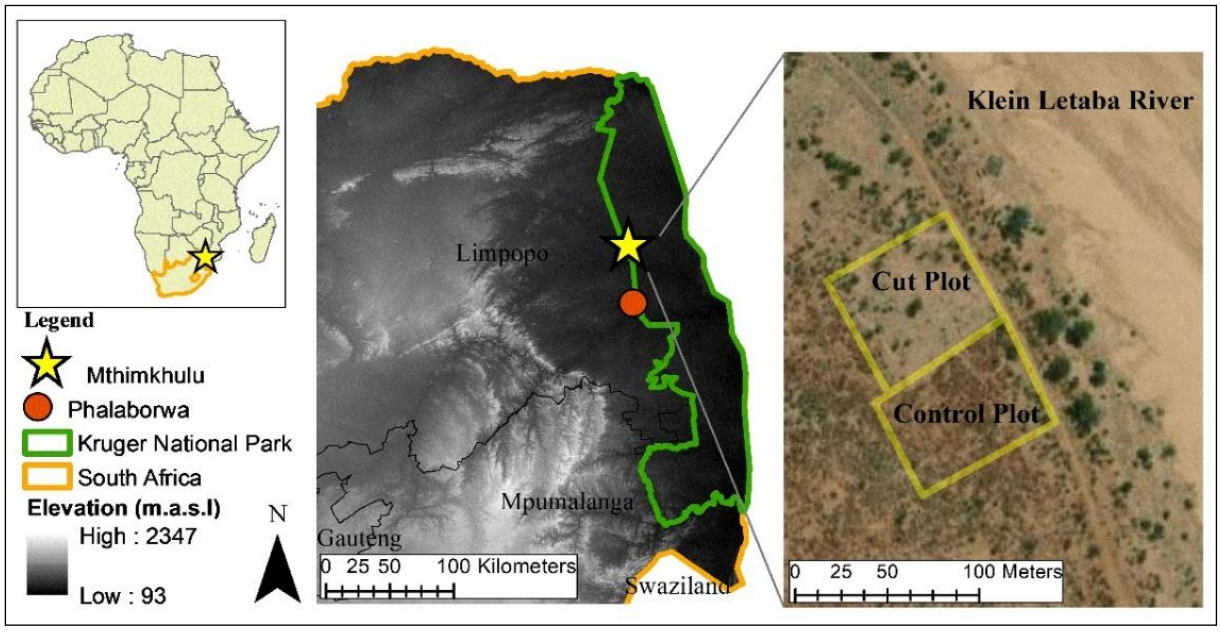


**Figure 3.1 Location of the Mthimkhulu Game Reserve in the Limpopo Province, north-eastern South Africa, and the location of the control and cut plots within the reserve.**

The cover of Mopane is extremely high in the Mthimkhulu Game Reserve, as well as surrounding areas, which is likely the result of woody encroachment that occurred in response to overgrazing by cattle over the past century. In 2014, the South African Environmental Observation Network (SAEON) established a long-term experimental woody plant clearing trial to determine the impact of Mopane cover on ecosystem processes. This comprises of five 'control' plots and five neighbouring 'cut' plots, each approximately 3600 $m^2$ in size. The control plots contain dense monotypic Mopane stands with occasional *Combretum imberbe* and *Vachellia tortilis*, and *Combretum apiculatum* and *Grewia bicolor* shrubs. The grass layer is sparse and consists mostly of annual Aristida species, with scattered tufts of *Urochloa mosambicensis* and *Panicum maximum*. The majority of the ground cover consists of bare soil and Mopane leaf litter for much of the year. The cut plots were mechanically cleared of Mopane trees by cutting all individuals shorter than four meters high, 1-2 times per year. No treatment has been applied to the control plots. For this study, one control plot and one neighbouring cut plot were selected for instrumentation and data collection (Figure 3.1). In this cut plot, the woody layer consisted of a few remaining Mopane trees taller than 4 m, and the grass layer was a thick sward dominated by *Urochloa mosambicensis*. The soil of both plots was an alluvial soil more than 1 m deep (an Oakleaf soil form in the South African Soil Classification System) (Soil Classification Working Group, 2018).

Identical surface renewal systems were deployed at the control and cut plots from mid-November 2019 to mid-June 2022, as well as an automatic weather station at the cut plot. At each plot, two week-long eddy covariance field campaigns were carried out alongside the surface renewal systems to determine $\alpha$ factors for SR1, and to test the validity of the SR1 and SRDT approaches for H estimation. The campaigns were conducted in different seasons, the first in the wet summer season (February 2020), and the second at the beginning of spring (October/November 2020) when conditions were drier (Figure 3.2).

**Figure 3.2 Vegetation and research equipment at the control plot in the summer (top-left) and spring (top-right) campaigns, and the cut plot in the summer (bottom-left) and spring (bottom-right) campaigns.**

### *3.3.2 Instrumentation*

The automatic weather station measured solar irradiance (CMP3, Kipp & Zonen, Delft, The Netherlands), air temperature and relative humidity (HMP60, Campbell Scientific Inc., Logan, UT, USA), wind speed and wind direction (Windsonic, Gill Instruments Ltd., Hampshire, UK) and rainfall (TR-525, Texas Electronics Inc., Dallas, TX, USA). All automatic weather station sensors were installed on a tripod at 2 m above a short grass surface, except for the rain gauge, which was installed with its orifice at 1.2 m above the ground.

The surface renewal systems each comprised of two unshielded 76 µm chromel-constantan fine-wire thermocouples (TCBR-3, Campbell Scientific Inc.) that measured high frequency air temperature at a sampling frequency of 10 Hz and at 0.4 s and 0.8 s time lags. The thermocouples were installed at 0.5 m and 1 m above the maximum expected canopy height (2.15 m and 0.55 m for the control and cut plots, respectively) and oriented toward the prevailing southerly wind direction to minimize wind distortion effects. Net radiation was measured with a net radiometer (NR Lite 2, Kipp and Zonen) installed 2 m above the ground and oriented toward the northerly direction. For G measurements, three soil heat flux plates (HFP01, Hukseflux Thermal Sensors, Delft, The Netherlands) were installed at a depth of 0.08 m, two soil temperature averaging soil thermocouple probes (TCAV, Campbell Scientific Inc.) were installed at depths of 0.02 m and 0.06 m above each soil heat flux plate and a soil volumetric water content sensor (CS655, Campbell Scientific Inc.) was installed at a depth of 0.1 m.

The surface renewal and automatic weather station sensors were coupled to the same data loggers (CR1000X, Campbell Scientific Inc.). The loggers were powered by 12 V rechargeable batteries. Throughout the measurement period, monthly visits were made to download the data, conduct general maintenance of the instruments and change batteries.

The eddy covariance system measured three-dimensional air movement (CSAT3, Campbell Scientific Inc.) and $H_20$ and $CO_2$ fluxes (EC150, Campbell Scientific Inc.). Following recommendations by Burba (2013), the eddy covariance sensors were installed in the constant flux layer roughly 2 m above the canopy, which allowed a fetch of approximately 200 m for the prevailing southerly wind at both plots. The eddy covariance sensors were oriented toward the prevailing southerly wind direction. Sensors at both plots were connected to an electronics panel (EC100, Campbell Scientific Inc.) and data logger (CR3000, Campbell Scientific Inc.) running the EasyFlux DL program (Campbell Scientific 2020).

### *3.3.3 Theory*

#### 3.3.3.1 Surface renewal

Surface renewal analysis is based on the Coherent Structure Theory (van Atta 1977), which assumes that air parcels near a canopy are continuously replaced or ‘renewed’ by ambient air parcels descending from the atmosphere above. While in contact with the canopy, there is

heating or cooling of the air parcels, due to heat exchange between the air and canopy elements. Using high-frequency (10 Hz, 10 samples per second) air temperature measurements taken near or above the canopy and plotting them against time, the temperature fluctuations of these individual air parcels exhibit organized coherent structures, which resemble ramp events. Using the structure function approach developed by van Atta (1977), the dimensions of these ramps, amplitude, α (°C) and ramp period, τ (s), can be determined. Knowing the mean values of the amplitude and duration of the temperature ramps allows for an estimate of the heat exchange of the air parcel with the canopy, and thus, an estimate of the H to or from the canopy (Paw U 1995, Zapata and Martínez-Cob 2002, Rosa and Tanny 2015, Haymann *et al*. 2019). $H_{SR}$ (W m$^{-2}$) can be calculated over the sampling period using the following equation (Savage 2017):

$$H_{SR} = z\rho C_\rho \frac{\alpha}{\tau} \tag{3.1}$$

where, z is the measurement height above the soil surface (m), ρ is the density of air (kg m$^{-3}$), $C_\rho$ is the specific heat of air (J kg$^{-1}$ °C$^{-1}$) and $\frac{\alpha}{\tau}$ is the rate of air temperature change (°C s$^{-1}$).

To estimate $H_{SR}$ using Equation 3.1, mean values of α and τ parameters for each sampling period are determined using the Van Atta structure-function method (van Atta 1977). The high-frequency air temperature measurements are used to determine the second-, third-, and fifth-order of the air temperature structure functions $S^n(r)$ ($n$ = 2, 3 and 5) for each sampling period according to the equation (Zapata and Martínez-Cob 2002):

$$S^n(r) = \frac{1}{m-j} \sum_{i=1+j}^{m} (T_i - T_{i-j})^n \tag{3.2}$$

where, $m$ is the number of data points measured at a frequency, f (Hz) within a t min interval, $j$ is the number of sample lags between data points corresponding to a time lag, $r$, and $T_i$ is the $i$-th temperature sample measurement. The $r$ can be calculated as the sample lag divided by the sampling frequency ($r = j/f$).

The mean value for the α for each sampling period can be determined by combining the second-, third-, and fifth-order of the structure function and solving the following equation for the real roots (Zapata and Martínez-Cob 2002):

$$\alpha^3 + \left[10S^2(r) - \frac{S^5(r)}{S^3(r)}\right]\alpha + 10S^3(r) = 0 \tag{3.3}$$

The $\tau$ can be calculated using the third-order structure function by the equation (Savage 2017):

$$\tau = -\frac{\alpha^3 r}{S^3(r)} \tag{3.4}$$

For SR1, H requires a α factor, which is derived from the regression slope of a simple linear regression forced through the origin between uncalibrated $H_{SR1}$ estimates and concurrent H measurements obtained with a standard flux measurement method (Mengistu and Savage 2010a).

For SRDT, H requires a correction factor (ß) obtained using the Dissipation Theory (Castellví and Snyder 2009a, Mengistu and Savage 2010a):

$$ß = \frac{1.66\alpha(z-d)}{\pi z \sigma T} \tag{3.5}$$

where, $d$ is the zero-plane displacement (determined as $d$ = 2/3 h, where h is the vegetation canopy height), $\pi$ is Pi and $\sigma$T is the standard deviation of air temperature.

Using calibrated $H_{SR1}$ estimates ($H_{SR1'}$) or $H_{SRDT}$ estimates, in combination with concurrent Rn (W m$^{-2}$) and G (W m$^{-2}$) measurements, $LE_{SR}$ (W m$^{-2}$) can be calculated by solving for the residual of the shortened energy balance equation (Mengistu and Savage 2010b):

$$LE_{SR} = Rn - G - H_{SR} \tag{3.6}$$

$Rn$ can be measured directly using a net radiometer and the $G$ can be calculated using the following equation (Campbell Scientific 2016):

$$G = G_{0.08\,m} + S \tag{3.7}$$

where, $G_{0.08\,m}$ is the soil heat flux at 0.08 m (W m$^{-2}$) measured using soil heat flux plates and $S$ is the change in soil heat storage above the flux plates (°C).

$S$ can be calculated using the following equation (Campbell Scientific 2016):

$$S = \frac{\Delta T_s C_s d}{t} \tag{3.8}$$

where, $\Delta T_s$ is the change in soil temperature (°C), $C_s$ is the heat capacity of moist soil (J kg$^{-1}$ °C$^{-1}$), $d$ is the depth of the soil heat flux plate (m) and $t$ is the output interval (s).

$C_s$ can be calculated using the following equation (Campbell Scientific 2016):

$$C_s = \rho_b C_d + \theta_v \rho_w C_w \tag{3.9}$$

where, $\rho_b$ is the bulk density, $C_d$ is the heat capacity of a dry mineral soil (J kg$^{-1}$ °C$^{-1}$), $\theta_v$ is the soil volumetric water content (0.1 m), $\rho_w$ is the density of water and $C_w$ is the heat capacity of water (J kg$^{-1}$ °C$^{-1}$).

$LE_{SR}$ (W m$^{-2}$) during unstable conditions is converted to actual $ET_{SR}$ (mm) using the latent heat of evaporation, $L$ (2.45 MJ kg$^{-1}$) and the following equation (Shapland *et al*. 2012):

$$ET_{SR} = \frac{LE_{SR}}{L} \tag{3.10}$$

Elaboration of the theory relating to SR1 can be found in Paw U *et al*. (1995), Snyder *et al*. (1996), Spano *et al*. (2000) and Castellví and Snyder (2010), and in Castellví and Snyder (2009a) and Castellví and Gavilán (2021) for SRDT.

3.3.3.2 Eddy covariance

Eddy covariance uses a high-response gas analyzer and a 3D sonic anemometer to directly measure the vertical flux of H. High frequency point-sampling measurements of three vertical wind speed components, air temperature and water vapour ($H_2O$) concentrations are measured simultaneously above a plant canopy to compute their covariance (Pozníková *et al*. 2018):

$H_{EC}$ (W $m^{-2}$), for any averaging period can be calculated using the following equation (Pozníková *et al*. 2018):

$$H_{EC} = \rho \times C_{\rho} \times \overline{w'T'} \quad (3.11)$$

where, $\rho$ is the density of air (kg $m^{-3}$), $C_{\rho}$ is the specific heat of air at constant pressure (J $kg^{-1}$ °$C^{-1}$) and $w'T'$ is the covariance between vertical wind speed and air temperature (m $s^{-1}$ °C). The over bar symbolizes a time-averaged value.

$LE_{EC}$ and $ET_{EC}$ can be calculated in the same manner as the surface renewal approaches (as described in Section 3.3.3.1).

Additional theory relating to the eddy covariance method can be found in Rinne and Ammann (2012) and Burba (2013).

### *3.3.4 Data processing*

The surface renewal fine-wire thermocouples measured air temperature at a frequency of 10 Hz for half-hourly sampling periods. The second-, third- and fifth-order air temperature structure functions were also calculated for each sampling period using the air temperature measurements lagged by 0.4 s and 0.8 s time lags. These data were processed using Savage's (2017) SR1 and SRDT spreadsheets, which uses Equations 3.1-3.4 to calculate half-hourly $H_{SR1}$ and $H_{SRDT}$ for each thermocouple and time lag combination. The SRDT calculations further required the mean and standard deviation of air temperature. For SR1, H was calibrated using a α factor calculated using eddy covariance campaign data, and for SRDT, H was corrected using a ß factor (Equation 3.5), which was calculated in the SRDT spreadsheet using vegetation canopy height and air temperature measurements. Soil heat flux was calculated using Equations 3.7-3.9. Thereafter, the $H_{SR1'}$, $H_{SRDT}$, Rn and G measurements, and the energy balance equation (Equation 3.6), were used to estimate half-hourly $LE_{SR1}$ and $LE_{SRDT}$.

The eddy covariance measurements were processed using EasyFlux DL software on the data logger, to generate half-hourly $H_{EC}$ (W $m^{-2}$) (Equation 3.11). EasyFlux DL despiked and filtered the 10 Hz data, applied corrections for coordinate system rotation (the double rotation method), frequency response and air density changes (using WPL equations) and converted from buoyancy flux to $H_{EC}$. These corrections are described in detail in the Easyflux DL manual

(Campbell Scientific 2020). EasyFlux DL provides quality flags numbered from 1 to 9 (high to low quality) for each half-hourly data point. Following recommendations by Foken *et al.* (2012), this study excluded H flux data with a flag of 9. This resulted in at least 99% of the half-hourly H fluxes collected during unstable atmospheric conditions being accepted for both campaigns. Half-hourly $LE_{EC}$ was calculated in the same manner as $LE_{SR}$, using Rn and G measurements, and the energy balance equation (Equation 3.6).

For SR1, a calibration using eddy covariance campaign data was performed to obtain the α factors. Linear regressions forced through the origin between half-hourly uncalibrated $H_{SR1}$ estimates and concurrent $H_{EC}$ measurements were performed. The slope of these regressions represented the α factors. H data from the summer and spring campaigns was combined into one dataset, which allowed for one α factor to be calculated for the entire measurement period.

Finally, LE and ET were calculated for the SR1, SRDT and eddy covariance methods for the measurement period, as described in Section 3.3.3. Half-hourly ET data were summed for each day to calculate daily ET totals and the daily ET totals were summed from 1 October to 30 September for the three hydrological years of the study to calculate the annual ET totals.

Only data collected during unstable atmospheric conditions when evaporation takes place were considered in this study. Unstable conditions were defined as being when Rn was positive ($R_n > 0$) and the third-order temperature structure function under both lags was negative ($S_r^3 < 0$) (Savage 2014). Data collected during periods when rainfall occurred was omitted from analysis. Minor gaps in the data record occurred due to thermocouple damage, instrument malfunction, power failure and the COVID-19 lockdown, which restricted access to the site. This missing data was patched using data from the backup thermocouple or from the other plot.

### *3.3.5 Performance evaluation*

Linear regression analysis was used to assess the validity of the SR1 calibration and to compare $H_{SR1'}$ and $H_{SRDT}$ estimates against $H_{EC}$ measurements, to determine the surface renewal approach and thermocouple and time lag combination most appropriate for LE and ET estimation. The coefficient of determination ($R^2$), root mean square error (RMSE), mean bias error (MBE) and mean absolute error (MAE) were calculated to evaluate the quality of the relationships. Coefficient of determination values close to one, MBE values close to zero and

low RMSE and MAE values were desired. Root mean square error, $MBE$ and $MAE$ can be calculated using the following equations (Dimitriadou and Nikolakopoulos 2022).

$$RMSE = \sqrt{\frac{\sum_{i=1}^{n}(x_i - y_i)^2}{n}} \quad (3.12)$$

$$MBE = \frac{\sum_{i=1}^{n}(x_i - y_i)}{n} \quad (3.13)$$

$$MAE = \frac{\sum_{i=1}^{n}|x_i - y_i|}{n} \quad (3.14)$$

where $x_i$ is the $i$-th $H_{SR1}$ and $H_{SRDT}$ estimated values, $y_i$ is the $i$-th reference $H_{EC}$ values, and $n$ is the number of half-hourly compared records.

## 3.4 Results

### *3.4.1 Weather conditions during the eddy covariance campaigns*

Eddy covariance data for the summer campaign were obtained from 12 February to 18 February 2020 at the cut plot and from 19 February to 25 February 2020 at the control plot. For the spring campaign, eddy covariance data were obtained from 23 October to 29 October 2020 at the cut plot and from 30 October to 5 November 2020 at the control plot. Only two days of the campaigns received significant rainfall, including one day during the summer-control campaign, which received 27 mm of rainfall, and one day during the spring-control campaign, which received 25 mm of rainfall. Temperatures were warm during all campaigns, with average daily air temperatures ranging between 21.6°C and 31.8°C. The maximum temperature recorded was 37.5°C and the minimum was 13.5°C. Solar radiation was high on most days, except for several days when there was rain or cloud. Daily wind speeds averaged below 2.3 m $s^{-1}$, however, the first two days of the spring-control campaign experienced slightly windier daily average conditions of over 3 m $s^{-1}$.

### *3.4.2 Estimation of the SR1 calibration factor*

Linear regressions between half-hourly, uncalibrated $H_{SR1}$ estimates and $H_{EC}$ measurements at the control and cut plots are shown in Figures 3.3 and 3.4. Individual regressions were

performed for each thermocouple and time lag combination. The α factors represented by the slope of the regressions ranged between 0.96 and 1.05 at the control plot and 1.04 and 1.29 at the cut plot. Similar α factors were found for the two measurement heights, however, higher α factors were obtained for the 0.8 s time lags than for the 0.4 s time lags.

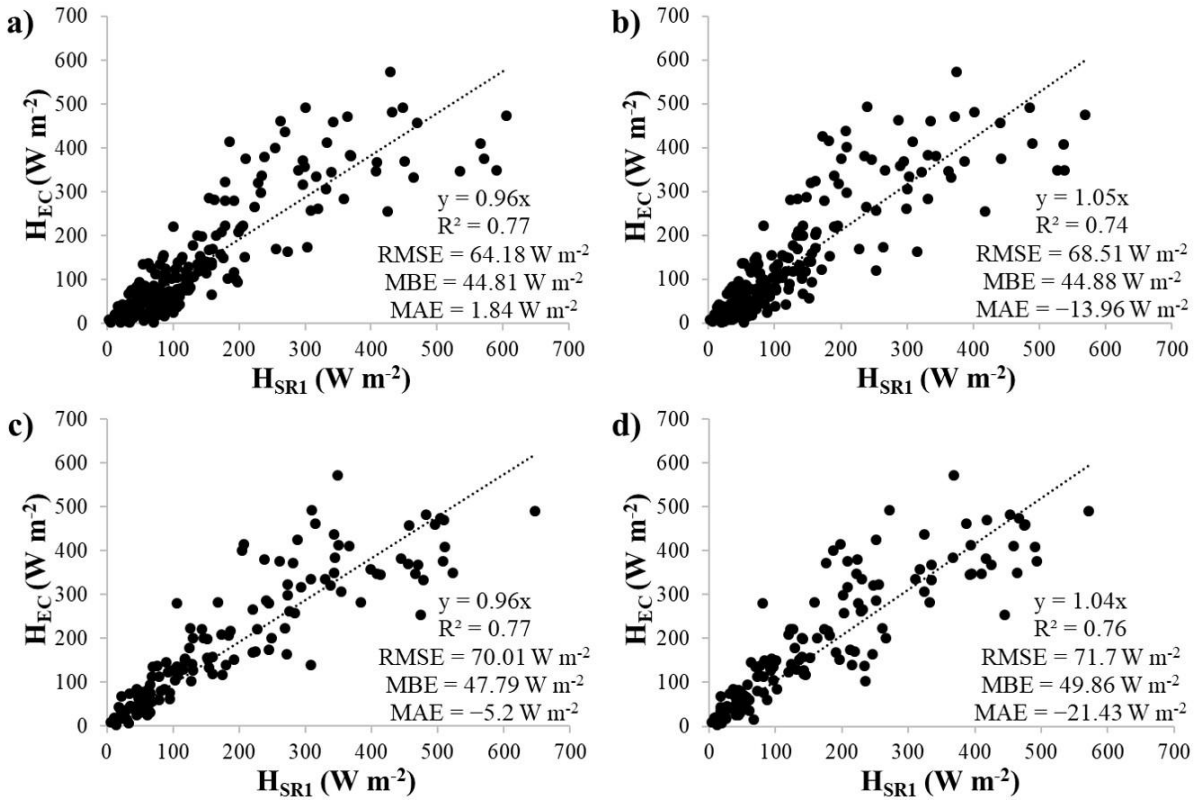


**Figure 3.3 Linear regression analysis between surface renewal 1 sensible heat flux ($H_{SR1}$) and eddy covariance sensible heat flux ($H_{EC}$) at the control plot for the upper thermocouple using time lags of (a) 0.4 s and (b) 0.8 s and the lower thermocouple using time lags of (c) 0.4 s and (d) 0.8 s.**

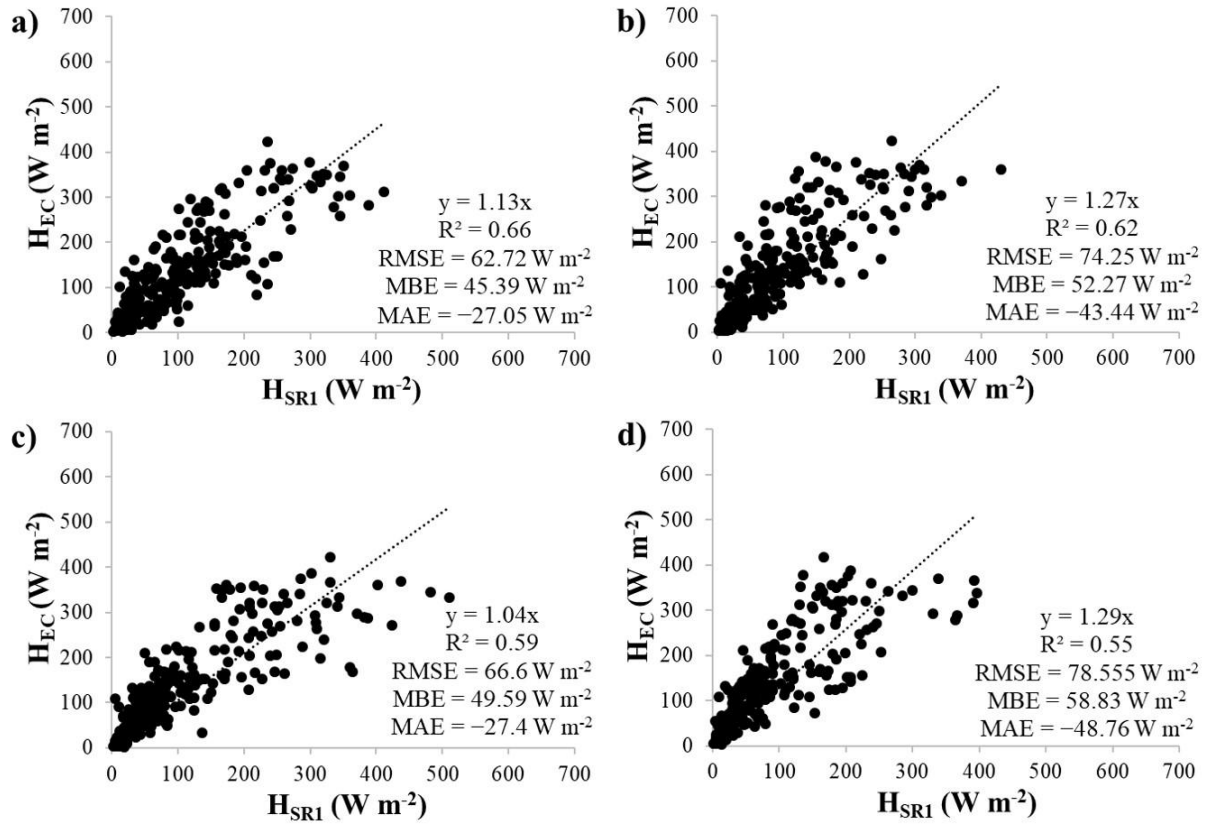


**Figure 3.4 Linear regression analysis between surface renewal 1 sensible heat flux ($H_{SR1}$) and eddy covariance sensible heat flux ($H_{EC}$) at the cut plot for the upper thermocouple using time lags of (a) 0.4 s and (b) 0.8 s and the lower thermocouple using time lags of (c) 0.4 s and (d) 0.8 s.**

The calibration regressions clearly showed that the optimal height and time lag for SR1 sampling at the site was the upper thermocouple and the 0.4 s time lag. Higher $R^2$ values, lower RMSE and MBE values and MAE values closer to zero were obtained at both plots. Therefore, the $H_{SR1}$ estimates were adjusted using these calculated α factors (0.96 and 1.13 for the control and cut plot, respectively), to obtain calibrated $H_{SR1'}$ estimates.

### *3.4.3 Validity of SR1 and SRDT*

Linear regressions of the $H_{SR1'}$ and $H_{SRDT}$ estimates were compared to the $H_{EC}$ measurements for the upper thermocouple and 0.4 s time lag at both plots (Figures 3.5 and 3.6). The $H_{SR1'}$ estimates agreed well with $H_{EC}$, with slopes close to 1 (0.96 and 0.84 for the control and cut plots, respectively). However, the $H_{SRDT}$ estimates did not show good agreement with $H_{EC}$, with slopes that well exceeded 1 (2.31 and 1.49 for the control and cut plots, respectively), indicating that $H_{SRDT}$ underestimated $H_{EC}$. In addition, the SRDT approach predicted $H_{EC}$ with

much higher errors (RMSE values of 124.55 W $m^{-2}$ and 93.29 W $m^{-2}$, MBE values of 84.15 W $m^{-2}$ and 70.17 W $m^{-2}$, and MAE values of −81.65 W $m^{-2}$ and −68.93 W $m^{-2}$ for the control and cut plots, respectively), compared to the errors predicted by the SR1 approach (RMSE values of 63.73 W $m^{-2}$ and 61.15 W $m^{-2}$, MBE values of 44.46 W $m^{-2}$ and 44.27 W $m^{-2}$, and MAE values of 3.64 W $m^{-2}$ and −13.53 W $m^{-2}$ for the control and cut plots, respectively).

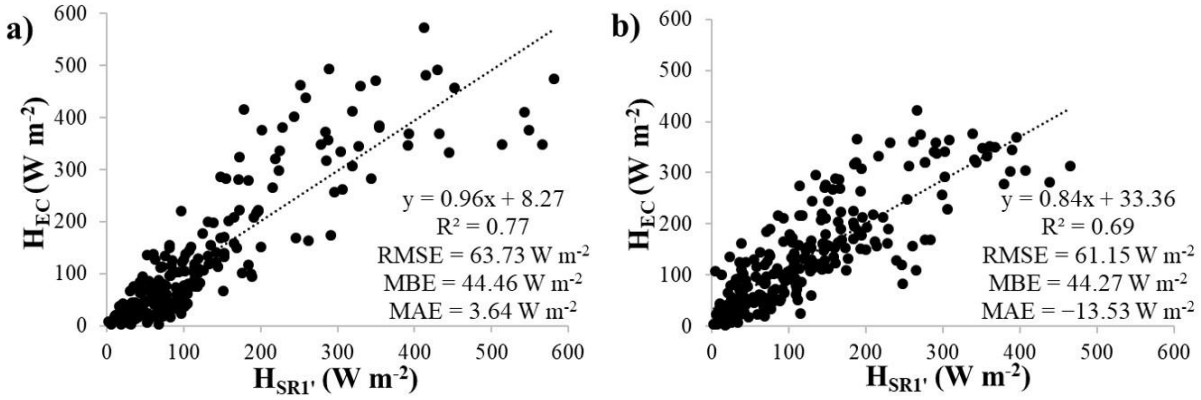


**Figure 3.5 Linear regression analysis between calibrated surface renewal 1 sensible heat flux ($H_{SR1'}$) and eddy covariance sensible heat flux ($H_{EC}$) for the upper thermocouple using the 0.4 s time lag at the (a) control and (b) cut plots.**

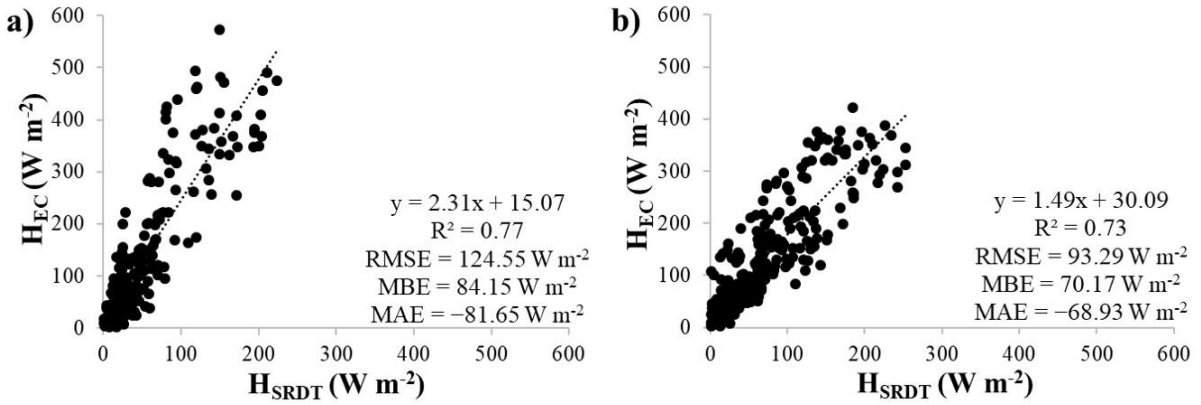


**Figure 3.6 Linear regression analysis between surface renewal dissipation theory sensible heat flux ($H_{SRDT}$) and eddy covariance sensible heat flux ($H_{EC}$) for the upper thermocouple using the 0.4 s time lag at the (a) control and (b) cut plots.**

The diurnal variation of half-hourly $H_{SR1'}$ and $H_{SRDT}$ for the upper thermocouple and 0.4 s time lag was compared against $H_{EC}$ for one day during the two campaigns at the plots (Figure 3.7), to further validate $H_{SR1'}$ and $H_{SRDT}$ estimates against $H_{EC}$ measurements. The Rn

and G measurements are also shown to better understand their relationship with $H_{EC}$ and $H_{SR}$. The days shown were selected as those that were warm, sunny and had no rainfall. Sensible heat flux for all methods was generally positive throughout the day, with the lowest values in the morning and late afternoon and the highest values around midday. Surface renewal 1 H tended to agree well with $H_{EC}$, however, it slightly underestimated $H_{EC}$ throughout the day of the spring campaign at the cut plot. Surface renewal dissipation theory H also tended to follow the $H_{EC}$ trends, but largely underestimated $H_{EC}$. Sensible heat flux for all methods followed the same diurnal trends as Rn and G. Eddy covariance H, $H_{SR1}$, $H_{SRDT}$ and Rn values were close to 0 in the early morning, increasing steadily until they peaked around noon. They then dropped back to around 0 in the early evening. Soil heat flux also peaked around noon, but was often negative in the morning and in the early evening hours.

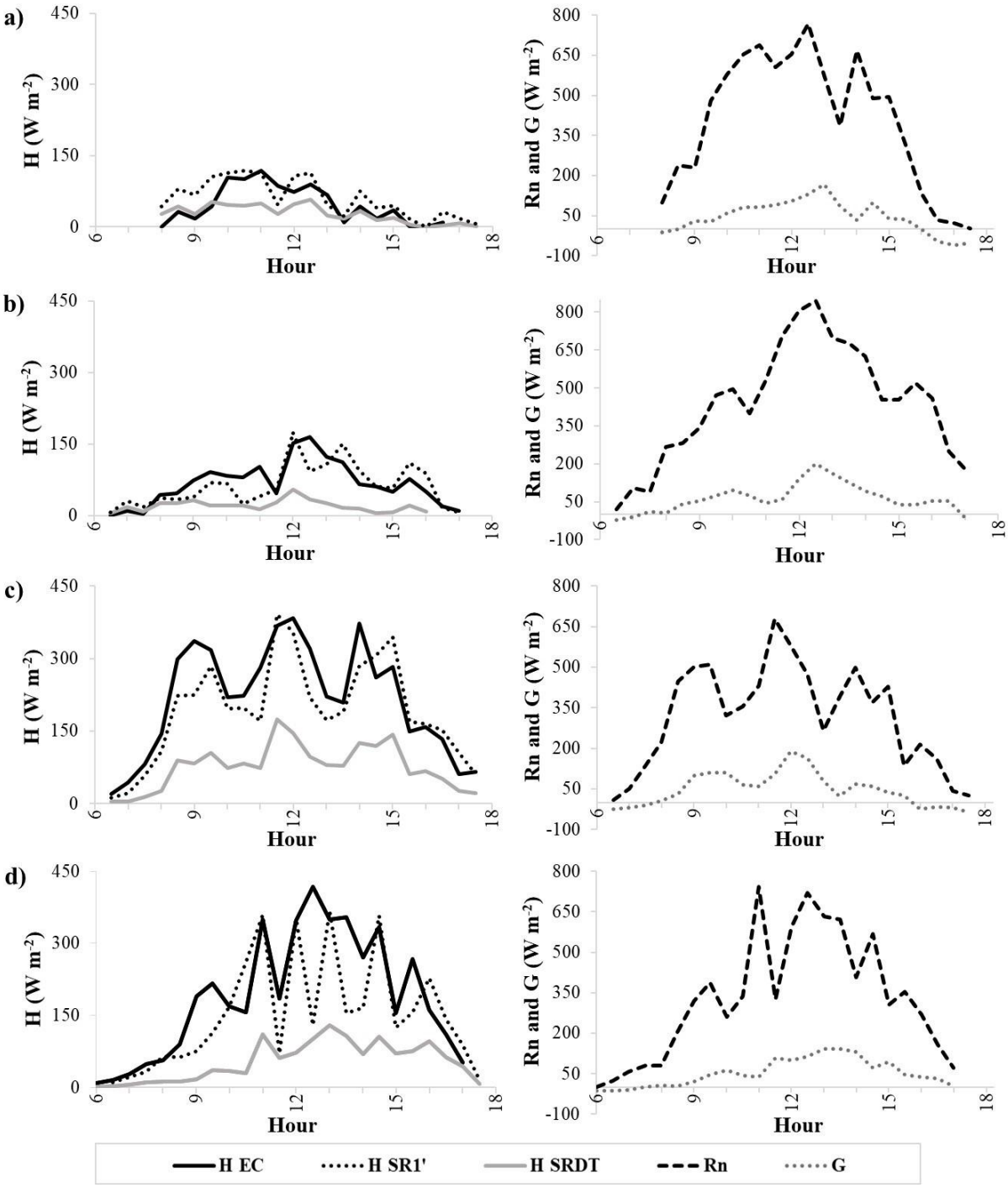


**Figure 3.7 Diurnal variation of half-hourly eddy covariance sensible heat flux ($H_{EC}$), calibrated surface renewal 1 sensible heat flux ($H_{SR1'}$), surface renewal dissipation theory sensible heat flux ($H_{SRDT}$), net radiation (Rn) and soil heat flux (G) for one day during the summer campaign at the (a) control and (b) cut plot and the spring campaign at the (c) control and (d) cut plot.**

Based on these statistics and observations, SR1 was deemed the most suitable surface renewal approach for H estimation at the site. Therefore, $H_{SR1'}$ estimates were used to estimate LE and ET for the long-term measurement period.

### *3.4.4 Long-term daily ET and energy balance flux measurements*

A seven-day moving average was calculated for the daily ET in an effort to minimize fluctuations and make trends more visible (Figure 3.8a). This revealed a strong seasonal pattern in ET at both plots, with high responses to rainfall. Higher ET occurred in the wetter summer months (December, January and February), averaging approximately 3 mm per day and reaching a maximum of approximately 5 mm per day, whereas the ET was much lower during the drier winter months (June, July and August), averaging approximately 1 mm per day. The lower ET in winter reflects the deciduous nature of the vegetation, resulting in a cessation of transpiration and ET primarily comprised of soil water evaporation by the end of the dry season.

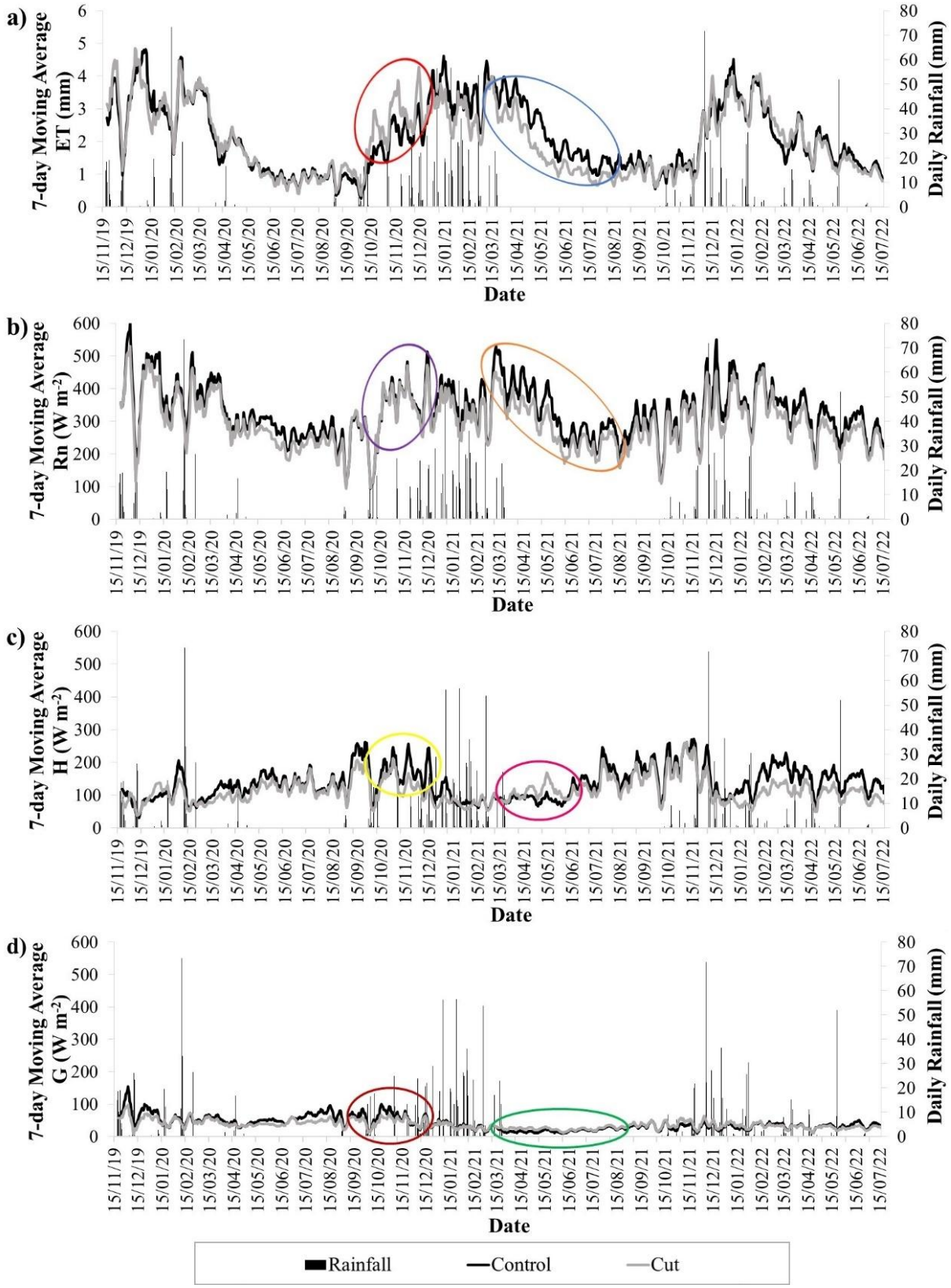


**Figure 3.8 Seven-day moving averages for (a) evapotranspiration (ET), (b) net radiation (Rn), (c) sensible heat flux (H) and (d) soil heat flux (G) during unstable conditions at the control and cut plots, and the daily rainfall for the measurement period.**

The control and cut plots had similar daily ET rates over most of the measurement period. However, after the first spring rains, the cut plot had higher ET peaks than the control plot, particularly for the 2020–2021 hydrological year (highlighted by the red oval, Figure 3.8a). This suggests that the grasses at the cut plot were able to expand their leaf area and initiate transpiration more rapidly than the Mopane once soil water became available, which fits with phenology observations (*pers. obs.*). Mopane typically flushed their leaves after the grasses, and thereafter ET rates at the control plot rapidly increased until they equaled that of the cut plot for the remainder of the summer. As rainfall decreased in autumn, vegetation senesced, resulting in a rapid drop in the ET to low rates that continued throughout winter. Grass leaves generally senesced before Mopane leaves, which was particularly evident in the autumn and winter of the 2020–2021 hydrological year when the control plot maintained higher ET rates than the cut plot (blue oval, Figure 3.8a). This slow decrease in ET and higher ET into autumn and winter of the Mopane, in comparison to the grassland, shows how different vegetation structures and physiologies respond differently to the same climatic conditions. The offset in their responses may have been a result of the Mopane keeping its leaves until late into the dry season to meet a seasonal growth cycle, or the Mopane's large rooting systems may have been able to access deeper soil water than the grasses as the upper soil layers dried up.

Figure 3.8b–d shows the seven-day moving averages of Rn, H and G at the control and cut plots over the measurement period. Net radiation followed similar diurnal trends and seasonal patterns as ET. H and G were smaller components of the energy balance and they did not replicate the ET trends well, nor was their seasonal pattern as strong as ET. Throughout the measurement period, the Rn was higher at the control plot than at the cut plot, indicating that the Mopane trees resulted in less emitted and reflected infrared radiation, likely a result of their dense canopies. Therefore, more energy was available to drive ET at the control plot. However, during spring of the 2020–2021 hydrological year, there was a gradual increase in Rn at the cut plot, causing the difference in Rn between the plots to become smaller (purple oval, Figure 3.8b). Over this same period, H was lower at the cut plot than at the control plot (yellow oval, Figure 3.8c). These trends in Rn and H indicate that once soil water became available with the first spring rains, rapid greening of the grass swards occurred at the cut plot before the emergence of new leaves on the Mopane at the control plot. The G was also higher at the control plot over this period (maroon oval, Figure 3.8d), indicating more shading of the soil layer and confirming that the grasses at the cut plot had a higher green leaf area. Therefore, there was higher potential for transpiration at the cut plot over this period. Over the autumn-

winter period of the same 2020–2021 hydrological year, the difference in canopy cover is noticeable by the higher Rn at the control plot, indicating that the Mopane still had active leaves, whereas the grassland was in senescence (orange oval, Figure 3.8b). Sensible heat flux increased at the cut plot over this period (pink oval, Figure 3.8c), likely due to a lack of water available to the grasses, limiting their transpiration. Notably, the difference in G between the plots was minimal over this period (green oval, Figure 3.8d), indicating that the leaf area at both sites was similar, the difference being that the control likely had actively transpiring leaves with a high radiant absorptivity, whereas the grass in senescence had a higher reflectance.

### *3.4.5 Annual ET*

The cumulative ET at the plots and the rainfall for the 2019–2020, 2020–2021 and 2021–2022 hydrological years of the study are shown in Figure 3.9a–c. The cumulative ET was comparable at the plots for the 2019–2020 and 2021–2022 years, totaling approximately 655 mm and 580 mm in 2019–2020 and 2021–2022, respectively. However, these years had missing ET data: for the first month and a half of 2019–2020 and the last two and a half months of 2021-2022. For the 2020–2021 year, for which there was a full data record, ET differences occurred between the plots. Increases in ET at the control plot lagged the cut plot, again indicating the more rapid growth and expansion of the grass leaf canopies following the first spring rainfall. Further into the growing season after the good summer rains, ET of the Mopane increased rapidly, shown by the steeper slope of the accumulated ET at the control plot. The ET at the control plot eventually equaled the ET at the cut plot in the beginning of the dry season, and thereafter exceeded the ET at the cut plot for the duration of the dry season. In total, the annual ET at the control plot (854 mm) exceeded the annual ET at the cut plot (762 mm) by 12%.

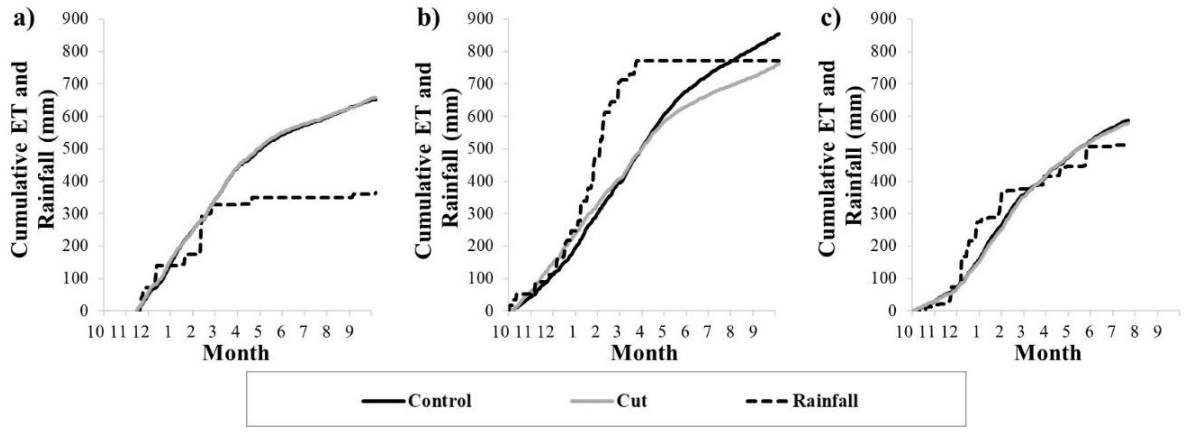


**Figure 3.9 The cumulative evapotranspiration (ET) at the control and cut plots and rainfall for the (a) 2019–2020, (b) 2020–2021 and (c) 2021–2022 hydrological years.**

The three hydrological years showed high inter-annual variability in the timing and amount of rainfall. 2019–2020 was the driest year and received an annual total rainfall of 364.7 mm, which was lower than the average for the site. However, this was significantly lower than the annual ET estimated for both plots. In fact, the annual ET exceeded the annual rainfall at the control and cut plots by 80%. 2020–2021 was a very wet year, receiving an annual rainfall of 770.9 mm, while the 2021–2022 year had a more typical rainfall of 511.6 mm (the latter is likely close to the total rainfall that occurred for the 2021–2022 year as the missing data fell over the dry season). For 2020–2021, the annual ET at the cut plot was similar to the annual rainfall, but the ET at the control plot exceeded the annual rainfall by 11%. For 2021–2022, the annual ET exceeded the annual rainfall at the control and cut plots by 15% and 13%, respectively.

The exceedance of the annual rainfall by the annual ET suggests that rainfall may not be the only source of water used by the vegetation during dry periods. Grasses have shallow roots and Mopane are typically shallow-rooted trees, with most of their roots being found within the first 0.6 m of soil (Smit and Rethman 1998), therefore, it is probable that the vegetation supplemented its water use with water that accumulated in the soil during previous wet seasons. There is also the possibility that the vegetation, particularly the larger trees, used water from deeper soil stores or groundwater that rose to within the rooting depth by capillary action or hydraulic lift. The water tables are likely shallow, or perched, since the plots are located near the riparian area of the Klein Letaba River.

## 3.5 Discussion

### *3.5.1 SR1 calibration*

There are no previously determined α factors for semi-arid, savanna-type vegetation against which our α factors can be compared. However, previous studies that have carried out calibrations between $H_{SR1}$ estimates and $H_{EC}$ measurements during unstable conditions for various plant canopies have reported α factors within the range of our estimates (our α factors ranged between 0.96 and 1.29). For example, in a montane catchment in South Africa, regression slopes of 0.89–0.92 have been reported for *Leucosidea sericea* and 0.81–0.86 for *Pteridium aquilinium* (Gray *et al*. 2021, Gray *et al*. 2022). Internationally, regression slopes of 1.1 have been reported for rice in Spain (Castellví *et al*. 2006) ,0.97–1 for grass in the United States (Castellví *et al*. 2008), 1.01–1.07 for cotton in Israel (Rosa *et al*. 2013), 0.73 and 1.15

for rice and wheat crops in Egypt (El-Magd *et al*. 2020) and 0.68 for a tea plantation in China (Wang *et al*. 2021).

Similar α factors were found for the two measurement heights, despite previous studies having found that the α factor decreases with increasing measurement height (Spano *et al*. 2000, Castellví 2004, Mengistu and Savage 2010a, Rosa *et al*. 2013, Mekhmandarov *et al*. 2015, Rosa and Tanny 2015, Hu *et al*. 2018, Dzikiti *et al*. 2019). However, higher α factors were obtained for the 0.8 s time lags than for the 0.4 s time lags, in agreement with Zapata and Martínez-Cob (2001), Mengistu and Savage (2010) and Gray *et al.* (2021), who found higher α factors for longer time lags. Overall, $H_{SR1}$ for the upper thermocouple and 0.4 s time lag showed best agreement against $H_{EC}$.

### *3.5.2 Comparison between SR1, SRDT and eddy covariance for H estimation*

Surface renewal 1 H provided stronger regressions against $H_{EC}$ than $H_{SRDT}$, with regression slopes closer to 1, lower RMSE and MBE values and MAE values closer to zero. The previous studies that compared $H_{SRDT}$ estimates and $H_{EC}$ measurements found better agreement than this study, which reported regression slopes of 2.31 and 1.49 for the control and cut plots, respectively. Gray *et al*. (2021) and Gray *et al*. (2022) reported regression slopes of 0.85–0.92 over *Leucosidea sericea* and 0.91–1.03 over *Pteridium aquilinium,* and Castellví and Snyder (2009b) reported a slope of 1.09 over grass in the United States. In addition, $H_{SR1'}$ followed the diurnal trends more closely than $H_{SRDT}$, which largely underestimated $H_{EC}$. An adjustment to the correction factor would be required to use the SRDT approach at the site. However, the RMSE values for the $H_{SR1'}$ regressions were relatively high in comparison to previous studies. The RMSE values for the $H_{SR1'}$ regressions at the control and cut plots were 63.73 W $m^{-2}$ and 78.55 W $m^{-2}$, respectively, whereas Gray *et al.* (2021) and Gray *et al.* (2022), using the same instrumentation, reported RMSE's of 36.74 W $m^{-2}$ and –38.39 W $m^{-2}$ over *Leucosidea sericea* and 39.56 W $m^{-2}$ and –41.84 W $m^{-2}$ over *Pteridium aquilinium*. Other international SR1 studies reported RMSE values ranging between 16 W $m^{-2}$ and 42 W $m^{-2}$ (Castellví *et al*. 2006, Castellví *et al*. 2008, Rosa and Tanny 2015, Wang *et al.* 2021) The RMSE values for the $H_{SRDT}$ regressions were also very high in comparison to other studies, with values of 124.55 W $m^{-2}$ and 93.29 W $m^{-2}$ for the control and cut plots, respectively. Gray *et al.* (2021) and Gray *et al.* (2022) reported RMSE's of 36.18 W $m^{-2}$–37.26 W $m^{-2}$ over *Leucosidea sericea* and 38.77 W $m^{-2}$–41.8 W $m^{-2}$ over *Pteridium aquilinium*, and Castellví and Snyder (2009a) reported a RMSE of 52 W $m^{-2}$ over grass. However, Castellví and Gavilán (2021) compared

$LE_{SRDT}$ to lysimeter LE measurements over short fescue grass in Spain and found high RMSE's, ranging between 93 W $m^{-2}$ and 136 W $m^{-2}$.

### *3.5.3 ET measurements*

A review of the available literature revealed only one study involving annual ET in situ measurements for a semi-arid savanna in South Africa. Dzikiti *et al*. (2019) used data from a FLUXNET eddy covariance system located in Skukuza in the Kruger National Park at an ecotone between *Combretum apiculatum* and *Senegalia nigrescens* savanna types. The eddy covariance flux tower is situated approximately 170 km south of the Mthimkhulu Game Reserve, but has a higher MAP of approximately 547 mm. Over their two-year study period (2010 and 2011), Dzikiti *et al*. (2019) measured an average annual ET of 610 mm and an average annual rainfall of only 323 mm. These results are within a fair range of our estimates for 2019–2020, the driest of the three years when the annual ET at both plots was significantly higher than the annual rainfall. Dzikiti *et al*. (2019) also measured a maximum daily ET of 5 mm, which was the same as the maximum seven-day moving average ET estimated for all three summers of our study.

The annual ET at both plots exceeded the annual rainfall, indicating that the vegetation may access deep soil water stores or groundwater. In a previous study at the Mthimkhulu Game Reserve site, Wedel *et al*. (2021) determined that Mopane used deeper soil water than grasses using stable isotopes, but no groundwater samples were taken to verify whether groundwater was a source of water used by the vegetation. Several studies that have measured ET for other vegetation types in South Africa have also found that the annual ET exceeded the annual rainfall. Dzikiti *et al*. (2017) found that the annual ET of an arid woodland invaded by *Prosopis* was approximately four times higher than the rainfall. Isotopic analysis results confirmed that the *Prosopis* used groundwater. Palmer *et al*. (2020) found that the annual ET of indigenous Albany thicket exceeded the annual rainfall by 7% over three hydrological years. Palmer *et al.* (2020) suggested that the Albany thicket was likely supported by groundwater, but this was not confirmed.

## 3.6 Conclusions

The SR1 approach with eddy covariance calibration was found to be a viable method for estimating ET in a Mopane-encroached, semi-arid savanna located in north-eastern South Africa. Over the three hydrological years of the study, ET was highly seasonal and was

typically highest during the wet season when it responded to increased soil water availability and increased Rn. For the two drier years of the study, the removal of Mopane trees had little effect on ET and all rainfall was evaporated irrespective of the density of woody plants. However, for the wettest year of the study, the annual ET at the control plot (Mopane) was 12% higher than at the cut plot (grassland). These results support the hypothesis that woody encroachment in semi-arid savannas can increase ET, at least during years of above-average rainfall, and thus may reduce groundwater and soil water profile recharge. Another significant finding of the study was that the annual ET at both plots was able to exceed the annual rainfall. Further isotope studies are needed to confirm the water sources used by the vegetation, and to understand the source of the accumulated water that is available in dry years. Further research on ET-soil water processes at the Mthimkhulu Game Reserve is also recommended, to advance our understanding of the relationship between vegetation structure, vegetation water consumption and water supplies in semi-arid savannas.

### 3.7 References


Acharya, B.S.; Hao, Y.; Ochsner, T.E.; Zou, C.B. Woody plant encroachment alters soil hydrological properties and reduces downward flux of water in tallgrass prairie. *Plant Soil* 2017, *414*, 379–391.

Acocks, J.P.H. *Veld Types of South Africa*, 3rd ed.; Memoirs of the Botanical Survey of South Africa No. 57; Botanical Research Institute: Pretoria, South Africa, 1988.

Afinowicz, J.D.; Munster, C.L.; Wilcox, B.P. Modelling effects of brush management on the rangeland water budget: Edwards Plateau, Texas. *J. Am. Water Resour. Assoc.* 2005, *41*, 181–193.

Archer, S.R.; Andersen, E.M.; Predick, K.I.; Schwinning, S.; Steidl, R.J.; Woods, S.R. Woody Plant Encroachment: Causes and Consequences. In *Rangeland Systems: Processes, Management and Challenges*; Briske, D.D., Ed.; Springer: Gewerbestrasse, Switzerland, 2017; 25–84.

Burba, G. *Eddy Covariance Method for Scientific, Industrial, Agricultural and Regulatory Applications*; LI-COR Biosciences: Lincoln, NE, USA, 2013.

Campbell Scientific. EASYFLUX DL CR3000OP for CR3000 and Open-Path Eddy-Covariance System Revision: 3/18. 2020. Available online: https://s.campbellsci.com/documents/us/manuals/easyflux-dl.pdf (accessed on 14 August 2022).

Campbell Scientific. Model HFP01SC Self-Calibrating Soil Heat Flux Plate Revision: 10/16. 2016. Available online: https://s.campbellsci.com/documents/us/manuals/hfp01sc.pdf (accessed on 14 August 2022).

Castellví, F.; Perez, P.J.; Ibañez, M. A method based on high frequency temperature measurements to estimate sensible heat flux avoiding the height dependence. *Water Resour. Res.* 2002, *38*, 1084. https://doi.org/10.1029/2001WR000486.

Castellví, F. Combining surface renewal analysis and similarity theory: A new approach for estimating sensible heat flux. *Water Resour. Res.* 2004, *40*, W05201.

Castellví, F.; Martínez-Cob, A.; Pérez-Coveta, O. Estimating sensible and latent heat fluxes over rice using surface renewal. *Agric. For. Meteorol.* 2006, *139*, 164–169.

Castellví, F.; Snyder, R.L.; Baldocchi, D.D. Surface energy-balance closure over rangeland grass using the eddy covariance method and surface renewal analysis. *Agric. For. Meteorol.* 2008, *148*, 1147–1160.

Castellví, F.; Snyder, R.L. On the performance of surface renewal analysis to estimate sensible heat flux over two growing rice fields under the influence of regional advection. *J. Hydrol.* 2009a, *375*, 546–553.

Castellví, F.; Snyder, R.L. Combining the dissipation method and surface renewal analysis to estimate scalar fluxes from the time traces over rangeland grass near Ione (California). *Hydrol. Process.* 2009b, *23*, 842–857.

Castellví, F.; Snyder, R.L. A comparison between latent heat fluxes over grass using a weighing lysimeter and surface renewal analysis. *J. Hydrol.* 2010, *381*, 213–220.

Castellví, F.; Gavilán, P. Estimation of the latent heat flux over irrigated short fescue grass for different fetches. *Atmosphere* 2021, *12*, 322.

Clulow, A.D.; Everson, C.S.; Mengistu, M.G.; Jarmain, C.; Jewitt, G.P.W.; Price, J.S.; Grundling, P.L. Measurement and modelling of evaporation from a coastal wetland in Maputaland. *Hydrol. Earth Syst. Sci.* 2012, *16*, 3233–3247.

Deng, Y.; Li, X.; Shi, F.; Hu, X. Woody plant encroachment enhanced global vegetation greening and ecosystem water-use efficiency. *Glob. Ecol. Biogeogr.* 2021, *30*, 2337–2353.

Dimitriadou, S.; Nikolakopoulos, K.G. Development of the Statistical Errors Raster Toolbox with Six Automated Models for Raster Analysis in GIS Environments. *Remote Sens.* 2022, *14*, 5446.

Dye, P.J.; Gush, M.B.; Everson, C.S.; Jarmain, C.; Clulow, A.; Mengistu, M.; Geldenhuys, C.J.; Wise, R.; Scholes, R.J.; Archibald, S.; *et al*. *Water-Use in Relation to Biomass of Indigenous Tree Species in Woodland, Forest and/or Plantation Conditions*; Report TT361/08; Water Research Commission: Pretoria, South Africa, 2008.

Dzikiti, S.; Ntshidi, Z.; Le Maitre, D.C.; Bugan, R.D.H.; Mazvimavi, D.; Schachtschneider, K.; Jovanovic, N.Z.; Pienaar, H.H. Assessing water use by *Prosopis* invasions and Vachellia karroo trees: Implications for groundwater recovery following alien plant removal in an arid catchment in South Africa. *For. Ecol. Manag.* 2017, *398*, 153–163.

Dzikiti, S.; Jovanovic, N.Z.; Bugan, R.D.H.; Ramoelo, A.; Majozi, N.P.; Nickless, A.; Cho, M.A.; Le Maitre, D.C.; Ntshidi, Z.; Pienaar, H.H. Comparison of two remote sensing models for estimating evapotranspiration: Algorithm evaluation and application in seasonally arid ecosystems in South Africa. *J. Arid Land* 2019, *11*, 495–512.

El-Magd, A.A.; Attaher, S.M.; Snyder, R.L. Evaluation of surface renewal vs. eddy covariance methods to estimate cereal crops evapotranspiration. *J. Soil Sci. Agric. Eng.* 2020, *11*, 845–851.

Ferreria, S.; Harmse, A. Kruger National Park: Tourism development and issues around the management of large numbers of tourists. *J. Ecotourism* 2014, *13*, 16–34.

Foken, T.; Leuning, R.; Oncley, S.R.; Mauder, M.; Aubinet, M. Corrections and data quality control. In *Eddy Covariance*; Aubinet, M., Vesala, T., Papale, D., Eds.; Springer: Dordrecht, The Netherlands, 2012; pp. 85–131.

Gray, B.A.; Toucher, M.L.; Savage, M.J.; Clulow, A.D. The potential of surface renewal for determining sensible heat flux for indigenous vegetation for a first-order montane catchment. *Hydrol. Sci. J.* 2021, *66*, 1015–1027.

Gray, B.A.; Toucher, M.L.; Savage, M.J.; Clulow, A.D. Seasonal evapotranspiration over an invader vegetation (*Pteridium aquilinum*) in a degraded montane grassland using surface renewal. *J. Hydrol. Reg.* 2022, *40*, 101012.

Haymann, N.; Lukyanova, V.; Tanny, J. Effects of variable fetch and footprint on surface renewal measurements of sensible and latent heat fluxes in cotton. *Agric. For. Meteorol.* 2019, *268*, 63–73.

Hsieh, C.I.; Katul, G.G. Dissipation methods, Taylor's hypothesis, and stability correction functions in the atmospheric surface layer. *J. Geophys. Res.* 1997, *102*, 16391–16405.

Hu, Y.; Buttar, N.A.; Tanny, J.; Snyder, R.L.; Savage, M.J.; Lakhiar, I.A. Surface renewal application for estimating evapotranspiration: A review. *Adv. Meteorol.* 2018, *2018*, 1690714.

Huxman, T.E.; Wilcox, B.P.; Breshears, D.D.; Scott, R.L.; Snyder, K.A.; Small, E.E.; Hultine, K.; Pockman, W.T.; Jackson, R.B. Ecohydrological implications of woody plant encroachment. *Ecology* 2005, *86*, 308–319.

Kambatuku, J.R.; Cramer, M.D.; Ward, D. Overlap in soil water sources of savanna woody seedlings and grasses. *Ecohydrology* 2013, *6*, 464–473. https://doi.org/10.1002/eco.1273.

Kennedy, A.D.; Potgieter, A.L.F. Fire season affects size and architecture of *Colophospermum mopane* in southern African savannas. *Plant Ecol.* 2003, *167*, 179–192.

Kormos, P.R.; Marks, D.; Pierson, F.B.; Williams, C.J.; Hardegree, S.P.; Havens, S.; Hedrick, A.; Bates, J.D.; Svejcar, T.J. Ecosystem water availability in Juniper versus Sagebrush snow-dominated rangelands. *Rangel. Ecol. Manag.* 2017, *70*, 116–128.

MacGregor, S.D.; O'Connor, T.G. Patch dieback of *Colophospermum mopane* in a dysfunctional semi-arid African savanna. *Austral Ecol.* 2002, *27*, 385–395.

Makhado, R.A.; Mapaure, I.; Potgieter, M.J.; Luus-Powell, W.J.; Saidi, A.T. Factors influencing the adaptation and distribution of *Colophospermum mopane* in southern Africa's Mopane savannas—A review. *Bothalia* 2014, *44*, 1–9.

Mekhmandarov, Y.; Pirkner, M.; Achiman, O.; Tanny, J. Application of the surface renewal technique in two types of screenhouses: Sensible heat flux estimates and turbulence characteristics. *Agric. For. Meteorol.* 2015, *203*, 229–242.

Mengistu, M.G.; Savage, M.J. Open water evaporation estimation for a small shallow reservoir in winter using surface renewal. *J. Hydrol.* 2010a, *380*, 27–35.

Mengistu, M.G.; Savage, M.J. Surface renewal method for estimating sensible heat flux. *Water SA* 2010b, *36*, 9–18.

Mucina, L.; Rutherford, M.C. *The Vegetation of South Africa, Lesotho and Swaziland*; Strelitzia 19, South African National Biodiversity Institute: Pretoria, South Africa, 2006.

Palmer, A.R.; Ezenne, G.I.; Choruma, D.J.; Gwate, O.; Mantel, S.K.; Tanner, J.L. A comparison of three models used to determine water fluxes over the albany thicket, Eastern Cape, South Africa. *Agric. For. Meteorol.* 2020, *288–289*, 107984.

Paw U, K.T.; Qiu, J.; Su, H.B.; Watanabe, T.; Brunet, Y. Surface renewal analysis: A new method to obtain scalar fluxes. *Agric. For. Meteorol.* 1995, *74*, 119–137.

Poblete-Echeverría, C.; Sepúlveda-Reyes, D.; Ortega-Farías, S. Effect of height and time lag on the estimation of sensible heat flux over a drip-irrigated vineyard using the surface renewal (SR) method across distinct phenological stages. *Agric. Water Manag.* 2014, *141*, 74–83.

Pozníková, G.; Fischera, M.; van Kesterend, B.; Orsága, M.; Hlavinkaa, P.; Žalud, Z.; Trnka, M. Quantifying turbulent energy fluxes and evapotranspiration in agricultural field conditions: A comparison of micrometeorological methods. *Agric. Water Manag.* 2018, *209*, 249–263.

Rinne, J.; Ammann, C. Disjunct Eddy Covariance Method. In *Eddy Covariance A Practical Guide to Measurement and Data Analysis*; Aubinet, M., Vesala, T., Papale, D., Eds.; Springer: Dordrecht, The Netherlands, 2012; pp. 291–307.

Rosa, R.; Dicken, U.; Tanny, J. Estimating evapotranspiration from processing tomato using the surface renewal technique. *Biosyst. Eng.* 2013, *114*, 406–413.

Rosa, R.; Tanny, J. Surface renewal and eddy covariance measurements of sensible and latent heat fluxes of cotton during two growing seasons. *Biosyst. Eng.* 2015, *136*, 149–161.

Sala, O.E.; Maestre, F.T. Grass–woodland transitions: Determinants and consequences for ecosystem functioning and provisioning of services. *J. Ecol.* 2014, *102*, 1357–1362.

Savage, M.J. Web-Based Teaching, Learning and Research Using Real-Time Data from Field-Based Agrometeorological Measurement Systems. MScAgric Dissertation, University of KwaZulu-Natal, Durban, South Africa, 2014.

Savage, M.J. Estimation of grass reference evaporation and sensible heat flux using surface renewal and Monin-Obukhov similarity theory: A simple implementation of an iterative method. *J. Hydrol*. 2017, *547*, 742–754.

Schreiner-McGraw, A.P.; Vivoni, E.R.; Ajami, H.; Sala, O.E.; Throop, H.L.; Peters, D.P.C. Woody Plant Encroachment has a Larger Impact than Climate Change on Dryland Water Budgets. *Sci. Rep.* 2020, *10*, 8112.

Scott, R.L.; Huxman, T.E.; Williams, D.G.; Goodrich, D.C. Ecohydrological impacts of woody-plant encroachment: Seasonal patterns of water and carbon dioxide exchange within a semiarid riparian environment. *Glob. Change Biol.* 2006, *12*, 311–324.

Shapland, T.M.; McElrone, A.J.; Snyder, R.L.; Paw U, K.T. Structure function analysis of two-scale scalar ramps. Part II: Ramp characteristics and surface renewal flux estimation. *Bound.-Layer Meteorol.* 2012, *145*, 27–44.

Smit, G.N.; Rethman, N.F.G. Root biomass, depth distribution and relations with leaf biomass of *Colophospermum mopane*. *S. Afr. J. Bot.* 1998, *64*, 38–43.

Smit, G.N.; Rethman, N.F.G. The influence of tree thinning on the soil water in a semi-arid savanna of southern Africa. *J. Arid Environ.* 2000, *44*, 41–59.

Smit, G.N. An approach to tree thinning to structure southern African savannas for long-term restoration from bush encroachment. *J. Environ. Manag.* 2004, *71*, 179–191.

Snyder, R.L.; Spano, D.; Paw U, K.T. Surface renewal analysis for sensible and latent heat flux density. *Bound.-Layer Meteorol.* 1996, *77*, 249–266.

Soil Classification Working Group. *Soil Classification: A Natural and Anthropogenic System for South Africa*; Agricultural Research Council—Institute for Soil, Climate and Water: Pretoria, South Africa, 2018.

Spano, D.; Snyder, R.L.; Duce, P.; Paw U, K.T. Estimating sensible and latent heat flux densities from grapevine canopies using surface renewal. *Agric. For. Meteorol.* 2000, *104*, 171–183.

Stafford, W.; Birch, C.; Etter, H.; Blanchard, R.; Mudavanhu, S.; Angelstame, P.; Blignaut, J.; Ferreira, L.; Marais, C. The economics of landscape restoration: Benefits of controlling bush encroachment and invasive plant species in South Africa and Namibia. *Ecosys. Serv.* 2017, *27*, 193–202.

Stevens, N.; Swemmer, A.M.; Ezzy, L.; Erasmus, B.F.N. Investigating potential determinants of the distribution limits of a savanna woody plant: *Colophospermum mopane. J. Veg. Sci*. 2013, *25*, 363–373.

Stevens, N. What shapes the range edge of a dominant African savanna tree, *Colophospermum mopane*? A demographic approach. *Ecol. Evol.* 2021, *11*, 3726–3736.

Suvočarev, K.; Shapland, T.M.; Snyder, R.L.; Martinez-Cob, A. Surface renewal performance to independently estimate sensible and latent heat fluxes in heterogeneous crop surfaces. *J. Hydrol.* 2014, *509*, 83–93.

Van Atta, C.W. Effect of coherent structures on structure functions of temperature in the atmospheric boundary layer. *Arc. Mech.* 1977, *29*, 161–171.

Wang, J.; Buttar, N.A.; Hu, Y.; Lakhiar, I.A.; Javed, Q.; Shabbir, A. Estimation of sensible and latent heat fluxes using surface renewal method: Case study of a tea plantation. *Agronomy* 2021, *11*, 179.

Wedel, E.R.; Nippert, J.B.; Swemmer, A.M. Lowveld savanna bush cutting alters tree-grass interactions. In Proceedings of the XXIV International Grassland Congress, Virtual, 25–29 October 2021.

Whitecross, M.A.; Archibald, S.; Witkowski, E.T.F. Do freeze events create a demographic bottleneck for *Colophospermum mopane*? *S. Afr. J. Bot.* 2012, *83*, 9–18.

Zapata, N.; Martínez-Cob, A. Estimation of sensible and latent heat flux from natural sparse vegetation surfaces using surface renewal. *J. Hydrol.* 2001, *254*, 215–228.

Zapata, N.; Martínez-Cob, A. Evaluation of the surface renewal method to estimate wheat evapotranspiration. *Agric. Water Manag.* 2002, *55*, 141–157.

**Lead into Chapter 4**

It was also important to investigate the influence of woody plant thinning on soil hydrological processes because any changes to the movement and distribution of water in the soil can have a direct impact on the production of surface runoff, deep drainage and/or groundwater recharge. Therefore, at the same experimental woody plant clearing trial in a semi-arid savanna, a field-scale paired-plot experiment was conducted, with soil water content, soil temperature and evapotranspiration (ET) measured in plots that had been thinned of the dominant woody plant species (*Colophospermum mopane*) and adjacent encroached plots over a two-and-a-half-year period. Surface infiltration tests were also carried out.

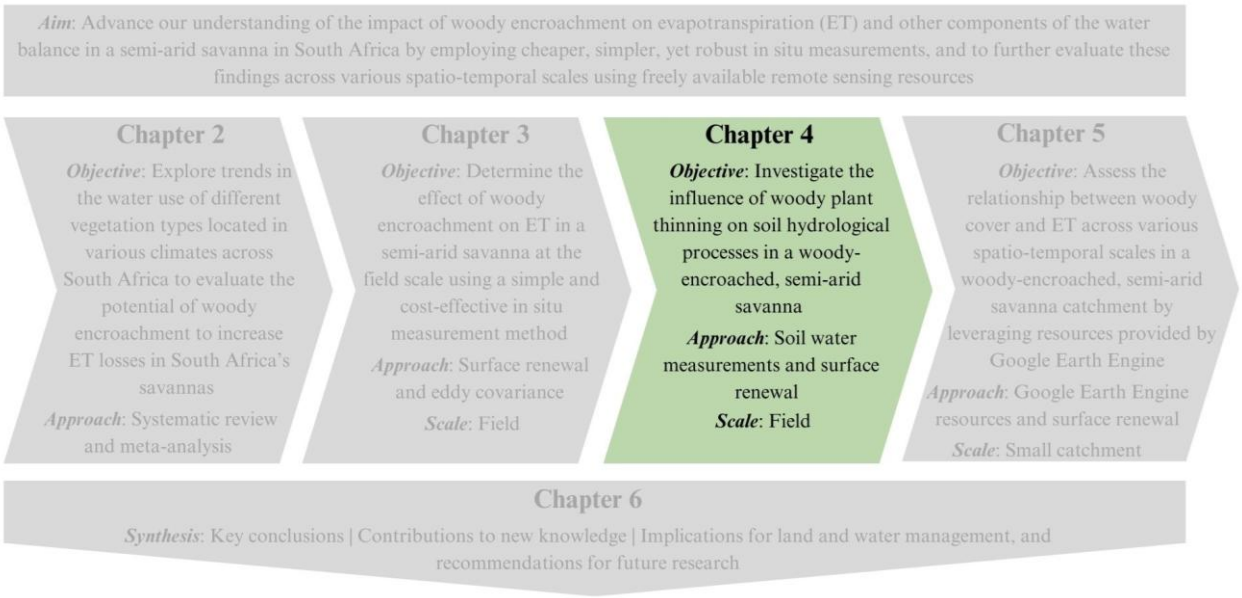

# 4 THE INFLUENCE OF WOODY PLANT THINNING ON SOIL HYDROLOGICAL PROCESSES: A PAIRED PLOT EXPERIMENT IN A WOODY-ENCROACHED, SEMI-ARID SAVANNA

## 4.1 Abstract

During the past 150 years, grassy biomes in drylands across the globe have undergone a shift from grass to woody dominance, a phenomenon commonly termed woody encroachment. The hydrological implications are of concern because a change in the dominant plant functional type can alter rainfall interception, plant water uptake and soil hydrological processes, with potentially significant implications for streamflow and groundwater recharge at the landscape scale. Removal of woody plants has long been proposed as a management strategy for increasing water yields, despite a lack of empirical evidence to prove its effectiveness. The current study investigated how woody plant thinning influenced soil hydrological processes in a woody-encroached, semi-arid savanna in South Africa. Over a two-and-a-half-year period, a field-scale paired-plot experiment was conducted, with soil water content, soil temperature and evapotranspiration (ET) measured in plots that had been thinned of the dominant woody plant species (*Colophospermum mopane*) and adjacent encroached plots. Surface infiltration tests were also carried out. Thinning had minor effects on soil water in the soil profile and soil temperature, and no pronounced effect on daily ET. Only one set of infiltration tests indicated a significant increase in infiltration following thinning. This contradicts the results of some similar studies in dryland savannas but is consistent with others. Whether thinning can increase the production of surface runoff or groundwater recharge over a longer time period in this study system requires further investigation.

***Keywords:*** *drylands, indigenous woody encroachment, surface runoff, groundwater recharge,* Colophospermum mopane*, climate variability, drought*

## 4.2 Introduction

Many grasslands and open savannas across the globe have seen a progressive increase in woody vegetation during the last 150 years (Bazan *et al*. 2012, Fan *et al*. 2019). This shift from grass to woody dominance, commonly termed woody encroachment, has primarily occurred in dryland ecosystems under semi-arid and subhumid climates, where annual potential evapotranspiration exceeds annual rainfall (Wilcox *et al*. 2022). Global increases in atmospheric $CO_2$ concentrations, regional shifts in climate and local-scale anthropogenic disturbances (e.g., changes in grazing regimes, fire suppression), are widely regarded as the

primary drivers (O'Connor *et al*. 2014, Stevens *et al*. 2016, Archer *et al*. 2017). Given the shortage of water in dryland ecosystems, which are simultaneously experiencing increasing climate variability, more intense and frequent drought, and increasing demands for freshwater, the hydrological implications of encroachment are of concern (Logan and Brunsell 2015, Acharya *et al*. 2018). It is believed that woody encroachment is decreasing streamflow and groundwater recharge because an increase in woody plant cover has the potential to increase rainfall interception and evapotranspiration, and decrease infiltration, leading to reduced soil water storage and deep drainage (Bazan *et al*. 2012, Acharya *et al*. 2018).

Removal of woody plants using various control methods (e.g., manual, mechanical, chemical, biological or fire) has long been proposed as a land management strategy to augment streamflow and groundwater recharge (Dugas *et al*. 1998, Keen *et al*. 2023). However, this can be costly and labour-intensive, and there is a lack of empirical evidence to prove its effectiveness, especially in drylands (Wilcox *et al*. 2005, Eldridge and Ding 2020). The few experimental studies that have been carried out in drylands indicate that a catchment's hydrological response to woody plant removal can be highly variable (Acharya *et al*. 2018). Woody plant removal can either increase (Dugas *et al*. 1998, Afinowicz *et al.* 2005, Moore *et al*. 2012, Ochoa *et al*. 2018, Durfee and Ochoa 2021, Wilcox *et al*. 2022), decrease (Leite *et al*. 2020, Schreiner-McGraw *et al*. 2020, Wilcox *et al*. 2022), or have little to no effect (Wilcox *et al*. 2005, Wilcox and Huang 2010, Bazan *et al*. 2012, Cardella Dammeyer *et al*. 2016) on streamflow and/or groundwater recharge. Ultimately, the hydrological response is determined not only by the degree of woody cover, but also by the climate, soil type and geology, topographic location, and spatial scale of the woody plant removal (Dugas *et al*. 1998, Acharya *et al*. 2018).

To fully comprehend the potential impact of woody encroachment or its removal on streamflow and/or groundwater recharge, it is necessary to first understand how woody plant cover influences the partitioning of rainfall into other hydrological processes within a catchment, i.e., evapotranspiration (ET), soil water storage and movement, infiltration and surface runoff (Huxman *et al*. 2005). Furthermore, how the change in root systems and/or organic matter inputs from woody plants affect soil properties or soil structure, which is critical in determining the subsurface soil's ability to hold and move water (Acharya *et al*. 2018). Changes to these hydrological processes and soil properties can have a direct influence on the

production of surface runoff, deep drainage and/or groundwater recharge (Acharya *et al*. 2018, Wilcox *et al*. 2022).

Most dryland studies agree that higher woody cover can translate to higher evapotranspiration losses, even if this is minor (Dugas *et al*. 1998, Afinowicz *et al*. 2005, Scott *et al*. 2014, Kormos *et al*. 2017, Ochoa *et al*. 2018, Wilcox *et al*. 2022). However, studies investigating the influence of woody cover on soil hydrological processes have reported more contradictory findings (Acharya *et al*. 2017).

Woody encroachment is prevalent in South Africa, affecting an estimated 10 to 20 million hectares of natural vegetation (Wigley *et al*. 2010, Buitenwerf *et al*. 2012, Munyati and Sinthumule 2016, Symeonakis *et al*. 2016, Marston *et al*. 2017, Skowno *et al*. 2017, Stafford *et al.* 2017, Maphanga *et al*. 2024). One of the most affected regions is the Greater Kruger National Park, the country's largest conservation area (Ferreria and Harmse 2014, Marston *et al*. 2017). The potential hydrological implications of woody encroachment in the Greater Kruger National Park is concerning, particularly in the northern part, because it experiences very dry conditions with a mean annual precipitation (MAP) of 375-475 mm (Bunting *et al*. 2016). To exacerbate the situation, global climate change models predict hotter and drier conditions for this region in coming decades (Bunting *et al*. 2016). The northern Greater Kruger National Park region is also projected to experience an increase in the cover of *Colophospermum mopane* (Mopane), one of the region's dominant woody encroacher species (Bunting *et al*. 2016). Little is known about Mopane's water-use strategies, but its predominantly shallow and lateral root system is thought to be an adaptation that enables it to share the same soil niche as grasses and other herbaceous plants and successfully compete for available soil water (Smit and Rethman 1998, Smit 2004). Mopane has also been reported to have a deeper taproot, allowing it to shift its water uptake into deeper soil water sources during dry periods (Sebego 1999).

This study investigated how woody plant thinning in a woody-encroached, semi-arid savanna influenced soil hydrological processes. Over a two-and-a-half-year period, a field-scale, paired-plot experiment was conducted in a semi-arid savanna ecosystem located in the northern Greater Kruger National Park region, South Africa. We hypothesized that thinning would lead to wetter soil profiles and higher soil water storage due to increased infiltration and reduced ET losses. If confirmed, large-scale woody plant thinning operations could promote

increased water yields in semi-arid savannas, thereby reducing their vulnerability to drought-related water shortages under global climate change.

## 4.3 Materials and methods

### *4.3.1 The study site and experimental design*

The study was conducted at an experimental woody plant clearing trial in the Mthimkhulu Game Reserve (23°31′46” S; 31°06′12” E) located in the Limpopo Province, north-eastern South Africa (Figure 4.1a). The Mthimkhulu Game Reserve borders the Kruger National Park with the Klein Letaba River, a tributary of the Groot Letaba river, separating the two. The climate of the area is semi-arid, with a mean annual temperature of 21.6°C and a MAP of 467 mm (Mucina and Rutherford 2006, Aldworth *et al*. 2023). The summers are hot and experience the majority of the annual rainfall, which falls mainly as high-intensity, short-duration thunderstorms, whereas winters are mild, dry and frost-free (Mucina and Rutherford 2006). The terrain is relatively flat with an elevation ranging between 300 m and 370 m above sea level (Mucina and Rutherford 2006). The geology is dominated by granites (Mucina and Rutherford 2006). The soils are characterized as shallow red-yellow apedals with good drainage, and are more than 1 m deep (Mucina and Rutherford 2006, Aldworth *et al*. 2023). The vegetation type of the Mthimkhulu Game Reserve is classified as Lowveld Mopaneveld, which is typically dominated by Mopane trees or shrubs (Mucina and Rutherford 2006). The reserve comprises of dense, monospecific Mopane stands scattered with *Combretum imberbe* (Leadwood), *Vachellia tortilis* (Umbrella thorn) and *Combretum apiculatum* (Red bushwillow) trees, and *Grewia bicolor* (Twotone raisin) shrubs. The grass layer is sparse, and dominated by annual *Aristida* species. Larger perennial species, such as *Urochloa mosambicensis* (Gonyagrass) and *Panicum maximum* (Guinea grass) are less common and are mostly found under tree and shrub canopies. Between Mopane stands, it is common for there to be patches of bare ground (typically a few meters in width) scattered with leaf litter.

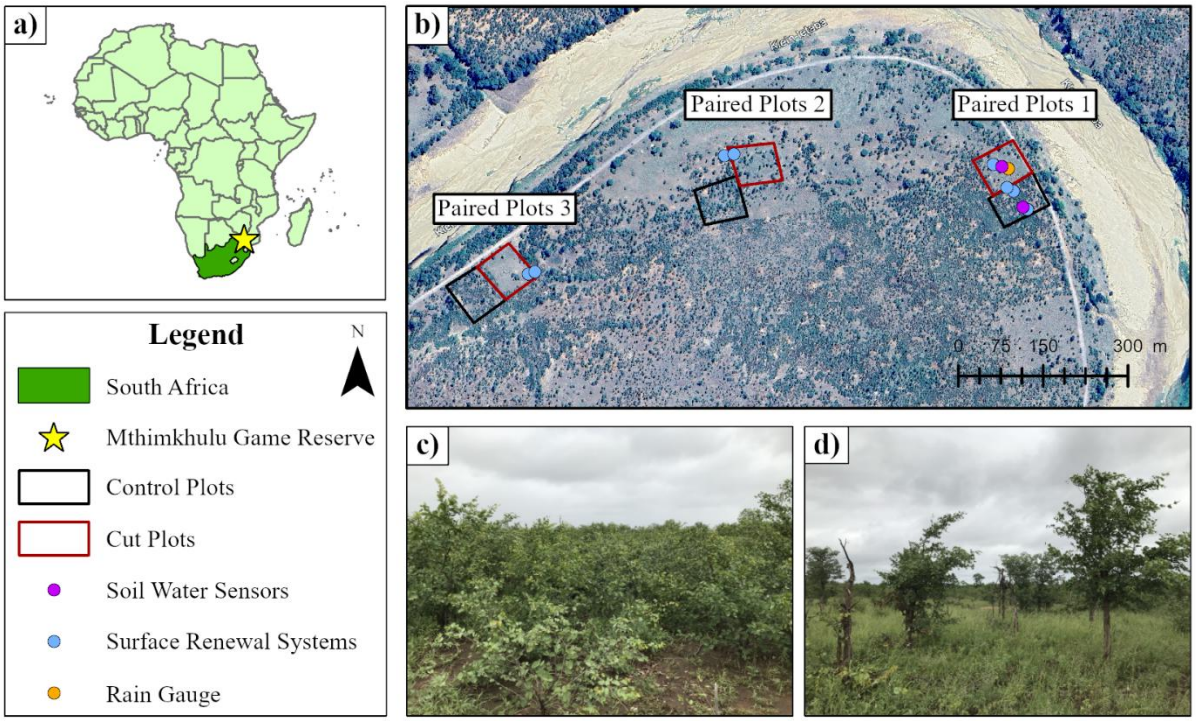


**Figure 4.1 a) Location of the Mthimkhulu Game Reserve in north-eastern South Africa, b) layout of paired plots 1, 2 and 3, and sensors in the Mthimkhulu Game Reserve, c) the vegetation in the control and d) cut plots.**

The Mthimkhulu trial was set up on an ancient alluvial floodplain of the Klein Letaba River and comprised of three paired 'control' and 'cut' plots positioned adjacent to one another (Figure 4.1b). Paired plot 1 was established in October 2014, and paired plots 2 and 3 in June 2015. Each control and cut plot were approximately 60×60 m in size. The control plots were left undisturbed and comprised of dense Mopane thickets, whereas the cut plots were thinned of Mopane less than 4 m in height (Figures 4.1c and 4.1d). The cut plots had an open savanna canopy structure, with a few large Mopane trees and scattered shrubs. Thinning was done by cutting individuals stems by hand, close to ground level. Roots were left undisturbed. Cut individuals resprouted vigorously at the start of the experiment, but all resprouting stems were cut to ground level 1-4 times per year (Table 4.3, *Appendix B*). Approximately 18% of the cut individuals had died by 2019, at the start of this study, and this rose to 80% by 2022.

Differences in vegetation structure of the plots are described by Wedel *et al*. (2024). Canopy cover of the woody vegetation, sampled with step-point transects, was approximately three times lower in the cut plots (Figure 4.6, *Appendix B*). Annual grass biomass, measured by

clipped peak standing biomass, was between 1.4 and 2.2 times higher in the cut plots (Figure 4.7, *Appendix B*).

### *4.3.2 Measurements of soil hydrological properties*

Soil samples were collected in paired plot 1 for measuring soil texture and bulk density. Undisturbed soil cores (98.13 $cm^3$ rings) were collected at depths of 100 mm, 300 mm and 500 mm to measure soil bulk density. To determine soil texture, an auger was used to collect mixed soil samples in sections of 200 mm increments at 0-200 mm, 200-400 mm and 400-600 mm depths at three sampling points in each plot. At each sampling point, any herbaceous vegetation and leaf litter was removed to expose the soil. The soil samples were put into labeled plastic bags and stored in a laboratory in cool conditions until processing. Soil bulk density was measured after oven drying the soil samples at 105 $^oC$ for 24 hours. Soil texture was determined by particle-size analysis using the dual hydrometer (Gee and Bauder 1986) and sieve method. The hydrometer method was used for the fine fractions of clay (< 0.002 mm) and silt (0.002 mm-0.02 mm), while sieving was used for the coarse sand fractions (0.02 mm-2 mm). Particle size distribution was analysed in accordance with the South African Soil Classification System (Soil Classification Working Group, 2018).

Infiltration tests were conducted at paired plot 1 in September 2021, at the end of the dry season, and at paired plots 1, 2 and 3 in July 2024 (middle of the dry season). Double ring infiltrometers (Bouwer 1986) were used, comprising of an outer ring with a diameter of 600 mm, and an inner ring with a diameter of 400 mm. Both rings had depths of 100 mm. Infiltration tests were repeated three to four times in grassy and bare soil areas of the control and cut plots. In the control plot, tests were carried out near Mopane stems and in canopy interspaces. Any herbaceous plants or litter present on the ground surface were left undisturbed prior to tests. The infiltrometer rings were hammered into the ground to a depth of around 30 mm and filled with water, taking care to avoid disturbance to the soil. A timer was started immediately, and the drop in the water level of the inner ring was recorded together with the time elapsed to determine the rate of water drop (i.e., the infiltration rate). A comparable water level in the outer ring to that in the inner ring was maintained throughout the tests. Both rings were re-filled with water when the inner ring's water levels had dropped substantially. Monitoring of the readings continued until a constant infiltration rate was obtained. Using the infiltration datasets acquired, cumulative infiltration versus time characteristic curves were plotted for each test repetition.

### *4.3.3 Field measurements*

Field measurements of soil volumetric water content, soil temperature and ET were carried out between December 2019 and mid-July 2022. Soil volumetric water content was measured in all three paired plots, while soil temperature and ET were only measured in paired plot 1. All measurements were replicated in both the control and cut plots. Rainfall was monitored at an automatic weather station in the cut plot of paired plot 1 using a tipping bucket rain gauge (TR-525, Texas Electronics Inc., Dallas, TX, USA) installed with its orifice at 1.2 m above the ground.

Soil volumetric water content ($mm^3\ mm^{-3}$) was measured using soil water content sensors (CS655, Campbell Scientific Inc., Logan, UT, USA) connected to CR1000X (Campbell Scientific Inc.) and CR300 (Campbell Scientific Inc.) data loggers. Soil pits were dug and sensors were installed horizontally into the undisturbed soil matrix at 100 mm, 300 mm and 800 mm depths in all three paired plots. In paired plot 1, an additional set of sensors were installed at 100 mm, 300 mm and 500 mm depths. Following sensor installation, each soil pit was backfilled with the same layer of excavated soil and carefully compacted. In the control plots, the sensors were installed beneath canopies and in canopy interspaces.

Soil water storage (mm) of the upper 600 mm or 900 mm of the soil profile was calculated using the following equation (Zou *et al*. 2014):

$$SWS = \sum_{i=1}^{n} \theta_{vi} \times d_i \tag{4.1}$$

where, soil water storage is the soil water storage, $\theta_v$ is the soil volumetric water content and $d_i$ is the soil layer depth (mm). The $d_i$ ranged between 200 mm and 350 mm, depending on the depth of the sensors.

Evapotranspiration ($mm\ d^{-1}$) was estimated using the residual of the energy balance (REB) method, where the shortened energy balance equation (i.e., LE = Rn−G−H) is solved to obtain latent heat flux (LE) using net radiation (Rn), soil heat flux (G) and sensible heat flux (H) estimates. Net radiation ($W\ m^{-2}$) was measured with a net radiometer (NR Lite 2, Kipp & Zonen, Delft, The Netherlands) and G ($W\ m^{-2}$) was determined using measurements from soil heat flux plates (HFP01, Hukseflux Thermal Sensors, Delft, The Netherlands), averaging soil thermocouple probes (TCAV, Campbell Scientific, Inc.), soil volumetric water content sensors

(CS655, Campbell Scientific Inc.) and soil bulk density. Sensible heat flux (W $m^{-2}$) was estimated using the surface renewal method, specifically the surface renewal 1 (SR1) approach, which has been found to be the most suitable surface renewal approach for estimating ET at the Mthimkhulu trial (Aldworth *et al.* 2023). The surface renewal systems measured high frequency air temperature using chromel-constantan fine-wire thermocouples (76 µm diameter) (TCBR-3, Campbell Scientific Inc.). The thermocouples, along with the Rn and G sensors, were connected to CR1000X (Campbell Scientific Inc.) data loggers.

Surface renewal 1 H estimates require site-specific calibration against a standard flux measurement method, to account for uneven heating of the air parcel below the sensor. Therefore, week-long eddy covariance campaigns were carried out alongside the surface renewal systems during the summer of February 2020 and the spring of October-November 2020. The eddy covariance systems measured three-dimensional wind speed and air temperature using a sonic anemometer (CSAT3, Campbell Scientific Inc.), and $H_20$ and $CO_2$ fluxes using a fast response gas analyzer (EC150, Campbell Scientific Inc.). The eddy covariance sensors were connected to an electronics panel (EC100, Campbell Scientific Inc.) and a CR3000 data logger (Campbell Scientific Inc.) programed with EasyFlux DL software (Campbell Scientific 2020).

More information relating to the theory of the SR1 and eddy covariance methods, layout of the sensors, the methods used to process the SR1 and eddy covariance data, and the calibration process are described in Aldworth *et al.* (2023).

Soil temperature data was obtained from the averaging soil thermocouple probes from the surface renewal systems. The probes were installed at depths of 20 mm and 60 mm.

### *4.3.4 Statistical analysis*

Differences in infiltration rates between the control and cut plots were analysed by fitting the 'Philip Two Term Model' (Philip 1957), which is still widely used for comparing double-ring infiltration data (Jha *et al*. 2019, Rahmati *et al*. 2018):

$$I(t) = S_p\, t^{0.5} + A\, t \qquad (4.2)$$

where $I(t)$ is the cumulative infiltration at time $t$, $S_p$ is soil sorptivity (mm/min$^{0.5}$), a function of initial soil water content and soil water diffusivity, and $A$ is a parameter providing an estimate of field-saturated hydraulic conductivity (mm min$^{-1}$).

This model was fit to the data for each replicate in each paired plot, with separate models for the 2021 and 2024 samples from paired plot 1, using the *nls* function in the R package 'nlme'. Estimates of $S_p$ and $A$ were then analysed using ANOVA, and differences between the control and cut plots for each paired plot tested with post-hoc tests of least square means, with a Bonferroni adjustment for multiple comparisons.

The time series of soil volumetric water content data for each sensor showed strong serial autocorrelation, non-stationarity and non-normality, and most had large sections of missing data. This precluded the fitting of a typical regression time-series model for comparing means between control and cut plots. Instead, a subsampling, permutation approach was used. Differences between control and cut plot soil volumetric water content values were calculated for each 5-minute sampling interval, for each pair of sensors at each depth in each plot. Sub-samples of 100 difference values were then randomly selected from each pair, and a mean difference calculated. This was iterated 10 000 times to produce a sampling distribution of means, and the 95% range of these was used as the test of whether the mean difference was significantly greater than zero.

## 4.4 Results

### *4.4.1 Soil properties*

Following the South African Soil Classification System (Soil Classification Working Group, 2018), the dominant soil form in the experimental trial area was an alluvial Oakleaf. The soil texture at paired plot 1 was similar in both the control and cut plots. The soils were mostly sandy loams or sandy clay loams, with a high average sand fraction (46-78%), and lower silt (12-29%) and clay (8-29%) fractions (Table 4.4, *Appendix B*). The soil bulk density for the upper 0.6 m of the soil profile was also similar between the plots, with a mean soil bulk density of 1.57 g cm$^{-3}$ and 1.52 g cm$^{-3}$ in the control and cut plots, respectively (Table 4.5, *Appendix B*).

### *4.4.2 Soil infiltrability*

The initial soil infiltration tests in 2021 at paired plot 1 revealed higher infiltration rates for the cut plot compared to the control plot (Figure 4.2a). Although not as pronounced, this same pattern was also evident in the 2024 tests for paired plots 1 (Figure 4.2b). This was reflected by the ANOVA of the infiltration model parameters for paired plot 1 - both $S_p$ and $A$ were significantly greater in the cut plot in 2021, and $A$ greater in 2024 (Table 4.1). In paired plots 2 and 3, infiltration in the control and cut plots appeared to be similar and the parameters were not significantly different (Figures 4.2c and 4.2d).

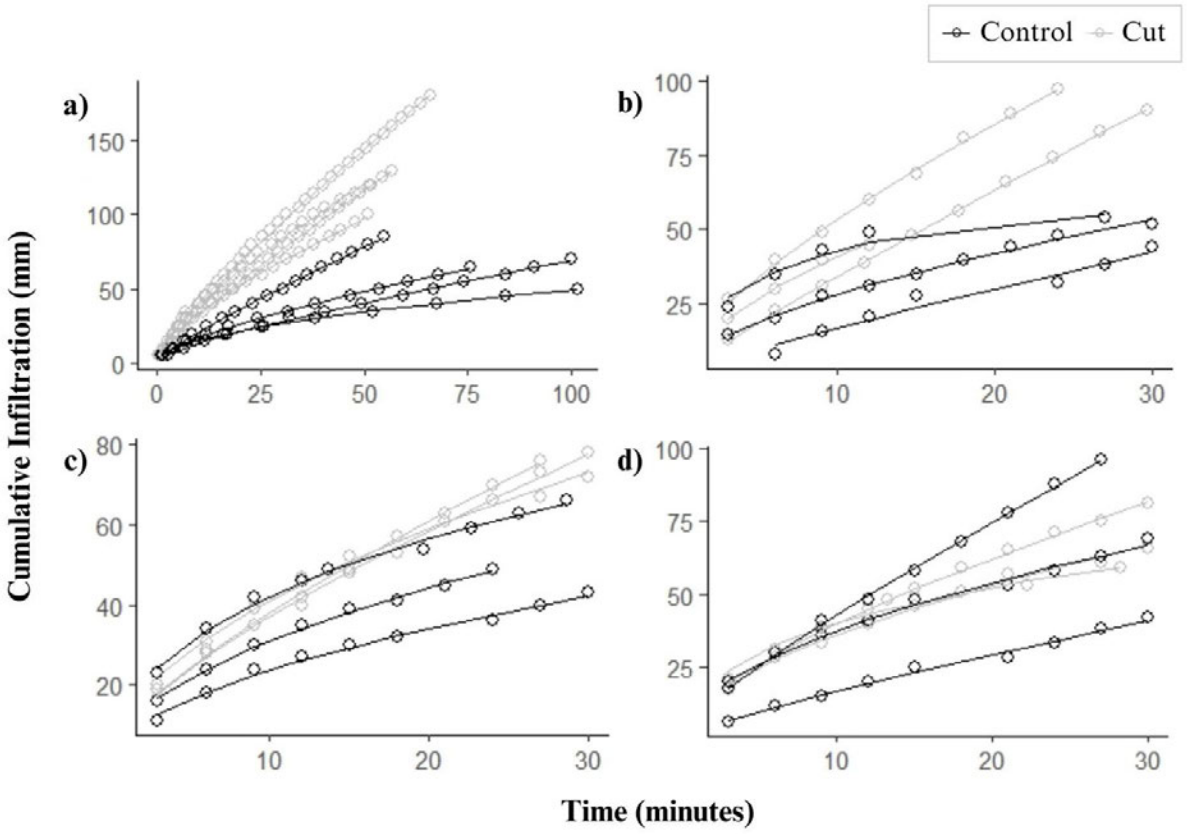


**Figure 4.2 Cumulative infiltration versus time curves at paired plot 1 for tests conducted in a) September 2021 and b) July 2024, and c) paired plot 2 and d) paired plot 3 for tests conducted in July 2024. The dotted lines are best-fit curves for each repetition of the infiltration tests.**

**Table 4.1 Contrasts for least square means of the $S_p$ and $A$ parameters estimated for the fitting of the Philip Two Term Model to the double ring infiltration data.**

| Contrast | Group | Estimate | SE | df | t ratio | p value |
|---|---|---|---|---|---|---|
| $S_p$ | Plot 1 2021 | 3.40 | 0.93 | 18 | 10.90 | < 0.01 |
| | Plot 1 2024 | -1.07 | 3.98 | 18 | -0.27 | 0.79 |
| Cut - Control | Plot 2 2024 | -0.82 | 3.98 | 18 | -0.21 | 0.84 |
| | Plot 3 2024 | 5.11 | 3.98 | 18 | 1.29 | 0.22 |
| $A$ | Plot 1 2021 | 0.91 | 0.34 | 18 | -2.7 | < 0.01 |
| | Plot 1 2024 | 1.7 | 0.74 | 18 | 2.3 | 0.04 |
| Cut - Control | Plot 2 2024 | 0.91 | 0.74 | 18 | 1.2 | 0.24 |
| | Plot 3 2024 | -0.98 | 0.74 | 18 | -1.3 | 0.21 |

### *4.4.3 Soil water and temperature*

The rainfall season began in spring and continued into autumn during the three hydrological years of the study, with the greatest number of rainfall days typically occurring in summer (Figure 4.3a). Except for several days of low rainfall in the 2021-2022 hydrological year, no rainfall occurred in winter. These highly seasonal rainfall patterns were reflected in the soil volumetric water content across all plots, with the wettest soil conditions occurring during the summer (up to 0.45 $mm^3\,mm^{-3}$ across the soil profile), and the driest occurring during the winter (between 0.03 $mm^3\,mm^{-3}$ and 0.25 $mm^3\,mm^{-3}$ across the soil profile) (Figures 4.8 – 4.11, *Appendix B*).

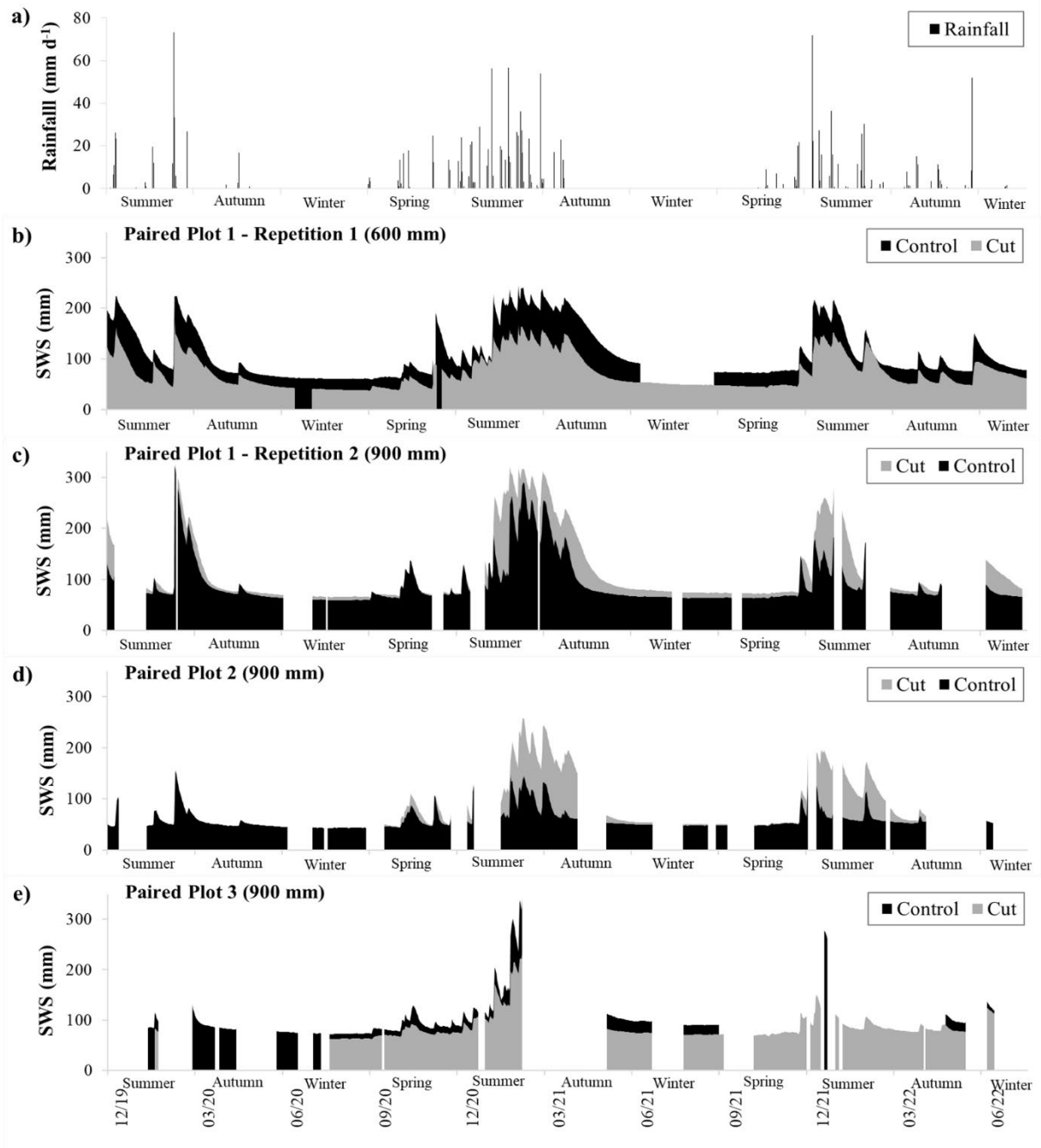


**Figure 4.3 Daily a) rainfall and b)-e) soil water storage (SWS) for the upper 600 mm or 900 mm of the soil profile for paired plots 1, 2 and 3 over the measurement period.**

The soil water data indicated a lack of a consistent effect of woody plant thinning on soil volumetric water content and soil water storage across the three paired plots (Figure 4.3b – 4.3e). Mean soil volumetric water content differed between each sensor pair at each paired plot, but differences were relatively small, with mean differences ranging from 0.01 to 0.05 $mm^3$ $mm^{-3}$ (Table 4.2). These differences were consistent across depths within each pair of control and cut plots, but not consistent across the three paired plots. In two of the paired plots, soil

volumetric water content and soil water storage were on average higher in the cut plots relative to the paired control plots, while in the third paired plot, the cut plots had drier soils. While differences for the first replicate in paired plot 1 were not tested statistically, the pattern here was clearly similar to that of paired plot 3, and opposite to that of the second repetition at paired plot 1. Differences in soil volumetric water content and soil water storage between the control and cut plots were greatest in summer and less pronounced in winter, and differences in soil volumetric water content between the plots increased with soil depth.

**Table 4.2 Means of the differences between soil volumetric water content between sensors of the same depth in each pair of control and cut plots. Differences were cut minus control (i.e. a positive value indicates greater soil volumetric water content in the cut plot). Means and confidence intervals were calculated from 10 000 iterations of 100 subsamples randomly selected from the time series of differences between each sensor pair.**

| Paired Plot | Depth (mm) | Mean Difference (mm3 mm-3) | 95% Confidence Interval | |
|---|---|---|---|---|
| | | | Lower | Upper |
| 1 | 10 | 0.036 | 0.029 | 0.043 |
| | 30 | 0.02 | 0.013 | 0.028 |
| | 80 | 0.024 | 0.016 | 0.033 |
| 2 | 10 | 0.052 | 0.044 | 0.061 |
| | 30 | 0.028 | 0.019 | 0.037 |
| | 80 | 0.04 | 0.027 | 0.053 |
| 3 | 10 | -0.009 | -0.006 | -0.013 |
| | 30 | -0.022 | -0.018 | -0.026 |
| | 80 | -0.038 | -0.026 | -0.039 |

The mean and minimum daily soil temperatures (soil $T_{mean}$ and $T_{min}$) were similar in the control and cut plots throughout the measurement period (Figures 4.4a and 4.4c). However, there were differences in the maximum daily soil temperatures (soil $T_{max}$) between the plots leading up to and during some season transitions, particularly in the 2020-2021 hydrological year (Figure 4.4b). In the winter and spring, the control plot had a higher soil $T_{max}$ than the cut plot, but in autumn, the cut plot was higher. This pattern continued into the next 2021-2022 hydrological year throughout the spring and into the first half of summer.

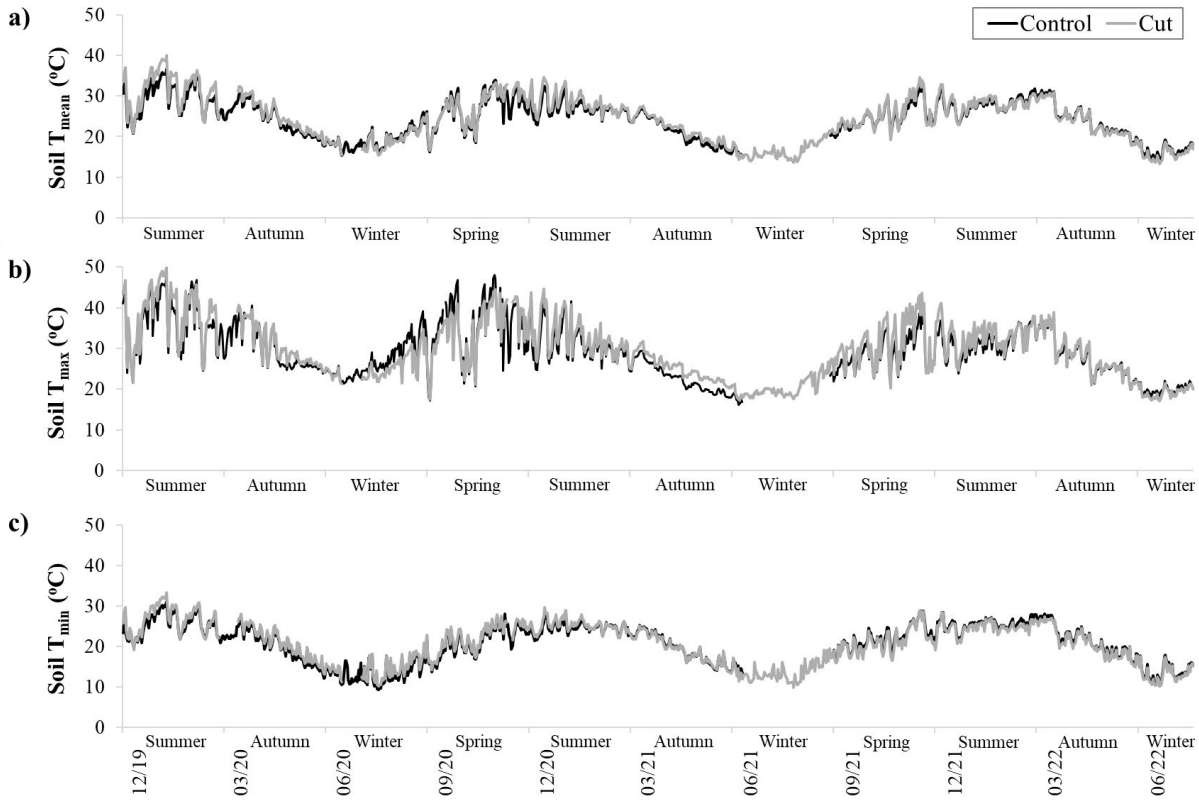


**Figure 4.4 Mean, maximum and minimum daily soil temperature (Soil $T_{mean}$, $T_{max}$ and $T_{min}$) measured in the upper 60 mm of the soil over the measurement period.**

### *4.4.4 Evapotranspiration losses*

Similar to the observations of soil water, ET reflected the highly seasonal patterns of rainfall, with the highest ET occurring in summer and the lowest in winter (Figures 4.5a and 4.5b). Differences in ET between the control and cut plots were only apparent during the season transitions of the 2020-2021 hydrological year. At the start of the wet season in spring, the cut plot had higher ET than the control plot, but as the wet season progressed into autumn and winter, the control plot had higher ET than the cut plot.

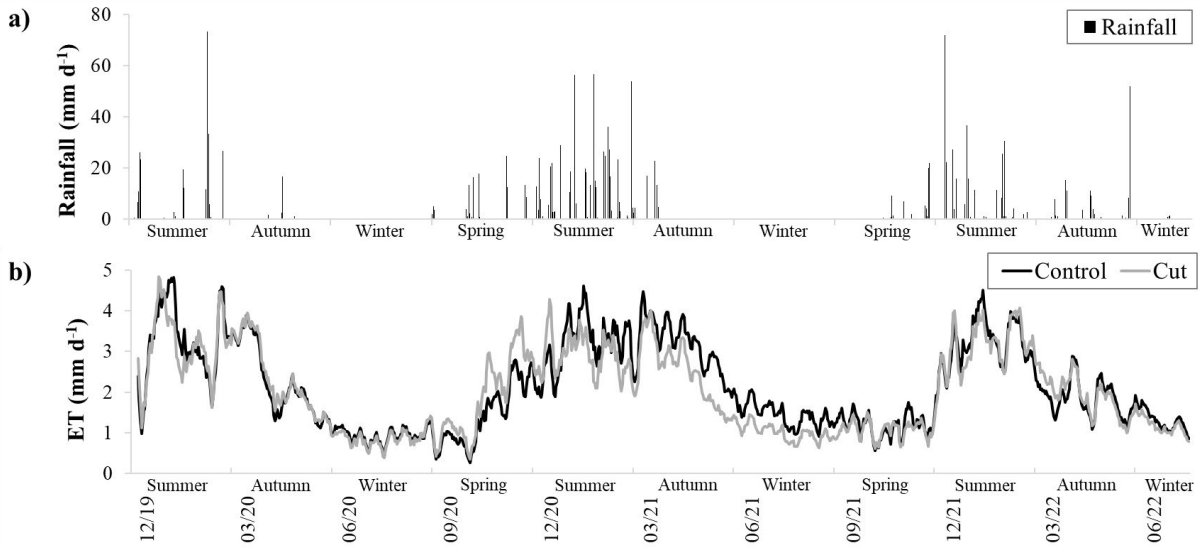


**Figure 4.5 Daily a) rainfall and b) evapotranspiration (ET) over the measurement period. Evapotranspiration is a seven-day moving average to minimize fluctuations and make trends more visible.**

## 4.5 Discussion

Our findings suggest that woody plant thinning had little effect on soil water storage, infiltration and ET at the daily and plot scales. The differences in mean soil volumetric water content between the control and cut plots were relatively small, and no consistent effect of thinning was observed across the three paired plots. Likewise, differences in infiltration were not consistent across the three plots. The ET measurements revealed that thinning only led to differences in daily ET during some season transitions, and these differences were relatively small and variable.

Prior studies on the effect of woody cover on soil water report contradictory findings. On the one hand, higher woody cover led to increased soil water content (Pierce and Reich 2010, Fan *et al.* 2019, Geissler *et al.* 2019), which was generally attributed to the fact that patches of woody plants improved infiltration rates following rainfall events, thereby increasing the amount of water stored in the upper soil layers beneath their canopies. In contrast, higher woody cover resulted in lower soil water content due to the greater water uptake of woody plants (Li and Wilson 1998, Smit and Rethman 2000). In contradiction to many of these studies, we anticipated that the recovery of the grass layer after thinning would promote infiltration and increase soil water due to a greater cover of grass tufts and a higher density of grass roots.

Furthermore, that the decomposed roots of the dead Mopane that remained after cutting would encourage infiltration by enhancing soil microporosity, creating preferential flow *channels* and increasing total organic matter. When digging the soil pits for the soil water sensors, we observed that the soils in the encroached control plots were compacted compared to the cut plots. It is common for woody-encroached sites in drier areas to be highly vulnerable to surface sealing and soil compaction, due to the exposure of bare soils to raindrop impact and trampling by large mammals (Smit and Rethman 2000). However, our infiltration tests did not indicate such changes had occurred. The soil properties analysis supports our soil water findings, as soil texture and bulk density were similar in the control and cut plots. The relatively minor change in ET was also consistent with the small and inconsistent differences found for soil volumetric water content. We expected that reduced ET losses after thinning would increase soil water in the cut plots, however, a previous study at the Mthimkhulu trial by Aldworth *et al*. (2023) discovered that thinning had a major effect on reducing ET only after a longer time period.

Although there were dense Mopane thickets and understorey grasses present in the control plots, it was common for there to be large patches of bare ground between stands. It is likely that soil evaporation from these patches was less than the transpiration of the Mopane trees and the grasses, thus reducing the actual ET in these plots. There were fewer bare soil batches in the cut plots, where grass cover and biomass was higher. Therefore, it is likely that the Mopane trees in the control plots had higher transpiration than the grass layer in the cut plots, but the occurrence of bare batches (with relatively lower evaporation) led to approximately equal ET across both types of plots. We anticipated that Mopane would have had more of an influence on soil water because of its shallow, lateral root system and deeper taproot (Smit 2004, Sebego 1999), allowing it to be a successful competitor against grasses for available soil water. Mopane roots may have also been able to encourage hydraulic lift, a process where plant roots facilitate the movement of deep soil water to shallower depths (Graz 2008, Yu and D'Odorico 2015). Fan *et al.* (2019), Potts *et al*. (2010) and Geissler *et al*. (2019) suggested that hydraulic lift was a potential explanation for the higher soil water content at their sites. Shading by the Mopane's dense canopies and litter accumulation may have also affected soil water, as Pierce and Reich (2009) suspected at their site. The soils in the encroached control plots would have received much more shading throughout the year, which we would expect to lower soil evaporation and temperatures, and hence allow the soils to hold more water. However, soil temperatures were generally comparable between the control and cut plots throughout the measurement period.

The fairly small sample size and short measurement period of our study's field measurements, a consequence of time and cost constraints, contributed to uncertainty in our results. Soil water can be highly spatially variable, even at small scales (Räsänen *et al*. 2020), necessitating many replications to account for this variation. Root decomposition and soil property changes caused by thinning will take time, and only with a longer measurement record may these effects on soil water become more evident. Therefore, replicating soil water sensors within our plots over longer measurement periods may have been necessary to detect any treatment effects with confidence. The use of standardized soil depths to interpret soil volumetric water content in soil profiles also introduces uncertainty in the soil water patterns. A focus on diagnostic soil horizons may be more appropriate for accounting for variations in soil hydrological processes caused by textural differences in the soil horizons, which may be missed if more than one probe is installed in the same horizon. The issue of lag effects in the hydrological response also raises questions. There have been few similar studies that have discussed lag effects, one of which was conducted by Dugas *et al*. (1998), who found that removing woody plants only reduced ET losses for two years after treatment. Our experimental plots were established in 2014 and 2015, thus thinning had been carried out for 4 to 5 years by the time that the field measurements began. Therefore, we expected our study did capture medium-term effects of thinning.

The inconsistent results from various studies investigating the effect of woody plant cover on surface runoff and/or groundwater recharge in dryland ecosystems, including this study, make it clear that more extensive, long-term research is necessary to establish a general and global understanding of the topic. Such studies need to consider the many factors that can result in site-specific patterns, including the seasonality and intensity of rainfall, antecedent soil moisture (especially in shallow soil), infiltration capacity and deep recharge. Such research will become increasingly important as we experience more and more water shortages due to climate variability and drought, and the implementation of management strategies to strengthen our resilience becomes more critical.

### 4.6 Conclusion

Our study demonstrated that thinning of woody plants in a woody-encroached, semi-arid savanna in South Africa had only minor effects on soil hydrological processes within the time frame of our study. Although our study involved experimental plots where woody cover was reduced for more than four years, greater differences may yet emerge in the long-term, as

further changes to the herbaceous layer, and possibly soil structure, occur. Whether such changes would ever be large enough to substantially alter surface runoff and groundwater recharge still requires investigation. As climate change is expected to increase the occurrence and intensity of drought, and water shortages in this water-stressed study region, assessment of the longer-term impacts of such thinning would be valuable. Furthermore, additional studies like this one are needed to understand why thinning results in significant hydrological changes in some ecosystems but not others, and what the primary determinants of these differences are. With this knowledge, we will be able to establish the role that woody encroachment control strategies can play in aiding sustainable water resource management.

### 4.7 References


Acharya BS, Hao Y, Ochsner TE, Zou CB. 2017. Woody plant encroachment alters soil hydrological properties and reduces downward flux of water in tallgrass prairie. *Plant Soil* 414: 379-391. https://doi.org/10.1007/s11104-016-3138-0.

Acharya BS, Kharel G, Zou CB, Wilcox BP, Halihan T. 2018. Woody plant encroachment impacts on groundwater recharge: A review. *Water* 10(10): 1466. https://doi.org/10.3390/w10101466.

Afinowicz JD, Munster CL, Wilcox BP. 2005. Modeling effects of brush management on the rangeland water budget: Edwards Plateau, Texas. *JAWRA Journal of the American Water Resources Association* 41(1): 181-193. https://doi.org/10.1111/j.1752-1688.2005.tb03727.x.

Aldworth TA, Toucher ML, Clulow AD, Swemmer AM. 2023. The effect of woody encroachment on evapotranspiration in a semi-arid Savanna. *Hydrology* 10(1), 9. https://doi.org/10.3390/hydrology10010009.

Archer SR, Andersen EM, Predick KI, Schwinning S, Steidl RJ, Woods SR. 2017. Woody plant encroachment: causes and consequences. *Rangeland Systems: Processes, Management and Challenges* 25-84. https://doi.org/10.1007/978-3-319-46709-2.

Bazan RA, Wilcox BP, Munster C, Gary M. 2013. Removing woody vegetation has little effect on conduit flow recharge. *Ecohydrology* 6(3): 435-443. https://doi.org/10.1002/eco.1277.

Buitenwerf R, Bond WJ, Stevens N, Trollope W. 2012. Increased tree densities in South African savannas :> 50 years of data suggests $CO_2$ as a driver. *Global Change Biology* 18(2): 675-684. https://doi.org/10.1111/j.1365-2486.2011.02561.x.

Bouwer H. 1986. Intake rate: cylinder infiltrometer. In Klute A (ed.). Methods of Soil Analysis, Part 1, 2nd ed. Physical and Mineralogical Methods. American Society of Agronomy and Soil Science Society of America. Madison, Wisconsin, USA.

Bunting EL, Fullman T, Kiker G, Southworth J. 2016. Utilization of the SAVANNA model to analyze future patterns of vegetation cover in Kruger National Park under changing

climate. *Ecological Modelling* 342: 147-160. http://doi.org/10.1016/j.ecolmodel.2016.09.012.

Campbell Scientific. 2020. EASYFLUX DL CR3000OP for CR3000 and Open-Path Eddy-Covariance System Revision: 3/18. https://s.campbellsci.com/documents/us/manuals/easyflux-dl.pdf [accessed 14 August 2023].

Cardella Dammeyer H, Schwinning S, Schwartz BF, Moore GW. 2016. Effects of juniper removal and rainfall variation on tree transpiration in a semi-arid karst: evidence of complex water storage dynamics. *Hydrological Processes 30*(24), 4568-4581. https://doi.org/10.1002/hyp.10938.

Dugas WA, Hicks RA, Wright P. 1998. Effect of removal of *Juniperus ashei* on evapotranspiration and runoff in the Seco Creek watershed. *Water Resources Research* 34(6): 1499-1506. https://doi.org/10.1029/98WR00556.

Durfee N, Ochoa CG. 2021. The seasonal water balance of western-juniper-dominated and big-sagebrush-dominated watersheds. *Hydrology* 8(4): 156. https://doi.org/10.3390/hydrology8040156.

Eldridge DJ, Ding J. 2021. Remove or retain: ecosystem effects of woody encroachment and removal are linked to plant structural and functional traits. *New Phytologist* 229(5): 2637-2646. https://doi.org/10.1111/nph.17045.

Fan Y, Li XY, Huang H, Wu XC, Yu KL, Wei JQ, Zhang CC, Wang P, Hu X, D'Odorico P. 2019. Does phenology play a role in the feedbacks underlying shrub encroachment? *Science of the Total Environment* 657: 1064-1073. https://doi.org/10.1016/j.scitotenv.2018.12.125.

Ferreira S, Harmse A. 2014. Kruger National Park: Tourism development and issues around the management of large numbers of tourists. *Journal of Ecotourism* 13(1): 16-34. https://doi.org/10.1080/14724049.2014.925907.

Gee GW, Bauder JW. 1986. Particle-size analysis. In Klute A (ed). Methods of Soil Analysis, Part 1, 2nd ed. Agronomy Monograph No 9. American Society of Agronomy and Soil Science Society of America. Madison, Wisconsin, USA.

Geissler K, Hahn C, Joubert D, Blaum N. 2019. Functional responses of the herbaceous plant community explain ecohydrological impacts of savanna shrub encroachment. *Perspectives in Plant Ecology, Evolution and Systematics* 39: 125458. https://doi.org/10.1016/j.ppees.2019.125458.

Graz FP. 2008. The woody weed encroachment puzzle: gathering pieces. *Ecohydrology* 1: 340-348. https://doi.org/10.1002/eco.28.

Huxman TE, Wilcox BP, Breshears DD, Scott RL, Snyder KA, Small EE, Hultine K, Pockman WT, Jackson RB. 2005. Ecohydrological implications of woody plant encroachment. *Ecology* 86(2): 308-319. https://doi.org/10.1890/03-0583.

Jha MK, Mahapatra S, Mohan C, Pohshna C. 2019. Infiltration characteristics of lateritic vadose zones: Field experiments and modeling. *Soil and Tillage Research* 187: 219-234. https://doi.org/10.1016/j.still.2018.12.007.

Keen RM, Nippert JB, Sullivan PL, Ratajczak Z, Ritchey B, O'Keefe K, Dodds WK. 2023. Impacts of riparian and non-riparian woody encroachment on tallgrass prairie ecohydrology. *Ecosystems* 26(2): 290-301.

Kormos PR, Marks D, Pierson FB, Williams CJ, Hardegree SP, Havens S, Hedrick A, Bates JD, Svejcar TJ. 2017. Ecosystem water availability in juniper versus sagebrush snow-dominated rangelands. *Rangeland Ecology & Management* 70(1): 116-128. https://doi.org/10.1016/j.rama.2016.05.003.

Leite PA, Wilcox BP, McInnes KJ. 2020. Woody plant encroachment enhances soil infiltrability of a semiarid karst savanna. *Environmental Research Communications* 2(11): 115005. https://doi.org/10.1088/2515-7620/abc92f.

Li X, Wilson SD. 1998. Facilitation among woody plants establishing in an old field. *Ecology* 79(8): 2694-2705. https://doi.org/10.1890/0012-9658.

Logan KE, Brunsell NA. 2015. Influence of drought on growing season carbon and water cycling with changing land cover. *Agricultural and Forest Meteorology* 213: 217-225. https://doi.org/10.1016/j.agrformet.2015.07.002.

Maphanga T, Shoko C, Sibanda M, Thamaga KH, Dube T. 2024. Understanding the spatio-temporal distribution of bush encroachment in savannah rangelands, South Africa. *Geocarto International* 39(1): 2366515. https://doi.org/10.1080/10106049.2024.2366515.

Marston CG, Aplin P, Wilkinson DM, Field R, O'Regan HJ. 2017. Scrubbing up: multi-scale investigation of woody encroachment in a southern African Savannah. *Remote Sensing* 9(5): 419. https://doi.org/10.3390/rs9050419.

Moore GW, Barre DA, Owens MK. 2012. Does shrub removal increase groundwater recharge in southwestern Texas semiarid rangelands? *Rangeland Ecology & Management* 65(1): 1-10. https://doi.org/10.2111/REM-D-11-00055.1.

Mucina L, Rutherford MC. 2006. *The Vegetation of South Africa, Lesotho and Swaziland*; Strelitzia 19, South African National Biodiversity Institute: Pretoria, South Africa.

Munyati C, Sinthumule NI. 2016. Change in woody cover at representative sites in the Kruger National Park, South Africa, based on historical imagery. *SpringerPlus* 5: 1-23. https://doi.org/10.1186/s40064-016-3036-1.

Ochoa CG, Caruso P, Ray G, Deboodt T, Jarvis WT, Guldan SJ. 2018. Ecohydrologic connections in semiarid watershed systems of central Oregon USA. *Water* 10(2): 181. https://doi.org/10.3390/w10020181.

O'Connor TG, Puttick JR, Hoffman MT. 2014. Bush encroachment in southern Africa: changes and causes. *African Journal of Range & Forage Science 31*(2): 67-88. http://dx.doi.org/10.2989/10220119.2014.939996.

Philip JR. 1957. The theory of infiltration: 3. Moisture profiles and relation to experiment. *Soil Science*, 84(2): 163-178.

Pierce AM, Reich PB. 2010. The effects of eastern red cedar (*Juniperus virginiana*) invasion and removal on a dry bluff prairie ecosystem. *Biological Invasions* 12: 241-252. https://doi.org/10.1007/s10530-009-9446-z.

Potts DL, Scott RL, Bayram S, Carbonara J. 2010. Woody plants modulate the temporal dynamics of soil moisture in a semi-arid mesquite savanna. *Ecohydrology: Ecosystems, Land and Water Process Interactions, Ecohydrogeomorphology*, 3(1): 20-27. https://doi.org/10.1002/eco.91.

Rahmati M, Weihermüller L, Vanderborght J, Pachepsky YA, Mao L, Sadeghi SH, Moosavi N, Kheirfam H, Montzka C, Van Looy K, Toth B. 2018. Development and analysis of the Soil Water Infiltration Global database. *Earth System Science Data* 10(3): 1237-1263. https://doi.org/10.5194/essd-10-1237-2018.

Räsänen M, Merbold L, Vakkari V, Aurela M, Laakso L, Beukes JP, Van Zyl PG, Josipovic M, Feig G, Pellikka P, Rinne J. 2020. Root-zone soil moisture variability across African savannas: From pulsed rainfall to land-cover switches. *Ecohydrology* 13(5): 1-20. https://doi.org/10.1002/eco.2213.

Schreiner-McGraw AP, Vivoni ER, Ajami H, Sala OE, Throop HL, Peters DP. 2020. Woody plant encroachment has a larger impact than climate change on dryland water budgets. *Scientific reports* 10(1): 8112. https://doi.org/10.1038/s41598-020-65094-x.

Scott RL, Huxman TE, Barron-Gafford GA, Darrel Jenerette G, Young JM, Hamerlynck EP. 2014. When vegetation change alters ecosystem water availability. *Global Change Biology* 20(7): 2198-2210. https://doi.org/10.1111/gcb.12511.

Sebego RJ. 1999. The ecology and distribution limits of *Colophospermum mopane* in southern Africa. *Botswana Notes & Records* 31(1): 53-72.

Skowno AL, Thompson MW, Hiestermann J, Ripley B, West AG, Bond WJ. 2017. Woodland expansion in South African grassy biomes based on satellite observations (1990–2013): general patterns and potential drivers. *Global Change Biology* 23(6): 2358-2369. https://doi.org/10.1111/gcb.13529.

Smit GN, Rethman, NFG. 1998. Root biomass, depth distribution and relations with leaf biomass of *Colophospermum mopane*. *South African Journal of Botany* 64(1): 38-43. https://doi.org/10.1016/S0254-6299(15)30825-5.

Smit GN, Rethman NFG. 2000. The influence of tree thinning on the soil water in a semi-arid savanna of southern Africa. *Journal of Arid Environments* 44(1): 41-59. https://doi.org/10.1006/jare.1999.0576.

Smit GN. 2004. An approach to tree thinning to structure southern African savannas for long-term restoration from bush encroachment. *Journal of Environmental Management* 71: 179-191. https://doi:10.1002/2016WR019951.

Soil Classification Working Group. 2018. Soil Classification: A Natural and Anthropogenic System for South Africa; Agricultural Research Council—Institute for Soil, Climate and Water: Pretoria, South Africa.

Stafford W, Birch C, Etter H, Blanchard R, Mudavanhu S, Angelstame P, Blignaut, J, Ferreira L, Marais C. 2017. The economics of landscape restoration: Benefits of controlling bush encroachment and invasive plant species in South Africa and Namibia. *Ecosystem Services* 27: 193-202. http://dx.doi.org/10.1016/j.ecoser.2016.11.021.

Stevens N, Lehmann CE, Murphy, BP, Durigan G. 2016. Savanna woody encroachment is widespread across three continents. *Global Change Biology* 23(1): 235-244. https://doi.org/10.1111/gcb.13409.

Symeonakis E, Petroulaki K, Higginbottom T. 2016. Landsat-based woody vegetation cover monitoring in southern African savannahs. *The International Archives of the Photogrammetry, Remote Sensing and Spatial Information Sciences* 41: 563-567. https://doi.org/10.5194/isprs-archives-XLI-B7-563-2016.

Wedel ER, Nippert JB, O'Connor RC, Nkuna P, Swemmer AM. 2024. Repeated bush clearing as a mechanism for savanna recovery following bush encroachment. *Journal of Applied Ecology*. https://doi.org/10.1111/1365-2664.14666.

Wigley BJ, Bond WJ, Hoffman MT. 2010. Thicket expansion in a South African savanna under divergent land use: local vs. global drivers? *Global Change Biology* 16(3): 964-976. https://doi.org/10.1111/j.1365-2486.2009.02030.x.

Wilcox BP, Owens MK, Knight RW and Lyons RK. 2005. Do woody plants affect streamflow on semiarid karst rangelands? *Ecological Applications* 15(1): 127-136. https://doi.org/10.1890/04-0664.

Wilcox BP, Basant S, Olariu H, Leite PA. 2022. Ecohydrological connectivity: A unifying framework for understanding how woody plant encroachment alters the water cycle in drylands. *Frontiers in Environmental Science* 10: 934535. https://doi.org/10.3389/fenvs.2022.934535.

Wilcox BP and Huang Y. 2010. Woody plant encroachment paradox: Rivers rebound as degraded grasslands convert to woodlands. *Geophysical Research Letters* 37(7): 1-5. https://doi.org/10.1029/2009GL041929.

Yu K, D'Odorico P. 2015. Hydraulic lift as a determinant of tree–grass coexistence on savannas. *New Phytologist* 207(4): 1038-1051. https://doi.org/10.1111/nph.13431.

Zou CB, Turton DJ, Will RE, Engle DM, Fuhlendorf SD. 2014. Alteration of hydrological processes and streamflow with juniper (*Juniperus virginiana*) encroachment in a mesic grassland catchment. *Hydrological Processes* 28(26): 6173-6182. https://doi.org/10.1002/hyp.10102.

## APPENDIX B

**Table 4.3 Mopane cutting schedule at the paired plots from 2014-2024.**

| Plot | Year | Jan | Feb | Mar | Apr | May | Jun | Jul | Aug | Sep | Oct | Nov | Dec |
|---|---|---|---|---|---|---|---|---|---|---|---|---|---|
| 1 | 2014 | | | | | | | | | | ■ | | |
| 1 | 2015 | | | | | ■ | | | | | | | ■ |
| 1 | 2016 | | | | | | | | | | | | ■ |
| 1 | 2017 | | ■ | | | ■ | | | | | | | |
| 1 | 2018 | ■ | | | | | | ■ | | | | | |
| 1 | 2019 | | | | ■ | | | ■ | | | | ■ | |
| 1 | 2020 | ■ | | ■ | | | | | | ■ | | ■ | |
| 1 | 2021 | | | ■ | | | ■ | | | | | | ■ |
| 1 | 2022 | ■ | | | | | | | | | ■ | | |
| 1 | 2023 | ■ | | | | ■ | | | | | | ■ | |
| 1 | 2024 | ■ | | | | ■ | | | | | | ■ | |
| 2 | 2015 | | | | | | ■ | | | | | | |
| 2 | 2016 | | | | | | | | | | | | ■ |
| 2 | 2017 | | ■ | | | ■ | | | | | | | |
| 2 | 2018 | ■ | | | | | | ■ | | | | | |
| 2 | 2019 | | | | ■ | | | ■ | | | | ■ | |
| 2 | 2020 | ■ | | ■ | | | | | | ■ | | ■ | |
| 2 | 2021 | | | ■ | | | ■ | | | | ■ | | ■ |
| 2 | 2022 | ■ | | | | | | | | | ■ | | |
| 2 | 2023 | ■ | | | | ■ | | | | | | ■ | |
| 2 | 2024 | ■ | | | | ■ | | | | | | ■ | |
| 3 | 2015 | | | | | | ■ | | | | | | |
| 3 | 2016 | | | | | | | | | | | | ■ |
| 3 | 2017 | | ■ | | | ■ | | | | | | | |
| 3 | 2018 | ■ | | | | | | ■ | | | | | |
| 3 | 2019 | | | | ■ | | | ■ | | | | ■ | |
| 3 | 2020 | ■ | | ■ | | | | | | ■ | | ■ | |
| 3 | 2021 | | | ■ | | | ■ | | | | | | ■ |
| 3 | 2022 | ■ | | | | | | | | | ■ | | |
| 3 | 2023 | ■ | | | | ■ | | | | | | ■ | |
| 3 | 2024 | ■ | | | | ■ | | | | | | ■ | |

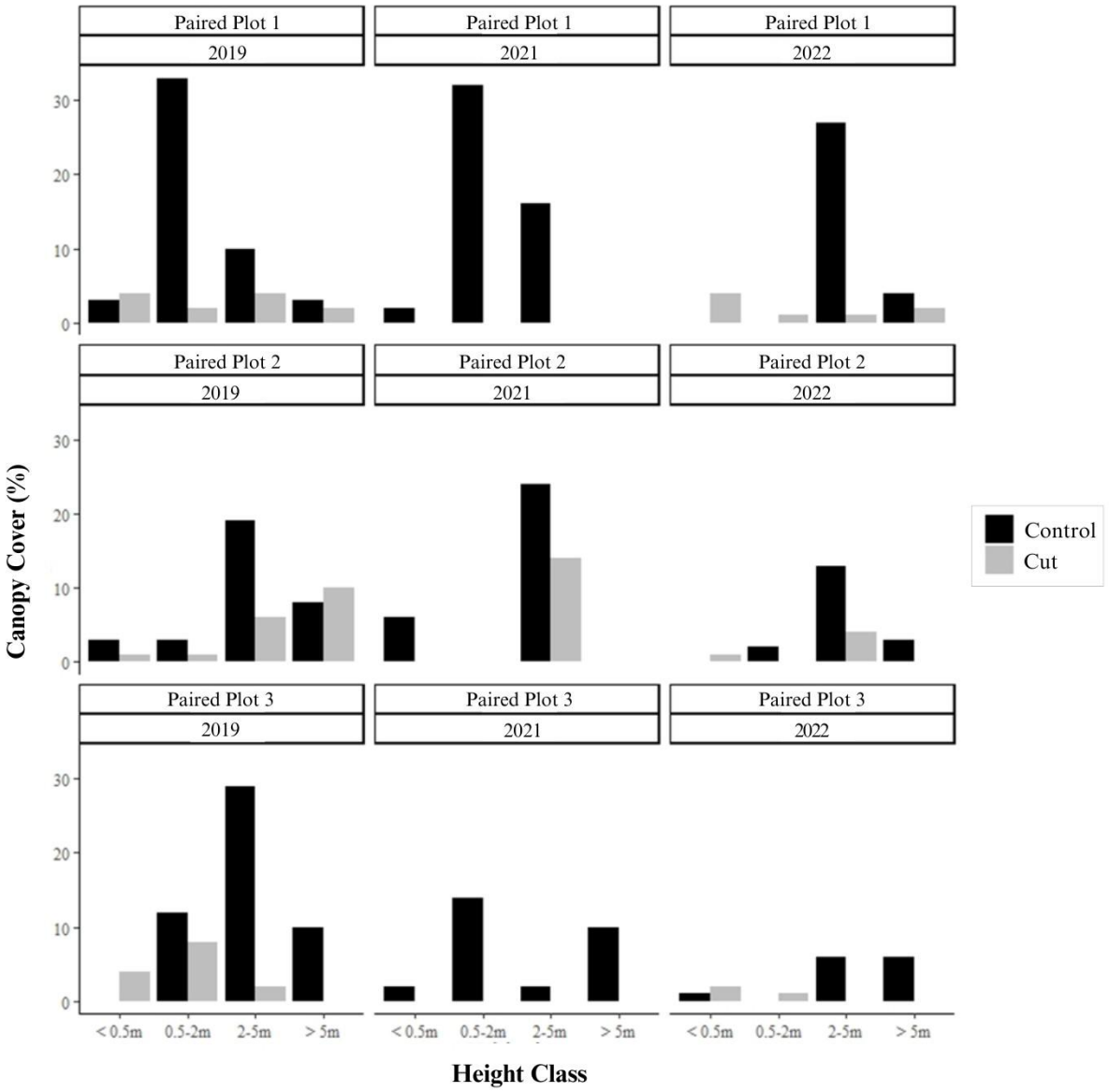


**Figure 4.6 Canopy cover (%) vs height class of the trees and/or shrubs in the paired plots for 2019, 2021 and 2022. This data is based on a step-point transect study by Wedel *et al.* (2024).**

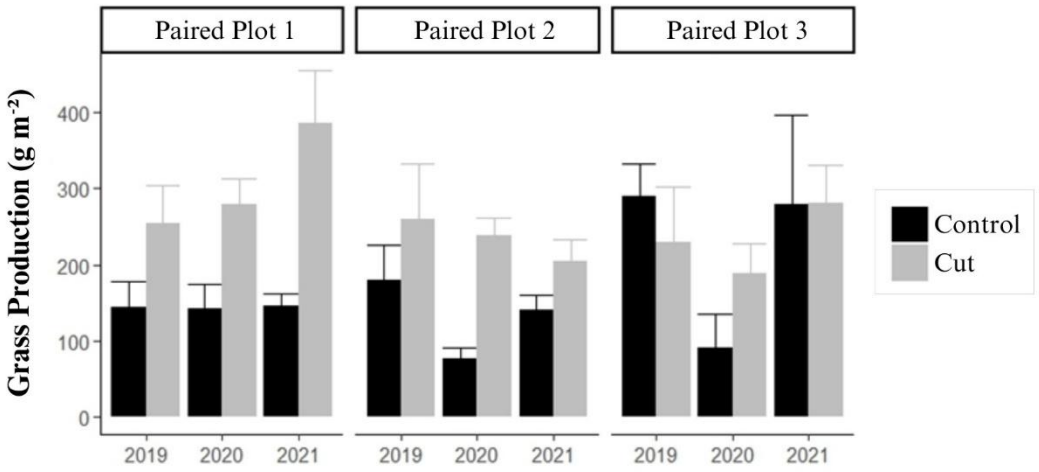


**Figure 4.7 Grass production (g $m^{-2}$) in the paired plots for 2019-2021.**

**Table 4.4 Soil texture at paired plot 1.**

| Plot | Soil Depth (mm) | Coarse Silt and Sand (0.02 - 2 mm) (%) | Fine Silt (0.02 - 0.002 mm) (%) | Clay (< 0.002 mm) (%) | Texture Class |
|---|---|---|---|---|---|
| Control | 0-200 | 69 | 18 | 13 | Sandy Loam |
| | 200-400 | 52 | 40 | 8 | Loam |
| | 400-600 | 60 | 16 | 25 | Sandy Clay Loam |
| | 0-200 | 56 | 24 | 20 | Sandy Clay Loam |
| | 200-400 | 55 | 20 | 25 | Sandy Clay Loam |
| | 400-600 | 54 | 17 | 29 | Sandy Clay Loam |
| | 0-200 | 70 | 18 | 12 | Sandy Loam |
| | 200-400 | 54 | 28 | 18 | Sandy Loam |
| | 400-600 | 63 | 15 | 22 | Sandy Clay Loam |
| Cut | 0-200 | 73 | 17 | 10 | Sandy Loam |
| | 200-400 | 71 | 15 | 14 | Sandy Loam |
| | 400-600 | 72 | 13 | 15 | Sandy Loam |
| | 0-200 | 52 | 29 | 19 | Loam |
| | 200-400 | 54 | 24 | 22 | Sandy Clay Loam |
| | 400-600 | 46 | 28 | 26 | Loam |
| | 0-200 | 78 | 12 | 10 | Sandy Loam |
| | 200-400 | 74 | 12 | 14 | Sandy Loam |
| | 400-600 | 72 | 14 | 14 | Sandy Loam |

**Table 4.5 Bulk density at paired plot 1.**

| Plot | Soil Depth (mm) | Bulk Density (g $cm^{-3}$) |
|---|---|---|
| Control | 100 | 1.56 |
| | 300 | 1.51 |
| | 600 | 1.65 |
| | **Mean** | 1.57 |
| Cut | 100 | 1.51 |
| | 300 | 1.57 |
| | 600 | 1.49 |
| | **Mean** | 1.52 |

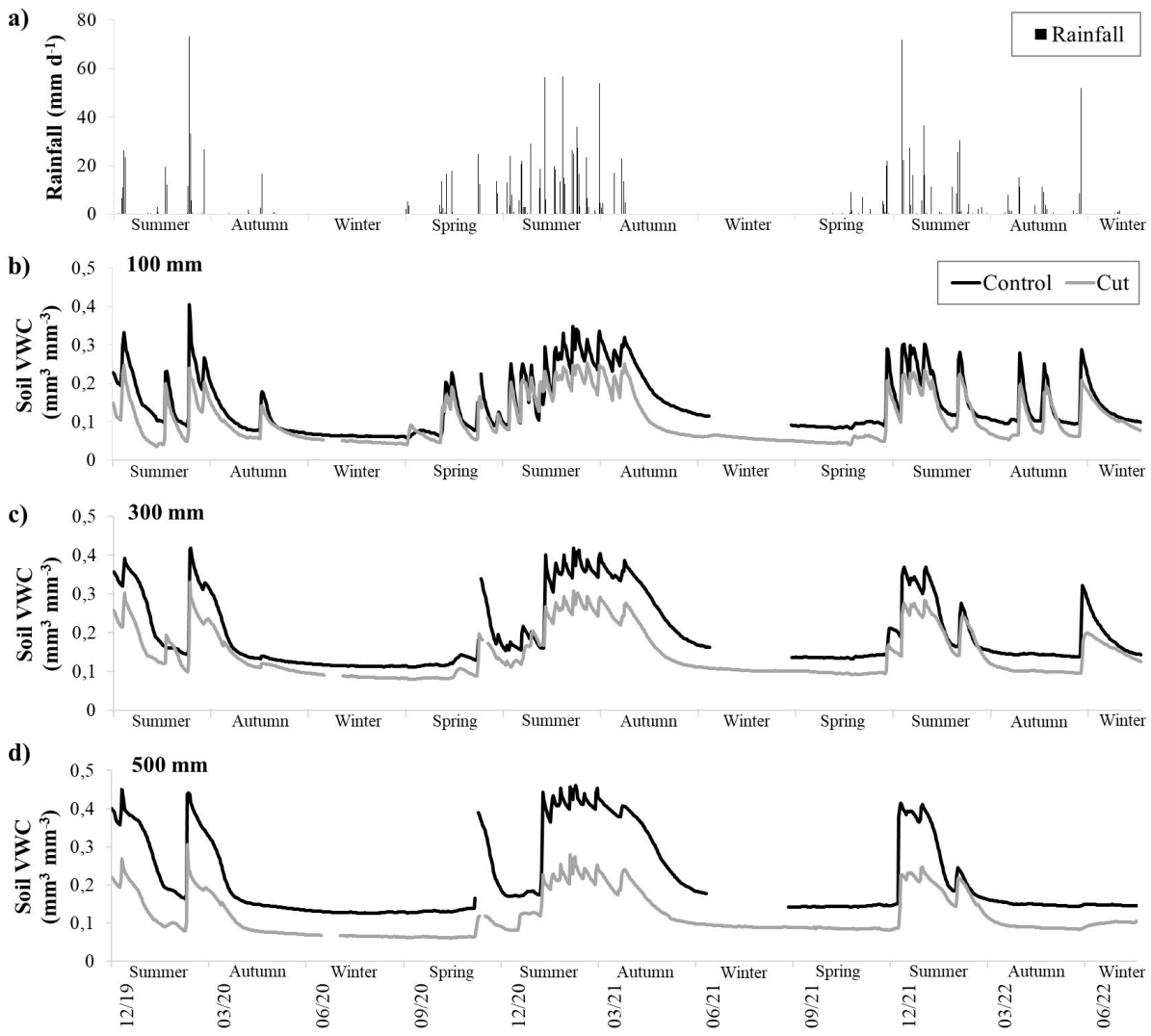


**Figure 4.8 Daily a) rainfall and b)-d) soil volumetric water content (VWC) at 100 mm, 300 mm and 500 mm soil depths for paired plot 1 - repetition 1 over the measurement period.**

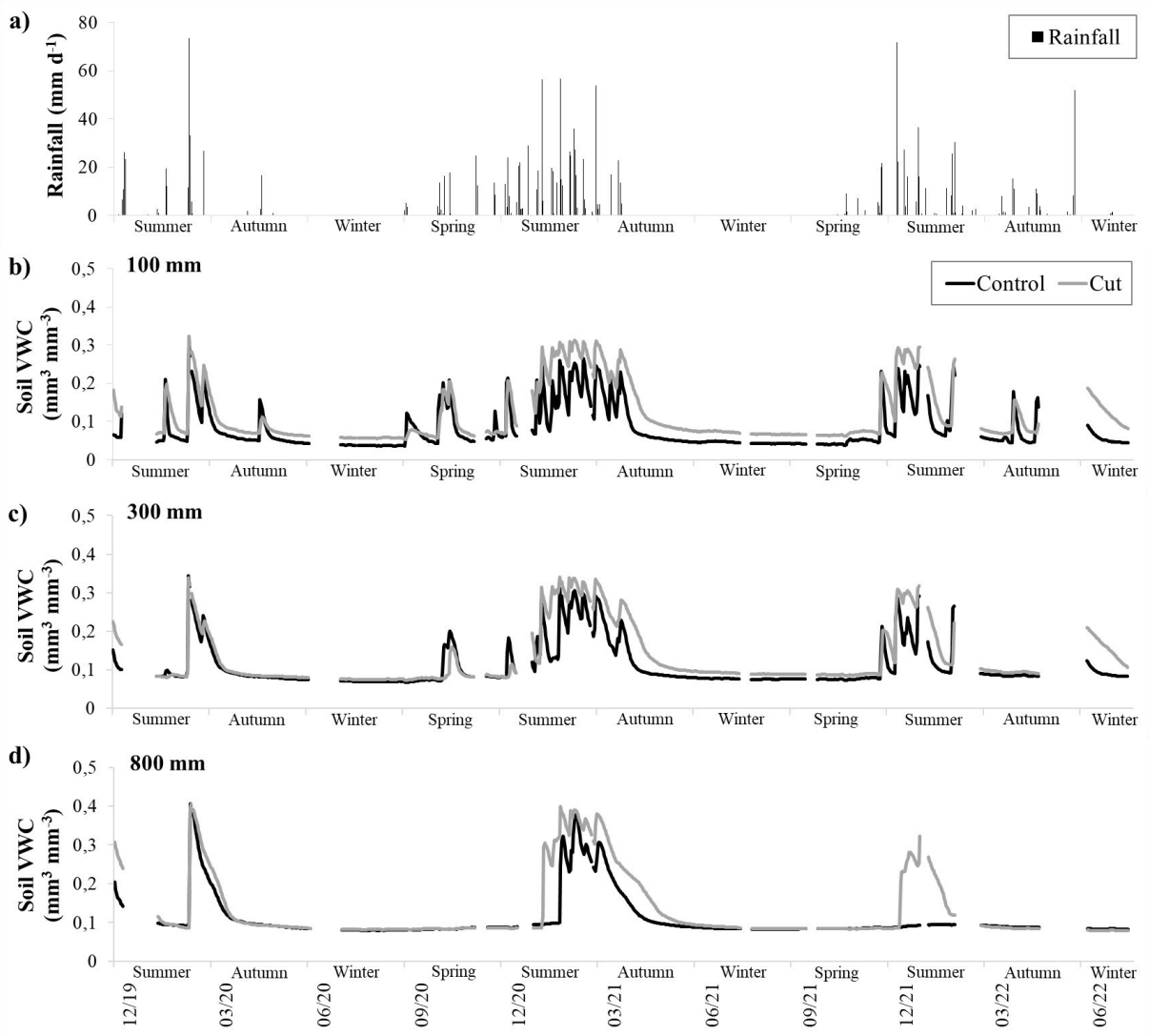


**Figure 4.9 Daily a) rainfall and b)-d) soil volumetric water content (VWC) at 100 mm, 300 mm and 800 mm soil depths for paired plot 1 - repetition 2 over the measurement period.**

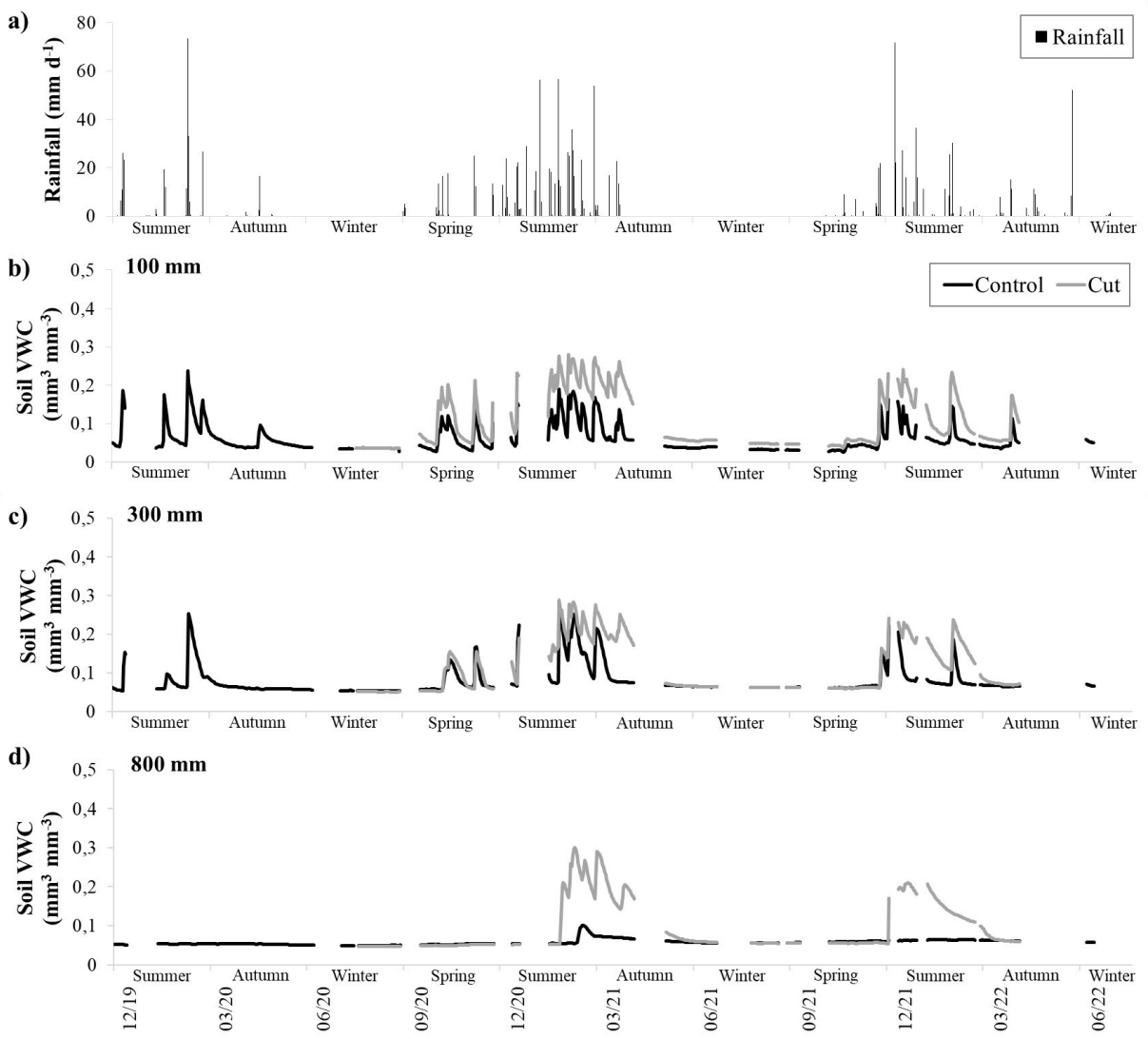


**Figure 4.10 Daily a) rainfall and b)-d) soil volumetric water content (VWC) at 100 mm, 300 mm and 800 mm soil depths for paired plot 2 over the measurement period.**

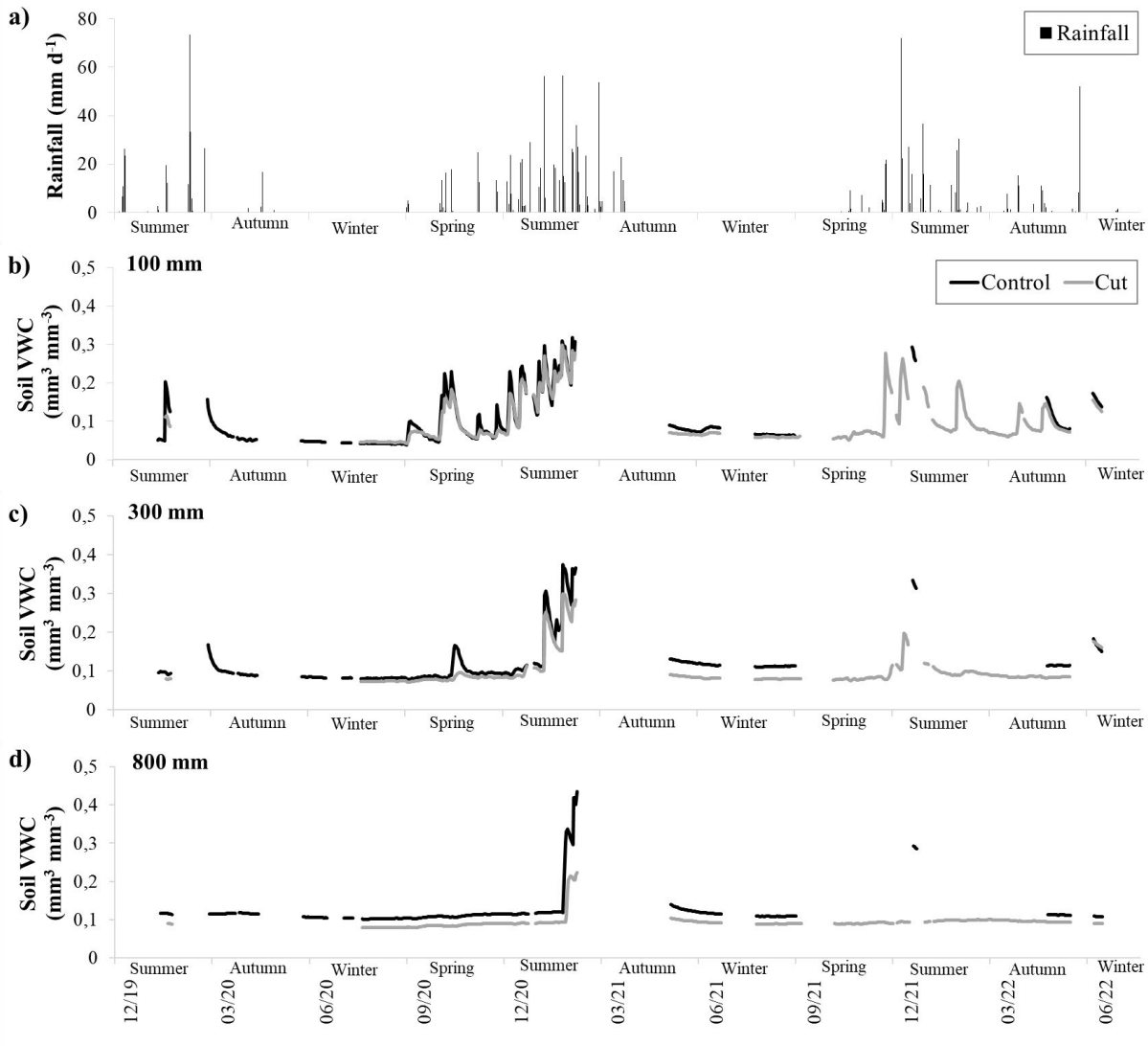


**Figure 4.11 Daily a) rainfall and b)-d) soil volumetric water content (VWC) at 100 mm, 300 mm and 800 mm soil depths for paired plot 3 over the measurement period.**

**Lead into Chapter 5**

In the final research paper, freely available and relatively user-friendly resources provided by Google Earth Engine were leveraged to assess the relationship between woody cover and evapotranspiration (ET) across various spatio-temporal scales in a woody-encroached, semi-arid savanna catchment. Woody cover was mapped using Sentinel-2 imagery and Gradient Tree Boost algorithms within the Google Earth Engine platform, while remotely sensed ET estimates were obtained from Earth Engine Evapotranspiration Flux (EEFlux) validated by in situ surface renewal measurements.

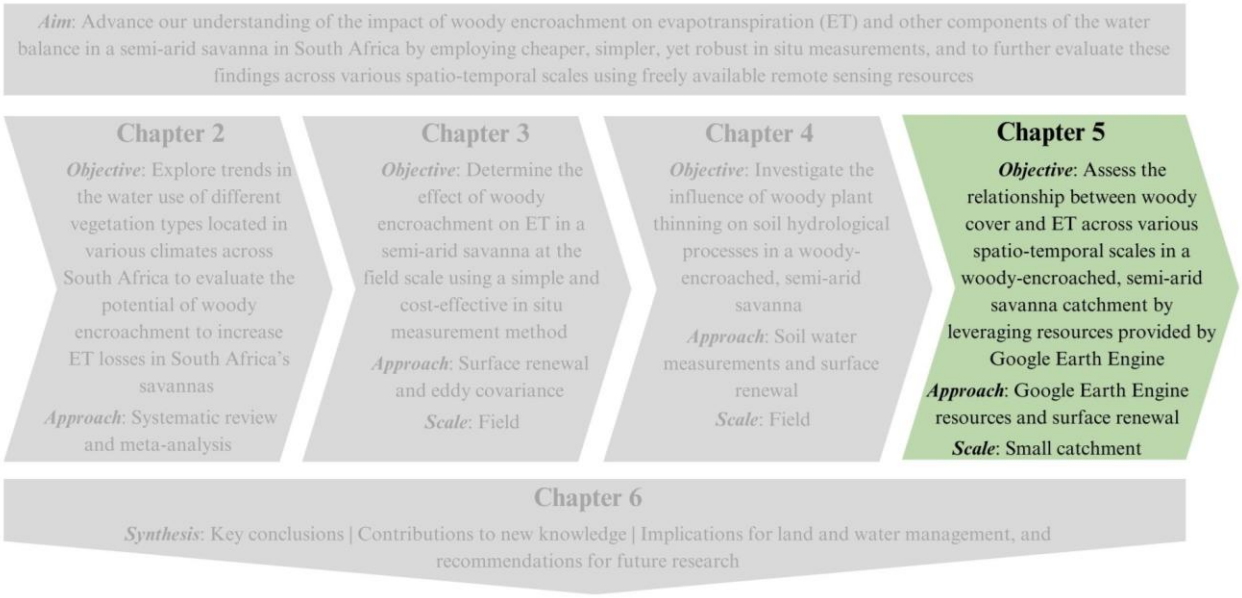

# 5 ASSESSING THE RELATIONSHIP BETWEEN WOODY COVER AND EVAPOTRANSPIRATION ACROSS VARIOUS SPATIO-TEMPORAL SCALES IN A SEMI-ARID SAVANNA CATCHMENT

## 5.1 Abstract

Savannas across the globe are undergoing large-scale degradation in the form of woody encroachment, a phenomenon where native woody plants are gradually increasing in abundance at the expense of herbaceous vegetation. Given that it is widely believed that increases in woody cover lead to associated increases in evapotranspiration (ET), and savannas are generally located in arid or semi-arid regions where climate change is projected to exacerbate the recurrent water scarcity conditions, considerable concern has been raised. In this study, freely available and relatively user-friendly resources provided by Google Earth Engine were leveraged to assess the relationship between woody cover and ET across various spatio-temporal scales in a woody-encroached, semi-arid savanna catchment. Woody cover was mapped using Sentinel-2 imagery and Gradient Tree Boost supervised pixel-based classification algorithms within the Google Earth Engine platform, while remotely sensed ET estimates were obtained from Earth Engine Evapotranspiration Flux (EEFlux) validated by in situ surface renewal measurements. Our results demonstrate that, while woody encroachment can increase ET in semi-arid savannas, this increase occurs gradually over time and typically only during wet seasons and wet years. Moreover, this increase only becomes evident at larger scales. These findings suggest that if woody plant removal operations are carried out, any hydrological benefits of increased catchment water yields may only manifest over time and may be limited to wet seasons or extended wet periods. Large-scale implementation and long-term monitoring will also be necessary. These findings open discussion regarding the viability of large-scale woody plant removal operations as a management strategy in woody-encroached, semi-arid savanna catchments. The benefits to other ecosystem services - such as changed carrying capacity, carbon sequestration, soil nutrient cycling and biodiversity - that are provided or improved in addition to greater water yields may need to be considered when assessing the viability of woody plant removal operations.

***Keywords:*** *Land use and land cover change, woody encroachment, Google Earth Engine, EEFlux, hydrological processes*

## 5.2 Introduction

Savannas comprise about one fifth of the earth's surface and hence play a significant role in carbon, energy and water budgets, biodiversity conservation, and the provision of ecosystem services critical to human well-being (Sankaran *et al*. 2005, Tsalyuk *et al*. 2017). However, savannas are undergoing large-scale degradation as a result of land use and land cover change (LULCC), altered herbivore and fire management regimes, climate change and rising atmospheric $CO_2$ (Stevens *et al*. 2017, Tsalyuk *et al*. 2017). Consequently, this has led to woody encroachment, a phenomenon where native woody plants are gradually increasing in abundance at the expense of grasses and other herbaceous vegetation (Devine *et al*. 2017, Stevens *et al*. 2017, Zhang *et al*. 2019). Increases in woody cover are widely hypothesised to lead to associated increases in evapotranspiration (ET) (Acharya *et al*. 2018). Given increases in ET can translate to potential reductions in streamflow and/or groundwater recharge, and hence reduced water yields, considerable concern has been raised (Acharya *et al*. 2017, Acharya *et al*. 2018, Wang *et al*. 2018). Reduced water yields are particularly worrisome in savanna catchments since they are generally located in arid or semi-arid regions, where water is limited or only available seasonally and droughts are frequent. Furthermore, global climate projections for many of these regions suggest that ET (typically the largest loss in the water balance of savanna regions) will increase and the recurrent water scarcity conditions will likely be exacerbated and become more variable (Andreu *et al*. 2018, Nisa *et al*. 2021). Therefore, understanding any changes in savanna ET associated with woody encroachment is crucial for informing water resource management and planning (Acharya *et al*. 2018).

Determining the degree to which woody encroachment impacts ET or water yields in savanna regions is challenging because there are very few long-term ET monitoring programs in savannas worldwide. The global ET monitoring network, known as FLUXNET, currently has nine registered savanna sites (https://fluxnet.org/sites/site-list-and-pages/, Weerasinghe *et al.* 2020). Besides FLUXNET, in situ measurements of ET in savannas are limited, localised, and the data are only available for short periods, ranging from several days to a few years (Jovanovic *et al*. 2015, Wang *et al*. 2018). This is largely due to the high cost and labour-intensive nature of the micrometeorological methods required to measure ET, which include weighing lysimeters, Bowen Ratio Energy Balance, eddy covariance, surface renewal and scintillometry (Alemayehu *et al*. 2017, Khosa *et al.* 2019, Awada *et al*. 2021). In situ ET measurements are also limited in savanna regions because these vegetation types are predominantly present in developing countries where logistics are challenging, and funds and

resources are often limited (Blin and Suárez 2023). Furthermore, regular maintenance is necessary for micrometeorological methods, but savannas are typically found in remote locations that can be difficult to access (Tsalyuk *et al*. 2017, Oliveira *et al*. 2018).

Given the scarcity and short duration of in situ ET measurements in savannas, there remains uncertainty about the spatial and temporal variability of ET caused by woody encroachment (Heilman *et al*. 2008). However, recent advances in remote sensing-based ET models provide a promising alternative to bridge these observational gaps (Alemayehu *et al*. 2017, Oliveira *et al*. 2018, Laipelt *et al*. 2021). These models generally use thermal infrared observations from satellite sensors to derive a surface energy balance from which latent heat flux (LE), and subsequently ET, may be calculated (da Silva *et al*. 2015, Nassar *et al*. 2022). Some of the most commonly used surface energy balance models include the Surface Energy Balance Algorithm for Land (SEBAL), Mapping Evapotranspiration at High Resolution using Internalized Calibration (METRIC), Atmosphere-Land Exchange Inverse (ALEXI), Simplified Surface Energy Balance (SSEBop), Surface Energy Balance System (SEBS), Two-Source Energy Balance (TSEB), Simplified Surface Energy Balance Index (S-SEBI) and the disaggregated ALEXI Model (DisALEXI) (Laipelt *et al*. 2021, Khoshnood *et al*. 2023). Surface energy balance models have many advantages, such as being inexpensive and repeatable for ongoing monitoring, as well as having the ability to accurately estimate ET across multiple spatial and temporal scales (Alemayehu *et al*. 2017, de Sousa Junior *et al.* 2022). However, they are highly complex and require a trained expert in surface energy balance modelling to calibrate and run the model (Poudel *et al*. 2021). The ET retrieval process is also computationally intensive and time-consuming (Venancio *et al.* 2020), and users must obtain a variety of model inputs, which are often not readily available and may need to undergo a substantial amount of pre-processing before the algorithms can be applied (Venancio *et al.* 2020, Alsanjar and Cetin 2024).

The limitations of surface energy balance models have led to their integration into cloud computing platforms (i.e., Google Earth Engine, Earth on Amazon Web Services, Microsoft Planetary Computer, Microsoft Azure), which have the ability to simplify remote sensing applications, manage computationally demanding processing tasks, and assist with issues related to massive data volumes (Xu *et al*. 2022, Amani *et al*. 2020, Praticò *et al*. 2021). One example is the integration of the METRIC Model into the Google Earth Engine platform via a graphical user interface known as Earth Engine Evapotranspiration Flux (EEFlux) (Allen *et al*. 2007, Kadam *et al.* 2021, Poudel *et al.* 2021). By using Landsat-5, -7, -8 or -9 images that are

already stored in Google Earth Engine, EEFlux enables users to freely obtain maps of ET in a matter of minutes for any terrestrial land area worldwide (de Oliveira Costa *et al*. 2020). Evapotranspiration maps are available from 1984 to the present and have a spatial resolution of 30 m and a temporal resolution of eight days (Carrasco-Benavides *et al.* 2022, Blin and Suárez 2023). A major drawback of EEFlux is that ET can only be estimated under clear sky conditions with no cloud cover (Salem *et al*. 2024).

Accurate detection and mapping of woody cover is critical if we are to understand the influence of woody encroachment on ET in savannas. However, ground-based assessments of woody cover, like in situ ET measurements, are expensive, time-consuming and labour-intensive (Norton *et al*. 2022). Moreover, mapping at the scale at which woody encroachment occurs, and continuously quantifying change are often impossible tasks for assessments conducted on the ground (Shekede *et al*. 2015, Fundisi *et al*. 2022). Remote sensing has been demonstrated to be an alternative tool for mapping and monitoring LULCC across a range of spatial and temporal scales (Zurqani *et al.* 2018, Praticò *et al*. 2021). Light Detection and Ranging (LiDAR) data and object-based image analysis using very high resolution imagery (≤1 m) (e.g., Quickbird, Worldview) are preferred remote sensing approaches for mapping woody cover since they are almost equivalent to field measurements and can detect individual woody plants (Ludwig *et al*. 2016, Zhang *et al.* 2019, Filippelli *et al*. 2020). These approaches are, however, not feasible beyond the local scale, due to the limited spatial coverage of the data that is currently archived, and the high expense of acquiring new data for large areas. They are also limited by the frequency that data are able to be collected (Ludwig *et al*. 2016, Zhang *et al*. 2019, Filippelli *et al*. 2020). Consequently, pixel-based classification algorithms (e.g., Gradient Tree Boost, Random Forest) together with freely available moderate resolution satellite imagery (e.g., Landsat, Sentinel) have widely been used to map woody vegetation (Zhang *et al*. 2019, Filippelli *et al*. 2020, Holden *et al*. 2021, Rabelo *et al*. 2021). Sentinel-2 imagery has become widely used since the twin satellites sentinel-2A and -2B were launched in 2015 and 2017 (Djamai and Fernandes 2018). The 10 m spatial resolution and five-day revisit frequency of the Sentinel-2 satellites have made it possible to map more accurately the presence of dense woody areas across broad spatio-temporal scales (Zhang *et al*. 2019, Filippelli *et al*. 2020). Recently, machine learning algorithms have emerged as an option to improve large-scale woody encroachment mapping (e.g., Ludwig *et al*. 2019, Tooley *et al*. 2024).

Given the extent of woody encroachment throughout the world's dryland savannas, regional water budgets and groundwater recharge rates may be further impacted if woody encroachment is indeed increasing ET. Consequently, in this study, freely available and relatively user-friendly resources provided by Google Earth Engine were leveraged to assess the relationship between woody cover and ET across various spatio-temporal scales in a woody-encroached, semi-arid savanna catchment located in South Africa. The study region has undergone an increase in woody cover in recent decades (Munyati *et al*. 2011, Buitenwerf *et al*. 2012, Munyati and Sinthumule 2016, Symeonakis *et al*. 2016, Marston *et al*. 2017, Zhou *et al*. 2021, Maphanga *et al*. 2024), and water supplies are severely constrained, a situation that is likely to worsen in the future due to the projected impacts of drought and climate change (Pollard and du Toit 2011, Kanjere *et al*. 2014). A prior plot-scale study conducted in the study catchment by Aldworth *et al*. (2022) found that woody encroachment had little effect on daily ET, but it did increase annual ET by 12% in the wet year of the study. Therefore, the main research question that we sought to answer in this study was whether the increase in ET caused by woody encroachment is more evident over greater spatial and temporal scales? Before this could be determined, the study needed to answer two additional research questions. First, can pixel-based classification algorithms and moderate resolution satellite imagery effectively map woody cover in heterogenous savanna environments? Second, what is the potential of EEFlux for estimating ET in semi-arid savanna vegetation in southern Africa?

## 5.3 Methodology

### *5.3.1 Study catchment*

The quaternary B82J catchment (796 $km^2$) is situated in the north-eastern part of South Africa, and is one of 23 quaternary catchments (i.e., the country's principal water management unit) that make up the Letaba River catchment (Figure 5.1). It drains into the Klein Letaba River, a major tributary of the Letaba River. Most of the catchment falls within the Kruger National Park, the largest conservation area in South Africa (Ferreria and Harmse 2014). The western part of the catchment comprises of small private game reserves, as well as the communal villages of Phalakubeni, Ka-Sabulane and Macene.

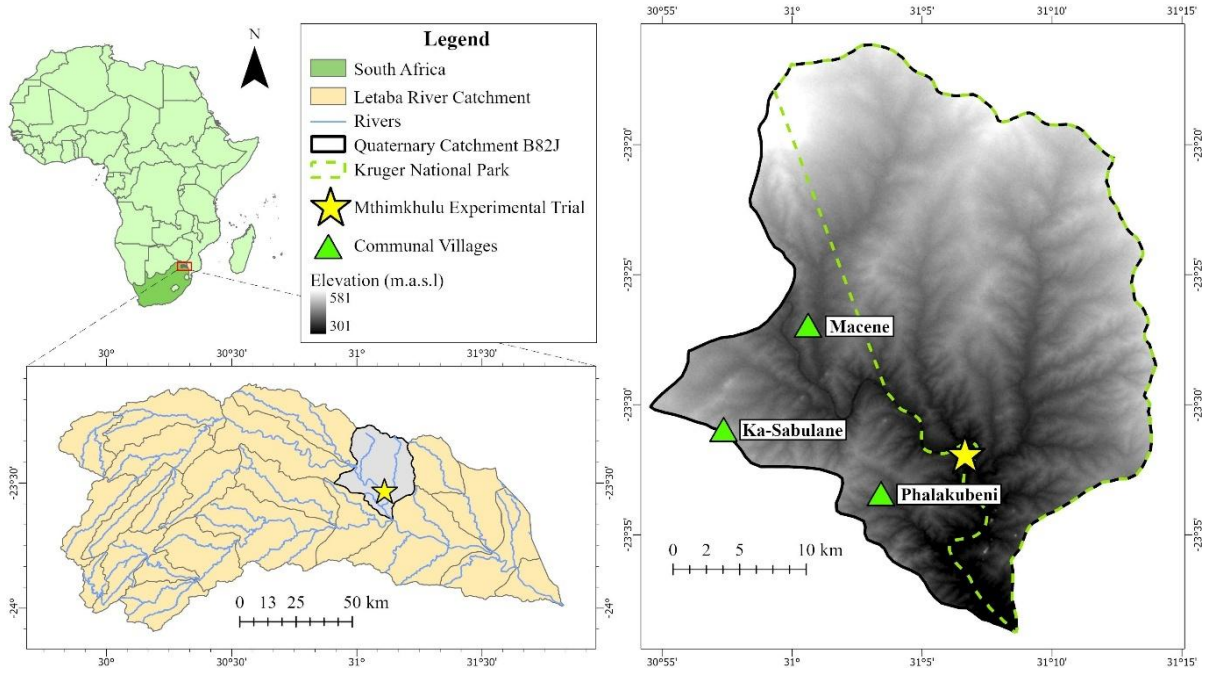


**Figure 5.1 Location of the quaternary B82J and the Mthimkhulu experimental trial in Africa.**

The vegetation of quaternary B82J is classified as Lowveld Mopaneveld, a savanna with dense shrubs interspersed with sporadic trees and a sparse grass layer (Mucina and Rutherford 2006). *Colophospermum mopane* (Kirk ex Benth) Kirk éx J. Léonard (Mopane) is the predominant shrub and tree species, but there are also the occasional *Combretum imberbe* (Leadwood) and *Vachellia tortilis* (Umbrella thorn) trees and *Grewia bicolor* (Twotone raisin) shrubs scattered amidst the Mopane. The annual *Aristida* species predominate in the sparse grass layer, with tufts of *Urochloa mosambicensis* (Gonyagrass) and *Panicum maximum* (Guinea grass) scattered throughout. The elevation is relatively flat, ranging between ~300 m and ~400 m above sea level, but there are several prominent hills to the north with the highest point at ~580 m above mean sea level (Mucina and Rutherford 2006). Approximately three quarters of the quaternary B82J is underlain by granites and gneiss, and the soils are typically red-yellow apedals that are shallow and well drained (Mucina and Rutherford 2006).

The study area has a semi-arid climate and experiences a mean annual precipitation (MAP) of ~476 mm according to a rainfall station located at the outlet of quaternary B82J (Mucina and Rutherford 2006, WR2012). Rainfall is highly seasonal, occurring mainly during the summer months (October to March). January and February are the peak rainfall months

(Kennedy and Potgieter 2003, Mucina and Rutherford 2006). Winters are extremely dry and the region seldom experiences frost (Mucina and Rutherford 2006).

### *5.3.2 Experimental trial and surface renewal validation measurements*

Due to the availability of observed ET data, quaternary B82J was chosen as the study catchment. In situ ET measurements were made over a two-and-a-half-year-period (mid-November 2019 to mid-July 2022) at an experimental woody plant thinning trial (23°31′31” S; 31°06′48” E) located in the Mthimkhulu Private Game Reserve within the catchment (Figures 5.1 and 5.2). The Mthimkhulu trial was set up on an ancient alluvial floodplain of the Klein Letaba River and consisted of four paired plots, namely paired plots 1, 2, 3 and 4. Each paired plot had one undisturbed ‘control’ plot that was encroached by Mopane and one ‘cut’ plot consisting of an open canopy structured savanna with a few tall trees and scattered shrubs. In the cut plots, individual Mopane trees and shrubs less than four meters in height were cut to ground level 1-4 times per year, thereby ‘thinning’ the cover of woody plants. Paired plot 1 was first established in October 2014, paired plot 2 in June 2015 (enlarged in July 2021), paired plot 3 in July 2016 and paired plot 4 in October 2020. The smaller plots averaged about 5 000 $m^2$ in size, whereas the larger plots averaged about 14 000 $m^2$.

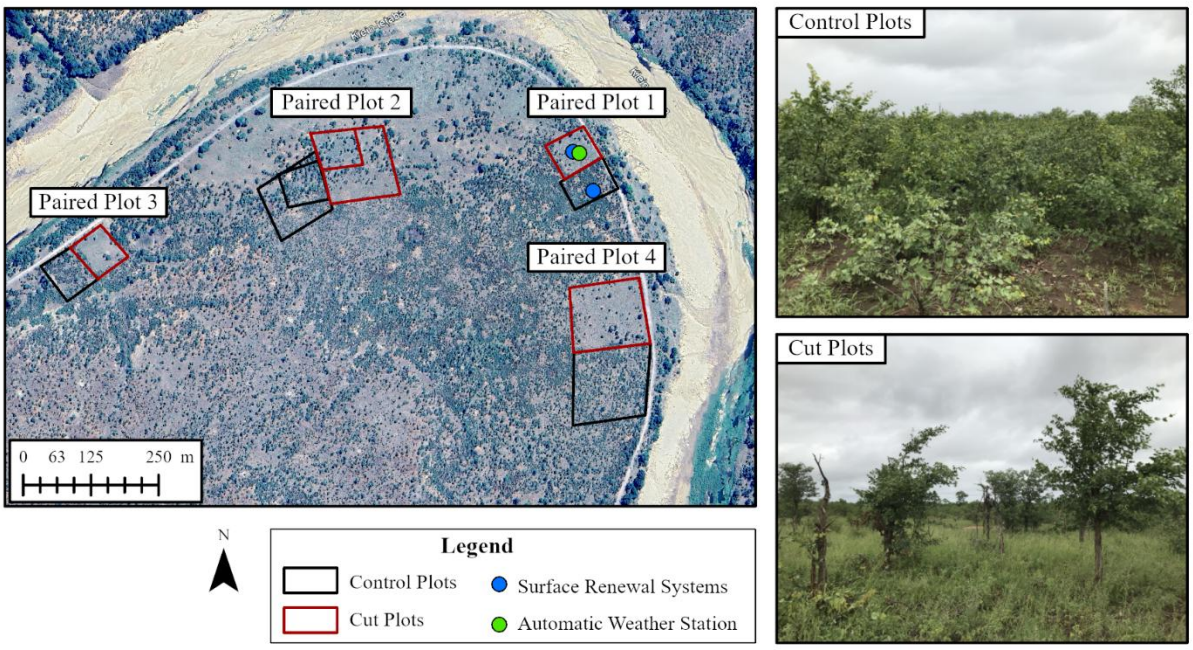


**Figure 5.2 Layout of the paired plots at the Mthimkhulu experimental trial and the location of the research equipment within paired plot 1. Vegetation in the control and cut plots are shown on the right.**

The setup for the in situ ET measurements included two surface renewal systems installed in the control and cut plots at paired plot 1. The surface renewal systems continuously measured the energy balance components of sensible heat flux (H, W $m^{-2}$), net radiation (Rn, W $m^{-2}$) and soil heat flux (G, W $m^{-2}$). The latent heat flux (W $m^{-2}$) was obtained by solving the residual of the shortened energy balance equation (i.e., LE = Rn−G−H). Thereafter, LE was converted to actual $ET_{SR}$ (mm) using the latent heat of evaporation (L, 2.45 MJ $kg^{-1}$) (Shapland *et al*. 2012, Rosa and Tanny 2015). The surface renewal 1 (SR1) method, which has previously been identified as the most suitable surface renewal approach for measuring H at the Mthimkhulu trial, was used to measure H (Aldworth *et al.* 2022). SR1 H measurements require site-specific calibration against a standard flux measurement method (Mengistu and Savage 2010). Therefore, two eddy covariance field campaigns of one week each were carried out alongside the surface renewal systems at each plot to determine site-specific calibration factors (α). It was presumed that the surface renewal and eddy covariance measurements were representative of the entirety of the plots.

An automatic weather station was also set up at paired plot 1 to monitor the site's climatic conditions, including the rainfall, solar irradiance, temperature, relative humidity, and wind speed and direction. Aldworth *et al*. (2022) provide a detailed description of the surface renewal, eddy covariance and automatic weather station instrumentation, the theory of the methods, and the calibration and ET measurement procedure.

### *5.3.3 Woody cover mapping*

Supervised pixel-based classification algorithms were applied to Sentinel-2 images in Google Earth Engine to differentiate between woody cover and non-woody cover in the study catchment. The Sentinel-2 images were obtained through Google Earth Engine from the COPERNICUS/S2_SR collection, a publicly available collection of Level 2A bottom-of-atmosphere corrected images (Zhang *et al*. 2019). Sentinel-2 has 13 spectral bands that range from visible and near infrared to shortwave infrared. The bands have different spatial resolutions; bands 2, 3, 4, and 8 have a 10 m spatial resolution, bands 5, 6, 7, 8A, 11 and 12 have a 20 m spatial resolution, and bands 1, 9 and 10 have a 60 m spatial resolution (Bayas *et al*. 2022, Pech-May *et al*. 2022). The bands allow for the calculation of a number of vegetation indices used in classification. The vegetation indices used in this study to classify woody cover and non-woody cover are provided in Table 5.2 *(Appendix C*).

Woody cover maps were generated for four hydrological years (i.e., 01 October to 30 September) between 2019 and 2023. The Sentinel-2 image collection was filtered for the summer months of December to March since Mopane is a deciduous species, and this is the time of year when Mopane will most easily be detected by the classifiers due to its green leaves. Mopane leaves shed or senesce in the dry season, making the Mopane more difficult to detect during the drier months. The image collection was also filtered to only include images with a cloud cover of < 5%. The filtered images for each summer period were composited and a median value for each pixel was calculated. The classifiers used included the Gradient Tree Boost, Random Forest and Support Vector Machine methods, which have all been shown to be robust approaches for land use land cover classifications (Zhang *et al*. 2019, Bayas *et al*. 2022, Pech-May *et al*. 2022). We compared the performance of the three classifiers by employing an iterative process, where each classifier's performance was assessed using the default hyper-parameters.

To train and validate the classifications, training and validation data were collected within Google Earth Engine using very-high spatial resolution Google Earth imagery from the 2023 year (Zhang *et al*. 2019). Training and validation data consisted of sample points collected for areas representing woody and non-woody cover classes. A total of 1 600 training and validation data points were obtained for the classification. This included 800 points for each of the woody cover and non-woody cover classes. The classifier was trained using 70% of the sample points, with the remaining 30% used as validation data to test the classification result as part of the statistical accuracy assessment (Pech-May *et al*. 2022). Given that the training and validation data were only collected in 2023, the statistical accuracy assessment was performed for the 2022-2023 year. The statistical accuracy assessment involved the construction of a confusion matrix, from which the producer's, user's and overall accuracies, and kappa statistics for each land cover class were calculated (Story and Congalton 1986, Congalton 1991, Congalton and Green 2009).

### *5.3.4 Earth Engine Evapotranspiration Flux ET data product*

Earth Engine Evapotranspiration Flux derives a surface energy balance from thermal and short-wave infrared bands of Landsat images and then employs the METRIC Model to estimate $LE$ (W $m^{-2}$) as a residual of the surface energy balance equation (Equation 5.1) (Allen *et al*. 2015, Blin and Suárez 2023):

$$LE = Rn - G - H \tag{5.1}$$

where, $Rn$ is the net radiation (W $m^{-2}$), $G$ is the soil heat flux (W $m^{-2}$), and $H$ is the sensible heat flux (W $m^{-2}$). The $LE$ is estimated at the exact moment of satellite image acquisition for each 30 m x 30 m pixel of the Landsat image (Carrasco-Benavides *et al*. 2022).

The instantaneous ET ($ET_i$, mm $h^{-1}$) for each pixel is then calculated using Equation 5.2:

$$ET_i = 3600 \frac{LE_i}{\lambda \rho w} \tag{5.2}$$

where, $3600$ converts seconds to hours, $\lambda$ is the latent heat of vaporization (J $kg^{-1}$), and ρw is the density of water (~1000 kg $m^{-3}$) (Poudel *et al*. 2021, de Oliveira Costa *et al*. 2020).

Thereafter, the $ET_i$ is converted to a fraction of the reference ET ($ET_oF$) using the instantaneous alfalfa reference ET ($ET_o$) according to Equation 5.3. The $ET_oF$ is similar to the traditional crop coefficient ($K_c$) (de Oliveira Costa *et al*. 2020, Blin and Suárez 2023).

$$ET_oF = \frac{ET_i}{ET_o} \tag{5.3}$$

The $ET_o$ is calculated using the Standardized Penman-Monteith equation (Poudel *et al*. 2021) and hourly gridded weather data from Climate Forecast System version 2 (CFSv2), which includes solar radiation, wind speed, specific humidity and air temperature data (Blin and Suárez 2023). Earth Engine Evapotranspiration Flux also uses CFSv2 data to calibrate the image's surface energy balance by assigning $ET_oF$ values to the 'hot' and 'cold' pixels of the image's surface temperature spectrum (de Oliveira Costa *et al*. 2020, Carrasco-Benavides *et al*. 2022).

Finally, to convert ET from the satellite image acquisition time to daily actual ET ($ET_a$, mm $d^{-1}$), the $ET_oF$ is multiplied by the daily $ET_o$ for each individual pixel, according to Equation 5.4. The $ET_oF$ at the time of the satellite image acquisition and the $ET_oF$ over the 24-hour period are assumed to be constant (de Oliveira Costa *et al*. 2020, Blin and Suárez 2023).

$$ET_a = ET_oF \times ET_o \tag{5.4}$$

Earth Engine Evapotranspiration Flux ET maps were obtained from the EEFlux website (https://eeflux-level1.appspot.com, version 0.20.17, accessed on 20 January 2025) every eight days between 1990 and 2023. Before downloading the maps, EEFlux provides a cloud cover percentage for each image and allows the user to visualise where there is cloud cover within the image. For this study, only EEFlux maps with < 10% cloud cover were downloaded. Certain pixels in all Landsat-7 images obtained after 31 May 2003 exhibited null ET values due to a malfunction of the scan line corrector. These maps were still used where pixels had ET values.

### *5.3.5 Validation of EEFlux ET estimates*

Linear regression analysis was used to validate the $ET_{EEFlux}$ estimates against the observed $ET_{SR}$ measurements. Validation was carried out for each surface renewal system at paired plot 1 over the two-and-a-half-year measurement period. The plot boundaries were used to define the footprint of the $ET_{SR}$ measurements, and a region of interest for which the daily $ET_{EEFlux}$ estimates were extracted and analyzed. Using EEFlux ET maps and ArcGIS Pro software, the mean value of pixels within these plot boundaries were calculated. To eliminate bias from pixels that fell mostly beyond the plot boundaries, only whole or nearly whole pixels (~ >75%) located within the plot boundaries were used in the calculations. Finally, the daily $ET_{EEFlux}$ estimates were summed and validated against the daily $ET_{SR}$ measurements. The statistical indices used for validation included the coefficient of determination ($R^2$), root mean square error (RMSE), mean bias error (MBE), and the Willmott (1981) index of agreement (d) (de Oliveira Costa *et al*. 2020). The optimal values of $R^2$ and the d index are one, and RMSE and MBE values that are close to zero (Bennett *et al*. 2013)

### *5.3.6 Spatio-temporal assessment of the woody cover-ET relationship*

Long-term time series of the difference in daily ET between the control and cut plots were created using all available EEFlux maps between 1990 and 2023 in order to illustrate any changes in ET that may have occurred in the experimental plots over time, particularly after

the thinning of woody plants. Separate time series were created for each of the four paired plots. The daily $ET_{EEFlux}$ estimates were calculated in the same manner as in the EEFlux validation process. The time series of daily $ET_{EEFlux}$ estimates indicated the timing of woody plant thinning, allowing for the visual detection of any differences in ET that may have occurred after thinning. Furthermore, the mean daily $ET_{EEFlux}$ for twenty selected areas (A-T) with higher woody cover (i.e., highly dense woody vegetation) and lower woody cover (i.e., less dense woody vegetation) were calculated and compared between 1990 and 2023 to determine whether woodier areas had greater ET on a larger scale over time. To be classified as higher or lower woody cover, the woody cover maps for all four hydrological years had to agree on whether the area had highly dense or less dense woody vegetation. Datasets for 13 higher and 7 lower woody cover areas were collected. These datasets were used to create cumulative curves and box plots that allowed the average (mean and median) and spread (interquartile range) of daily $ET_{EEFlux}$ for the higher and lower woody cover areas to be compared.

We also performed a statistical analysis on the $ET_{EEFlux}$ time series datasets for the higher and lower woody cover areas as part of the spatio-temporal assessment of the woody cover-ET relationship. The Mann-Kendall trend (Mann 1945, Kendall 1975) and Sen's slope (Sen 1968) tests were used in RStudio. The Mann-Kendall test was used to identify statistically significant trends in the time series, and Sen's slope was used to calculate the magnitude of that trend. The Mann-Kendall test accepts the null hypothesis when the p-value exceeds the significance level ($\alpha = 0.05$), indicating that there is no statistically significant trend in the time series. If the p-value is below the significance level ($\alpha = 0.05$), the null hypothesis is rejected and the alternative hypothesis is accepted, indicating a statistically significant trend in the time series. A positive Z value indicates that the time series has an increasing trend, whereas a negative Z value indicates a decreasing trend. The positivity or negativity of the Sen's slope value can also confirm an increasing or decreasing trend.

## 5.4 Results

### *5.4.1 Classification of current woody cover in the quaternary catchment B82J*

The Gradient Tree Boost, Random Forest and Support Vector Machine classifiers performed comparably for the classification of woody cover in the study catchment, but Gradient Tree Boost and Random Forest marginally outperformed Support Vector Machine (Figure 5.9,

*Appendix C*). The classification results using the Gradient Tree Boost classifier for the 2022-2023 hydrological year showed high accuracies when tested against the validation data (Figure 5.3). The overall accuracy was 90%, and producers and user's accuracies for the woody cover and non-woody cover classes ranged between 86% and 93%. The Kappa statistic was 0.79, indicating strong agreement between the classification result and the validation data.


**Figure 5.3 Woody cover classification (10 m spatial resolution) using the Gradient Tree Boost classifier in the quaternary B82J for the 2019-2020, 2020-2021, 2021-2022 and 2022-2023 hydrological years. The classification results are provided for the 2022-2023 year.**

The woody cover maps revealed that the quaternary B82J had a high woody cover, accounting for 57% to 60% of the total catchment area. Despite agreement on the degree of woody cover across years, the spatial distribution of woody cover differed. However, all years agreed that there was higher cover in the north-eastern and eastern areas of the catchment.

Lower woody cover was also clearly visible in the vicinity of the small communal villages. The 2020-2021 and 2022-2023 years depicted high woody cover in the southern area of the catchment. It could be argued that the maps indicated lower woody cover in the western area of the catchment within the Kruger National Park, but there was only a clear distinction between lower woody cover in the Kruger National Park and higher woody cover outside the Kruger National Park at the Kruger National Park fence line for the 2022-2023 year in the central area.

### *5.4.2 Earth Engine Evapotranspiration Flux performance*

The relationship between daily $ET_{SR}$ measurements and $ET_{EEFlux}$ estimates was compared on 39 days in total (Figure 5.4). The majority of the days were from the dry season, as there was a scarcity of usable EEFlux maps during the wet season due to the high incidence of cloud cover. The comparisons revealed slopes of 0.87 and 0.76, $R^2$ values of 0.68 and 0.59, and RMSE values of 0.80 mm $d^{-1}$ and 0.98 mm $d^{-1}$, for the control and cut plots, respectively. These errors indicate that the $ET_{EEFlux}$ estimates have been underestimated. The MBE values were negative, further indicating that EEFlux underestimated ET, with values of -0.25 mm $d^{-1}$ and -0.26 mm $d^{-1}$ for the control and cut plots, respectively. The index d, on the other hand, revealed that EEFlux was accurate, with values of 0.86 and 0.84 for the control and cut plots, respectively.

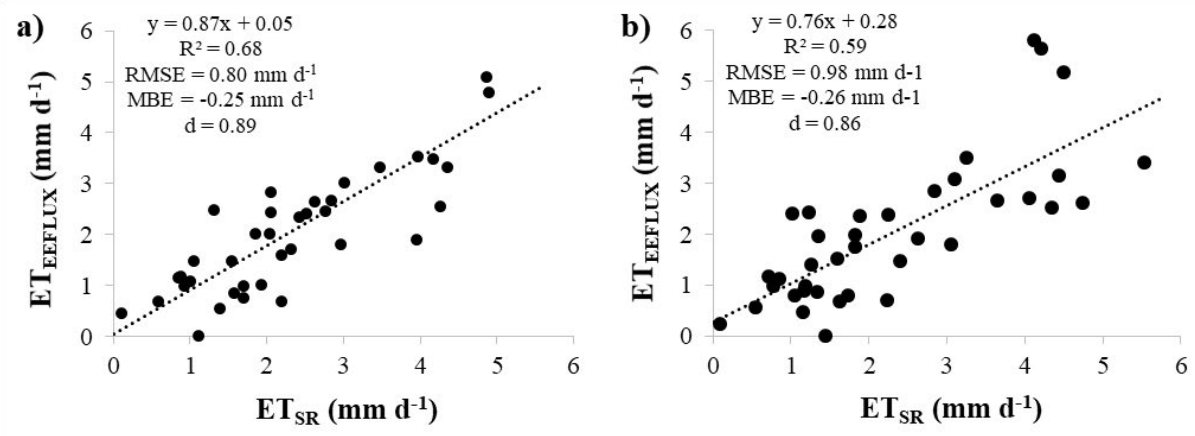


**Figure 5.4 Comparisons of daily surface renewal evapotranspiration ($ET_{SR}$) measurements and Earth Engine Evapotranspiration Flux evapotranspiration ($ET_{EEFlux}$) estimates during the measurement period for the a) control and b) cut plots.**

The time series of the daily $ET_{SR}$ measurements and $ET_{EEFlux}$ estimates for the measurement period revealed that the $ET_{EEFlux}$ in both plots captured the strong seasonality of ET measured by the SR1 method (Figure 5.5). Earth Engine Evapotranspiration Flux accurately reproduced the maximum peaks reached in the summer, as well as the gradual increases and decreases in ET during the season transitions. Maximum $ET_{EEFlux}$ values during the summer season reached between 5.00 mm $d^{-1}$ and 5.50 mm $d^{-1}$, which is comparable with the maximum $ET_{SR}$ values observed of around 5.00 mm $d^{-1}$. However, $ET_{EEFlux}$ consistently underestimated $ET_{SR}$ in both plots in 2019 and 2020. In 2021 and 2022, $ET_{SR}$ and $ET_{EEFlux}$ were more comparable in both plots, although there was still a general pattern of underestimation, except for several days, particularly in the summer, where $ET_{EEFlux}$ overestimated $ET_{SR}$. However, given the scarcity of usable EEFlux maps for the summer months, it can't be confirmed as a trend.

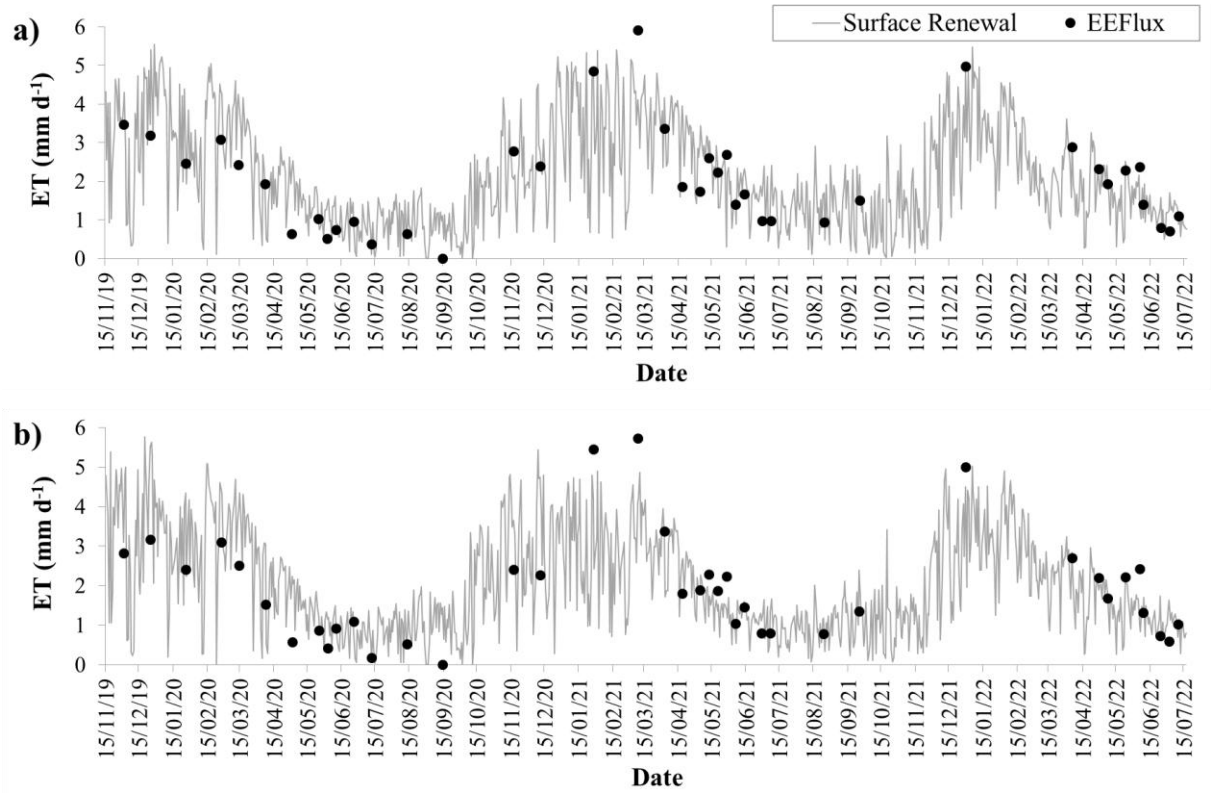


**Figure 5.5 Time-series of daily surface renewal evapotranspiration ($ET_{SR}$) measurements and Earth Engine Evapotranspiration Flux evapotranspiration ($ET_{EEFlux}$) estimates during the measurement period for the a) control and b) cut plots.**

### *5.4.3 Woody cover-ET relationship at the plot scale*

The long-term time series (1990-2023) of the difference in daily $ET_{EEFlux}$ between the control and cut plots at the four paired plots are presented in Figure 5.6. From 1990 to 1999, there were

fewer data points since only Landsat-5 images were available, but from 1999, 2013 and 2021, there were more data points due to the launches of Landsat-7, -8 and -9, respectively. At paired plots 1 and 4, before woody plant thinning, the control and cut plots had comparable ET, or the control plot measured slightly higher ET. This pattern did not change to a large extent after thinning, with the exception of a few days when the control plot measured higher ET. Most of these days occurred during the wet season, which was also when the largest differences in ET between the plots occurred. At paired plots 2 and 3, before thinning, the cut plot generally tended to have a higher ET than the control. However, as at paired plot 1, after thinning, there were more days where the control plot had a higher ET, particularly during the wet season. However, there were several days at paired plot 2, and most days at paired plot 3, where the cut plot measured higher ET.

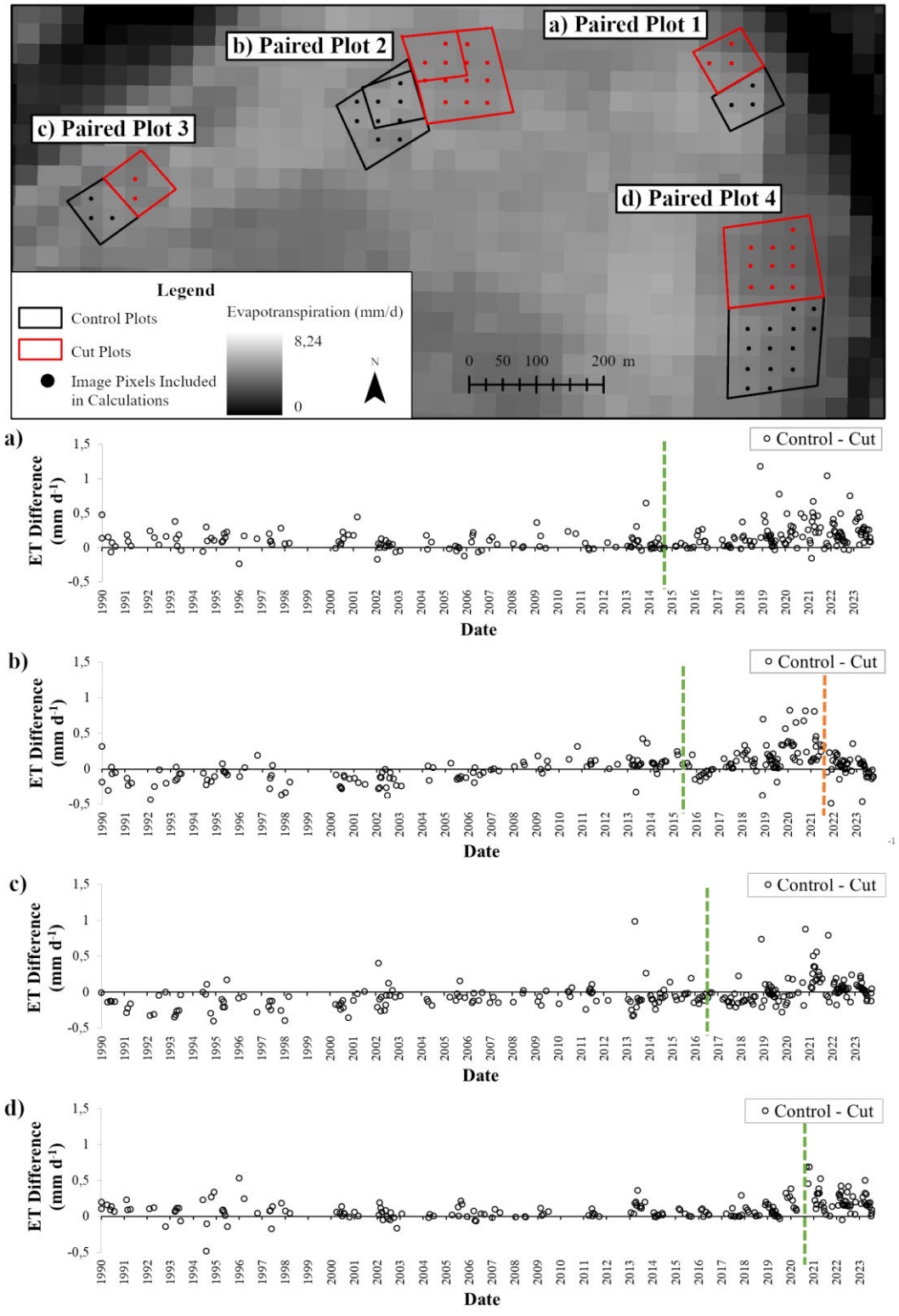


**Figure 5.6 Long-term time series (1990–2023) demonstrating the difference in daily Earth Engine Evapotranspiration Flux evapotranspiration ($ET_{EEFlux}$) between the control and cut plots at paired plots 1, 2, 3 and 4. The green dashed lines in the graphs indicate when cutting took place in the cut plots, and the orange dashed line in paired plot 2 indicates when the plots were expanded in size.**

### *5.4.4 Woody cover-ET relationship at the catchment scale*

The daily $ET_{EEFlux}$ maps for the quaternary B82J revealed high spatial variability in savanna vegetation ET (Figure 5.7). On several days, $ET_{EEFlux}$ appeared to be higher in the catchment's northern areas, as well as in the eastern side outside the Kruger National Park on several days during the wet season. The dry season maps generally agreed that $ET_{EEFlux}$ was lower in the southern part of the catchment. The locations of the three communal villages also appeared to have lower $ET_{EEFlux}$. On DOY 287 of 2022, $ET_{EEFlux}$ was significantly reduced over a substantial portion of the catchment as a result of the occurrence of a widespread fire. Clear differences in daily $ET_{EEFlux}$ patterns were observed during the wet and dry season. During the wet season, much higher $ET_{EEFlux}$ was observed, reaching a maximum of around 5.50 mm $d^{-1}$. Cumulative graphs of daily $ET_{EEFlux}$ revealed that the higher woody cover areas generally generated a higher cumulative $ET_{EEFlux}$ compared to the lower woody cover areas (Figure 5.8a). There were, however, several lower woody cover areas that had a higher cumulative $ET_{EEFlux}$ compared to some of the higher woody cover areas. The cumulative $ET_{EEFlux}$ for higher woody cover areas ranged from 213.4 mm to 370.4 mm, while the lower woody cover areas ranged from 185.0 mm to 264.4 mm. Box plots also revealed that the woodier areas generally had higher mean and median daily $ET_{EEFlux}$ values than the less woody areas (Figure 5.8b and Table 5.3, *Appendix C*). The woodier areas also generally had larger first and third quartiles than the less woody areas, and an interquartile range that was comparable or greater.

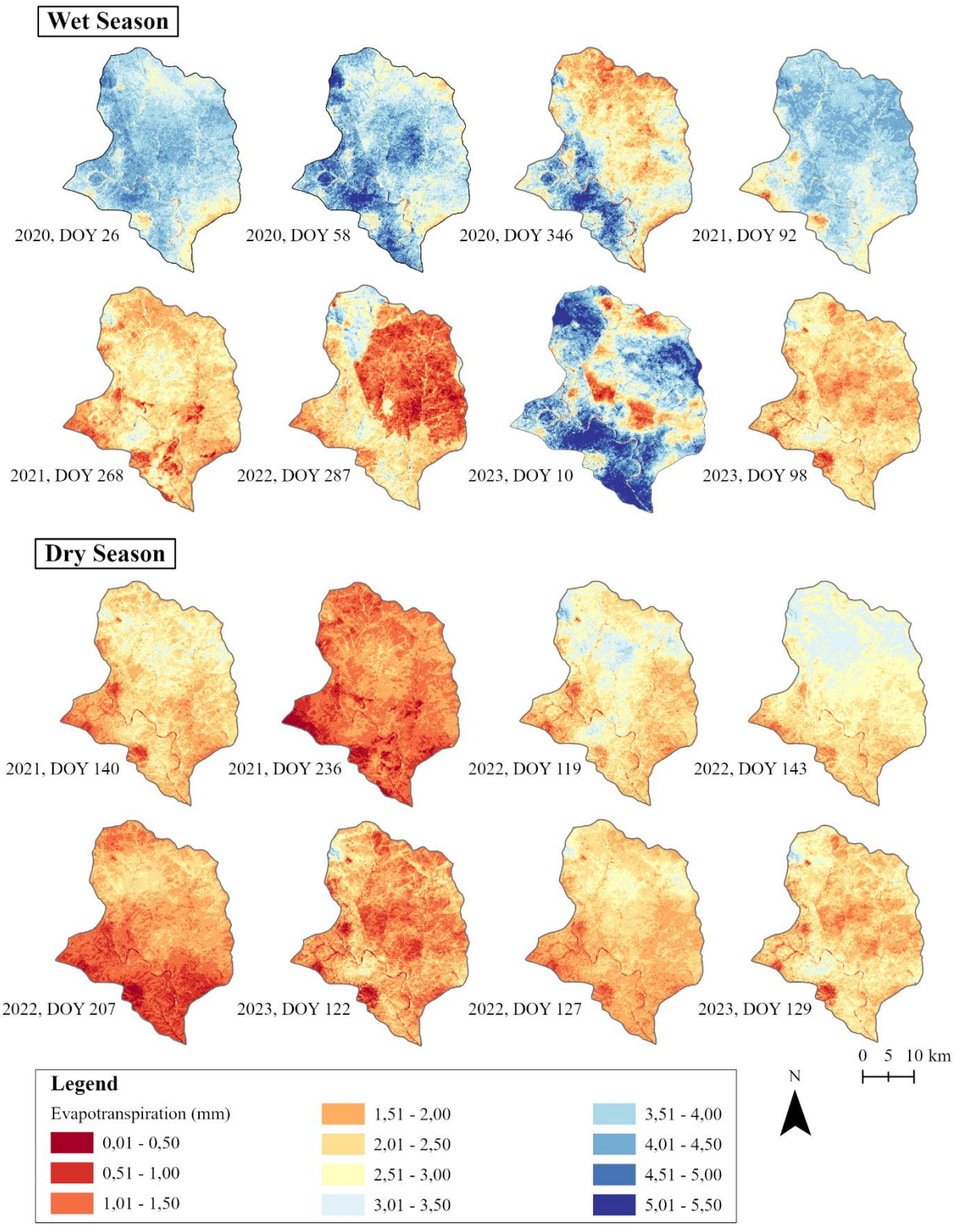


**Figure 5.7 Spatial patterns of daily evapotranspiration (ET) derived from Earth Engine Evapotranspiration Flux (EEFlux) for the quaternary B82J on days representative of the wet (October-March) and dry (April-September) seasons during the 2020-2023 years.**

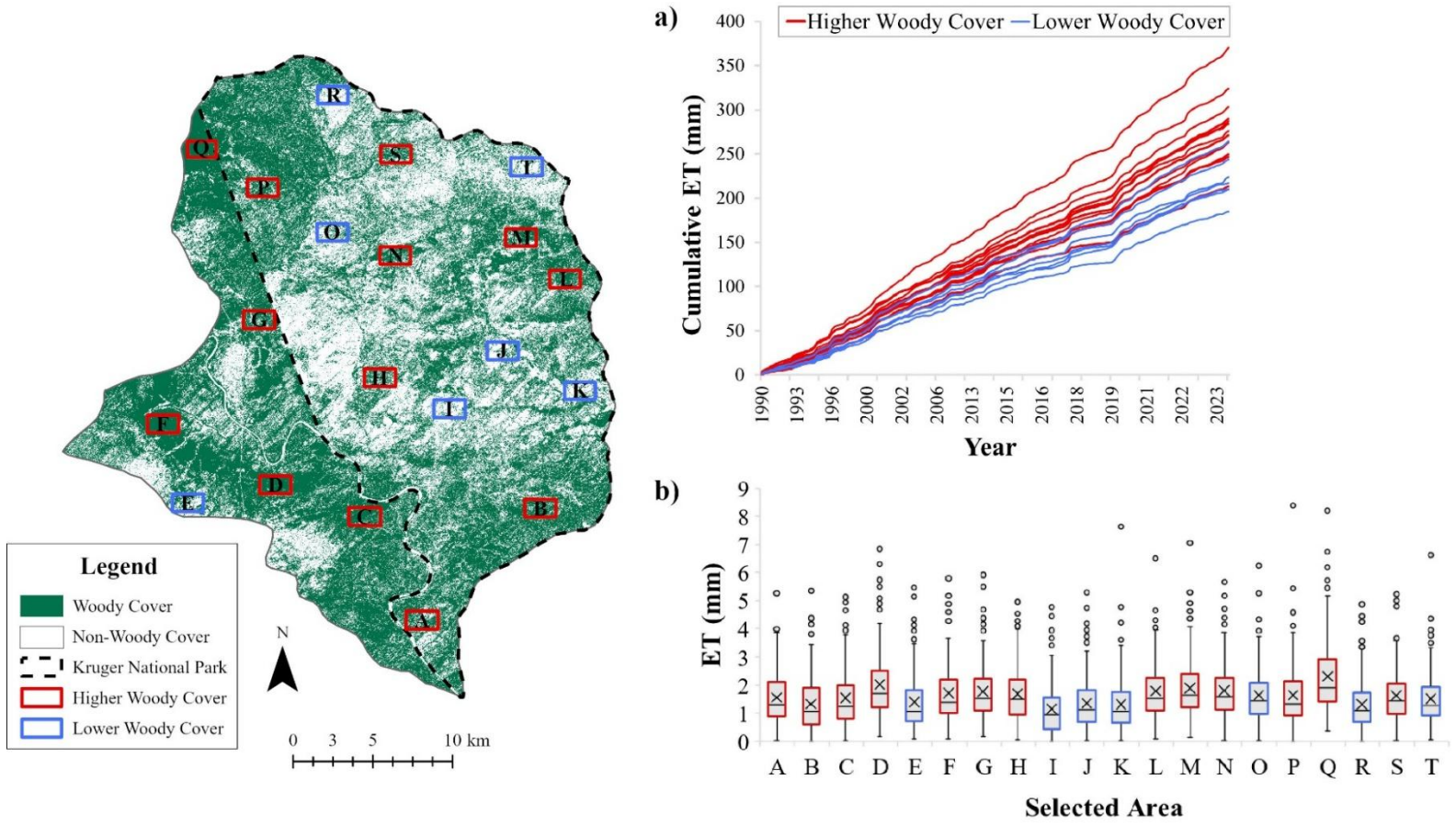


**Figure 5.8 Spatio-temporal variation in daily Earth Engine Evapotranspiration Flux (EEFlux) evapotranspiration ($ET_{EEFLUX}$) depicted by a) cumulative curves, and b) box plots for higher and lower woody cover areas between 1990 and 2023. The cumulative curve totals are only for 161 days that (EEFlux) data was available. Each box plot displays the minimum, maximum, median, mean, and first and third quartiles. Outliers are represented by the dots; these are points that fall outside of the 150% inter-quartile range. The quaternary B82J map is given as a reference to show the location of the higher and lower woody cover areas.**

Table 5.1 shows the results of the Mann-Kendall trend and Sen's slope tests for the $ET_{EEFlux}$ time series for areas A-T. The Mann-Kendall trend test revealed that only four areas (M, N, P and T) showed statistically significant trends over time (p-values < 0.05). All of these areas showed positive Z and Sen's slope values, Mann-Kendall parameter (S), Variance (varS) and Kendall's tau, indicating increasing trends in $ET_{EEFlux}$. Most areas showed increasing trends; only areas E and G showed decreasing trends, but neither of these trends were statistically significant.

**Table 5.1 Mann-Kendall trend and Sen's slope test statistics for the $ET_{EEFlux}$ time series (1990-2023) for higher and lower woody cover areas A-T.**

| Area | Woody Cover | Z value | p-value | α | S | varS | Kendall's tau | Sen's slope | Trend |
|---|---|---|---|---|---|---|---|---|---|
| **A** | Higher | 0.89 | 0.375 | 0.05 | 608 | 467971.3 | 0.05 | 0.0013 | Increasing |
| **B** | Higher | 0.29 | 0.776 | 0.05 | 196 | 467971.3 | 0.02 | 0.0004 | Increasing |
| **C** | Higher | 0.20 | 0.844 | 0.05 | 136 | 467971.3 | 0.01 | 0.0003 | Increasing |
| **D** | Higher | 1.10 | 0.271 | 0.05 | 754 | 467971.3 | 0.06 | 0.0018 | Increasing |
| **E** | Lower | -0.63 | 0.531 | 0.05 | -430 | 467971.3 | -0.03 | -0.0008 | Decreasing |
| **F** | Higher | 0.07 | 0.941 | 0.05 | 52 | 467971.3 | 0.01 | 0.0001 | Increasing |
| **G** | Higher | -0.19 | 0.853 | 0.05 | -128 | 467971.3 | -0.01 | -0.0003 | Decreasing |
| **H** | Higher | 0.74 | 0.459 | 0.05 | 508 | 467971.3 | 0.04 | 0.0010 | Increasing |
| **I** | Lower | 0.49 | 0.622 | 0.05 | 338 | 467971.3 | 0.03 | 0.0006 | Increasing |
| **J** | Lower | 0.77 | 0.441 | 0.05 | 528 | 467971.3 | 0.04 | 0.0010 | Increasing |
| **K** | Lower | 1.21 | 0.226 | 0.05 | 830 | 467971.3 | 0.06 | 0.0015 | Increasing |
| **L** | Higher | 1.95 | 0.052 | 0.05 | 1332 | 467971.3 | 0.10 | 0.0025 | Increasing |
| **M** | Higher | 2.00 | 0.046 | 0.05 | 1366 | 467971.3 | 0.11 | 0.0026 | Increasing |
| **N** | Higher | 2.79 | 0.005 | 0.05 | 1910 | 467971.3 | 0.15 | 0.0040 | Increasing |
| **O** | Lower | 1.64 | 0.102 | 0.05 | 1120 | 467971.3 | 0.09 | 0.0023 | Increasing |
| **P** | Higher | 3.18 | 0.001 | 0.05 | 2178 | 467971.3 | 0.17 | 0.0048 | Increasing |
| **Q** | Higher | 1.82 | 0.069 | 0.05 | 1244 | 467971.3 | 0.10 | 0.0027 | Increasing |
| **R** | Lower | 1.30 | 0.194 | 0.05 | 890 | 467971.3 | 0.07 | 0.0015 | Increasing |
| **S** | Higher | 1.82 | 0.069 | 0.05 | 1246 | 467971.3 | 0.10 | 0.0026 | Increasing |
| **T** | Lower | 1.97 | 0.049 | 0.05 | 1348 | 467971.3 | 0.10 | 0.0023 | Increasing |

Acronym key: Significance level (α) Mann-Kendall parameter (S), Variance (varS).

## 5.5 Discussion

The purpose of this study was to assess the relationship between woody cover and ET across various spatio-temporal scales in a woody-encroached, semi-arid savanna catchment using freely available and relatively user-friendly resources provided by Google Earth Engine. Here, we discuss the three research questions that the study sought to answer. First, can pixel-based classification algorithms and moderate resolution satellite imagery effectively map woody cover in heterogenous savanna environments? Second, what is the potential of EEFlux for estimating ET in semi-arid savanna vegetation? Finally, is the increase in ET caused by woody encroachment more evident over greater spatial and temporal scales? We also discuss the limitations and uncertainties of the study.

### *5.5.1 Can pixel-based classification algorithms and moderate resolution satellite imagery effectively map woody cover in heterogenous savanna environments?*

The accuracy assessment for the 2022-2023 year classification revealed that the mapping of woody cover in the quaternary catchment B82J was done with high accuracy. However, the spatial distribution of woody cover varied between the four hydrological years. Rainfall exhibited high inter-annual variability, with the 2020-2021 year being very wet, which may have led to differences in leaf area index, and thus, different distributions of woody cover classified. We found that woody cover was accurately mapped in densely wooded areas, but either over- or under-classified in sparsely wooded areas when visually comparing the classified maps to Google Earth's very high resolution imagery. Sentinel-2 imagery's 10 m x 10 m pixels are larger than the crown area of a typical savanna woody plant, which is likely to result in inaccurate woody cover mapping in sparsely wooded areas. A similar issue has been reported by Zhang *et al*. (2019) who mapped woody cover over an arid and semi-arid savanna environment in the West African Sahel using a Support Vector Machine classifier and Sentinel-1 and -2 imagery. They discovered that the amount of woody cover was overestimated because smaller tree crowns were classified as a single 10 x 10 m pixel.

No field-based ground truthing data was collected to further validate the classifications. Validation data was gathered from very high resolution Google Earth imagery as with the resources available for this study, we were unable to cover the entire study area. The site is not only remote and difficult to access, but it is also hazardous due to the presence of dangerous wild animals, particularly when conducting surveys on foot. One of the study's primary goals was to create a more pragmatic approach that involved quick, simple and inexpensive methods.

Although the accuracy metrics indicated that the classifier performed well in reproducing the training data, this may not be a true reflection of what is happening on the ground. It would be preferable to verify the accuracy of the woody cover mapping with ground truthing data, but we considered the method adequate for capturing the general pattern of savanna vegetation's woody and grass components. We also only collected training and validation data for the 2022-2023 year, but produced woody cover maps for an additional three years. Therefore, we only performed the validation for the 2022-2023 year and assumed that the model performed satisfactorily in the other years. Given that the goal of this study was to identify broad spatial patterns and trends across time, we only required an indication of where the higher and lower woody cover areas were. The woody cover maps were created primarily to compare them to the $ET_{EEFlux}$ maps, which had a lower spatial resolution of 30 m.

### *5.5.2 What is the potential of EEFlux for estimating ET in semi-arid savanna vegetation?*

The validation of the $ET_{EEFlux}$ estimates against the observed $ET_{SR}$ measurements revealed that EEFlux performed reasonably well in estimating daily ET at the experimental plots, despite an underestimation of ET. Prior studies by Salem *et al*. (2004) and Foolad *et al*. (2018) also report a general underestimation of $ET_{EEFlux}$ estimates when compared to in situ ET observations and ET calculated by the METRIC Model in both agricultural land uses and natural vegetation types across North America and Europe. Salem *et al*. (2004) and Foolad *et al*. (2018), however, presented errors significantly higher than those of this study. Our results can also be considered reasonable when compared to prior studies that have validated ET estimates obtained from various surface energy balance models against in situ eddy covariance ET measurements in savanna environments (Ruhoff *et al*. 2012, da Silva *et al*. 2015, Gokool *et al*. 2017, Kunstmann *et al*. 2018, Oliviera *et al*. 2018, Gokool *et al*. 2020, Burchard-Levine *et al*. 2021, Carpintero *et al*. 2021, Senay *et al*. 2022). Many of these studies also report an over- or underestimation of ET by surface energy balance models, especially during conditions of water stress.

Various reasons can explain the underestimation of $ET_{EEFlux}$ estimates, such as inadequate or erroneous data inputs into the METRIC Model, problems with calibration, and modelling errors in estimating G (Laipelt *et al*. 2021). Moreover, it is possible that a deficiency within the METRIC Model contributes to its poorer performance in drier regions. Savannas are often data-scarce and lack extensive monitoring networks, especially those outside North America and Europe, therefore inaccurate data inputs from ground measurements are probably largely to blame (Laipelt *et al*. 2021). Salem *et al*. (2004) suggested that this may be due to EEFlux

employing gridded weather datasets rather than ground truth weather data, which causes the $ET_{EEFlux}$ estimates to suffer from aridity biases common to gridded weather datasets. Grid-based weather datasets typically present low precipitation amounts, resulting in an underestimation of the fraction of reference ET, and hence actual ET.

Given the study's objectives, the $ET_{EEFlux}$ estimates were considered reasonably accurate for the purposes of the research. However, in agreement with Salem *et al*. (2024), EEFlux is still a work in progress that requires further improvement and validation efforts. Despite this, it could be a very valuable tool in data-scarce settings without monitoring networks.

### *5.5.3 Is the increase in ET caused by woody encroachment more evident over greater spatial and temporal scales?*

In the previous study at the Mthimkhulu trial by Aldworth *et al*. (2022), the daily in situ $ET_{SR}$ measurements indicated that woody encroachment did not have a significant effect on daily ET, however this study discovered that the daily $ET_{EEFlux}$ estimates showed some variation between the control and cut plots. The overall $ET_{EEFlux}$ patterns were generally comparable in the control and cut plots before and after woody plant thinning, however, there were more days after woody plant thinning when the control plot recorded greater ET, particularly during the wet season. Despite the fact that the $ET_{EEFlux}$ estimates were generally underestimated when compared to the $ET_{SR}$ measurements, the results for the control and cut plots were consistent (i.e., they both showed statistically similar indices and underestimated $ET_{EEFlux}$ to a similar degree). Therefore, when comparing $ET_{EEFlux}$ estimates between the plots, the pattern of difference should be representative of the pattern of difference between the paired plots.

At the catchment scale, it became evident that woodier areas had greater ET. The daily $ET_{EEFlux}$ maps for the quaternary B82J revealed that areas with higher woody cover, such as in the northern and eastern areas of the catchment, generally had higher ET. The woodier areas also generally exhibited higher cumulative $ET_{EEFlux}$ during the period between 1990 and 2023, as well as higher mean and median daily $ET_{EEFlux}$ values, and first and third quartiles. The $ET_{EEFlux}$ maps also revealed that it was particularly during the wet season that the woodier areas had greater ET than the less woody areas, which was consistent with the field-scale $ET_{EEFlux}$ results. This is most likely due to increased water availability during the wet season, resulting in a higher potential for plant water uptake and ET. Gradual temporal changes in ET were also discernible at the catchment scale. According to the Mann-Kendall and Sen's slope tests, most

of the areas within the catchment indicated increasing trends in ET between 1990 and 2023, although only in four of the twenty areas was this statistically significant.

### *5.5.4 Uncertainties and limitations*

It has already been acknowledged that EEFlux is still a work in progress and requires improved data inputs, but one factor beyond our control is the shortage of usable EEFlux maps, particularly for the wet season, due to the high incidence of cloud cover and the malfunctioning scan line corrector. Given that the majority of $ET_{EEFlux}$ data came from dry season days, this brings some uncertainty to our analysis and trend identification, particularly during the wet season when we expect woody cover to have the greatest effect on ET, as indicated by the in situ surface renewal measurements performed at the experimental trial (Aldworth *et al*. 2022). We could obtain more usable EEFlux data if Sentinel-2 data was integrated into EEFlux instead of the Landsat data because Sentinel-2 satellites have a higher temporal resolution. This study investigated how woody cover affects ET, but we cannot predict the hydrological response if woody plant thinning is carried out, or if there will be lag effects. Few studies have investigated lag effects following the removal of woody plants, including Dugas *et al*. (1998), who discovered reduced ET losses in a small catchment for only two years after treatment. We also did not investigate how elevation, slope and soil texture influence spatial variation in ET. Higher altitudes appeared to have higher ET, as seen in the north-eastern part of the catchment, but this was also the woodiest area and may have received more rainfall, making it difficult to determine whether the higher ET was due to higher woody cover, higher elevation or higher rainfall. This could be investigated further at more sites in future studies. We also need to be cautious in assuming that the increasing ET is caused by increased woody cover, because we know that temperature rises are occurring in the Greater Kruger National Park region because of climate change (Bunting *et al*. 2016), which would also contribute to rising ET.

## 5.6 Conclusion

This study provides alternative, relatively user-friendly and low-cost methods for mapping woody cover and ET in semi-arid savannas, allowing the relationship between woody cover and ET to be assessed across various spatio-temporal scales in a woody-encroached, semi-arid savanna catchment. Our results demonstrate that, while woody encroachment can increase ET in semi-arid savannas, this increase occurs gradually over time and typically only during wet seasons and wet years. Moreover, this increase only becomes evident at larger scales. These findings suggest that if woody plant removal operations are carried out, any hydrological

benefits (i.e., reduced ET losses and increased water yields) may only manifest over time. Moreover, rather than being sustained year-round or occurring every year, increased water yields may be limited to wet seasons or extended wet periods. In semi-arid savannas, it is during these wet seasons and years when groundwater and soil water stores are replenished. However, if woody plants use more water during wet seasons and years, this replenishment may not occur. Therefore, if woody plant densities are not reduced, systems may be unable to recover from dry spells and years, and groundwater depletion may become increasingly apparent over time. It is also evident that any effective woody plant removal efforts aimed at increasing water yields will require large-scale implementation and long-term monitoring. If increased water yields from woody plant removal are only likely to occur on a large scale, during select periods after a prolonged period in semi-arid savanna catchments, and these operations are both costly and labour-intensive, then it might beg the question whether this is an effective management approach? These findings open discussion regarding the viability of large-scale woody plant removal operations as a management strategy in woody-encroached, semi-arid savanna catchments. The benefits to other ecosystem services - such as changed carrying capacity, carbon sequestration, soil nutrient cycling and biodiversity - that are provided or improved in addition to greater water yields may need to be considered when assessing the viability of woody plant removal operations.

### 5.7 References


Acharya, B.S., Hao, Y., Ochsner, T.E. and Zou, C.B., 2017. Woody plant encroachment alters soil hydrological properties and reduces downward flux of water in tallgrass prairie. *Plant and Soil*, 414, 379-391. https://doi.org/10.1007/s11104-016-3138-0.

Acharya, B.S., Kharel, G., Zou, C.B., Wilcox, B.P. and Halihan, T., 2018. Woody plant encroachment impacts on groundwater recharge: A review. *Water,* 10 (10), 1466. https://doi.org/10.3390/w10101466.

Aldworth, T.A., Toucher, M.L., Clulow, A.D. and Swemmer, A.M., 2022. The effect of woody encroachment on evapotranspiration in a semi-arid savanna. *Hydrology*, 10 (1), 9. https://doi.org/10.3390/hydrology10010009.

Alemayehu, T., van Griensven, A., Senay, G.B. and Bauwens, W., 2017. Evapotranspiration mapping in a heterogeneous landscape using remote sensing and global weather datasets: Application to the Mara Basin, East Africa. *Remote Sensing*, 9 (4), 390. https://doi.org/10.3390/rs9040390.

Allen, R.G., Tasumi, M. and Trezza, R., 2007. Satellite-based energy balance for mapping evapotranspiration with internalized calibration (METRIC) - Model. *Journal of Irrigation and Drainage Engineering*, 133 (4), 380-394. http://dx.doi.org/10.1061/(ASCE)0733-9437(2007)133:4(380).

Allen, R.G., Morton, C., Kamble, B., Kilic, A., Huntington, J., Thau, D., Gorelick, N., Erickson, T., Moore, R., Trezza, R. and Ratcliffe, I., 2015. EEFlux: A Landsat-based evapotranspiration mapping tool on the Google Earth Engine. In 2015 ASABE/IA Irrigation Symposium: Emerging Technologies for Sustainable Irrigation-A Tribute to the Career of Terry Howell, Sr. Conference Proceedings (pp. 1-11). *American Society of Agricultural and Biological Engineers*.

Alsanjar, O. and Cetin, M., 2024. Comparison of actual evapotranspiration by the google earth engine evapotranspiration flux (EEFlux) to the METRIC model using remote sensing data and in-situ climate observations. In BIO Web of Conferences (Vol. 85, p. 01073). *EDP Sciences*. https://doi.org/10.1051/bioconf/20248501073.

Amani, M., Ghorbanian, A., Ahmadi, S.A., Kakooei, M., Moghimi, A., Mirmazloumi, S.M., Moghaddam, S.H.A., Mahdavi, S., Ghahremanloo, M., Parsian, S. and Wu, Q., 2020. Google earth engine cloud computing platform for remote sensing big data applications: A comprehensive review. *IEEE Journal of Selected Topics in Applied Earth Observations and Remote Sensing*, 13, 5326-5350.

Andreu, A., Kustas, W.P., Polo, M.J., Carrara, A. and González-Dugo, M.P., 2018. Modeling surface energy fluxes over a dehesa (oak savanna) ecosystem using a thermal based two-source energy balance model (TSEB) I. *Remote Sensing*, 10 (4), 567. https://doi.org/10.3390/rs10040567.

Awada, H., Di Prima, S., Sirca, C., Giadrossich, F., Marras, S., Spano, D. and Pirastru, M., 2021. Daily actual evapotranspiration estimation in a mediterranean ecosystem from landsat observations using SEBAL approach. *Forests*, 12 (2), 189. https://doi.org/10.3390/f12020189.

Bayas, S., Sawant, S., Dhondge, I., Kankal, P. and Joshi, A., 2022. Land use land cover classification using different ml algorithms on sentinel-2 imagery. In Advanced machine intelligence and signal processing (pp. 761-777). Singapore: *Springer Nature Singapore*. https://doi.org/10.1007/978-981-19-0840-8_59.

Bennett, N.D., Croke, B.F., Guariso, G., Guillaume, J.H., Hamilton, S.H., Jakeman, A.J., Marsili-Libelli, S., Newham, L.T., Norton, J.P., Perrin, C. and Pierce, S.A., 2013. Characterising performance of environmental models. *Environmental Modelling & Software*, 40, 1-20. http://dx.doi.org/10.1016/j.envsoft.2012.09.011.

Blin, N. and Suárez, F., 2023. Evaluating the contribution of satellite-derived evapotranspiration in the calibration of numerical groundwater models in remote zones using the EEFlux tool. *Science of the Total Environment*, 858, 159764. http://dx.doi.org/10.1016/j.scitotenv.2022.159764.

Bolyn, C., Michez, A., Gaucher, P., Lejeune, P. and Bonnet, S., 2018. Forest mapping and species composition using supervised per pixel classification of Sentinel-2 imagery. *Biotechnologie, Agronomie, Société et Environnement*, 22(3). https://doi.org/10.25518/1780-4507.16524.

Burchard-Levine, V., Nieto, H., Riaño, D., Migliavacca, M., El-Madany, T.S., Guzinski, R., Carrara, A. and Martín, M.P., 2021. The effect of pixel heterogeneity for remote sensing-

based retrievals of evapotranspiration in a semi-arid tree-grass ecosystem. *Remote Sensing of Environment*, 260, 112440. https://doi.org/10.1016/j.rse.2021.112440.

Carpintero, E., Anderson, M.C., Andreu, A., Hain, C., Gao, F., Kustas, W.P. and González-Dugo, M.P., 2021. Estimating evapotranspiration of mediterranean oak savanna at multiple temporal and spatial resolutions. Implications for water resources management. *Remote Sensing*, 13(18), 3701. https://doi.org/10.3390/rs13183701.

Carrasco-Benavides, M., Ortega-Farías, S., Gil, P.M., Knopp, D., Morales-Salinas, L., Lagos, L.O., de la Fuente, D., López-Olivari, R. and Fuentes, S., 2022. Assessment of the vineyard water footprint by using ancillary data and EEFlux satellite images. Examples in the Chilean central zone. *Science of The Total Environment*, 811, 152452. http://dx.doi.org/10.1016/j.scitotenv.2021.152452.

Congalton, R.G., 1991. A review of assessing the accuracy of classifications of remotely sensed data. *Remote Sensing of Environment*, 37(1), 35-46. https://doi.org/10.1016/0034-4257(91)90048-B.

Congalton, R.G., and Green, K., 2009. Assessing the accuracy of remotely sensed data: principles and practices. 2nd ed. Boca Raton, FL, USA: Lewis Publishers. https://doi.org/10.1201/9781420055139.

de Oliveira Costa, J., José, J.V., Wolff, W., de Oliveira, N.P.R., Oliveira, R.C., Ribeiro, N.L., Coelho, R.D., da Silva, T.J.A., Bonfim-Silva, E.M. and Schlichting, A.F., 2020. Spatial variability quantification of maize water consumption based on Google EEflux tool. *Agricultural Water Management*, 232, 106037. https://doi.org/10.1016/j.agwat.2020.106037.

da Silva, B.B., Wilcox, B.P., da Silva, V.D.P.R., Montenegro, S.M.G.L. and de Oliveira, L.M.M., 2015. Changes to the energy budget and evapotranspiration following conversion of tropical savannas to agricultural lands in São Paulo State, Brazil. *Ecohydrology*, 8(7), 1272-1283. https://doi.org/10.1002/eco.1580.

Devine, A.P., McDonald, R.A., Quaife, T. and Maclean, I.M., 2017. Determinants of woody encroachment and cover in African savannas. *Oecologia*, 183, 939-951. https://doi.org/10.1007/s00442-017-3807-6.

Djamai, N. and Fernandes, R., 2018. Comparison of SNAP-derived Sentinel-2A L2A product to ESA product over Europe. *Remote Sensing*, 10(6), 926. https://doi.org/10.3390/rs10060926.

Dugas, W.A., Hicks, R.A. and Wright, P., 1998. Effect of removal of *Juniperus ashei* on evapotranspiration and runoff in the Seco Creek watershed. *Water Resources Research*, 34(6) 1499-1506. https://doi.org/10.1029/98WR00556.

Ferreira, S. and Harmse, A., 2014. Kruger National Park: Tourism development and issues around the management of large numbers of tourists. *Journal of Ecotourism*, 13(1), 16-34. https://doi.org/10.1080/14724049.2014.925907.

Filippelli, S.K., Vogeler, J.C., Falkowski, M.J. and Meneguzzo, D.M., 2020. Monitoring conifer cover: Leaf-off lidar and image-based tracking of eastern redcedar encroachment in

central Nebraska. *Remote Sensing of Environment*, 248, 111961. https://doi.org/10.1016/j.rse.2020.111961.

Foolad, F., Blankenau, P., Kilic, A., Allen, R.G., Huntington, J.L., Erickson, T.A., Ozturk, D., Morton, C.G., Ortega, S., Ratcliffe, I. and Franz, T.E., 2018. Comparison of the automatically calibrated Google Evapotranspiration Application—EEFlux and the manually calibrated METRIC application. http://dx.doi.org/10.20944/preprints201807.0040.v1

Fundisi, E., Tesfamichael, S.G. and Ahmed, F., 2022. A combination of Sentinel-1 RADAR and Sentinel-2 multispectral data improves classification of morphologically similar savanna woody plants. *European Journal of Remote Sensing*, 55(1), 372-387. https://doi.org/10.1080/22797254.2022.2083984.

Gokool, S., Jarmain, C., Riddell, E., Swemmer, A., Lerm Jr, R. and Chetty, K.T., 2017. Quantifying riparian total evaporation along the Groot Letaba River: A comparison between infilled and spatially downscaled satellite derived total evaporation estimates. *Journal of Arid Environments*, 147, 114-124. http://dx.doi.org/10.1016/j.jaridenv.2017.07.014.

Gokool, S., Riddell, E., Jarmain, C., Chetty, K., Feig, G. and Thenga, H., 2020. Evaluating the accuracy of satellite-derived evapotranspiration estimates acquired during conditions of water stress. *International Journal of Remote Sensing*, 41(2), 704-724. https://doi.org/10.1080/01431161.2019.1646940.

Heilman, J.L., Litvak, M.E., McInnes, K.J., Kjelgaard, J.F., Kamps, R.H. and Schwinning, S., 2014. Water-storage capacity controls energy partitioning and water use in karst ecosystems on the Edwards Plateau, Texas. *Ecohydrology*, 7(1), 127-138. http://dx.doi.org/10.1002/eco.1327.

Holden, P.B., Rebelo, A.J. and New, M.G., 2021. Mapping invasive alien trees in water towers: A combined approach using satellite data fusion, drone technology and expert engagement. *Remote Sensing Applications: Society and Environment*, 21, 100448. https://doi.org/10.1016/j.rsase.2020.100448.

Huxman, T.E., Wilcox, B.P., Breshears, D.D., Scott, R.L., Snyder, K.A., Small, E.E., Hultine, K., Pockman, W.T. and Jackson, R.B., 2005. Ecohydrological implications of woody plant encroachment. *Ecology*, 86(2), 308-319. https://doi.org/10.1890/03-0583.

Jovanovic, N., Mu, Q., Bugan, R.D. and Zhao, M., 2015. Dynamics of MODIS evapotranspiration in South Africa. *Water SA*, 41(1), 79-90. http://dx.doi.org/10.4314/wsa.v41i1.11.

de Sousa Junior, M.F., Fonseca, L.M.G. and Bendini, H.D.N., 2022. Estimation of Water Use in Center Pivot Irrigation Using Evapotranspiration Time Series Derived by Landsat: A Study Case in a Southeastern Region of the Brazilian Savanna. *Remote Sensing*, 14(23), 5929. https://doi.org/10.3390/rs14235929.

Kanjere, M., Thaba, K. and Lekoana, M., 2014. Water Shortage Management at Letaba Water Catchment Area in Limpopo Province, of South Africa. *Mediterr. J. Soc. Sci*, 5, 1356.

Kadam, S.A., Stöckle, C.O., Liu, M., Gao, Z. and Russell, E.S., 2021. Suitability of Earth Engine Evaporation Flux (EEFlux) estimation of evapotranspiration in rainfed crops. *Remote Sensing*, 13(19), 3884. https://doi.org/10.3390/rs13193884.

Kendall, M.G., 1975. Rank Correlation Methods. Griffin: London.

Kennedy, A.D. and Potgieter, A.L.F., 2003. Fire season affects size and architecture of *Colophospermum mopane* in southern African savannas. *Plant Ecology*, 167, 179-192.

Khosa, F.V., Feig, G.T., Van der Merwe, M.R., Mateyisi, M.J., Mudau, A.E. and Savage, M.J., 2019. Evaluation of modeled actual evapotranspiration estimates from a land surface, empirical and satellite-based models using in situ observations from a South African semi-arid savanna ecosystem. *Agricultural and Forest Meteorology*, 279, 107706. https://doi.org/10.1016/j.agrformet.2019.107706.

Khoshnood, S., Lotfata, A., Mombeni, M., Daneshi, A., Verrelst, J. and Ghorbani, K., 2023. A spatial and temporal correlation between remotely sensing evapotranspiration with land use and land cover. *Water*, 15(6), 1068.

Kruskal, W.H. and Wallis, W.A., 1952. Use of ranks in one-criterion variance analysis. *Journal of the American statistical Association*, 47(260), 583-621.

Kumbula, S.T., Mafongoya, P., Peerbhay, K.Y., Lottering, R.T. and Ismail, R., 2019. Using sentinel-2 multispectral images to map the occurrence of the cossid moth (coryphodema tristis) in eucalyptus nitens plantations of Mpumalanga, South Africa. *Remote Sensing*, 11(3), 278. https://doi.org/10.3390/rs11030278.

Kunstmann, H., Oluwadare, A., Okogbue, E., Akinluyi, F., Arnault, J., Tayari, S., Hingerl, L., & Bliefernicht, J., 2018. Comparison of SEBAL estimated heat fluxes and evapotranspiration using field and remote sensing data in the Sudanian Savanna in West Africa. *International Journal of Agriculture and Environmental Research*, 4(2), 352-374.

Laipelt, L., Kayser, R.H.B., Fleischmann, A.S., Ruhoff, A., Bastiaanssen, W., Erickson, T.A. and Melton, F., 2021. Long-term monitoring of evapotranspiration using the SEBAL algorithm and Google Earth Engine cloud computing. *ISPRS Journal of Photogrammetry and Remote Sensing*, 178, 81-96. https://doi.org/10.1016/j.isprsjprs.2021.05.018.

Ludwig, A., Meyer, H. and Nauss, T., 2016. Automatic classification of Google Earth images for a larger scale monitoring of bush encroachment in South Africa. *International Journal of Applied Earth Observation and Geoinformation*, 50, 89-94. http://dx.doi.org/10.1016/j.jag.2016.03.003.

Ludwig, M., Morgenthal, T., Detsch, F., Higginbottom, T.P., Valdes, M.L., Nauß, T. and Meyer, H., 2019. Machine learning and multi-sensor based modelling of woody vegetation in the Molopo Area, South Africa. *Remote Sensing of Environment*, *222*, 195-203. https://doi.org/10.1016/j.rse.2018.12.019.

MacGregor, S.D. and O'Connor, T.G., 2002. Patch dieback of *Colophospermum mopane* in a dysfunctional semi-arid African savanna. *Austral Ecology*, 27, 385-395. https://doi.org/10.1046/j.1442-9993.2002.01192.x.

Mann, H.B., 1945. Nonparametric tests against trend. Econometrica: *Journal of the Econometric Society*, 245-259. https://doi.org/10.2307/1907187.

Mapaure, I., 1994. The distribution of *Colophospermum mopane* (Leguminosae-caesalpinioideae) in Africa. *Kirkia*, 1-5.

Mengistu, M.G. and Savage, M.J., 2010. Open water evaporation estimation for a small shallow reservoir in winter using surface renewal. *Journal of Hydrology*, 380(1-2), 27-35. https://doi.org/10.1016/j.jhydrol.2009.10.014

Mucina L, Rutherford MC. 2006. *The Vegetation of South Africa, Lesotho and Swaziland*; Strelitzia 19, South African National Biodiversity Institute: Pretoria, South Africa.

Nassar, A., Torres-Rua, A., Hipps, L., Kustas, W., McKee, M., Stevens, D., Nieto, H., Keller, D., Gowing, I. and Coopmans, C., 2022. Using remote sensing to estimate scales of spatial heterogeneity to analyze evapotranspiration modeling in a natural ecosystem. *Remote Sensing*, 14(2), 372. https://doi.org/10.3390/rs14020372.

Nisa, Z., Khan, M.S., Govind, A., Marchetti, M., Lasserre, B., Magliulo, E. and Manco, A., 2021. Evaluation of SEBS, METRIC-EEFlux, and QWaterModel actual evapotranspiration for a Mediterranean cropping system in southern Italy. *Agronomy*, 11(2), 345. https://doi.org/10.3390/agronomy11020345.

Norton, C.L., Hartfield, K., Collins, C.D.H., van Leeuwen, W.J. and Metz, L.J., 2022. Multi-temporal LiDAR and hyperspectral data fusion for classification of semi-arid woody cover species. *Remote Sensing*, 14(12), 2896. https://doi.org/10.3390/ rs14122896.

Oliveira, B.S., Moraes, E.C., Carrasco-Benavides, M., Bertani, G. and Mataveli, G.A.V., 2018. Improved albedo estimates implemented in the METRIC model for modeling energy balance fluxes and evapotranspiration over agricultural and natural areas in the Brazilian Cerrado. *Remote Sensing, 10*(8), 1181. https://doi.org/10.3390/rs10081181.

Pech-May, F., Aquino-Santos, R., Rios-Toledo, G. and Posadas-Durán, J.P.F., 2022. Mapping of land cover with optical images, supervised algorithms, and google earth engine. *Sensors*, 22(13), 4729. https://doi.org/10.3390/s22134729.

Pollard, S. and Du Toit, D., 2011. Towards adaptive integrated water resources management in southern Africa: The role of self-organisation and multi-scale feedbacks for learning and responsiveness in the Letaba and Crocodile catchments. *Water Resources Management,* 25(15), 4019-4035. https://doi.org/10.1007/s11269-011-9904-0.

Poudel, U., Stephen, H. and Ahmad, S., 2021. Evaluating irrigation performance and water productivity using EEFlux ET and NDVI. *Sustainability,* 13(14), 7967. https://doi.org/10.3390/su13147967.

Praticò, S., Solano, F., Di Fazio, S. and Modica, G., 2021. Machine learning classification of mediterranean forest habitats in google earth engine based on seasonal sentinel-2 time-series and input image composition optimisation. *Remote Sensing*, 13(4), 586. https://doi.org/10.3390/rs13040586.

Ren, S., Chen, X. and An, S., 2017. Assessing plant senescence reflectance index-retrieved vegetation phenology and its spatiotemporal response to climate change in the Inner Mongolian Grassland. *International Journal of Biometeorology,* 61, 601-612. https://doi.org/10.1007/s00484-016-1236-6.

Rosa, R. and Tanny, J., 2015. Surface renewal and eddy covariance measurements of sensible and latent heat fluxes of cotton during two growing seasons. *Biosystems Engineering*, 136, 149-161. http://dx.doi.org/10.1016/j.*Biosystemseng*.2015.05.012.

Ruhoff, A.L., Paz, A.R., Collischonn, W., Aragao, L.E., Rocha, H.R. and Malhi, Y.S., 2012. A MODIS-based energy balance to estimate evapotranspiration for clear-sky days in Brazilian tropical savannas. *Remote Sensing*, 4(3), 703-725. https://doi.org/10.3390/rs4030703.

Salem, F.K.A., Awad, S., Hamdar, Y., Kharroubi, S. and Jaafar, H., 2024. Utility-based regression and meta-learning techniques for modeling actual ET: Comparison to (METRIC-EEFLUX) model. *Artificial Intelligence in Agriculture*, 14, 43-55. https://doi.org/10.1016/j.aiia.2024.11.001.

Sankaran, M., Hanan, N.P., Scholes, R.J., Ratnam, J., Augustine, D.J., Cade, B.S., Gignoux, J., Higgins, S.I., Le Roux, X., Ludwig, F. and Ardo, J., 2005. Determinants of woody cover in African savannas. *Nature*, 438(7069), 846-849. https://doi.org/10.1038/nature04070.

Sebego, R.J., 1999. The ecology and distribution limits of *Colophospermum mopane* in southern Africa. *Botswana Notes & Records*, 31(1), 53-72.

Sen, P.K., 1968. Estimates of the regression coefficient based on Kendall's tau. *Journal of the American Statistical Association*, 63(324), 1379-1389.

Senay, G.B., Friedrichs, M., Morton, C., Parrish, G.E., Schauer, M., Khand, K., Kagone, S., Boiko, O. and Huntington, J., 2022. Mapping actual evapotranspiration using Landsat for the conterminous United States: Google Earth Engine implementation and assessment of the SSEBop model. *Remote Sensing of Environment*, 275, 113011. https://doi.org/10.1016/j.rse.2022.113011.

Shapland, T.M., Snyder, R.L., Smart, D.R. and Williams, L.E., 2012. Estimation of actual evapotranspiration in winegrape vineyards located on hillside terrain using surface renewal analysis. *Irrigation Science*, 30, 471-484. https://doi.org/10.1007/s00271-012-0377-6.

Shekede, M.D., Murwira, A. and Masocha, M., 2015. Wavelet-based detection of bush encroachment in a savanna using multi-temporal aerial photographs and satellite imagery. *International Journal of Applied Earth Observation and Geoinformation*, 35, 209-216. http://dx.doi.org/10.1016/j.jag.2014.08.019.

Smit, G.N. and Rethman, N.F.G., 1998. Root biomass, depth distribution and relations with leaf biomass of *Colophospermum mopane*. South African *Journal of Botany*, 64(1), 38-43.

Smit, G.N., 2004. An approach to tree thinning to structure southern African savannas for long-term restoration from bush encroachment. *Journal of Environmental Management*, 71(2), 179-191. https://doi.org/10.1016/j.jenvman.2004.02.005.

Stevens, N., Lehmann, C.E., Murphy, B.P. and Durigan, G., 2017. Savanna woody encroachment is widespread across three continents. *Global Change Biology*, 23(1), 235-244. https://doi.org/10.1111/gcb.13409.

Story, M. and Congalton, R.G., 1986. Accuracy assessment: a user's perspective. *Photogrammetric Engineering and Remote Sensing*, 52(3), 397-399.

Tooley, E.G., Nippert, J.B. and Ratajczak, Z., 2024. Evaluating methods for measuring the leaf area index of encroaching shrubs in grasslands: From leaves to optical methods, 3-D

scanning, and airborne observation. *Agricultural and Forest Meteorology*, *349*, 109964. https://doi.org/10.1016/j.agrformet.2024.109964.

Tsalyuk, M., Kelly, M. and Getz, W.M., 2017. Improving the prediction of African savanna vegetation variables using time series of MODIS products. ISPRS *Journal of Photogrammetry and Remote Sensing*, 131, 77-91. http://dx.doi.org/10.1016/j.isprsjprs.2017.07.012.

Venancio, L.P., Eugenio, F.C., Filgueiras, R., França da Cunha, F., Argolo dos Santos, R., Ribeiro, W.R. and Mantovani, E.C., 2020. Mapping within-field variability of soybean evapotranspiration and crop coefficient using the Earth Engine Evaporation Flux (EEFlux) application. *Plos one*, 15(7), 0235620. https://doi.org/10.1371/journal.pone.0235620.

Wang, J., Xiao, X., Zhang, Y., Qin, Y., Doughty, R.B., Wu, X., Bajgain, R. and Du, L., 2018. Enhanced gross primary production and evapotranspiration in juniper-encroached grasslands. *Global Change Biology*, 24(12), 5655-5667. https://doi.org/10.1111/gcb.14441.

Weerasinghe, I., Bastiaanssen, W., Mul, M., Jia, L. and Van Griensven, A., 2020. Can we trust remote sensing evapotranspiration products over Africa? *Hydrology and Earth System Sciences*, 24(3), 1565-1586. https://doi.org/10.5194/hess-24-1565-2020.

Wei, H.E., Grafton, M., Bretherton, M., Irwin, M. and Sandoval, E., 2022. Evaluation of the use of UAV-derived vegetation indices and environmental variables for grapevine water status monitoring based on machine learning algorithms and SHAP analysis. *Remote Sensing*, 14(23), 5918. https://doi.org/10.3390/rs14235918.

Willmott, C.J., 1981. On the validation of models. *Physical Geography*, 2(2), 184-194.

Water Resources of South Africa. 2012 Study (WR2012). Available online: http://waterresourceswr2012.co.za/ (accessed on 21 February 2024).

Xu, C., Du, X., Fan, X., Giuliani, G., Hu, Z., Wang, W., Liu, J., Wang, T., Yan, Z., Zhu, J. and Jiang, T., 2022. Cloud-based storage and computing for remote sensing big data: a technical review. *International Journal of Digital Earth*, 15(1), 1417-1445. https://doi.org/10.1080/17538947.2022.2115567.

Yang, H., Ming, B., Nie, C., Xue, B., Xin, J., Lu, X., Xue, J., Hou, P., Xie, R., Wang, K. and Li, S., 2022. Maize canopy and leaf chlorophyll content assessment from leaf spectral reflectance: estimation and uncertainty analysis across growth stages and vertical distribution. *Remote Sensing*, 14(9), 2115. https://doi.org/10.3390/rs14092115.

Yeom, J., Jung, J., Chang, A., Ashapure, A., Maeda, M., Maeda, A. and Landivar, J., 2019. Comparison of vegetation indices derived from UAV data for differentiation of tillage effects in agriculture. *Remote Sensing*, 11(13), 1548. https://doi.org/10.3390/rs11131548.

Zhang, W., Brandt, M., Wang, Q., Prishchepov, A.V., Tucker, C.J., Li, Y., Lyu, H. and Fensholt, R., 2019. From woody cover to woody canopies: How Sentinel-1 and Sentinel-2 data advance the mapping of woody plants in savannas. *Remote Sensing of Environment*, 234, 111465. https://doi.org/10.1016/j.rse.2019.111465.

Zurqani, H.A., Post, C.J., Mikhailova, E.A., Schlautman, M.A. and Sharp, J.L., 2018. Geospatial analysis of land use change in the Savannah River Basin using Google Earth

Engine. *International Journal of Applied Earth Observation and Geoinformation*, 69, 175-185. https://doi.org/10.1016/j.jag.2017.12.006.

## APPENDIX C

**Table 5.2 The vegetation indices used in classification.**

| Vegetation Spectral Index | Equation | Reference |
|---|---|---|
| Normalized Difference Vegetation Index (NDVI) | $\frac{(NIR - RED)}{(NIR + RED)}$ | Pech-May *et al.* 2022 |
| Green Normalized Difference Vegetation Index (GNDVI) | $\frac{(NIR - GREEN)}{(NIR + GREEN)}$ | Pech-May *et al.* 2022 |
| Red-edge Normalized Difference Vegetation Index (NDVIre) | $\frac{(NIR - Rededge1)}{(NIR + Rededge1)}$ | Filippelli *et al.* 2020 |
| Enhanced Vegetation Index (EVI) | $2.5 * \frac{(NIR - RED)}{(NIR + 6 * RED - 7.5 * BLUE + 1)}$ | Pech-May *et al.* 2022 |
| Soil Adjusted Vegetation Index (SAVI) | $\frac{(NIRnarrow - RED)}{(NIRnarrow + RED + 0.5)} * 1.5$ | Pech-May *et al.* 2022 |
| Simple Blue and Red-edge 1 Ratio (SR-BlueRededge1) | $\frac{BLUE}{REDedge1}$ | Bolyn *et al.* 2018 |
| Simple NIR and Red-edge 1 Ratio (SR-NIRnarrowRededge1) | $\frac{NIRnarrow}{REDedge1}$ | Bolyn *et al.* 2018 |
| Chlorophyll Index / Pigment Specific Simple Ratio | $\frac{NIR}{RED}$ | Bolyn *et al.* 2018 |
| Chlorophyll Green Index (Chlogreen) | $\frac{NIR}{GREEN} - 1$ | Yeom *et al.* 2019 |
| Built-up Area Index (BAI) | $\frac{(BLUE - NIR)}{(BLUE + NIR)}$ | Bolyn *et al.* 2018 |
| Leaf Carotenoid Content (Lcaroc) | $\frac{REDedge3}{(BLUE - REDedge1)}$ | Bolyn *et al.* 2018 |
| Leaf Chlorophyll Content (Lchloc) | $\frac{REDedge3}{REDedge1}$ | Bolyn *et al.* 2018 |
| Leaf Anthocyanin Content (LAnthoC) | $\frac{REDedge3}{(GREEN + Rededge1)}$ | Bolyn *et al.* 2018 |
| Modified Chlorophyll Absorption in Reflectance Index (Mcari) | $(REDedge1 - RED) - 0.2 * (REDedge1 - GREEN) * \left(\frac{REDedge1}{RED}\right)$ | Wei *et al.* 2022 |

| | | |
|---|---|---|
| Plant Senescence Reflectance Index (PSRI) | $\frac{(RED - GREEN)}{REDedge2}$ | Ren *et al*. 2017 |
| Plant Pigment Ratio (PPR) | $\frac{(GREEN - BLUE)}{(GREEN + BLUE)}$ | Yang *et al*. 2022 |
| Photosynthetic Vigour Ratio (PVR) | $\frac{(GREEN - RED)}{GREEN + RED}$ | Kumbula *et al.* 2019 |

**Table 5.3 Mean (x̄), Median (M), First Quartile (Q1), Third Quartile (Q3) and Interquartile Range (IQR) for the $ET_{EEFlux}$ time series (1990-2023) for higher and lower woody cover areas A-T.**

| Area | Woody Cover | x̄ | M | Q1 | Q3 | IQR |
|---|---|---|---|---|---|---|
| **A** | Higher | 1.55 | 1.29 | 0.88 | 2.11 | 1.24 |
| **B** | Higher | 1.33 | 1.07 | 0.61 | 1.88 | 1.27 |
| **C** | Higher | 1.53 | 1.22 | 0.81 | 2.00 | 1.18 |
| **D** | Higher | 2.01 | 1.69 | 1.21 | 2.49 | 1.28 |
| **E** | Lower | 1.39 | 1.07 | 0.72 | 1.82 | 1.10 |
| **F** | Higher | 1.71 | 1.38 | 1.01 | 2.17 | 1.16 |
| **G** | Higher | 1.77 | 1.52 | 1.09 | 2.18 | 1.09 |
| **H** | Higher | 1.68 | 1.49 | 0.95 | 2.18 | 1.23 |
| **I** | Lower | 1.15 | 0.95 | 0.44 | 1.53 | 1.09 |
| **J** | Lower | 1.35 | 1.13 | 0.70 | 1.81 | 1.11 |
| **K** | Lower | 1.30 | 1.07 | 0.65 | 1.75 | 1.10 |
| **L** | Higher | 1.78 | 1.53 | 1.09 | 2.21 | 1.12 |
| **M** | Higher | 1.88 | 1.63 | 1.21 | 2.35 | 1.14 |
| **N** | Higher | 1.80 | 1.58 | 1.12 | 2.26 | 1.13 |
| **O** | Lower | 1.64 | 1.44 | 0.98 | 2.08 | 1.10 |
| **P** | Higher | 1.64 | 1.33 | 0.91 | 2.13 | 1.22 |
| **Q** | Higher | 2.30 | 1.90 | 1.40 | 2.91 | 1.51 |
| **R** | Lower | 1.30 | 1.09 | 0.69 | 1.73 | 1.05 |
| **S** | Higher | 1.63 | 1.43 | 0.98 | 2.01 | 1.03 |
| **T** | Lower | 1.51 | 1.27 | 0.93 | 1.94 | 1.01 |

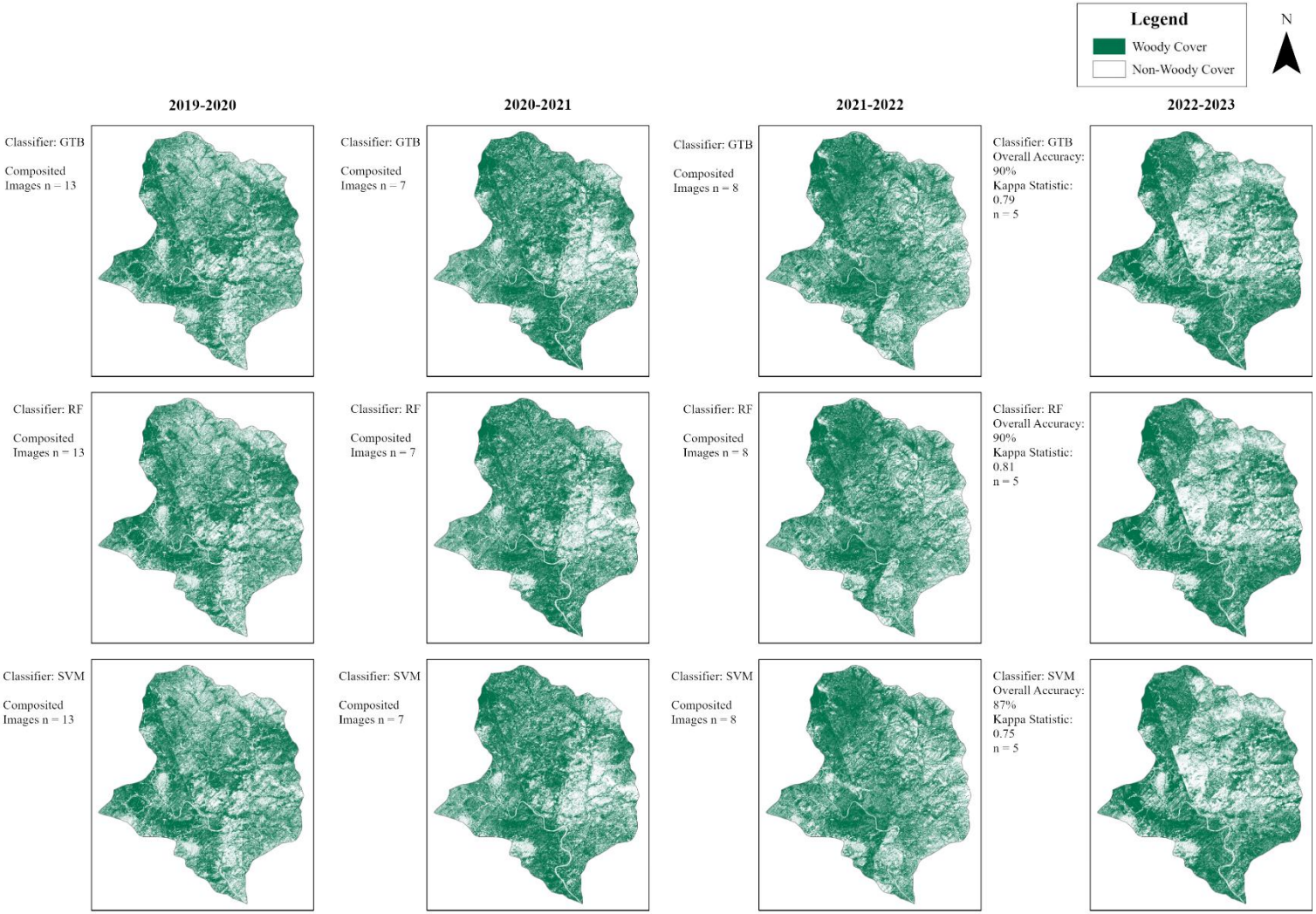


**Figure 5.9 The performance of the Gradient Tree Boost (GTB), Random Forest (RF) and Support Vector Machine (SVM) classifiers for the classification of woody cover and non-woody cover in the quaternary B82J for the four hydrological years of the study.**

**Lead into Chapter 6**

After addressing the objectives of the thesis in line with the main aim through the four research papers, we discussed the key conclusions from the research and how the research contributed to new knowledge. We also discussed recommendations for land management and future research.

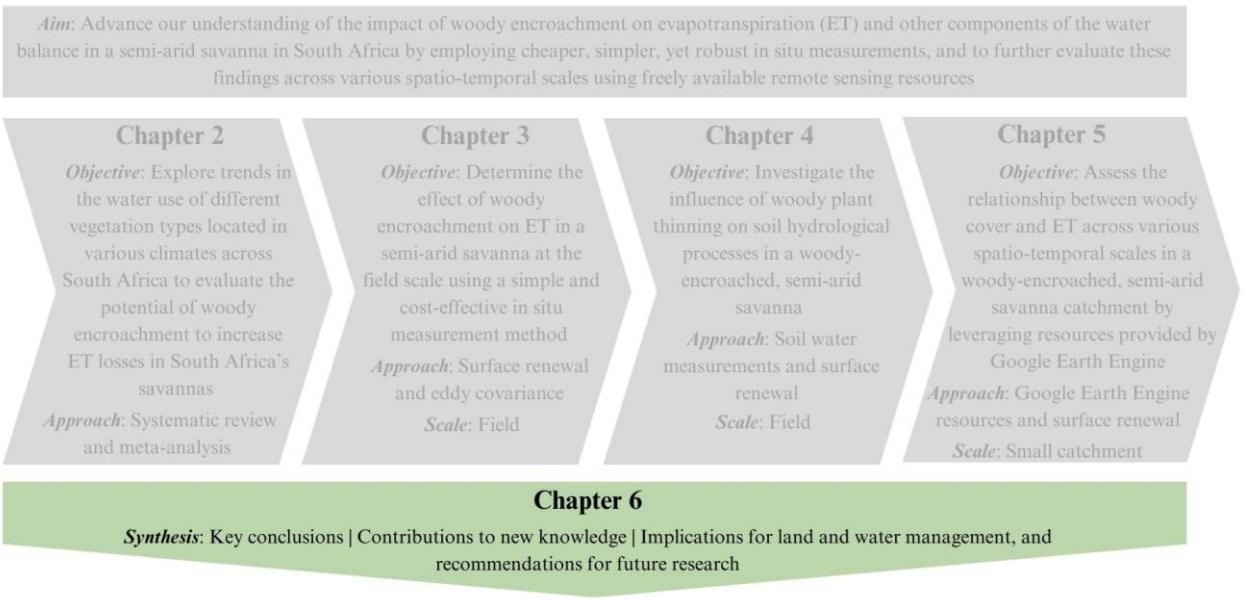

# 6 SYNTHESIS, KEY CONCLUSIONS AND RECOMMENDATIONS FOR FUTURE RESEARCH

## 6.1 Overview

The notion that woody encroachment increases evapotranspiration (ET) losses and adversely affects water resources (Acharya *et al*. 2018) raises the question of whether woody plant removal efforts should be undertaken in South Africa's woody-encroached savannas. However, insufficient hydrological research has been conducted in these environments to justify these expensive and labour-intensive operations. This is largely due to the fact that performing in situ measurements requires expensive and sophisticated equipment, which is particularly problematic in developing countries such as South Africa, where funds, resources and technical skills are scarce (Khosa *et al*. 2019, Awada *et al*. 2021, Gray *et al*. 2021). Therefore, the aim of this research was to explore the use of simple and affordable, yet robust methods to advance understanding of the impact of woody encroachment on ET and other water balance components in a semi-arid savanna in South Africa vulnerable to woody encroachment. In addition, the research sought to leverage recent advancements in remote sensing technologies to assess the relationship between woody cover and ET across various spatio-temporal scales. This knowledge may be crucial in informing land management planning and justifying large-scale woody plant removal in regions undergoing woody encroachment in South Africa's savannas in order to conserve water resources.

The research comprised of four individual, but linked, research papers, each of which were reported as a chapter of the thesis. The first research paper coupled a systematic review and meta-analysis approach to synthesize information from vegetation water use studies conducted in South Africa to evaluate the likelihood that woody encroachment is increasing ET losses in the country's savannas, and thereby, justify the necessity for further research on this topic (Chapter 2). The second research paper presented in situ ET estimates made using the surface renewal measurement technique at an existing experimental woody plant clearing trial in a semi-arid South African savanna, where the density of *Colophospermum mopane* (Mopane) is extremely high. Over three hydrological years, ET measurements were made in 'cut' plots that had undergone regular woody plant thinning treatments (grassland), as well as paired 'control' plots where no treatment had been applied (Mopane thicket) to determine the effect of woody encroachment on ET (Chapter 3). Soil measurements carried out in the paired plots to evaluate the influence of woody plant thinning on soil hydrological processes, including soil water

content, soil temperature and surface infiltration, were presented in the third research paper (Chapter 4). Lastly (fourth research paper), the relationship between woody cover and ET was assessed for the study catchment across various spatio-temporal scales using freely available and relatively user-friendly resources provided by Google Earth Engine (Chapter 5).

We first revisit the aims and objectives of the thesis as a reminder before discussing the key conclusions from the research.

## 6.2 Revisiting the aims and objectives

The overall aim of this thesis was to advance our understanding of the impact of woody encroachment on ET and other components of the water balance in a semi-arid savanna in South Africa by employing cheaper, simpler, yet robust in situ measurements, and to further evaluate these findings across various spatio-temporal scales using freely available remote sensing resources.

To achieve the overall aim, the following four objectives were defined:

1. Explore trends in the water use of different vegetation types located in various climates across South Africa to evaluate the potential of woody encroachment to increase ET losses in South Africa's savannas (Chapter 2).

2. Determine the effect of woody encroachment on ET in a semi-arid savanna at the field scale using a simple and cost-effective in situ measurement method (Chapter 3).

3. Investigate the influence of woody plant thinning on soil hydrological processes in a woody-encroached, semi-arid savanna (Chapter 4).

4. Assess the relationship between woody cover and ET across various spatio-temporal scales in a woody-encroached, semi-arid savanna catchment by leveraging freely available and relatively user-friendly resources provided by Google Earth Engine (Chapter 5).

### 6.3 Key conclusions from the research

The first key conclusion is that woody encroachment in semi-arid savannas can increase ET losses, however, this is a gradual process that is only distinguishable during wet seasons or extended wet periods. The findings of the combined systematic review and meta-analysis first provided support for this conclusion, which was subsequently corroborated by the analysis of the in situ and remotely sensed ET estimates. Previous studies demonstrating that ET increases with increasing woody densities have been carried out in wetter climates (MAP > 700 mm), or in riparian zones, where vegetation likely had access to other water sources besides rainfall (Acharya *et al*. 2018). Research on this topic has been far less abundant in arid and semi-arid climates, such as our research region, where it is argued that most, if not all, precipitation is used for ET regardless of vegetation type (Huxman *et al*. 2005, Schreier-McGraw *et al*. 2020). It has also been argued that because woody encroachment species are indigenous, they are conservative water users (Calder and Dye 2001, Dye *et al*. 2008), and hence woody encroachment should not be able to significantly increase ET, if at all. However, contrary to these beliefs, our research demonstrated that indigenous woody encroachment can increase ET in semi-arid savannas, but this occurs gradually over time and is dependent on water availability.

The analysis of the in situ and remotely sensed ET estimates over various spatial scales in the study catchment revealed that the increase in ET in semi-arid savannas caused by woody encroachment only becomes evident at larger scales. The field-scale $ET_{SR}$ estimates for the experimental plots showed that woody encroachment only caused a change in ET during some season transitions, but these changes were variable and not pronounced, whereas the $ET_{EEFlux}$ estimates for the experimental plots showed that there were some days during the wet season when the encroached plots had higher ET than the thinned plots. However, after analysis of the $ET_{EEFlux}$ estimates at the catchment scale and over larger areas of the catchment, it became evident that woodier areas had greater ET than less woody areas.

To obtain in situ ET measurements for the study catchment, surface renewal was investigated as an alternative method to eddy covariance. The surface renewal 1 (SR1) approach with eddy covariance calibration was found to produce reliable ET estimates with reasonable accuracy over semi-arid savanna-type vegetation. Prior studies have reported on the successful application of surface renewal for estimating ET over a wide range of surfaces (Hu *et al*. 2018), however, this study was the first to assess surface renewal's applicability for use

in semi-arid savanna vegetation. The validation test for the two surface renewal approaches, SR1 (Snyder *et al*. 1996) and surface renewal dissipation theory (SRDT, Castellví and Snyder 2009), against week-long eddy covariance campaigns for sensible heat flux (H) estimation revealed that the SRDT approach underestimated H, with poorer agreement than previous studies comparing $H_{SRDT}$ estimates and $H_{EC}$ measurements in grassy vegetation types. However, $H_{SR1}$ estimates agreed well with $H_{EC}$ measurements, despite relatively high RMSE values. As a result, it was determined that in our study location, SR1 was the most viable approach for measuring long-term and continuous ET.

Following the validity assessment of the SR1 and SRDT approaches for H estimation, SR1 was used to calculate the daily LE and ET for the measurement period. An analysis of these measurements along with the rainfall and energy balance flux measurements revealed that ET in semi-arid savannas is highly seasonal, rising during the wet season in response to increased soil water availability and higher net radiation (Rn), and dropping significantly during the dry season due to low soil water availability and the deciduous nature of the vegetation. Observations in the field revealed that the grass swards greened rapidly with the first spring rains before the emergence of the new Mopane leaves, but the Mopane kept their leaves much longer into the dry season, resulting in longer transpiring seasons and hence greater ET over time. The ET trends also exhibited a strong response to the distribution of annual rainfall, which dictated the overall pattern of soil water availability, and hence, the dynamics of vegetation water use. The deciduous nature of the Mopane and the seasonal dormancy of the grasses also greatly influenced these trends. Rn showed similar diurnal and seasonal patterns to ET, whereas sensible heat flux (H) and soil heat flux (G) were smaller components of the energy balance and did not accurately replicate the ET trends, nor did they exhibit a strong seasonal pattern like ET. Therefore, we could assume that Rn, rather than H and G, had a greater influence on ET.

The analysis of the soil volumetric water content and soil water storage measurements in the experimental plots revealed that woody plant thinning had minor effects on water volumes in the soil profile. The differences in mean soil volumetric water content between the control and cut plots were relatively small, and no consistent effect of thinning was observed across the three paired plots. Prior studies on the effect of woody cover on soil water report contradictory findings; higher woody cover can lead to higher soil water content (Pierce and Reich 2010, Fan *et al*. 2019, Geissler *et al*. 2019), or lower soil water content (Li and Wilson

1998, Smit and Rethman 2000). However, no prior studies report negligible effects. Only one set of infiltration tests indicated a significant increase in infiltration following thinning. The soil properties analysis supported our soil water findings, as soil texture and bulk density were similar in the control and cut plots.

Supervised pixel-based classification algorithms were applied to Sentinel-2 images in Google Earth Engine to map woody cover in the study catchment. The accuracy assessment used to test the classification results revealed that Sentinel-2 imagery and Gradient Tree Boost algorithms accurately captured woody cover over large scales. However, in sparsely wooded areas, woody cover tended to be over- or under-classified. Previous studies by Zhang *et al*. (2019) and Holden *et al*. (2021), who used similar methods to map woody cover in heterogeneous landscapes, agree that distinguishing between woody plants, trees and other vegetation types is difficult for Sentinel-2's spatial resolution, despite indicating good accuracy statistics, resulting in an under- or over-estimation of woody cover. The mapping of woody cover could have been improved with higher spatial resolution imagery, however, higher spatial resolution imagery isn't publicly available, nor is it produced as frequently or on such a large scale, which does not align with the aims of this thesis. As the focus of this research was on broad spatial patterns and trends throughout time, the mapping method and data source used were adequate for the purposes of the research.

For mapping ET in the study catchment, the Earth Engine Evapotranspiration Flux (EEFlux) product (Allen *et al*. 2007), which integrates the Mapping Evapotranspiration at High Resolution using Internalized Calibration (METRIC) Model and Landsat imagery into Google Earth Engine, was evaluated against the in situ $ET_{SR}$ estimates. It was found that EEFlux was able to estimate daily ET in semi-arid savanna vegetation with a reasonable level of accuracy, despite a general pattern of underestimation. Prior research on EEFlux has mostly tested the product over croplands that are either irrigated or located in wetter climates, and these studies have indicated good results (Bchir *et al*. 2021, Kadam *et al*. 2021, Nisa *et al*. 2021, Poudel *et al*. 2021, Rojas-Villalobos *et al*. 2022). However, very few studies have investigated its application in savannas or other heterogeneous landscapes, and those that have, have reported poor results (Foolad *et al*. 2018, Salem *et al*. 2024). The findings of Foolad *et al*. (2018) and Salem *et al*. (2024) did, however, agree that EEFlux underestimated ET in natural vegetation types.

The study thus met the aims and objectives while also contributing to new knowledge.

## 6.4 Contributions to new knowledge

- Provided a summary and comparison of the relevant literature to enhance understanding of vegetation water usage in South Africa, which revealed that woody encroachment has the potential to increase ET in the country's savannas (Objective 1).

- Undertook the first known validation of two surface renewal approaches, SR1 and SRDT, over semi-arid savanna-type vegetation, and demonstrated that the SR1 approach with eddy covariance calibration can provide ET estimates with reasonable accuracy (Objective 2).

- Provided the first in situ and remotely sensed ET estimates for woody-encroached, semi-arid savanna vegetation in South Africa, providing evidence that woody encroachment can increase ET in semi-arid savannas, however, this is typically a gradual process that is only distinguishable during wet seasons or extended wet periods (Objective 2 and 4).

- Evaluated the impact of woody encroachment on ET across various spatial scales in a semi-arid savanna, which revealed that the increase in ET caused by woody encroachment becomes more evident as the scale of observation increases (Objective 4).

- Provided evidence that woody plant thinning in woody-encroached, semi-arid savannas had minor effects on soil hydrological processes (Objective 3).

- Demonstrated that savanna vegetation can be mapped over large areas in southern Africa with reasonable accuracy using Sentinel-2 imagery and supervised pixel-based classification algorithms within Google Earth Engine (Objective 4).

- Confirmed the ability of EEFlux for estimating ET with a reasonable level of accuracy in semi-arid savanna vegetation in southern Africa (Objective 4).

## 6.5 Implications for land and water management, and recommendations for future research

Accurate in situ ET observations are critical in understanding the hydrological response of savanna systems to woody encroachment, and serve as an invaluable source of data for the calibration and validation of model simulations employed in these studies (Khosa *et al*. 2019). However, aside from the Council for Scientific and Industrial Research's (CSIR) three eddy covariance flux towers, in situ ET measurements in South Africa's savannas are scarce and usually only available for short time periods (Khosa *et al*. 2019). Common practice is to replicate ET measurements only once and have short measurement campaigns. However, ET is temporally and spatially variable in savannas, necessitating long-term monitoring and repeated replications of measurements over large areas to accurately capture mean conditions and variations in these environments (Alemayehu *et al*. 2017, Awada *et al*. 2021). The limited number of campaigns are largely due to the well-established ET micrometeorological methods being costly to establish and operationally complex, yet in South Africa and other developing countries, funds and technical skills are limited for such research (Khosa *et al.* 2019, Awada *et al*. 2021, Gray *et al*. 2021). These methods also typically require site homogeneity with a relatively large fetch, and ongoing maintenance, whereas South Africa's savannas are heterogeneous vegetation types that are typically located in remote areas which are not easy to access (Castellví and Gavilán 2021). Furthermore, the risks of vandalism, theft and fire, which are frequent occurrences, and wild animals and pests, which can interfere with expensive equipment, are high (Clulow *et al*. 2012, Gray *et al*. 2021). All things considered, it is imperative that we conduct in situ ET monitoring in South Africa's savannas, but it is critical that we identify affordable methods that are implementable and meet requirements. This study revealed that the lesser-known SR1 method is a reliable alternative to other more established methods, such as eddy covariance. However, a major drawback of the SR1 approach is that it still requires calibration against an independent and accountable method (Suvočarev *et al*. 2014). It is therefore, recommended that more testing and development be undertaken on alternative surface renewal approaches that do not require calibration, such as the SRDT (Castellví and Snyder 2009) and SR2 (Castellví *et al*. 2002; 2004) approaches, particularly in semi-arid savanna vegetation. It is also possible that new methods and instrumentation that overcome these limitations may be released in the near future. Thus, the first recommendation is to ***establish ET observation networks in savannas utilizing simple, inexpensive and low maintenance technologies for long-term monitoring.***

Empirical studies using ground observations can only cover a limited number of sites, hence simulation modelling and remote sensing methods may be more effective for assessing the hydrological impacts of woody encroachment in large catchments with spatial heterogeneity and environmental gradients (Castellví *et al*. 2016). Catchment hydrological models have long been used to compute ET patterns in catchments and explore various vegetation management scenarios, however, to ensure accuracy they require significant field data that is often unavailable, thus their results are often viewed with skepticism. However, during the last two decades, the use of satellite remote sensing models for ET estimation has advanced significantly (Alemayehu *et al*. 2017, Weerasinghe *et al.* 2020, Laipelt *et al*. 2021). The high-resolution, wide coverage, frequent updates, and consistent quality of remotely sensed ET data are some of the advantages (Alemayehu *et al*. 2017). In our research, we tested a remote sensing product called EEFlux to obtain reliable ET estimates, and this was the first evaluation of EEFlux in a dry savanna environment to the best of our knowledge. Earth Engine Evapotranspiration Flux integrates a surface energy balance model known as the Mapping Evapotranspiration at High Resolution using Internalized Calibration (METRIC) Model into Google Earth Engine (Kadam *et al.* 2021, Poudel *et al.* 2021). The comparison of $ET_{EEFlux}$ estimates to in situ $ET_{SR}$ estimates revealed an underestimation of $ET_{EEFlux}$. It is often the case that remote sensing products work well in the place where they are developed but perform poorly in other climates and vegetation types. Several factors could influence the inconsistency between EEFlux and surface renewal derived ET, but it is most likely caused by poor data input due to South Africa's sparse or non-existent weather data networks. These results indicate that EEFlux still requires improvement and more validation efforts in the savanna regions of southern Africa, and most likely in other data scarce natural environments throughout the world. Another drawback of EEFlux was that the Landsat imagery had a high amount of cloud cover, especially during the wet season. Unfortunately, cloud cover cannot be avoided when using Landsat imagery. This resulted in a shortage of usable EEFlux maps during the wet season. Future research must focus on improving remote sensing models, especially to obtain accurate ET estimates in natural environments with sparse ground-based data networks. This could involve local parameterization and other improvements to EEFlux, as well as more integrations of surface energy balance models into Google Earth Engine or other cloud computing platforms. The use of imagery from other satellites that is not impacted by cloud cover must also be considered in these models. Thus, the second recommendation is to ***increase the use of remote sensing-based ET models in natural vegetation types for further validation and to enable hydrological assessments over various spatio-temporal scales.***

In natural systems, surface runoff is controlled by factors such as ET, interception, antecedent soil moisture (particularly in shallow soil), infiltration capacity and rainfall intensity, whereas the potential for deep recharge is determined by deep soil water volumes, hydraulic conductivity, porosity and fractures. Exploration of these factors that were not investigated in this research is important to gain a more comprehensive understanding of the hydrological processes in these systems, as well as the impact of woody encroachment on each individual process. In particular, very few studies have focused on the effect of woody encroachment on deep drainage and groundwater recharge, especially in semi-arid regions. An improved understanding of the impact of woody encroachment on deep drainage/groundwater recharge is especially important because a reduction in deep drainage/groundwater recharge has the potential to reduce baseflow in catchments, which is linked to streamflow and groundwater depletion (Acharya *et al*. 2017b). Stable isotopes and geophysical methods may be effective tools for studying deep drainage and groundwater recharge (Acharya *et al*. 2018). There have also been few studies to determine the effect of woody encroachment on interception, which, given the dense canopies of encroacher species, may significantly lower the effective rainfall received in these systems. Thus, the third recommendation is to ***further investigate the effect of woody encroachment on all hydrological processes, particularly the effect on deep soil drainage, groundwater recharge and interception*.**

Water flow pathways in savannas can be tracked using stable isotopes of oxygen and hydrogen. Analysing the isotopic compositions of plant and soil water may be able to provide valuable insight on the differences in grass and woody plant water uptake strategies, as well as the hydrologic linkage between transpiration, soil water and groundwater (Acharya *et al*. 2018). Therefore, stable isotopes could be a valuable tool for future investigations on how changes in vegetation water consumption and vegetation structure brought about by woody encroachment can affect the production of surface runoff and the downward flow of water into deep soil and groundwater aquifers. Stable isotopes may also help us to answer other questions that were raised during our research, such as whether savanna plants are able to utilize additional water sources besides rainfall during dry periods, including deeper soil water or groundwater? Are tree roots capable of facilitating hydraulic lift of deep soil water or groundwater to depths within their rooting zones? Thus, the fourth recommendation is to ***use stable isotope methods to improve understanding of vegetation water use dynamics in woody-encroached savannas and the impact of woody encroachment on the production of surface runoff and groundwater recharge*.**

The findings of the research indicate that in order to reduce ET losses and increase catchment water yields in South Africa's semi-arid savannas, large scale woody plant removal efforts must be implemented. However, further research is needed to fully evaluate the effects of removal and determine the extent to which increased water yield is possible. Furthermore, if there is potential for greater yields in pristine regions (i.e., protected areas) versus modified land use types. Finally, the optimal strategies for woody plant removal and restoring land for increasing yields should be investigated. For example, to what degree of woody plant thinning is best, and whether manual removal methods, arboricides, fire etc. should be used. In addition, it must be determined how long after thinning, increased yields can be expected or whether these effects will be lagged. Furthermore, will riparian or upland areas experience greater yields? A combination of remote sensing tools, hydrological modelling and in situ experiments is recommended for these studies. Thus, the fifth recommendation is to ***further investigate woody plant removal methods and best land management practices that promote increased catchment water yields at various altitudinal locations*.**

Global climate change is expected to alter rainfall and temperature regimes, as well as increase atmospheric $CO_2$ levels. These changes will likely shift plant functional types, and hence alter ET, interception, infiltration, and subsurface flow, all of which have potential to have a substantial impact on streamflow and groundwater recharge, especially in water-limited ecosystems (Acharya *et al*. 2018). As such, the changing climate must be considered when studying the hydrological implications of woody encroachment. Savanna landscapes are projected to be highly sensitive to climate change, with our study area expected to become hotter and drier in coming decades. Studies also agree that woody cover will increase in our study region (Bunting *et al*. 2016). The combined effects of climate change and woody encroachment are largely uncertain, but by assessing the possible vegetation and ET changes under various climate change scenarios, we may begin to determine the vulnerability of this savanna environment and the urgency of woody encroachment management interventions. Thus, the sixth and final recommendation is to ***investigate woody cover-ET changes under various climate change scenarios to establish the future impacts of woody encroachment on water resources and the need for management interventions.***

## 6.6 References

Acharya, B.S., Hao, Y., Ochsner, T.E. and Zou, C.B., 2017a. Woody plant encroachment alters soil hydrological properties and reduces downward flux of water in tallgrass prairie. *Plant and Soil*, *414*, 379-391.

Acharya, B.S., Halihan, T., Zou, C.B. and Will, R.E., 2017b. Vegetation controls on the spatio-temporal heterogeneity of deep moisture in the unsaturated zone: A hydrogeophysical evaluation. *Scientific Reports*, *7*(1), 1499.

Acharya, B.S., Kharel, G., Zou, C.B., Wilcox, B.P. and Halihan, T., 2018. Woody plant encroachment impacts on groundwater recharge: A review. *Water*, *10*(10): 1466.

Alemayehu, T., Van Griensven, A., Senay, G.B. and Bauwens, W., 2017. Evapotranspiration mapping in a heterogeneous landscape using remote sensing and global weather datasets: Application to the Mara Basin, East Africa. *Remote Sensing*, *9*(4), 390.

Allen, R.G., Tasumi, M. and Trezza, R., 2007. Satellite-based energy balance for mapping evapotranspiration with internalized calibration (METRIC) - Model. *Journal of Irrigation and Drainage Engineering*, *133*(4), 380-394.

Awada, H., Di Prima, S., Sirca, C., Giadrossich, F., Marras, S., Spano, D. and Pirastru, M., 2021. Daily actual evapotranspiration estimation in a mediterranean ecosystem from Landsat observations using SEBAL approach. *Forests*, *12*(2), 189.

Bchir, A., M'nassri, S., Dhib, S., Amri, A.E. and Mulla, D., 2021. Estimating and mapping evapotranspiration in olive groves of semi-arid Tunisia using empirical formulas and satellite remote sensing. *Arabian Journal of Geosciences*, *14*(24), 2717.

Bunting, E.L., Fullman, T., Kiker, G. and Southworth, J., 2016. Utilization of the SAVANNA model to analyze future patterns of vegetation cover in Kruger National Park under changing climate. *Ecological Modelling*, *342*, 147-160.

Calder, I.R. and Dye, P., 2001. Hydrological impacts of invasive alien plants. *Land Use and Water Resources Research*, *1*(1732-2016-140259).

Castellví, F., Perez, P.J. and Ibanez, M., 2002. A method based on high-frequency temperature measurements to estimate the sensible heat flux avoiding the height dependence. *Water Resources Research*, *38*(6), 20-1.

Castellví, F., 2004. Combining surface renewal analysis and similarity theory: A new approach for estimating sensible heat flux. *Water Resources Research*, *40*(5).

Castellví, F. and Snyder, R.L., 2009. Combining the dissipation method and surface renewal analysis to estimate scalar fluxes from the time traces over rangeland grass near Ione (California). *Hydrological Processes*, *23*, 842–857.

Castellví, F., Cammalleri, C., Ciraolo, G., Maltese, A. and Rossi, F., 2016. Daytime sensible heat flux estimation over heterogeneous surfaces using multitemporal land-surface temperature observations. *Water Resources Research*, *52*(5), 3457-3476.

Castellví, F. and Gavilán, P., 2021. Estimation of the latent heat flux over irrigated short fescue grass for different fetches. *Atmosphere*, *12*(3), 322.

Clulow, A.D., Everson, C.S., Mengistu, M.G., Jarmain, C., Jewitt, G.P.W., Price, J.S. and Grundling, P.L., 2012. Measurement and modelling of evaporation from a coastal wetland in Maputaland, South Africa. *Hydrology and Earth System Sciences*, *16*(9), 3233-3247.

Dye, P. J., Gush, M. B., Everson, C. S., Jarmain, C., Clulow, A., Mengistu, M., ... & Savage, M. J. (2008). Water-use in relation to biomass of indigenous tree species in woodland, forest and/or plantation conditions. *Water Research Commission Report*, (361/08).

Eldridge, D.J., Wang, L. and Ruiz-Colmenero, M., 2015. Shrub encroachment alters the spatial patterns of infiltration. *Ecohydrology*, *8*(1), 83-93.

Fan, Y., Li, X.Y., Huang, H., Wu, X.C., Yu, K.L., Wei, J.Q., Zhang, C.C., Wang, P., Hu, X. and D'Odorico, P., 2019. Does phenology play a role in the feedbacks underlying shrub encroachment? *Science of the Total Environment*, *657*, 1064-1073.

Foolad, F., Blankenau, P., Kilic, A., Allen, R.G., Huntington, J.L., Erickson, T.A., Ozturk, D., Morton, C.G., Ortega, S., Ratcliffe, I. and Franz, T.E., 2018. Comparison of the automatically calibrated Google Evapotranspiration Application—EEFlux and the manually calibrated METRIC application.

Geissler, K., Hahn, C., Joubert, D. and Blaum, N., 2019. Functional responses of the herbaceous plant community explain ecohydrological impacts of savanna shrub encroachment. *Perspectives in Plant Ecology, Evolution and Systematics 39*, 125458.

Gray, B.A., Toucher, M.L., Savage, M.J. and Clulow, A.D., 2021. The potential of surface renewal for determining sensible heat flux for indigenous vegetation for a first-order montane catchment. *Hydrological Sciences Journal*, *66*(6), 1015-1027.

Holden, P.B., Rebelo, A.J. and New, M.G., 2021. Mapping invasive alien trees in water towers: A combined approach using satellite data fusion, drone technology and expert engagement. *Remote sensing applications: Society and Environment*, *21*, 100448.

Hu, Y., Buttar, N.A., Tanny, J., Snyder, R.L., Savage, M.J. and Lakhiar, I.A., 2018. Surface renewal application for estimating evapotranspiration: A review. *Advances in Meteorology*, *2018*(1), 1690714.

Huxman, T.E., Wilcox, B.P., Breshears, D.D., Scott, R.L., Snyder, K.A., Small, E.E., Hultine, K., Pockman, W.T. and Jackson, R.B., 2005. Ecohydrological implications of woody plant encroachment. *Ecology*, *86*(2), 308-319.

Kadam, S.A., Stöckle, C.O., Liu, M., Gao, Z. and Russell, E.S., 2021. Suitability of Earth Engine Evaporation Flux (EEFlux) estimation of evapotranspiration in rainfed crops. *Remote Sensing*, *13*(19), 3884.

Khosa, F.V., Feig, G.T., Van der Merwe, M.R., Mateyisi, M.J., Mudau, A.E. and Savage, M.J., 2019. Evaluation of modeled actual evapotranspiration estimates from a land surface, empirical and satellite-based models using in situ observations from a South African semi-arid savanna ecosystem. *Agricultural and Forest Meteorology*, *279*, 107706.

Laipelt, L., Kayser, R.H.B., Fleischmann, A.S., Ruhoff, A., Bastiaanssen, W., Erickson, T.A. and Melton, F., 2021. Long-term monitoring of evapotranspiration using the SEBAL algorithm and Google Earth Engine cloud computing. *ISPRS Journal of Photogrammetry and Remote Sensing*, *178*, 81-96.

Li, X. and Wilson, S.D., 1998. Facilitation among woody plants establishing in an old field. *Ecology 79*(8): 2694-2705.

Niemeyer, R.J., Heinse, R., Link, T.E., Seyfried, M.S., Klos, P.Z., Williams, C.J. and Nielson, T., 2017. Spatiotemporal soil and saprolite moisture dynamics across a semi-arid woody plant gradient. *Journal of Hydrology*, *544*, 21-35.

Nisa, Z., Khan, M.S., Govind, A., Marchetti, M., Lasserre, B., Magliulo, E. and Manco, A., 2021. Evaluation of SEBS, METRIC-EEFlux, and QWaterModel actual evapotranspiration for a Mediterranean cropping system in southern Italy. *Agronomy*, *11*(2), 345.

Oliveira, R.S., Bezerra, L., Davidson, E.A., Pinto, F., Klink, C.A., Nepstad, D.C. and Moreira, A. 2005. Deep root function in soil water dynamics in cerrado savannas of central Brazil. *Functional Ecology*, *19*(4): 574-581.

Poudel, U., Stephen, H. and Ahmad, S., 2021. Evaluating irrigation performance and water productivity using EEFlux ET and NDVI. *Sustainability*, *13*(14), 7967.

Rojas Villalobos, H.L., 2022. Comparison of evaporation estimates from the REEM and EEFlux models in a shallow water body. Case: Bustillos Lake, Chihuahua, Mexico. Instituto de Arquitectura Diseño y Arte.

Salem, F.K.A., Awad, S., Hamdar, Y., Kharroubi, S. and Jaafar, H., 2024. Utility-based regression and meta-learning techniques for modeling actual ET: Comparison to (METRIC-EEFLUX) model. *Artificial Intelligence in Agriculture*, *14*, 43-55.

Schreiner-McGraw, A.P., Vivoni, E.R., Ajami, H., Sala, O.E., Throop, H.L. and Peters, D.P., 2020. Woody plant encroachment has a larger impact than climate change on dryland water budgets. *Scientific reports*, *10*(1), 8112.

Smit, G.N. and Rethman, N.F.G., 2000. The influence of tree thinning on the soil water in a semi-arid savanna of southern Africa. *Journal of Arid Environments*, *44*(1), 41-59.

Snyder, R.L., Spano, D., Paw U, K.T., 1996. Surface renewal analysis for sensible and latent heat flux density. *Boundary-Layer Meteorology*, *77*, 249-266.

Suvočarev, K., Shapland, T.M., Snyder, R.L. and Martínez-Cob, A., 2014. Surface renewal performance to independently estimate sensible and latent heat fluxes in heterogeneous crop surfaces. *Journal of Hydrology*, *509*, 83-93.

Weerasinghe, I., Bastiaanssen, W., Mul, M., Jia, L. and Van Griensven, A., 2020. Can we trust remote sensing evapotranspiration products over Africa? *Hydrology and Earth System Sciences*, *24*(3), 1565-1586.

Zhang, W., Brandt, M., Wang, Q., Prishchepov, A.V., Tucker, C.J., Li, Y., Lyu, H. and Fensholt, R., 2019. From woody cover to woody canopies: How Sentinel-1 and Sentinel-2 data advance the mapping of woody plants in savannas. *Remote Sensing of Environment*, *234*, 111465.

Zou, C.B., Turton, D.J., Will, R.E., Engle, D.M. and Fuhlendorf, S.D., 2014. Alteration of hydrological processes and streamflow with juniper (*Juniperus virginiana*) encroachment in a mesic grassland catchment. *Hydrological Processes*, *28*(26), 6173-6182.